Classical and Quantum Aspects of Infinite Derivative Field Theories and Infinite Derivative Gravity

Spyridon Talaganis

Master of Mathematics (University of Cambridge)

Physics

Department of Physics

Lancaster University

April 2018

A thesis submitted to Lancaster University for the degree of Doctor of Philosophy in the Faculty of Science and Technology

Abstract

The objective of this thesis is to study classical and quantum aspects of infinite derivative field theories and infinite derivative gravity. Infinite derivative theories of gravity can be made free from ghosts and classical singularities. In order to avoid ghosts, one modifies the graviton propagator by employing *entire* functions so that no new poles are introduced apart from the pole corresponding to the massless graviton of General Relativity.

Inspired by infinite derivative gravity, we consider an infinite derivative *scalar toy model* and demonstrate renormalisability when the loop-order is arbitrarily large. Moreover, scattering diagrams within the framework of infinite derivative field theories are explicitly evaluated and it is shown that the cross section can be made finite. Finally, we perform a Hamiltonian analysis of an infinite derivative gravitational theory with a simpler action containing only the Ricci scalar and compute the number of relevant degrees of freedom.

To my mother

Acknowledgements

First, I would like to thank my supervisor, Dr Jonathan Gratus, for his unwavering support and guidance. I would also like to thank Dr Jaroslaw Nowak, Dr David Burton and my collaborator, Dr Tirthabir Biswas.

I am very grateful to my colleagues, Aindriú Conroy, James Edholm, Ernestas Pukartas, Saleh Qutub, Ilia Teimouri and Lingfei Wang. In particular, I would like to thank my close friends, Saleh Qutub and Ilia Teimouri, for their continuous support. I would also like to thank all the people from whom I learnt mathematics and physics during the four years I spent at Trinity College, University of Cambridge. Moreover, I would like to express my gratitude to Onassis Foundation for funding me throughout my studies.

Last but not least, I would like to thank my family: my mother, my sister and my father.

Declaration

This thesis is my own work and no portion of the work referred to in this thesis has been submitted in support of an application for another degree or qualification at this or any other institute of learning.

"Carpe diem"
Horace.

Contents

List of Figures

List of abbreviations

CM: Centre-of-Mass

d.o.f.: degrees of freedom

EH: Einstein-Hilbert

e.o.m.: equation of motion

GR: General Relativity

IDG: Infinite Derivative theories of Gravity

LQG: Loop Quantum Gravity

QCD: Quantum ChromoDynamics

QED: Quantum ElectroDynamics

QFT: Quantum Field Theory

ST: String Theory

SUGRA: SuperGravity

SUSY: SuperSymmetry

UV: UltraViolet

Relevant Papers by the Author

Chapter 2

- T. Biswas and S. Talaganis, "String-Inspired Infinite-Derivative Theories of Gravity: A Brief Overview," *Mod. Phys. Lett. A* **30**, 1540009 (2015) [arXiv:1412.4256 [gr-qc]].

Chapter 3

- S. Talaganis, T. Biswas and A. Mazumdar, "Towards understanding the ultraviolet behavior of quantum loops in infinite-derivative theories of gravity," *Class. Quant. Grav.* **32**, 215017 (2015) [arXiv:1412.3467 [hep-th]].
- S. Talaganis, "Towards UV Finiteness of Infinite Derivative Theories of Gravity and Field Theories," arXiv:1704.08674 [hep-th].

Chapter 4

- S. Talaganis and A. Mazumdar, "High-Energy Scatterings in Infinite-Derivative Field Theory and Ghost-Free Gravity," *Class. Quant. Grav.* **33**, 145005 (2016) [arXiv:1603.03440 [hep-th]].

Chapter 5

- S. Talaganis and A. Teimouri, "Hamiltonian Analysis for Infinite Derivative Field Theories and Gravity," arXiv:1701.01009 [hep-th].

Appendix D

- S. Talaganis, "Slavnov Identities for Infinite Derivative Theory of Gravity," arXiv:1705.08569 [hep-th].

Appendix F

- S. Talaganis and A. Teimouri, "Scale of non-locality for a system of n particles," arXiv:1705.07759 [hep-th].

Appendix G

- A. Teimouri, S. Talaganis, J. Edholm and A. Mazumdar, "Generalised Boundary Terms for Higher Derivative Theories of Gravity," *JHEP* **1608**, 144 (2016) [arXiv:1606.01911 [gr-qc]].

Appendix H

- A. Conroy, A. Mazumdar, S. Talaganis and A. Teimouri, "Nonlocal gravity in D dimensions: Propagators, entropy, and a bouncing cosmology," *Phys. Rev. D* **92**, 124051 (2015) [arXiv:1509.01247 [hep-th]].

Chapter 1

Introduction

The impact of Albert Einstein's theory of General Relativity (GR) [1] on theoretical physics has been remarkable. Apart from being, probably, the most aesthetically pleasing and elegant physical theory formulated so far, GR has passed, to this day, all experimental and observational tests it has undergone. However, GR is not a flawless theory. At the classical level, it is beset by cosmological and black hole singularities. At the quantum level, it is perturbatively non-renormalisable and, thus, not complete in the ultraviolet (UV), that is, it is not complete at short distances or high energies.

Formulating a completely successful theory of quantum gravity [2, 3, 4, 5, 6] remains a goal to be achieved in theoretical physics. *Renormalisability* [1] plays a very important role in establishing a consistent theory of quantum gravity. In four-dimensional spacetime, pure gravity is UV finite at 1-loop order [8]. That is, at 1-loop order, the counterterms vanish on mass-shell. However, when gravity is coupled to matter, the theory is non-renormalisable. Now, at 2-loop order, pure gravity has a UV divergence [8, 9, 10, 11]. Since infinitely many local counterterms would be required to eliminate the divergences, pure gravity is said to be a non-renormalisable theory. By virtue of being non-renormalisable, pure gravity, as given by the Einstein-Hilbert action, is not a quantum theory of gravity, but, rather, an effective field theory, valid at scales much less than the (reduced) Planck mass $M_P \simeq 2.4 \times 10^{18}\ GeV$.

[1] It is also possible for renormalisability to be established non-perturbatively [7].

Non-local theories provide a promising approach to quantising gravity. What we mean by the concept of *locality* is, schematically, that a particle is only affected by its neighbouring environment [12, 13]. Thus, in a non-local theory, the behaviour of a particle may be impinged on by particles far away from it and interactions take place in a finite region of space. Among many attempts to quantise gravity, *i.e.*, string theory [14, 15], loop quantum gravity [16, 17], causal set approach [18], it can be readily observed that *non-locality* is present in many quantum gravitational theories; for instance, strings and branes are often regarded as non-local objects [19]. In string field theory (SFT) [20, 21], non-locality also plays an important role, for example, in p-adic strings [22], zeta strings [23] and strings quantised on a random lattice [24]. One may wonder whether non-locality is an essential attribute of spacetime.

String theory (ST) [14, 15] is a very well known candidate for a complete theory of quantum gravity. In string theory, strings are taken to be the most fundamental objects in nature and the excitations of strings give rise to particles. Within the framework of string theory, there has been substantial progress in unifying all interactions, that is, the strong force, the electroweak force and gravitation. On the other hand, in supergravity (SUGRA) [25], where both bosonic and fermionic degrees of freedom are present, divergences are eliminated when computing Feynman loop integrals. At two-loop order, there are no UV divergences, which is a striking result when juxtaposed with the two-loop divergences present in GR. However, supersymmetric theories of gravity are beset by various other shortcomings.

In this thesis, we shall focus on *infinite derivative* theories, which are a subclass of non-local theories [1]. Infinite derivative gravitational theories contain an infinite series of higher-derivative terms, that is, terms containing more than two derivatives of the metric tensor. Recently, there has been great interest in infinite derivative gravitational theories as to addressing the Big Bang singularity problem [41, 42, 43, 44, 45, 46] and other cosmological applications [47, 48, 49, 50, 51, 52, 53, 54]. In particular, in [41], an infinite derivative gravitational action was considered and cosmological non-singular bouncing solutions were obtained,

[1] Regarding non-local theories of quantum gravity, one may consult [26, 27, 28, 29, 30, 31, 32, 33, 34, 35, 36, 37, 38, 39, 40].

thereby precluding Big Bang and Big Crunch. Consequently, in [42, 43], further progress was made in that direction and links to inflation were explored. Such an infinite derivative gravitational action can modify the Raychaudhuri equation [55], thereby yielding a non-singular bouncing cosmology without violating the null energy conditions. Moreover, in the case of microscopic black holes with mass much smaller than the Planck mass, singularities are avoided if one considers the Newtonian approximation where the gravitational potential is very weak [56].

In string theory literature, one can find infinite derivative actions of the following form (see Appendix A for the conventions and notations used in this thesis),

$$S = \int d^D x \left[\frac{1}{2} \phi \mathcal{K}(\Box) \phi - V_{\texttt{int}}(\phi) \right], \tag{1.1}$$

where the kinetic operator $\mathcal{K}(\Box)$ contains an infinite series of higher-derivative terms and $\Box$ is the covariant d'Alembertian operator given by $\Box = g^{\mu\nu}\nabla_\mu \nabla_\nu$. For stringy toy models based on p-adic numbers [22, 57, 58, 59] or random lattices [24, 60, 61, 62, 63], we find that $\mathcal{K}(\Box) = e^{-\Box/M^2}$. In SFT [20], we have $\mathcal{K}(\Box) = (\Box - m^2)e^{-\Box/M^2}$, where m^2 and M^2 are proportional to the string tension. Perturbatively, these theories do not contain *ghosts*, that is, fields whose kinetic energy is negative (one can see Appendix B for more details on ghosts). In contrast, let us consider a fourth-order scalar theory where $\mathcal{K}(\Box) = \Box(1 - \frac{\Box}{m^2})$. Then the propagator is

$$\Pi(-k^2) \sim \frac{m^2}{k^2(k^2 + m^2)} = \frac{1}{k^2} - \frac{1}{k^2 + m^2}. \tag{1.2}$$

We observe that there are two poles and, hence, two physical states, but the massive pole has negative residue, denoting the presence of a ghost. Therefore, the classical theory is unstable while the quantum theory is not unitary [27] (see Appendix C). On the other hand, when the kinetic term has the form of an exponential, which is an *entire function* [1] with no zeroes, no new states (ghosts, etc) are introduced [41]. Many infinite derivative theoretical models in different

[1] An entire function is a function that is analytic at each point on the finite complex plane [64].

contexts have been proposed [65, 66, 67, 68, 69, 70, 71, 72, 73, 74, 75, 76, 77, 78, 79, 80, 81, 82, 83].

In [84, 85], Stelle proposed a four-derivative, quadratic in curvature gravitational theory which is perturbatively renormalisable. The action proposed by Stelle is given by

$$S = \int d^4x\sqrt{-g}\left[\alpha R + \beta R^2 + \gamma R^{\mu\nu}R_{\mu\nu}\right] \tag{1.3}$$

and, for aptly chosen values of the coupling constants α, β, γ, the theory is renormalisable. However, for these values, the theory contains a ghost. Let us point out that we do not have to include $R^{\mu\nu\lambda\sigma}R_{\mu\nu\lambda\sigma}$ terms in (1.3) since the four-dimensional Gauss-Bonnet action,

$$S_{GB} = \int d^4x\sqrt{-g}\left[R^{\mu\nu\lambda\sigma}R_{\mu\nu\lambda\sigma} - 4R^{\mu\nu}R_{\mu\nu} + R^2\right], \tag{1.4}$$

is an Euler topological invariant. The spin-2 component of the modified propagator is schematically given by

$$\Pi = \Pi_{GR} - \frac{\mathcal{P}^2}{k^2 + m^2}, \tag{1.5}$$

where Π_{GR} is the graviton propagator in General Relativity and is defined as follows,

$$\Pi_{GR} = \frac{\mathcal{P}^2}{k^2} - \frac{1}{2k^2}\mathcal{P}^0_s; \tag{1.6}$$

$\mathcal{P}^2$ and $\mathcal{P}^0_s$ are the spin-2 and spin-0 projector operators, respectively [86, 87]. We observe that there is an additional pole in the spin-2 sector of the propagator, which comes with a negative residue. It can be easily deduced that there is a massive spin-2 ghost, which is called the *Weyl ghost*, resulting in violation of unitarity.

On the other hand, it should be stressed that $f(R)$ gravity, which is given by the action [88]

$$S = \frac{1}{2}\int d^4x\sqrt{-g}f(R), \tag{1.7}$$

where $f(R)$ is a function of the Ricci scalar, is ghost-free but is also non-renormalisable. One prominent example of $f(R)$ theories of gravity with applications in primordial inflation is the Starobinsky model [89],

$$S = \frac{1}{2}\int d^4x\sqrt{-g}\left[M_P^2 R + \alpha_0 R^2\right], \tag{1.8}$$

where α_0 is a constant.

In [86], a tensor Lagrangian devoid of ghosts was presented and relevant applications in gravity were discussed. Accordingly, in [41, 90, 91], attempts were made to construct ghost-free, infinite derivative gravitational theories which may be able to resolve spacetime singularities such as the ones present inside the black holes and at the Big Bang. To that end, it has recently been shown one can avoid ghosts in the context of infinite derivative gravitational theories [33, 34, 37, 38, 56, 87] [1]. Furthermore, in [29, 97], infinite derivative Lagrangians were considered and the super-renormalisability of the theories was demonstrated [2]. The interplay between unitarity and renormalisability is an important factor in the formulation of a successful theory of quantum gravity.

Infrared Freedom and Asymptotic Freedom

If the coupling constant in a theory is small, the theory can be treated perturbatively. If the coupling constant increases as the energy scale increases and vanishes at long distances, the theory is said to be *infrared free* [12]; for example, QED is an infrared free theory. On the contrary, if the coupling constant decreases as the energy scale increases and vanishes at short distances, the theory is said to be *asymptotically free* [12]; for instance, QCD is an asymptotically free theory.

A covariant, quadratic in curvature, asymptotically free gravitational theory, which is devoid of ghosts and tachyons around constant curvature backgrounds,

[1] One may also consult [27, 39, 40, 92, 93, 94, 95, 96] for a discussion of unitarity in non-local theories.

[2] In [26, 28, 29, 31, 32], the propagator goes as $k^{-2\gamma-4}$, where $\gamma \geq 2$, in the UV.

was derived in [56, 87]. The form of the action S, which is an extension of (1.3), is given by

$$S = S_{EH} + S_{UV}, \tag{1.9}$$

$$= \frac{1}{2}\int d^4x\sqrt{-g}\left[M_P^2 R + R\mathcal{F}_1(\bar{\Box})R + R_{\mu\nu}\mathcal{F}_2(\bar{\Box})R^{\mu\nu} + R_{\mu\nu\lambda\sigma}\mathcal{F}_3(\bar{\Box})R^{\mu\nu\lambda\sigma}\right], \tag{1.10}$$

where S_{EH} is the Einstein-Hilbert action, S_{UV} constitutes the non-local modifications of GR, M_P is the Planck mass, $\bar{\Box} \equiv \Box/M^2$ and M is the mass scale at which the non-local modifications become important. The $\mathcal{F}_i$'s are infinite-derivative functions of $\bar{\Box}$ and satisfy the constraint

$$2\mathcal{F}_1(\bar{\Box}) + \mathcal{F}_2(\bar{\Box}) + 2\mathcal{F}_3(\bar{\Box}) = 0 \tag{1.11}$$

around a Minkowski background so that the action is *ghost-free* and corresponds to a massless graviton [56, 87]. In particular, we can choose the graviton propagator to be modulated by the exponential of an *entire function*, $a(-k^2) = e^{k^2/M^2}$ [41],

$$\Pi(-k^2) = \frac{1}{k^2 a(-k^2)}\left(\mathcal{P}^2 - \frac{1}{2}\mathcal{P}_s^0\right) = \frac{1}{a(-k^2)}\Pi_{GR}. \tag{1.12}$$

Note that the exponential of an entire function [1] does not give rise to poles. For an exponential entire function, the propagator becomes exponentially suppressed in the UV (see also applications regarding Regge behaviour [63] and Hagedorn transition [66, 67, 68]), while the vertex factors are exponentially enhanced. The fact that the propagators and vertex factors have opposing momentum dependence is a key feature of gauge theories. Meanwhile, in the IR, one recovers the physical graviton propagator of GR. In addition, this asymptotically free theory

[1] Notice that any entire function without zeroes, a, can be written as the exponential of an analytic function: $a(-k^2) = e^{\gamma(-k^2)}$, where γ is an analytic function of $-k^2$. If γ is polynomial and, in momentum space, $\gamma(-k^2) > 0$ as $k^2 \to \infty$, the propagator will be even more convergent than the exponential case [56, 87]. A similar action was proposed in [26, 27, 28, 29, 30], where it was shown that $a(-k^2)$ being an *entire* function is a sufficient condition for the renormalisability of infinite derivative gravity. Similar results were obtained in [31, 32].

addresses the classical singularities present in GR [56, 98]. This is in clear contrast with GR and other finite-order higher-derivative theories of gravity. Moreover, the UV behaviour of the theory is ameliorated, leading to convergent Feynman diagrams [98, 99, 100, 101, 102]. One may consult Appendix D with respect to the quantised infinite derivative gravitational action.

Inspired by the infinite-derivative gravitational action given by (1.10), we formulated a scalar toy model in [100] that captures the essential features of the UV behaviour of the aforementioned infinite derivative gravitational action. The action of the scalar toy model is given by

$$S_{\texttt{scalar}} = S_{\texttt{free}} + S_{\texttt{int}}, \tag{1.13}$$

$$= \int d^4x \left[\frac{1}{2}\phi\Box a(\bar{\Box})\phi + \frac{1}{4M_P}\left(\phi\partial_\mu\phi\partial^\mu\phi + \phi\Box\phi a(\bar{\Box})\phi - \phi\partial_\mu\phi a(\bar{\Box})\partial^\mu\phi\right)\right], \tag{1.14}$$

where $S_{\texttt{free}}$ is given by the quadratic in ϕ term, $S_{\texttt{int}}$ is given by the cubic in ϕ terms and $a(\bar{\Box}) = e^{-\bar{\Box}} \equiv e^{-\Box/M^2}$. The equation of motion for the action given by (1.14) satisfies the shift-scaling symmetry $\phi \to (1+\epsilon)\phi+\epsilon$, where ϵ is infinitesimal. In this thesis, we shall mainly focus on the above infinite derivative scalar toy model and study its UV quantum behaviour [98, 99, 100, 101, 102]; one may consult Chapters 2 & 3 for more details.

Scattering Amplitudes

Evaluating scattering amplitudes [103] has long been of extremely high importance in theoretical high-energy particle physics. When analysing scattering diagrams, the behaviour of the corresponding cross sections is probably the most interesting aspect of the theory under consideration. If the cross section blows up at high energies, this implies that the theory is not physical and the ramifications for the viability of the theory are severe. For scalar field theories containing more than two derivatives of the scalar field, the cross section generically diverges when the external momenta become very large. As we shall see later on, this need not be the case for infinite derivative scalar field theories. By dressing

propagators and vertices, one can tame and, actually, eliminate the external momentum divergences arising when calculating the scattering matrix element and the cross section. This means that the relevant cross sections are finite, which is a comforting result.

In [99], the UV behaviour of scattering diagrams within the context of an infinite derivative scalar toy model was investigated and it was found that the external momentum dependence of the scattering diagrams is convergent for large external momenta. That was achieved by dressing the bare vertices of the scattering diagrams by considering renormalised propagator and vertex loop corrections to the bare vertices. As the loop order increases, the exponents in the dressed vertices decrease and eventually become negative at sufficiently high loop-order; one may consult Chapter 4 for more details. Finally it would be very interesting to replicate these results within the framework of the infinite derivative gravitational theory given by (1.10).

Hamiltonian Formalism

Hamiltonian analysis provides a useful theoretical framework within which the stability or instability of a theory can be investigated and the number of physical degrees of freedom can be computed. To that end, it is well known that Ostrogradsky's theorem [104, 105] can help determine the stability of higher-derivative gravitational theories. Let us expound on this statement.

Let us consider a Lagrangian density of the form

$$\mathcal{L} = \mathcal{L}(q, \dot{q}, \ddot{q}), \tag{1.15}$$

which is non-degenerate on $\ddot{q}$, *i.e.*, $\frac{\partial^2 \mathcal{L}}{\partial \ddot{q}^2} \neq 0$, where dots indicate derivatives with respect to some parameter $\bar{\lambda}$. Then the Euler-Lagrange equation is given by

$$\frac{\partial \mathcal{L}}{\partial q} - \frac{d}{dt}\frac{\partial \mathcal{L}}{\partial \dot{q}} + \frac{d^2}{dt^2}\frac{\partial \mathcal{L}}{\partial \ddot{q}} = 0. \tag{1.16}$$

Because of the non-degeneracy of the Lagrangian, the initial data $q_0, \dot{q}_0, \ddot{q}_0, \dddot{q}_0$

determine the solutions. Making the following definitions,

$$Q_1 = q, \qquad P_1 = \frac{\partial \mathcal{L}}{\partial \dot{q}} - \frac{d}{dt}\frac{\partial \mathcal{L}}{\partial \ddot{q}}, \tag{1.17}$$

$$Q_2 = \dot{q}, \qquad P_2 = \frac{\partial \mathcal{L}}{\partial \ddot{q}}, \tag{1.18}$$

we can write $\ddot{q}$ in terms of Q_1, Q_2 and P_2, that is, $\ddot{q} = f(Q_1, Q_2, P_2)$. Hence, the Hamiltonian density can be expressed as [105, 106]

$$\mathcal{H} = P_1 Q_1 + P_2 f(Q_1, Q_2, P_2) - \mathcal{L}(Q_1, Q_2, f). \tag{1.19}$$

Such a theory exhibits instabilities. When the vacuum decays into both positive and negative kinetic energy states, this is termed the *Ostrogradsky instability*.

Higher-derivative gravitational theories usually exhibit the Ostrogradsky instability [19], which is normally signified by the presence of ghosts arising as extra poles in the propagator. The four-derivative gravitational theory proposed by Stelle is one such example. Nonetheless, $f(R)$ gravitational theories, which are given by (1.7), can be rendered ghost-free since $\ddot{q}$ cannot be written in terms of Q_1, Q_2, P_2. Let us also point out that there exists a single additional scalar degree of freedom in the propagator of such theories.

The Ostrogradsky argument relies on having a highest "momentum" associated with the highest derivative in the theory in which the energy is seen to be linear, as opposed to quadratic. However, the infinite derivative gravitational theory given by (1.10) contains an infinite set of derivatives where no such highest momentum operator can be readily identified, nor are there any extra poles in the propagator which could correspond to new degrees of freedom, ghosts or otherwise. In [107], the Hamiltonian analysis of an infinite derivative gravitational theory was presented and it is the focus of Chapter 5.

Summary of Results

In this section, we present various results within the context of infinite derivative field theories and infinite derivative gravity, which are not the main focus of this

thesis.

Field Equations

In [108], the most general, generally covariant, quadratic in curvature, infinite derivative gravitational action was studied. The full non-linear field equations for the theory were derived. Moreover, the corresponding Bianchi identities were explicitly checked while the linearised field equations around Minkowski spacetime were obtained. The linearised field equations around de Sitter (dS) spacetime can also be attained in a similar fashion [13].

Newtonian Potential

In [56], the Newtonian potential around the weak field limit of the infinite derivative gravitational theory given by (1.10) was looked into. Making the choice $a(\bar{\Box}) = e^{-\bar{\Box}}$ yields the following Newtonian potential,

$$\Phi(r) = -\frac{\kappa m_g \text{Erf}\left(\frac{Mr}{2}\right)}{8\pi r}, \tag{1.20}$$

where m_g is the mass of the object generating the gravitational potential. As $r \to \infty$, Minkowski space is recovered. On the other hand, as $r \to 0$, the potential tends to a constant. Therefore, the behaviour of the Newtonian potential is non-singular at short distances, as compared to the behaviour of the Newtonian potential in GR as $r \to \infty$. One may consult Appendix E for more details on the derivation of the potential.

In [109], the Newtonian potential in an infinite derivative gravitational theory was analysed, for which $a(\bar{\Box}) = e^{\gamma(\bar{\Box})}$ and γ is an entire function, and, at large distances, the Newtonian potential was shown to decrease as $1/r$. At short distances, the potential was found to be non-singular.

In [110], an even more expansive class of infinite derivative gravitational theories was probed, for which the Newtonian potential is non-singular and oscillating, thereby permitting the defocusing of null rays and geodesic completeness. By

use of the Raychaudhuri equation, the conditions for past-completeness of null geodesic congruences were presented while the Newtonian potential for the infinite derivative gravitational theory remains non-singular. Moreover, a class of Newtonian potentials bearing a supplemental degree of freedom in the scalar sector of the propagator was investigated and the potential of GR is recovered at large distances.

Scale of Non-locality

In [111], an infinite derivative scalar field theory toy model was considered. The infinite derivative function in the toy model was chosen to be $e^{-\Box/M^2}$. The mass scale M ensures that the exponent $-\Box/M^2$ is dimensionless and is called the scale of non-locality. It was demonstrated that, for such a theory, one can derive an effective mass scale M_{eff} which can be computed by evaluating the relevant scattering amplitudes for systems of n particles. The effective mass scale M_{eff} was found to be proportional to the mass scale of non-locality M and was, for large n, inversely proportional to the square root of the number of incoming particles in the scattering diagram, that is, $M_{\text{eff}} \sim M/\sqrt{n}$. Hence, the effective mass scale associated with the scattering amplitude was found to decrease as the number of incoming particles in the scattering diagram increased. Since, by dimensional analysis, one can relate the effective mass scale M_{eff} to the effective length scale L_{eff}, *i.e.*, $[L_{\text{eff}}] = [M_{\text{eff}}]^{-1}$, the effective length scale of non-locality L_{eff} was found to increase as the number of incoming particles in the scattering diagram increased; one can see Appendix F for more details.

Generalised Boundary Term

In [112], the generalised Gibbons-Hawking-York (GHY) boundary term for the infinite derivative gravitational action given by (1.10) was explicitly computed. In order for the boundary term to be written down, coframe slicing within the Arnowitt-Deser-Misner (ADM) decomposition of spacetime in four dimensions was utilised. When $\Box \to 0$, or $M \to \infty$, the GHY term for the Einstein-Hilbert action is recovered, serving as a check for the correctness of the generalised GHY

term presented in [112]. One may consult Appendix G for more details on the derivation of this result.

Wald Entropy

In [113], the gravitational Wald entropy of a static spherically symmetric black hole solution within the context of the infinite derivative gravitational action given by (1.10) was computed. In the non-linear regime, it was found that there exist corrections to the area law for the entropy [1]. In the linear regime, the gravitational Wald entropy was found to be given solely by the area law insofar as the massless graviton is the only propagating degree of freedom.
In [114], the gravitational Wald entropy for the infinite derivative gravitational action given by (1.10) around an (A)dS metric was evaluated and the corresponding corrections to the entropy were written down explicitly. Furthermore, the gravitational entropy of a non-singular bouncing cosmology at the bounce point for an infinite derivative gravitational action was presented. Finally, the propagator for the infinite derivative gravitational action given by (1.10) around D-dimensional Minkowski space was derived. One can see Appendix H for a concise discussion of Wald entropy in infinite derivative gravitational theories.

Entropy of a Rotating Black Hole

In [115], the entropy of a rotating black hole for different modified theories of gravity (for instance, $f(R)$ theories of gravity, $f(R, R_{\mu\nu})$ theories of gravity, etc) was derived. Furthermore, the corrections to the area law for the entropy in the context of a rotating black hole were computed for a higher-derivative gravitational action consisting of the Ricci scalar, the Ricci tensor and covariant

[1] The area law for the entropy is given by

$$S_{Wald} = \frac{A_H}{4G_N^{(D)}}, \tag{1.21}$$

where A_H is the area of the event horizon and $G_N^{(D)}$ is Newton's gravitational constant in D dimensions.

derivatives acting on them.

Singularities

In [55, 116], the formulation of a singularity-free, infinite derivative theory of gravity was discussed. First, the definition of a singularity was presented while the Raychaudhuri equation was motivated and derived. Applications in cosmology were also outlined and the construction of non-singular bouncing cosmologies in the context of an infinite derivative theory of gravity was considered. Finally, the conditions for defocusing of null rays around Minkowski and de Sitter spacetimes were obtained within the framework of an infinite derivative gravitational theory [13].

Infrared Modifications

In [117], non-local modifications to GR in the infrared (IR) were investigated. The gravitational action considered in [117] contains an infinite power series of inverse d'Alembertian ($1/\Box$) operators. The full non-linear field equations were derived and the corresponding Bianchi identities were verified. The corrections to the Newtonian potentials were also evaluated. For a non-local model characterised by the exponential of the inverse d'Alembertian, it was found that the gravitational field weakens at large distances. Finally, one may consult [118] for relevant thermodynamic applications.

1.1 Organisation of thesis

The content of the thesis is organised as follows:

Chapter 2: In this chapter, an infinite derivative scalar field theory toy model, which is inspired by the infinite derivative gravitational action given by (1.10), is motivated and derived. The modified superficial degree of divergence for the toy model is computed and contrasted with the superficial degree of divergence for GR.

Chapter 3: The focus of this chapter is the evaluation of Feynman integrals corresponding to Feynman diagrams within the framework of the infinite derivative scalar toy model presented in Chapter 2. The Feynman integrals for 1-loop & 2-loop 2-point diagrams are explicitly computed. Moreover, the dressed propagator is derived and Feynman diagrams where the bare propagator has been replaced with the dressed one are studied. At the end, the UV finiteness of n-loop, N-point diagrams constructed out of lower-loop, N_i-point diagrams with respect to both internal loop momenta and external momenta is analysed and the renormalisability of the scalar field theory is extensively discussed.

Chapter 4: Scattering amplitudes and, correspondingly, cross sections are evaluated in this chapter. First, this analysis is performed for a finite order, higher derivative scalar toy model. Next, it is carried out for an infinite derivative scalar field theory toy model. Subsequently, it is implemented for the infinite derivative scalar toy model derived in Chapter 2. For each case, the behaviour of the cross section when the external momenta become large is investigated and compared to that for the other cases.

Chapter 5: Hamiltonian analysis for an infinite derivative gravitational (IDG) action containing only the Ricci scalar is performed in this chapter. At the beginning, primary/secondary and first-class/second-class constraints are defined and the formula for computing the relevant physical degrees of freedom is presented. Later on, this analysis is applied to an infinite derivative scalar field theory. Finally, the fundamentals of ADM formalism are outlined,

leading to the classification of the constraints for the IDG action and the computation of the physical degrees of freedom in various cases.

Chapter 2

Infinite derivative gravity and scalar toy model

In this chapter, starting from the infinite derivative gravitational action given by (1.10), we motivate and derive our infinite derivative scalar toy model.

2.1 Superficial degree of divergence for General Relativity

Let us consider metric perturbations around a Minkowski background,

$$g_{\mu\nu} = \eta_{\mu\nu} + h_{\mu\nu}. \tag{2.1}$$

In GR, the propagator goes as k^{-2} where k denotes momentum (see (1.6) for the graviton propagator in GR), while the vertex factors go as k^2. This is the compensating feature which is a hallmark of gauge theories. Moreover, in D-dimensional spacetime, each loop momentum integration comes with a $d^D k$ integration measure. The superficial degree of divergence of a Feynman diagram in

GR is therefore given by [84]

$$E = DL - 2I + 2V, \tag{2.2}$$

where D is the dimensionality of spacetime, L is the number of loops, V is the number of vertices and I is the number of internal propagators. Using the following topological relation,

$$L = 1 + I - V, \tag{2.3}$$

we get

$$E = (D-2)L + 2. \tag{2.4}$$

In four-dimensional spacetime ($D = 4$), we obtain

$$E = 2L + 2. \tag{2.5}$$

Thus, the superficial degree of divergence increases as the number of loops increases, which is why GR is said to be a non-renormalisable theory.

In Stelle's four-derivative gravitational theory [84] (see (1.3)), the graviton propagator goes as k^{-4}, while the vertices go as k^4, leading to a constant degree of divergence,

$$E = 4. \tag{2.6}$$

In other words, the degree of divergence does not increase as the loop-order increases which enabled Stelle to prove that such a theory is renormalisable. Unfortunately, such a theory also contains a Weyl ghost which makes the theory non-unitary. We shall follow a different approach where we will introduce an infinite series of higher-derivative operators in a way that does not introduce any new states, ghosts or otherwise. We shall see that the divergence counting will also be different as it will be based on the exponents rather than the degree of the polynomial momentum dependences.

2.2 Derivation of infinite derivative gravitational action

The most general, quadratic in curvature, generally covariant four-dimensional gravitational action can be written as follows [56, 87],

$$S = S_{EH} + S_{UV}, \tag{2.7}$$

$$S_{EH} = \frac{1}{2}\int d^4x\sqrt{-g}M_P^2 R, \tag{2.8}$$

$$S_{UV} = \frac{1}{2}\int d^4x\sqrt{-g}\left(R_{\mu_1\nu_1\lambda_1\sigma_1}\mathcal{O}^{\mu_1\nu_1\lambda_1\sigma_1}_{\mu_2\nu_2\lambda_2\sigma_2}R^{\mu_2\nu_2\lambda_2\sigma_2}\right), \tag{2.9}$$

where S_{EH} is the Einstein-Hilbert action and S_{UV} represents the ultraviolet modifications of GR. The operator $\mathcal{O}^{\mu_2\nu_2\lambda_2\sigma_2}_{\mu_1\nu_1\lambda_1\sigma_1}$ maintains general covariance.

Expanding (2.9), we can write (2.7) as follows,

$$\begin{aligned}
S = \int d^4x\frac{\sqrt{-g}}{2}\Big[&M_P^2R + R\mathcal{F}_1(\Box)R + R\mathcal{F}_2(\Box)\nabla_\nu\nabla_\mu R^{\mu\nu} + R_{\mu\nu}\mathcal{F}_3(\Box)R^{\mu\nu}\\
&+ R^\nu_\mu\mathcal{F}_4(\Box)\nabla_\nu\nabla_\lambda R^{\mu\lambda} + R^{\lambda\sigma}\mathcal{F}_5(\Box)\nabla_\mu\nabla_\sigma\nabla_\nu\nabla_\lambda R^{\mu\nu} + R\mathcal{F}_6(\Box)\nabla_\mu\nabla_\nu\nabla_\lambda\nabla_\sigma R^{\mu\nu\lambda\sigma}\\
&+ R_{\mu\lambda}\mathcal{F}_7(\Box)\nabla_\nu\nabla_\sigma R^{\mu\nu\lambda\sigma} + R^\rho_\lambda\mathcal{F}_8(\Box)\nabla_\mu\nabla_\sigma\nabla_\nu\nabla_\rho R^{\mu\nu\lambda\sigma}\\
&+ R^{\mu_1\nu_1}\mathcal{F}_9(\Box)\nabla_{\mu_1}\nabla_{\nu_1}\nabla_\mu\nabla_\nu\nabla_\lambda\nabla_\sigma R^{\mu\nu\lambda\sigma} + R_{\mu\nu\lambda\sigma}\mathcal{F}_{10}(\Box)R^{\mu\nu\lambda\sigma}\\
&+ R^\rho{}_{\mu\nu\lambda}\mathcal{F}_{11}(\Box)\nabla_\rho\nabla_\sigma R^{\mu\nu\lambda\sigma} + R_{\mu\rho_1\nu\sigma_1}\mathcal{F}_{12}(\Box)\nabla^{\rho_1}\nabla^{\sigma_1}\nabla_\rho\nabla_\sigma R^{\mu\rho\nu\sigma}\\
&+ R_\mu^{\nu_1\rho_1\sigma_1}\mathcal{F}_{13}(\Box)\nabla_{\rho_1}\nabla_{\sigma_1}\nabla_{\nu_1}\nabla_\nu\nabla_\lambda\nabla_\sigma R^{\mu\nu\lambda\sigma}\\
&+ R^{\mu_1\nu_1\rho_1\sigma_1}\mathcal{F}_{14}(\Box)\nabla_{\rho_1}\nabla_{\sigma_1}\nabla_{\nu_1}\nabla_{\mu_1}\nabla_\mu\nabla_\nu\nabla_\lambda\nabla_\sigma R^{\mu\nu\lambda\sigma}\Big],
\end{aligned} \tag{2.10}$$

where we have integrated by parts where appropriate. It should be noted that the $\mathcal{F}_i$'s are analytic functions of $\bar{\Box}$ ($\Box$ is the covariant d'Alembertian operator given by $\Box = g^{\mu\nu}\nabla_\mu\nabla_\nu$ while, around a Minkowski background, we have $\Box = \eta^{\mu\nu}\partial_\mu\partial_\nu$),

$$\mathcal{F}_i(\bar{\Box}) = \sum_{n=0}^{\infty} f_{i_n}\bar{\Box}^n, \tag{2.11}$$

where $\bar{\Box} \equiv \Box/M^2$ and M is the mass scale at which the non-local modifications

become important. Furthermore, the f_{i_n}'s in (2.11) are real coefficients.

Using the antisymmetric properties of the Riemann tensor,

$$R_{(\mu\nu)\rho\sigma} = R_{\mu\nu(\rho\sigma)} = 0, \tag{2.12}$$

and the Bianchi identity

$$\nabla_\alpha R^\mu_{\ \nu\beta\gamma} + \nabla_\beta R^\mu_{\ \nu\gamma\alpha} + \nabla_\gamma R^\mu_{\ \nu\alpha\beta} = 0. \tag{2.13}$$

we have that (2.10) reduces to

$$\begin{aligned} S = \int d^4x \frac{\sqrt{-g}}{2} \Big[& M_P^2 R + R\mathcal{F}_1(\Box)R + R_{\mu\nu}\mathcal{F}_3(\Box)R^{\mu\nu} + R\mathcal{F}_6(\Box)\nabla_\mu\nabla_\nu\nabla_\lambda\nabla_\sigma R^{\mu\nu\lambda\sigma} \\ & + R_{\mu\nu\lambda\sigma}\mathcal{F}_{10}(\Box)R^{\mu\nu\lambda\sigma} + R^{\nu_1\rho_1\sigma_1}_{\ \ \ \ \mu}\mathcal{F}_{13}(\Box)\nabla_{\rho_1}\nabla_{\sigma_1}\nabla_{\nu_1}\nabla_\nu\nabla_\lambda\nabla_\sigma R^{\mu\nu\lambda\sigma} \\ & + R^{\mu_1\nu_1\rho_1\sigma_1}\mathcal{F}_{14}(\Box)\nabla_{\rho_1}\nabla_{\sigma_1}\nabla_{\nu_1}\nabla_{\mu_1}\nabla_\mu\nabla_\nu\nabla_\lambda\nabla_\sigma R^{\mu\nu\lambda\sigma} \Big]. \end{aligned} \tag{2.14}$$

Since we are considering perturbations around Minkowski space, the covariant derivatives become partial derivatives and commute freely. For example, one has

$$R\mathcal{F}_6(\Box)\nabla_\mu\nabla_\nu\nabla_\lambda\nabla_\sigma R^{\mu\nu\lambda\sigma} \simeq \frac{1}{2}R\mathcal{F}_6(\Box)\nabla_\mu\nabla_\nu\nabla_\lambda\nabla_\sigma R^{\mu\nu\lambda\sigma} + \frac{1}{2}R\mathcal{F}_6(\Box)\nabla_\mu\nabla_\nu\nabla_\lambda\nabla_\sigma R^{\mu\nu\lambda\sigma}. \tag{2.15}$$

Commuting covariant derivatives, we obtain

$$R\mathcal{F}_6(\Box)\nabla_\mu\nabla_\nu\nabla_\lambda\nabla_\sigma R^{\mu\nu\lambda\sigma} \simeq \frac{1}{2}R\mathcal{F}_6(\Box)\nabla_\nu\nabla_\mu\nabla_\lambda\nabla_\sigma R^{\mu\nu\lambda\sigma} + \frac{1}{2}R\mathcal{F}_6(\Box)\nabla_\mu\nabla_\nu\nabla_\lambda\nabla_\sigma R^{\mu\nu\lambda\sigma}, \tag{2.16}$$

where two expressions are defined to be equivalent (the equivalence is denoted by the sign "$\simeq$") if they differ by terms of third (or higher) order in products of the Riemann tensor. If we relabel the indices, we get

$$R\mathcal{F}_6(\Box)\nabla_\mu\nabla_\nu\nabla_\lambda\nabla_\sigma R^{\mu\nu\lambda\sigma} \simeq R\mathcal{F}_6(\Box)\nabla_\mu\nabla_\nu\nabla_\lambda\nabla_\sigma R^{(\mu\nu)\lambda\sigma} \simeq 0, \tag{2.17}$$

which vanishes due to the antisymmetric properties of the Riemann tensor which are given by (2.12).

Therefore, the "simplest" infinite derivative gravitational action that can modify the propagator of the graviton without introducing any new states is given by [56, 87]

$$S = S_{EH} + S_{UV}, \tag{2.18}$$

$$S_{EH} = \frac{1}{2}\int d^4x\sqrt{-g}M_P^2 R, \tag{2.19}$$

$$S_{UV} = \frac{1}{2}\int d^4x\sqrt{-g}\left[R\mathcal{F}_1(\bar{\Box})R + R_{\mu\nu}\mathcal{F}_2(\bar{\Box})R^{\mu\nu} + R_{\mu\nu\lambda\sigma}\mathcal{F}_3(\bar{\Box})R^{\mu\nu\lambda\sigma}\right]. \tag{2.20}$$

2.3 Propagator for infinite derivative gravitational action

If we consider metric perturbations around Minkowski space, $g_{\mu\nu} = \eta_{\mu\nu} + h_{\mu\nu}$, then the $\mathcal{O}(h^2)$ part of the following D-dimensional gravitational action (which is a generalisation of the gravitational action given by (2.18)-(2.20)),

$$S = \frac{1}{2}\int d^Dx\sqrt{-g}\left[M_P^2 R + R\mathcal{F}_1(\bar{\Box})R + R_{\mu\nu}\mathcal{F}_2(\bar{\Box})R^{\mu\nu} + R_{\mu\nu\lambda\sigma}\mathcal{F}_3(\bar{\Box})R^{\mu\nu\lambda\sigma}\right], \tag{2.21}$$

can be written as

$$S^{(2)} = \frac{1}{32\pi G_N^{(D)}}\int d^Dx\left[\frac{1}{2}h_{\mu\nu}\Box a(\bar{\Box})h^{\mu\nu} + h^\sigma_\mu b(\bar{\Box})\partial_\sigma\partial_\nu h^{\mu\nu}\right.$$
$$\left. + hc(\bar{\Box})\partial_\mu\partial_\nu h^{\mu\nu} + \frac{1}{2}h\Box d(\bar{\Box})h + h^{\lambda\sigma}\frac{f(\bar{\Box})}{2\Box}\partial_\sigma\partial_\lambda\partial_\mu\partial_\nu h^{\mu\nu}\right], \tag{2.22}$$

where $G_N^{(D)}$ is Newton's gravitational constant in D-dimensional spacetime and

$$R\mathcal{F}_1(\bar{\Box})R = \mathcal{F}_1(\bar{\Box})\left[h\Box^2 h + h^{\lambda\sigma}\partial_\sigma\partial_\lambda\partial_\mu\partial_\nu h^{\mu\nu} - 2h\Box\partial_\mu\partial_\nu h^{\mu\nu}\right], \tag{2.23}$$

$$\begin{aligned} R_{\mu\nu}\mathcal{F}_2(\bar{\Box})R^{\mu\nu} = \mathcal{F}_2(\bar{\Box})\Bigg[&\frac{1}{4}h\Box^2 h + \frac{1}{4}h_{\mu\nu}\Box^2 h^{\mu\nu} - \frac{1}{2}h^\sigma_\mu\Box\partial_\sigma\partial_\nu h^{\mu\nu} - \frac{1}{2}h\Box\partial_\mu\partial_\nu h^{\mu\nu} \\ &+ \frac{1}{2}h^{\lambda\sigma}\partial_\sigma\partial_\lambda\partial_\mu\partial_\nu h^{\mu\nu}\Bigg], \end{aligned} \tag{2.24}$$

$$R_{\mu\nu\lambda\sigma}\mathcal{F}_3(\bar{\Box})R^{\mu\nu\lambda\sigma} = \mathcal{F}_3(\bar{\Box})\left[h_{\mu\nu}\Box^2 h^{\mu\nu} - 2h^\sigma_\mu\Box\partial_\sigma\partial_\nu h^{\mu\nu} + h^{\lambda\sigma}\partial_\sigma\partial_\lambda\partial_\mu\partial_\nu h^{\mu\nu}\right]. \tag{2.25}$$

Hence, $a(\bar{\Box})$, $b(\bar{\Box})$, $c(\bar{\Box})$, $d(\bar{\Box})$ and $f(\bar{\Box})$ are as follows,

$$a(\bar{\Box}) = 1 + M_P^{-2}\left(\mathcal{F}_2(\bar{\Box})\Box + 4\mathcal{F}_3(\bar{\Box})\Box\right), \tag{2.26}$$

$$b(\bar{\Box}) = -1 - M_P^{-2}\left(\mathcal{F}_2(\bar{\Box})\Box + 4\mathcal{F}_3(\bar{\Box})\Box\right), \tag{2.27}$$

$$c(\bar{\Box}) = 1 - M_P^{-2}\left(4\mathcal{F}_1(\bar{\Box})\Box + \mathcal{F}_2(\bar{\Box})\Box\right), \tag{2.28}$$

$$d(\bar{\Box}) = -1 + M_P^{-2}\left(4\mathcal{F}_1(\bar{\Box})\Box + \mathcal{F}_2(\bar{\Box})\Box\right), \tag{2.29}$$

$$f(\bar{\Box}) = 2M_P^{-2}\left(2\mathcal{F}_1(\bar{\Box})\Box + \mathcal{F}_2(\bar{\Box})\Box + 2\mathcal{F}_3(\bar{\Box})\Box\right). \tag{2.30}$$

We observe that

$$a(\bar{\Box}) + b(\bar{\Box}) = 0, \tag{2.31}$$

$$c(\bar{\Box}) + d(\bar{\Box}) = 0, \tag{2.32}$$

$$b(\bar{\Box}) + c(\bar{\Box}) + f(\bar{\Box}) = 0. \tag{2.33}$$

The field equations are as follows,

$$\begin{aligned} -\kappa T_{\mu\nu} = \frac{1}{2}\Bigg[&a(\Box)\Box h_{\mu\nu} + b(\Box)\partial_\sigma(\partial_\mu h^\sigma_\nu + \partial_\nu h^\sigma_\mu) + c(\Box)\left(\partial_\nu\partial_\mu h + \eta_{\mu\nu}\partial_\sigma\partial_\tau h^{\sigma\tau}\right) \\ &+ d(\Box)\eta_{\mu\nu}\Box h + \frac{f(\Box)}{\Box}\partial_\mu\partial_\nu\partial_\sigma\partial_\tau h^{\sigma\tau}\Bigg], \end{aligned} \tag{2.34}$$

where $\kappa = 8\pi G_N^{(D)} = M_P^{-2}$ and $T_{\mu\nu}$ is the energy-momentum tensor. Employing the generalised Bianchi identity due to diffeomorphism invariance, $\nabla_\mu T^\mu_\nu = 0$, we

obtain

$$(c+d)\,\Box\partial_\nu h + (a+b)\,\Box\partial_\mu h^\mu_\nu + (b+c+f)\,\partial_\nu\partial_\alpha\partial_\mu h^{\alpha\mu} = 0. \tag{2.35}$$

We observe that (2.31)-(2.33) follow from (2.35).

One can express the field equations in terms of the inverse propagator $\Pi^{-1\sigma\tau}_{\mu\nu}$,

$$\Pi^{-1\rho\sigma}_{\mu\nu} h_{\rho\sigma} = \kappa T_{\mu\nu}, \tag{2.36}$$

Now, let us write down the spin projector operators in D-dimensional Minkowski space [86, 87, 114]:

$$\mathcal{P}^2_{\mu\nu\rho\sigma} = \frac{1}{2}(\theta_{\mu\rho}\theta_{\nu\sigma} + \theta_{\mu\sigma}\theta_{\nu\rho}) - \frac{1}{D-1}\theta_{\mu\nu}\theta_{\rho\sigma}, \tag{2.37}$$

$$\mathcal{P}^1_{\mu\nu\rho\sigma} = \frac{1}{2}(\theta_{\mu\rho}\omega_{\nu\sigma} + \theta_{\mu\sigma}\omega_{\nu\rho} + \theta_{\nu\rho}\omega_{\mu\sigma} + \theta_{\nu\sigma}\omega_{\mu\rho}), \tag{2.38}$$

$$(\mathcal{P}^0_s)_{\mu\nu\rho\sigma} = \frac{1}{D-1}\theta_{\mu\nu}\theta_{\rho\sigma}, \qquad (\mathcal{P}^0_w)_{\mu\nu\rho\sigma} = \omega_{\mu\nu}\omega_{\rho\sigma}, \tag{2.39}$$

$$(\mathcal{P}^0_{sw})_{\mu\nu\rho\sigma} = \frac{1}{\sqrt{D-1}}\theta_{\mu\nu}\omega_{\rho\sigma}, \qquad (\mathcal{P}^0_{ws})_{\mu\nu\rho\sigma} = \frac{1}{\sqrt{D-1}}\omega_{\mu\nu}\theta_{\rho\sigma}, \tag{2.40}$$

where

$$\theta_{\mu\nu} = \eta_{\mu\nu} - \frac{k_\mu k_\nu}{k^2} \quad \text{and} \quad \omega_{\mu\nu} = \frac{k_\mu k_\nu}{k^2}. \tag{2.41}$$

One may verify that

$$\eta_{\mu\nu} = \theta_{\mu\nu} + \omega_{\mu\nu}. \tag{2.42}$$

Going to momentum space ($\partial_\mu \to ik_\mu$ & $\Box \to -k^2$ on a flat background), we

obtain

$$\begin{aligned}
a(\Box)h_{\mu\nu} &\to\ a(-k^2)\left[\mathcal{P}^2+\mathcal{P}^1+\mathcal{P}^0_s+\mathcal{P}^0_w\right]_{\mu\nu}{}^{\rho\sigma}h_{\rho\sigma},\\
b(\Box)\partial_\sigma\partial_{(\nu}h^\sigma_{\mu)} &\to -b(-k^2)k^2\left[\mathcal{P}^1+2\mathcal{P}^0_w\right]_{\mu\nu}{}^{\rho\sigma}h_{\rho\sigma},\\
c(\Box)(\eta_{\mu\nu}\partial_\rho\partial_\sigma h^{\rho\sigma}+\partial_\mu\partial_\nu h) &\to\ -c(-k^2)k^2\left[2\mathcal{P}^0_w+\sqrt{D-1}\left(\mathcal{P}^0_{sw}+\mathcal{P}^0_{ws}\right)\right]_{\mu\nu}{}^{\rho\sigma}h_{\rho\sigma},\\
\eta_{\mu\nu}d(\Box)h &\to\ d(-k^2)\left[(D-1)\mathcal{P}^0_s+\mathcal{P}^0_w+\sqrt{D-1}\left(\mathcal{P}^0_{sw}+\mathcal{P}^0_{ws}\right)\right]_{\mu\nu}{}^{\rho\sigma}h_{\rho\sigma},\\
f(\Box)\partial^\sigma\partial^\rho\partial_\mu\partial_\nu h_{\rho\sigma} &\to\ f(-k^2)k^4(\mathcal{P}^0_w)_{\mu\nu}{}^{\rho\sigma}h_{\rho\sigma}.
\end{aligned}\tag{2.43}$$

We observe that the multiplets $\mathcal{P}^2,\mathcal{P}^1,\mathcal{P}^0_s,\mathcal{P}^0_w$ satisfy the following relation,

$$(\mathcal{P}^2+\mathcal{P}^1+\mathcal{P}^0_s+\mathcal{P}^0_w)_{\mu\nu\rho\sigma}=\frac{1}{2}(\eta_{\nu\rho}\eta_{\mu\sigma}+\eta_{\nu\sigma}\eta_{\mu\rho}).\tag{2.44}$$

Using (2.40), (2.41) and (2.44), we can express the inverse propagator (2.36) in terms of the spin projector operators $\mathcal{P}^i$, $i=1.\ldots,6$, which are given by (2.37)-(2.40):

$$\begin{aligned}
\Pi^{-1\rho\sigma}_{\mu\nu}h_{\rho\sigma}&=\sum_{i=1}^{6}C_i\mathcal{P}^i_{\mu\nu}{}^{\rho\sigma}h_{\rho\sigma}\\
&=\kappa(\mathcal{P}^2+\mathcal{P}^1+\mathcal{P}^0_s+\mathcal{P}^0_w)_{\mu\nu}{}^{\rho\sigma}T_{\rho\sigma}\\
&=\frac{1}{2}\kappa(\delta^\rho_\nu\delta^\sigma_\mu+\delta^\sigma_\nu\delta^\rho_\mu)T_{\rho\sigma}\\
&=\kappa T_{\mu\nu},
\end{aligned}\tag{2.45}$$

where the coefficients C_i are functions of k^2. Thus, (2.43) yields

$$\begin{aligned}
ak^2\mathcal{P}^2_{\mu\nu}{}^{\rho\sigma}h_{\rho\sigma}&=\kappa\mathcal{P}^2_{\mu\nu}{}^{\rho\sigma}T_{\rho\sigma},\\
(a+b)k^2\mathcal{P}^1_{\mu\nu}{}^{\rho\sigma}h_{\rho\sigma}&=\kappa\mathcal{P}^1_{\mu\nu}{}^{\rho\sigma}T_{\rho\sigma},\\
\left[(a+(D-1)d)k^2\mathcal{P}^0_s+(c+d)k^2\sqrt{D-1}\mathcal{P}^0_{sw}\right]_{\mu\nu}{}^{\rho\sigma}h_{\rho\sigma}&=\kappa(\mathcal{P}^0_s)_{\mu\nu}{}^{\rho\sigma}T_{\rho\sigma},\\
\left[(c+d)k^2\sqrt{D-1}\mathcal{P}^0_{ws}+(a+2b+2c+d+f)k^2\mathcal{P}^0_w\right]_{\mu\nu}{}^{\rho\sigma}h_{\rho\sigma}&=\kappa(\mathcal{P}^0_w)_{\mu\nu}{}^{\rho\sigma}T_{\rho\sigma}.
\end{aligned}\tag{2.46}$$

Consequently,

$$\begin{aligned}
\mathcal{P}^2{}_{\mu\nu}{}^{\rho\sigma} h_{\rho\sigma} &= \kappa \left(\frac{\mathcal{P}^2}{ak^2}\right)_{\mu\nu}{}^{\rho\sigma} T_{\rho\sigma}, \\
\mathcal{P}^1{}_{\mu\nu}{}^{\rho\sigma} T_{\rho\sigma} &= 0, \\
(\mathcal{P}^0_s)_{\mu\nu}{}^{\rho\sigma} h_{\rho\sigma} &= \kappa \frac{(\mathcal{P}_s)^0{}_{\mu\nu}{}^{\rho\sigma}}{(a-(D-1)c)k^2} T_{\rho\sigma}, \\
\kappa(\mathcal{P}^0_w)_{\mu\nu}{}^{\rho\sigma} T_{\rho\sigma} &= 0.
\end{aligned} \tag{2.47}$$

Hence, the D-dimensional propagator around Minkowski space is (the indices on the spin projector operators are suppressed)

$$\Pi^{(D)}(-k^2) = \frac{\mathcal{P}^2}{k^2 a(-k^2)} + \frac{\mathcal{P}^0_s}{k^2(a(-k^2)-(D-1)c(-k^2))}. \tag{2.48}$$

Therefore, the propagator in four dimensions ($D=4$) is given by [56, 87]

$$\Pi(-k^2) = \frac{\mathcal{P}^2}{k^2 a(-k^2)} + \frac{\mathcal{P}^0_s}{k^2\left(a(-k^2)-3c(-k^2)\right)}. \tag{2.49}$$

We want the scalar sector of (2.49) not to have any ghosts other than the benign ghost of GR, *i.e.*, the $k^2=0$ pole.

As a result, $a-3c$ in (2.49) can have at most one root [1]. Thus, $c(\bar{\Box})$ has to

[1]Suppose that you have a scalar propagator of the form $\Pi(-k^2) \sim 1/\bar{a}(-k^2)$ and that $\bar{a}$ is a power series with finitely many terms [41]. Therefore, $\bar{a}$ can be written as follows,

$$\bar{a}(-k^2) \sim (k^2+m_1^2)(k^2+m_2^2)\dots(k^2+m_n^2). \tag{2.50}$$

In order to avoid tachyons, one should have $m_i^2 > 0$. If there are at least two distinct poles (for instance, $m_1 \neq m_2$), then at least one of them is ghost-like since one of these poles shall have a negative residue.

To illustrate that, let us consider two adjacent poles, $k^2=-m_1^2$ and $k^2=-m_2^2$, where $m_1^2 < m_2^2$. Then we have

$$\bar{a}(-k^2) = (k^2+m_1^2)(k^2+m_2^2)\bar{\bar{a}}(-k^2). \tag{2.51}$$

Since the poles are adjacent, there are no more roots of $\bar{\bar{a}}(-k^2)$ in the range $-m_2^2 < k^2 < -m_1^2$. Hence, the sign of $\bar{\bar{a}}(-k^2)$ stays the same in this range, implying that the residues at $k^2=-m_1^2$ and $k^2=-m_2^2$ have different signs. Thus, one of the poles must be ghost-like.

be of the form

$$c(\bar{\Box}) = \frac{a(\bar{\Box})}{3}\left[1 + 2\left(1 - \frac{\Box}{m^2}\right)\tilde{c}(\bar{\Box})\right], \tag{2.52}$$

where $\tilde{c}(\bar{\Box})$ must be an entire function having no zeroes. Then, (2.49) becomes

$$\Pi(-k^2) = \frac{1}{a(-k^2)}\left[\frac{\mathcal{P}^2}{k^2} - \frac{1}{2\tilde{c}(-k^2)}\left(\frac{\mathcal{P}_s^0}{k^2} - \frac{\mathcal{P}_s^0}{k^2+m^2}\right)\right]. \tag{2.53}$$

To avoid tachyons, one should have $m^2 > 0$.

Choosing $f(\bar{\Box}) = 0$ implies $a(\bar{\Box}) = c(\bar{\Box})$, yielding the constraint

$$2\mathcal{F}_1(\bar{\Box}) + \mathcal{F}_2(\bar{\Box}) + 2\mathcal{F}_3(\bar{\Box}) = 0. \tag{2.54}$$

Moreover, (2.49) reduces to [56, 87]

$$\Pi(-k^2) = \frac{1}{a(-k^2)}\left(\frac{\mathcal{P}^2}{k^2} - \frac{\mathcal{P}_s^0}{2k^2}\right) = \frac{1}{a(-k^2)}\Pi_{GR}. \tag{2.55}$$

We choose $a(\bar{\Box})$ to be an *entire function* having no zeroes, thereby ensuring that no new propagating degrees of freedom are introduced. In the infrared (IR), that is, as $k^2 \to 0$, we have that $a(0) = 1$, so we recover the physical graviton propagator in GR:

$$\lim_{k^2\to 0}\Pi(-k^2) = \frac{\mathcal{P}^2}{k^2} - \frac{\mathcal{P}_s^0}{2k^2}. \tag{2.56}$$

2.4 Motivating infinite derivative scalar toy model

It is well known that the field equations of General Relativity exhibit a global scaling symmetry,

$$g_{\mu\nu} \to \lambda g_{\mu\nu}. \tag{2.57}$$

When we expand the metric around the Minkowski vacuum given by (2.1), the scaling symmetry translates to a symmetry for $h_{\mu\nu}$, whose infinitesimal version is given by

$$h_{\mu\nu} \to (1+\epsilon)h_{\mu\nu} + \epsilon\eta_{\mu\nu}, \tag{2.58}$$

where ϵ is infinitesimal. While we do not expect the scaling symmetry to be an unbroken fundamental symmetry of nature, the symmetry serves a rather useful purpose for us. It relates the free and interaction terms just like gauge symmetries do. Thus, we are going to use this combination of shift and scaling symmetry,

$$\phi \to (1+\epsilon)\phi + \epsilon, \tag{2.59}$$

to arrive at a scalar *toy model* whose propagator and vertices preserve the compensating nature found in infinite derivative gravity. Although this symmetry manifests itself only at the level of classical equations of motion, it will allow us to incorporate the compensating feature of exponential suppression and enhancement in propagators and interactions, respectively, which arises in infinite derivative gravity. Inspired by the discussion in the previous section, we will now consider a scalar *toy model* with a free action motivated by string field theory,

$$S_{\texttt{free}} = \frac{1}{2}\int d^4x \, \left(\phi \Box a(\bar{\Box})\phi\right), \tag{2.60}$$

where we are going to make the following choice [56, 87],

$$a(\bar{\Box}) = e^{-\bar{\Box}}. \tag{2.61}$$

In general, one is free to choose any entire function, while keeping in mind that $a(-k^2) \to 1$ as $k^2 \to 0$ so that the physical graviton propagator is recovered in the IR. It should be pointed out that the sign of the exponent in $a(\bar{\Box})$ is important in order to recover the correct Newtonian potential as shown in Refs. [56, 87] [1].

[1] If we had chosen $a(\bar{\Box})$ to be

$$a(\bar{\Box}) = e^{\bar{\Box}}, \tag{2.62}$$

where $M^2 > 0$, then we can perform the loop integrals for $a(\bar{\Box}) = e^{-\bar{\Box}}$, assuming $M^2 > 0$, and then analytically continue to $M^2 < 0$. Hence, the Newtonian potentials $\Phi(r)$ & $\Psi(r)$ would be given by

$$\Psi(r) = \Phi(r) = \frac{2im\pi^2}{M_p^2 r}\text{Erfi}\left(\frac{Mr}{2}\right), \tag{2.63}$$

where

$$\text{Erfi}(z) = \frac{\text{Erf}(iz)}{i} \tag{2.64}$$

2.5 Deriving infinite derivative scalar toy model

Now if we compute the $\mathcal{O}(h^3)$ part of the Einstein-Hilbert action given by (2.19), we obtain the following type of term:

$$h\partial_\mu h\partial^\mu h.$$

So let us compute the $\mathcal{O}(h^3)$ part of (2.20), keeping in mind that $\sqrt{-g} = 1 + \frac{1}{2}h + \frac{1}{8}h^2 - \frac{1}{4}h^\mu_\nu h^\nu_\mu + \mathcal{O}(h^3)$, where $h = h^\mu_\mu = \eta^{\mu\nu}h_{\mu\nu}$.

We shall need the following relation for the double sums appearing in the last two lines of (2.66):

$$T\delta(\bar{\Box}^n)S = \sum_{m=0}^{n-1} \bar{\Box}^m T\delta(\bar{\Box})\bar{\Box}^{n-m-1}S, \tag{2.65}$$

where $n \geq 1$. $\delta\left(\bar{\Box}\right)$ indicates the variation of the $\bar{\Box}$ operator and $\delta\left(\bar{\Box}^n\right)$ indicates the variation of the $\bar{\Box}^n$ operator. S and T are tensors constructed out of the Riemann curvatures and the metric.

Then, by applying integration by parts where appropriate, we obtain

$$\begin{aligned}
S^{(3)}_{UV} = {} & \frac{1}{2}\int d^4x\ \frac{1}{2}h\left[R^{(1)}\mathcal{F}_1(\bar{\Box})R^{(1)} + R^{(1)}_{\mu\nu}\mathcal{F}_2(\bar{\Box})R^{(1)\mu\nu} + R^{(1)}_{\mu\nu\lambda\sigma}\mathcal{F}_3(\bar{\Box})R^{(1)\mu\nu\lambda\sigma}\right] \\
& + \frac{1}{2}\int d^4x\left[2R^{(2)}\mathcal{F}_1(\bar{\Box})R^{(1)} + R^{(1)}_{\mu\nu}\mathcal{F}_2(\bar{\Box})R^{(2)\mu\nu} + R^{(2)}_{\mu\nu}\mathcal{F}_2(\bar{\Box})R^{(1)\mu\nu}\right. \\
& \left. + R^{(1)}_{\mu\nu\lambda\sigma}\mathcal{F}_3(\bar{\Box})R^{(2)\mu\nu\lambda\sigma} + R^{(2)}_{\mu\nu\lambda\sigma}\mathcal{F}_3(\bar{\Box})R^{(1)\mu\nu\lambda\sigma}\right] \\
& + \frac{1}{2}\sum_{n=1}^{\infty}\sum_{m=0}^{n-1}\int d^4x\left[f_{1_n}\bar{\Box}^m R^{(1)}\delta(\bar{\Box})\bar{\Box}^{n-m-1}R^{(1)} + f_{2_n}\bar{\Box}^m R^{(1)}_{\mu\nu}\delta(\bar{\Box})\bar{\Box}^{n-m-1}R^{(1)\mu\nu}\right. \\
& \left. + f_{3_n}\bar{\Box}^m R^{(1)}_{\mu\nu\lambda\sigma}\delta(\bar{\Box})\bar{\Box}^{n-m-1}R^{(1)\mu\nu\lambda\sigma}\right],
\end{aligned} \tag{2.66}$$

where $S^{(3)}_{UV}$ is the $\mathcal{O}(h^3)$ part of S_{UV} given in (2.9), $R^{(1)}$ is the $\mathcal{O}(h)$ part of the Ricci scalar R, $R^{(1)}_{\mu\nu}$ is the $\mathcal{O}(h)$ part of the Ricci tensor $R_{\mu\nu}$, $R^{(1)}_{\mu\nu\lambda\sigma}$ is the $\mathcal{O}(h)$

is the imaginary error function, admitting real values for real z. In that case, the Newtonian potential is purely imaginary, signifying an unphysical theory.

part of the Riemann tensor $R_{\mu\nu\lambda\sigma}$, $R^{(2)}$ is the $\mathcal{O}(h^2)$ part of the Ricci scalar R, $R^{(2)}_{\mu\nu}$ is the $\mathcal{O}(h^2)$ part of the Ricci tensor $R_{\mu\nu}$ and $R^{(2)}_{\mu\nu\lambda\sigma}$ is the $\mathcal{O}(h^2)$ part of the Riemann tensor $R_{\mu\nu\lambda\sigma}$. We have that $R^{\rho}{}_{\sigma\mu\nu} = \partial_\mu\Gamma^\rho_{\nu\sigma} - \partial_\nu\Gamma^\rho_{\mu\sigma} + \Gamma^\rho_{\mu\lambda}\Gamma^\lambda_{\nu\sigma} - \Gamma^\rho_{\nu\lambda}\Gamma^\lambda_{\mu\sigma}$. Moreover, $R_{\mu\nu} = R^{\sigma}{}_{\mu\sigma\nu}$ and $R = g^{\mu\nu}R_{\mu\nu}$. When we lower or raise an index in the Riemann tensors, that is always done with the use of $g_{\mu\nu} = \eta_{\mu\nu} + h_{\mu\nu}$ and $g^{\mu\nu} = \eta^{\mu\nu} - h^{\mu\nu} + \dots$ respectively. For instance, $R^{(2)\mu\nu} = \eta^{\mu\rho}\eta^{\nu\sigma}R^{(2)}_{\rho\sigma} - 2\eta^{\mu\rho}h^{\nu\sigma}R^{(1)}_{\rho\sigma}$ and $R^{(2)} = \eta^{\mu\nu}R^{(2)}_{\mu\nu} - h^{\mu\nu}R^{(1)}_{\mu\nu}$. Let us mention that

$$R^{(1)}_{\mu\nu\lambda\sigma} = \frac{1}{2}\left(\partial_\nu\partial_\lambda h_{\mu\sigma} + \partial_\mu\partial_\sigma h_{\nu\lambda} - \partial_\mu\partial_\lambda h_{\nu\sigma} - \partial_\nu\partial_\sigma h_{\mu\lambda}\right), \tag{2.67}$$

$$R^{(1)}_{\mu\nu} = \frac{1}{2}\left(\partial_\sigma\partial_\mu h^\sigma_\nu + \partial_\nu\partial_\sigma h^\sigma_\mu - \partial_\mu\partial_\nu h - \Box h_{\mu\nu}\right), \tag{2.68}$$

$$R^{(1)} = \partial_\mu\partial_\nu h^{\mu\nu} - \Box h. \tag{2.69}$$

Following the same method, we can derive the $\mathcal{O}(h^2)$ expressions for the Riemann tensors.

The terms involving double sums give rise to technical complications when evaluating the Feynman loop integrals. While several $\mathcal{F}_i$'s can satisfy (2.54), we make the following choice,

$$a(\bar{\Box}) = e^{-\bar{\Box}} \quad \& \quad \mathcal{F}_3(\bar{\Box}) = 0 \Rightarrow \mathcal{F}_1(\bar{\Box}) = -\frac{M_P^2}{2}\frac{e^{-\bar{\Box}} - 1}{\Box} = -\frac{\mathcal{F}_2(\bar{\Box})}{2}, \tag{2.70}$$

$a(\bar{\Box})$ having been defined in (2.26). Hence, we obtain a ghost-free infinite derivative gravitational action [56, 87],

$$S = \frac{M_P^2}{2}\int d^4x\sqrt{-g}\left\{R - \frac{1}{2}R\left[\frac{e^{-\bar{\Box}} - 1}{\Box}\right]R + R_{\mu\nu}\left[\frac{e^{-\bar{\Box}} - 1}{\Box}\right]R^{\mu\nu}\right\}. \tag{2.71}$$

Making these assumptions and enforcing a conformal flatness condition, $h_{\mu\nu} = \Omega^2(x)\,\eta_{\mu\nu}$, where $\Omega(x)$ is a smooth, strictly positive function ($\Omega^2 = h/4$ in four-dimensional spacetime) so as to get scalar-type gravitational terms, we obtain

the following types of $\mathcal{O}(h^3)$ terms:

$$\partial_\mu h \partial_\nu h \left(\frac{a(\bar{\Box})-1}{\Box}\right)\partial^\mu\partial^\nu h, \quad \partial_\rho h \partial^\rho h \left(\frac{a(\bar{\Box})-1}{\Box}\right)\Box h,$$
$$h\partial_\mu\partial_\nu h \left(\frac{a(\bar{\Box})-1}{\Box}\right)\partial^\mu\partial^\nu h, \quad h\Box h \left(\frac{a(\bar{\Box})-1}{\Box}\right)\Box h.$$

Inspired by the infinite derivative gravitational action given by (2.71), we wish to construct a scalar field theory *toy model* that will capture its essential properties and behaviour. After integrating by parts, the terms above which are relevant to the construction of such a scalar field theory *toy model* are

$$h\partial_\mu h\partial^\mu h, \quad h\Box h a(\bar{\Box})h, \quad h\partial_\mu h a(\bar{\Box})\partial^\mu h.$$

Therefore, if we choose the free part, $S_{\texttt{free}}$, of the action of our scalar field theory toy model to be given by (2.60), the interaction part, $S_{\texttt{int}}$, will be of the form

$$S_{\texttt{int}} = \frac{1}{M_P}\int d^4x \left(\alpha_1\phi\partial_\mu\phi\partial^\mu\phi + \alpha_2\phi\Box\phi a(\bar{\Box})\phi + \alpha_3\phi\partial_\mu\phi a(\bar{\Box})\partial^\mu\phi\right), \tag{2.72}$$

where α_1, α_2 and α_3 are real coefficients.

Hence, the action of our scalar toy model is given by

$$S_{\texttt{scalar}} = S_{\texttt{free}} + S_{\texttt{int}}, \tag{2.73}$$

where

$$S_{\texttt{free}} = \frac{1}{2}\int d^4x \left(\phi\Box a(\bar{\Box})\phi\right) \tag{2.74}$$

and

$$S_{\texttt{int}} = \frac{1}{M_P}\int d^4x \left(\alpha_1\phi\partial_\mu\phi\partial^\mu\phi + \alpha_2\phi\Box\phi a(\bar{\Box})\phi + \alpha_3\phi\partial_\mu\phi a(\bar{\Box})\partial^\mu\phi\right). \tag{2.75}$$

We want the equation of motion of $S_{\texttt{scalar}}$ to satisfy the following symmetry: $\phi \to (1+\epsilon)\phi + \epsilon$. This requirement [1] will fix the values of the coefficients α_1, α_2

[1] For the sake of convenience, we did not demand that $\delta S_{\texttt{scalar}} = 0$ but required, instead,

and α_3.

After integrating by parts, we can write $S_{\texttt{free}}$ and $S_{\texttt{int}}$ as follows:

$$S_{\texttt{free}} = \int d^4x \left(\frac{1}{2}\phi\Box\phi + \frac{1}{2}\phi\tilde{a}(\bar{\Box})\phi\right), \tag{2.76}$$

$$S_{\texttt{int}} = \frac{1}{M_P}\int d^4x \left[(\alpha_1+\alpha_3-2\alpha_2)\,\phi\partial_\mu\phi\partial^\mu\phi + \alpha_2\phi\Box\phi\tilde{a}(\bar{\Box})\phi + \alpha_3\phi\partial_\mu\phi\tilde{a}(\bar{\Box})\partial^\mu\phi\right], \tag{2.77}$$

where

$$\tilde{a}(\bar{\Box}) = a(\bar{\Box}) - 1. \tag{2.78}$$

Hence, $S_{\texttt{scalar}}$ can be written as

$$\begin{aligned} S_{\texttt{scalar}} = &\int d^4x \left(\frac{1}{2}\phi\Box\phi + \frac{1}{M_P}(\alpha_1+\alpha_3-2\alpha_2)\,\phi\partial_\mu\phi\partial^\mu\phi\right) \\ &+ \int d^4x \left(\frac{1}{2}\phi\tilde{a}(\bar{\Box})\phi + \frac{1}{M_P}\left(\alpha_2\phi\Box\phi\tilde{a}(\bar{\Box})\phi + \alpha_3\phi\partial_\mu\phi\tilde{a}(\bar{\Box})\partial^\mu\phi\right)\right). \end{aligned} \tag{2.79}$$

Each of the two lines in (2.79), when considered separately, should have invariant equations of motion under the symmetry: $\phi \to (1+\epsilon)\phi + \epsilon$. Let us write $S_{\texttt{scalar}}$ as

$$S_{\texttt{scalar}} = S_1 + S_2, \tag{2.80}$$

where S_1 is the first line in (2.79), and S_2 is the second line in (2.79).

If we vary S_1, we obtain

$$\begin{aligned} \delta S_1 &= \int d^4x \left(\epsilon\phi\Box\phi + \frac{\epsilon}{2}\Box\phi + \frac{1}{M_P}\left(3\epsilon\,(\alpha_1+\alpha_3-2\alpha_2)\,\phi\partial_\mu\phi\partial^\mu\phi + \epsilon\,(\alpha_1+\alpha_3-2\alpha_2)\,\partial_\mu\phi\partial^\mu\phi\right)\right) \\ &= \int d^4x \left(\epsilon\,(1+2\alpha_2-\alpha_1-\alpha_3)\,\phi\Box\phi + \frac{3\epsilon}{M_P}(\alpha_1+\alpha_3-2\alpha_2)\,\phi\partial_\mu\phi\partial^\mu\phi\right), \end{aligned} \tag{2.81}$$

up to a total divergence and after integrating by parts, it should be proportional

that $\delta S_{\texttt{scalar}}$ should be proportional to $S_{\texttt{scalar}}$.

to S_1. Therefore, we should have

$$1 + 2\alpha_2 - \alpha_1 - \alpha_3 = \frac{3}{2}. \tag{2.82}$$

Now, varying S_2 yields

$$\begin{aligned}\delta S_2 = &\int d^4x \left(\epsilon\phi\Box\tilde{a}(\bar{\Box})\phi + \frac{\epsilon}{2}\Box\tilde{a}(\bar{\Box})\phi + \frac{3\epsilon}{M_P}\alpha_2\phi\Box\phi\tilde{a}(\bar{\Box})\phi + \epsilon\alpha_2\Box\phi\tilde{a}(\bar{\Box})\phi \right. \\ &\left. + \frac{3\epsilon}{M_P}\alpha_3\phi\partial_\mu\phi\tilde{a}(\bar{\Box})\partial^\mu\phi + \epsilon\alpha_3\partial_\mu\phi\tilde{a}(\bar{\Box})\partial^\mu\phi \right) \\ = &\int d^4x \left(\epsilon\left(1 + \alpha_2 - \alpha_3\right)\phi\Box\tilde{a}(\bar{\Box})\phi + \frac{1}{M_P}\left(3\epsilon\alpha_2\phi\Box\phi\tilde{a}(\bar{\Box})\phi + 3\epsilon\alpha_3\phi\partial_\mu\phi\tilde{a}(\bar{\Box})\partial^\mu\phi\right) \right),\end{aligned} \tag{2.83}$$

up to a total divergence and after integration by parts. Again, it should be proportional to the original action, so

$$1 + \alpha_2 - \alpha_3 = \frac{3}{2}. \tag{2.84}$$

From (2.82) & (2.84), we get

$$\alpha_1 = \alpha_2 = \alpha_3 + \frac{1}{2}. \tag{2.85}$$

One solution satisfying (2.85) is given by

$$\alpha_1 = \alpha_2 = -\alpha_3 = \frac{1}{4}. \tag{2.86}$$

As a result, we can write

$$S_{\texttt{int}} = \frac{1}{M_P}\int d^4x \left(\frac{1}{4}\phi\partial_\mu\phi\partial^\mu\phi + \frac{1}{4}\phi\Box\phi a(\bar{\Box})\phi - \frac{1}{4}\phi\partial_\mu\phi a(\bar{\Box})\partial^\mu\phi \right). \tag{2.87}$$

Thus,

$$S_{\texttt{scalar}} = \int d^4x \left[\frac{1}{2}\phi\Box a(\bar{\Box})\phi + \frac{1}{4M_P}\left(\phi\partial_\mu\phi\partial^\mu\phi + \phi\Box\phi a(\bar{\Box})\phi - \phi\partial_\mu\phi a(\bar{\Box})\partial^\mu\phi\right)\right]. \tag{2.88}$$

2.6 Modified superficial degree of divergence for infinite derivative scalar toy model

Since every propagator comes with an exponential suppression, while every vertex comes with an exponential enhancement, the superficial degree of divergence, where we count exponents, is given by

$$E_{\text{modified}} = V - I. \tag{2.89}$$

By using the topological relation given in (2.3), we obtain

$$E_{\text{modified}} = 1 - L. \tag{2.90}$$

Thus, except for $L = 1$, $E_{\text{modified}} < 0$, and the corresponding loop amplitudes are superficially convergent. In the next chapter, we shall compute Feynman diagrams for our infinite derivative scalar toy model and investigate renormalisability.

2.7 Summary

In this chapter, we have written down the infinite derivative gravitational action which is the crux of this thesis. Moreover, we have presented the corresponding tree-level propagator when metric perturbations around a Minkowski background, $g_{\mu\nu} = \eta_{\mu\nu} + h_{\mu\nu}$, are considered. Inspired by the shift-scaling symmetries of the field equations in GR, we have motivated an infinite derivative scalar toy model which encapsulates the basic features and behaviour of infinite derivative gravity.

The free part of the infinite derivative scalar toy model gives rise to a propagator which is exponentially suppressed in the UV. Furthermore, after considering metric perturbations around a Minkowski background, we have computed the $\mathcal{O}(h^3)$ part of the infinite derivative gravitational theory given by (1.10). As a result, we derived the interaction terms in the infinite derivative scalar toy model. The interaction terms give rise to exponentially enhanced vertex factors. We observe that the propagator and the vertex factors exhibit opposing momentum dependence. This compensatory behaviour is a generic feature of gauge field theories.

Finally, we have derived the modified superficial degree of divergence for the infinite derivative scalar toy model. In contrast to the superficial degree of divergence for GR, where the superficial degree of divergence increases as the number of loops increases, rendering GR non-renormalisable, the modified superficial degree of divergence for the infinite derivative scalar toy model decreases as the number of loops L increases. Consequently, loop amplitudes are superficially convergent when $L > 1$. This fact is a promising hint as far as the renormalisability of the infinite derivative scalar toy model is concerned. In the next chapter, we shall explicitly compute Feynman diagrams within the framework of the infinite derivative scalar toy model with a view to making the scalar field theory renormalisable.

Chapter 3

Ultraviolet finiteness of Feynman diagrams

In this chapter, we consider the ultraviolet finiteness of Feynman diagrams within the context of infinite derivative theories.

Within the framework of infinite derivative field theories and gravity, we should start by explaining first what we mean by ultraviolet (UV) finiteness. When a Feynman diagram is finite in the UV, it means that the corresponding Feynman integral is convergent in the UV, *i.e.*, at very high energies (or short distances). That is, there are no UV divergences, with respect to the internal loop momentum variable k^μ. As far as renormalisability is concerned, this implies that no counterterms are required to cancel possible UV divergences. One should keep in mind that, if all UV divergences with respect to internal loop momenta, which arise in one-particle irreducible (1PI) diagrams, can be removed by adding to the action finitely many counterterms, renormalisability is automatically ensured.

Nevertheless, one could also study UV finiteness with respect to *external momenta*. For instance, when computing scattering diagrams, if the scattering diagram exhibits no external momentum growth, it is convergent in the UV, that is, for large external momenta. In that case, the corresponding cross section of the scattering diagram is finite and does not blow up when the external momenta become very large.

In this chapter, we shall derive the Feynman rules for propagators and vertices for the infinite derivative scalar toy model given by (1.14), show that scattering amplitudes for the scalar toy model are superficially convergent for $L > 1$, where L is the number of loops, that the highest divergence of the 1-loop, 2-point function with non-vanishing external momenta p & $-p$ is Λ^4, where Λ is a hard cutoff, and that the highest divergence of the 2-loop, 2-point function with vanishing external momenta is also Λ^4. In addition, we shall demonstrate that the dressed propagator is more exponentially suppressed than the bare propagator and that dressed vertices behave as exponentials of external momenta when the external momenta are large; therefore, by employing dressed propagators and dressed vertices, n-loop, 2- & 3-point diagrams constructed out of lower-loop, 2- & 3-point diagrams become finite in the UV with respect to internal loop momentum k^μ, that is, no UV divergences arise and no new counterterm is required.

Expanding on the results outlined above, we shall investigate UV finiteness with respect to both internal loop momenta and external momenta for the most general class of Feynman diagrams within the context of infinite-derivative field theories. Thus, we shall generalise the results presented in Refs. [99, 100] and show that, by employing dressed propagators and dressed vertices, n-loop, N-point diagrams constructed out of lower-loop, 2- & 3-point and, in general, N_i-point diagrams are finite in the UV with respect to the internal loop momentum k^μ while the exponential momentum dependences in those diagrams decrease as the loop-order increases and external momentum divergences are eliminated at sufficiently high loop-order. It should be pointed out that n-loop, N-point diagrams constructed out of lower-loop, N_i-point diagrams are the most general one-particle irreducible (1PI) Feynman diagrams.

3.1 Preliminaries

A Feynman diagram is said to be *one-particle irreducible* (1PI) if it cannot be cut in two by cutting a single propagator [119]. Green's functions can be constructed out of one-particle irreducible diagrams. Consequently, the value of

any S-matrix (or scattering amplitude, in general) is purely determined by one-particle irreducible diagrams.

When finitely many Feynman diagrams within the framework of a quantum field theory (QFT) superficially diverge, the theory is called *super-renormalisable* [119]. Now, when finitely many loop amplitudes superficially diverge with divergences arising at each loop-order, the theory is called *renormalisable* [119]. Finally, when all loop amplitudes diverge at a sufficiently high loop-order, the theory is called *non-renormalisable* [119].

In order to derive the *dressed* propagator, one should consider one-particle irreducible diagrams [120]. For example, the sum of the following geometric series containing infinitely many terms yields the dressed propagator $\widetilde{\Pi}(k^2)$:

$$\begin{aligned}\widetilde{\Pi}(k^2) = \Pi(k^2) &+ \Pi(k^2)\left[\Gamma(k^2)\right]\Pi(k^2) \\ &+ \Pi(k^2)\left[\Gamma(k^2)\right]\Pi(k^2)\left[\Gamma(k^2)\right]\Pi(k^2) \\ &\ldots\end{aligned} \tag{3.1}$$

where $\Pi(k^2)$ is the bare propagator and $\Gamma(k^2)$ is given by the sum of one-particle irreducible diagrams [1].

3.2 Feynman rules

All the Feynman integral computations in this thesis are carried out in Euclidean space after analytic continuation ($k_0 \to ik_0$ & $k^2 \to k_E^2$ using the mostly plus metric signature; we shall drop the E subscript for notational simplicity).

The propagator in momentum space is given by

$$\Pi(k^2) = \frac{-i}{k^2 e^{\bar{k}^2}}, \tag{3.2}$$

where barred 4-momentum vectors from now on will denote the momentum di-

[1] Wherever in this thesis the symbol Γ is used to denote a loop integral, we can write Γ as follows: $\Gamma = i\Gamma^{'}$ (dropping the prime, $i\Gamma$ is the convention usually used for loop integrals in the literature).

vided by the mass scale M. The vertex factor for three incoming momenta $k_1,\ k_2,\ k_3$ satisfying the following conservation law,

$$k_1 + k_2 + k_3 = 0\,, \tag{3.3}$$

is given by

$$\frac{1}{M_P} V(k_1, k_2, k_3) = \frac{i}{M_P} C(k_1, k_2, k_3) \left[1 - e^{\bar{k}_1^2} - e^{\bar{k}_2^2} - e^{\bar{k}_3^2}\right], \tag{3.4}$$

where

$$C(k_1, k_2, k_3) = \frac{1}{4}\left(k_1^2 + k_2^2 + k_3^2\right). \tag{3.5}$$

Let us briefly explain how we obtain the vertex factor. The first term originates from the term, $\frac{1}{4}\phi\partial_\mu\phi\partial^\mu\phi$, which using (3.3) in the momentum space, reads

$$-\frac{i}{2}(k_1 \cdot k_2 + k_2 \cdot k_3 + k_3 \cdot k_1) = \frac{i}{4}\left(k_1^2 + k_2^2 + k_3^2\right). \tag{3.6}$$

The second term comes from the terms, $\frac{1}{4}\phi\Box\phi a(\Box)\phi$, and $-\frac{1}{4}\phi\partial_\mu\phi a(\Box)\partial^\mu\phi$. In the momentum space, again using (3.3), we get

$$\frac{i}{4}\left(k_3 \cdot k_1 + k_1 \cdot k_2 - k_3^2 - k_2^2\right) e^{\bar{k}_1^2} = -\frac{i}{4}\left(k_1^2 + k_2^2 + k_3^2\right) e^{\bar{k}_1^2}. \tag{3.7}$$

The third and the fourth terms (3.4) arise in an identical fashion.

For future convenience, let us consider the special case when one of the momenta is zero. For instance, choosing $k_3 = 0$, we obtain $k_1 = -k_2 = k$, which then gives us

$$V(k) \equiv V(k, -k, 0) = -ik^2 e^{\bar{k}^2}. \tag{3.8}$$

We will also often encounter the square of the vertex factor, which is given by

$$\begin{aligned} V^2\left(k_1, k_2, k_3\right) = i^2 C^2(k_1, k_2, k_3) \Big[1 - 2e^{\bar{k}_1^2} - 2e^{\bar{k}_2^2} - 2e^{\bar{k}_3^2} + 2e^{\bar{k}_1^2} e^{\bar{k}_2^2} \\ + 2e^{\bar{k}_2^2} e^{\bar{k}_3^2} + 2e^{\bar{k}_3^2} e^{\bar{k}_1^2} + e^{2\bar{k}_1^2} + e^{2\bar{k}_2^2} + e^{2\bar{k}_3^2}\Big]. \end{aligned} \tag{3.9}$$

Figure 3.1: Left: 1-loop, 2-point diagram Γ_2. Right: The 1-loop, N-point diagram Γ_N. The dots indicate an arbitrary number of (bare) vertices and (bare) propagators for the scalar field.

3.3 1-loop, 2-point function with vanishing external momenta

Let us start with the 1-loop 2-point function. There is only one Feynman diagram as depicted in Fig. 3.1 (left). According to the Feynman rules, we have

$$\Gamma_2 = \frac{i}{2M_P^2}\int \frac{d^4k}{(2\pi)^4}\frac{V^2(k)}{i^2k^4e^{2\bar{k}^2}}. \tag{3.10}$$

Note that we are working in Euclidean space and that the symmetry factor is 2. The angular integrations can be performed trivially, see Appendix I.1 for details, as the integrand only depends on the norm of the external momentum, leaving us with

$$\Gamma_2 = \frac{i}{2M_P^2}\frac{4\pi}{(2\pi)^4}\int_0^\Lambda dk\ \frac{\pi k^3}{2}. \tag{3.11}$$

Integrating with respect to k from 0 to Λ, where Λ is a hard cutoff, we obtain

$$\Gamma_2 = \frac{i\Lambda^4}{64M_P^2\pi^2}. \tag{3.12}$$

We see that the integral goes like $\int d^4k$, and is therefore sensitive to the UV cutoff. This result is in complete accordance with the analysis of superficial degree of divergence according to which at 1-loop level the exponential non-locality does not affect the integrals. The divergence structure is exactly the same as that of

GR at 1-loop.

3.4 N-point function with vanishing external momenta

An interesting fact for gravitational theories is that the superficial degree of divergence does not depend on the number of external vertices. This is true both in GR, see (2.5), as well as in infinite derivative gravity and in infinite derivative scalar field theory, see (2.90). Let us then calculate the N-point function at one loop, see Fig. 3.1 (right). As one can see, the N-point diagram is not particularly different from the 2-point diagram; it is an N-polygon with N vertices and N edges. Thus, instead of a square of the propagator and vertex factor, one now has N powers of them:

$$\Gamma_N = \frac{i}{M_P^N}\int \frac{d^4k}{(2\pi)^4}\frac{V^N(k)}{i^N k^{2N} e^{N\bar{k}^2}} \tag{3.13}$$

$$= (-1)^N \frac{i\Lambda^4}{32 M_P^N \pi^2}, \tag{3.14}$$

where again Λ is the hard cutoff. As expected, its divergence is the same as that of the 2-point function precisely as predicted by the divergence power-counting. The above diagrams are also known as ring diagrams, and they contribute to the *effective potential*. The symmetry factor is $2N$ [1], and summing all the 1-loop

[1] It should be noted that the symmetry factor is equal to $2N$ when 1PI corrections to the effective potential are considered (the external points are not fixed in that case). When computing a Green's function, the symmetry factor is equal to 2 for $N = 1, 2$ and to 1 for $N > 2$.

diagrams, one obtains the 1-loop contribution to the effective potential,

$$V_{\text{eff}}^{(1)}(\phi) = i\sum_{N=1}^{\infty}\Gamma_N\phi^N \tag{3.15}$$

$$= \sum_{N=1}^{\infty}\frac{(-1)^{N+1}}{2N}\frac{\Lambda^4}{32M_P^N\pi^2}\phi^N \tag{3.16}$$

$$= \frac{\Lambda^4}{64\pi^2}\log\left(1+\frac{\phi}{M_P}\right), \tag{3.17}$$

as is typical, see also [70, 71, 121] for similar computations. In a theory of gravity, we do not expect to find such an effective potential as that would violate general covariance; diagrams coming from different order interactions must cancel the contributions. We obtain these terms in our *toy model* since the scaling symmetry is only a symmetry of the field equations and not the entire action, and therefore is expected to be broken at the quantum level.

The prescription that was used in [70] to eliminate these divergent terms while preserving the pole mass is to simply add an opposing counterterm. This is also the prescription that is followed in standard field theoretic calculations (renormalisation conditions), and we will adopt the same convention as we move on to higher-loop diagrams.

Our calculations corroborated the expected divergence structure, see (2.90), in infinite derivative theories, or any covariant theory of gravity for that matter. To prove renormalisability, the real challenge will be to demonstrate that once these 1-loop divergences (subdivergences) are eliminated by counterterms in higher loop subdiagrams, the remaining loop integrals yield finite results. This means that the higher than 1-loop diagrams cannot diverge more than the bare vertex. This is what we now want to check in the remaining sections.

Figure 3.2: Left: The 2-loop, 2-point diagram $\Gamma_{2,2a}$. Right: The 2-loop, 2-point diagram $\Gamma_{2,2b}$.

3.5 2-point function at 2-loop order

3.5.1 General structure

We wish to now investigate the second feature of the divergence formula (2.90), namely, that for higher than 1-loop no new divergences should emerge. Since there are always subdivergent 1-loop graphs within a 2-loop diagram, we do not expect in general finite results, but what we wish to find here is that the 2-loop graph should have the same divergence behavior as that of the 1-loop counterpart. In other words, they should diverge at most as Λ^4. This result will be in contrast with the case in GR, where the 2-loop diagrams diverge as Λ^6.

There are two Feynman diagrams as depicted in Fig. 3.2. The Feynman diagram with zero external momenta in Fig. 3.2 (left) is given by

$$\Gamma_{2,2a} = \frac{i^2}{2i^5 M_P^4} \int \frac{d^4k_1}{(2\pi)^4} \frac{d^4k_2}{(2\pi)^4} \frac{V(k_1)V(k_2)V^2(k_1,k_2,k_3)}{k_3^2 k_2^4 k_1^4 e^{\bar{k}_3^2} e^{2\bar{k}_2^2} e^{2\bar{k}_1^2}}, \tag{3.18}$$

where $k_3 = -k_1 - k_2$, and the expression is symmetric in k_1 and k_2. The numerator contains a sum of different exponents, so that the overall integral can be written in the form

$$\Gamma_{2,2a} = \frac{i}{2M_P^4} \int \frac{d^4k_1}{(2\pi)^4} \frac{d^4k_2}{(2\pi)^4} \frac{C^2}{k_1^2 k_2^2 k_3^2} \sum_i \lambda_i \exp[E_i(k_1,k_2)], \tag{3.19}$$

where C is given by (3.5) and the E_i's are quadratic polynomials of k_1 & k_2 and λ_i are constants taking on the values -2, -1, $+1$, $+2$. Firstly, let us note that one can always find linear combinations of $k_1,\ k_2$, call them $q_1,\ q_2$, such that E_i

is diagonal:

$$E_i = a_1 q_1^2 + a_2 q_2^2. \tag{3.20}$$

Now, depending upon the value of the a_i's, one can classify the terms in three groups:

(I) If both $a_1,\ a_2 < 0$, both the momentum integrals can be performed to provide a finite answer.

(II) If both a_i's are nonzero, but one of them is positive, then one can obtain the integrals by suitably analytically continuing results from the $a_i < 0$ to $a_i > 0$ region.

(III) Finally, there are cases when one of the a_i's is zero. We expect that this represents the divergent contribution from the 1-loop subdiagram embedded within the 2-loop graph. We shall check whether this provides a Λ^4 divergence, or a Λ^6 divergence as in GR.

3.5.2 Group (I) terms

Let us first look at the group (I) terms. The overall exponential factors for the group (I) type terms are given by

$$e^{-\bar{k}_1^2} e^{-\bar{k}_2^2} e^{-\bar{k}_3^2},\ e^{-\bar{k}_2^2} e^{-\bar{k}_1^2},\ e^{-\bar{k}_1^2} e^{-\bar{k}_3^2},\ e^{-\bar{k}_2^2} e^{-\bar{k}_3^2}.$$

The first integrand gives

$$\frac{3iM^6 \log(4/3)}{4096 M_P^4 \pi^4},$$

while each of the other three evaluates to

$$-\frac{iM^6(3+\log(4))}{2048 M_P^4 \pi^4}.$$

Summing, we obtain

$$\Gamma_{2,2,\mathtt{i}} = \frac{3iM^6}{2048 M_P^4 \pi^4}\left[\frac{1}{2}\log\left(\frac{4}{3}\right) - (3+\log 4)\right]. \tag{3.21}$$

3.5.3 Group (II) & (III) terms and the divergence structure

Next let us look at the integrals originating from the last three terms in (3.9). With overall exponents

$$e^{\bar{k}_1^2}e^{-\bar{k}_2^2}e^{-\bar{k}_3^2},\ e^{\bar{k}_2^2}e^{-\bar{k}_1^2}e^{-\bar{k}_3^2},\ e^{\bar{k}_3^2}e^{-\bar{k}_1^2}e^{-\bar{k}_2^2},$$

these form the group (II) set with one eigenvalue positive and one negative. These integrals can also be evaluated by employing suitable analytic continuation methods, see Appendix I.2 for details.

Again, all the terms contribute equally, yielding

$$\Gamma_{2,2,\texttt{ii}} = \frac{3iM^4}{4096\pi^4 M_P^4}\left(M^2\left(\log(4)-8\right)-4\Lambda^2\right). \tag{3.22}$$

We are left to tackle the group (III) terms originating from the fifth, sixth and seventh terms in (3.9), whose exponential contributions coming from the vertices are given by

$$e^{\bar{k}_1^2}e^{2\bar{k}_2^2}e^{\bar{k}_3^2},\ e^{\bar{k}_2^2}e^{2\bar{k}_1^2}e^{\bar{k}_3^2},\ e^{2\bar{k}_1^2}e^{2\bar{k}_2^2}.$$

Since the exponential contribution of the propagators is given by

$$e^{-2\bar{k}_1^2}e^{-2\bar{k}_2^2}e^{-\bar{k}_3^2},$$

the overall exponents, E_i, for the three above cases are

$$-\bar{k}_1^2,\ -\bar{k}_2^2,\ -\bar{k}_3^2.$$

Clearly, there is no exponential damping along the directions orthogonal to k_1, k_2 and k_3 respectively. Accordingly, while one of the momentum integrals is convergent due to the presence of the exponential, the other one can only be computed using a hard cutoff. The result is identical for all the three diagrams,

and one obtains

$$\Gamma_{2,2,\mathtt{iii}} = \frac{iM^2}{4096M_P^4\pi^4}\left[2M^4\left(6\log\left(\frac{\Lambda}{M}\right)+5e^{-\frac{\Lambda^2}{M^2}}-3\mathrm{Ei}\left(-\frac{\Lambda^2}{M^2}\right)+3\gamma-5\right)\right.$$
$$\left.+\,\Lambda^2M^2\left(e^{-\frac{\Lambda^2}{M^2}}+15\right)+\Lambda^4\left(6-e^{-\frac{\Lambda^2}{M^2}}\right)-\frac{\Lambda^6\mathrm{Ei}\left(-\frac{\Lambda^2}{M^2}\right)}{M^2}\right], \tag{3.23}$$

where

$$\mathrm{Ei}(z) \equiv -\fint_{-z}^{\infty} dt\ \frac{e^{-t}}{t} \tag{3.24}$$

is the exponential-integral function, see Ref. [122], and has a branch cut discontinuity in the complex z-plane running from 0 to ∞. The sign $\fint$ indicates that the principal value of the integral is taken. We note that, for large negative z, the Ei function falls off as a Gaussian and therefore can be ignored in the $\Lambda \to \infty$ limit. Moreover, γ is the Euler-Mascheroni constant,

$$\gamma = \lim_{n\to\infty}\left(\sum_{l=1}^{n}\frac{1}{l}-\log n\right). \tag{3.25}$$

Therefore, the surviving divergent pieces read

$$\Gamma_{2,2,\mathtt{iii}} = \frac{iM^2}{4096M_P^4\pi^4}\left[12M^4\log\left(\frac{\Lambda}{M}\right)+15\Lambda^2M^2+6\Lambda^4+2M^4\left(3\gamma-5\right)\right]. \tag{3.26}$$

Firstly, we see that the highest divergence is indeed proportional to Λ^4, as the superficial divergence argument suggested, and does not grow as Λ^6, as one would find in GR.

We note that all the results obtained in this section have been divided by a symmetry factor 2 for the diagram. Summing all the integrals, we obtain our

final result:

$$\Gamma_{2,2a} = \frac{iM^2}{4096M_P^4\pi^4}\left[M^4\left(12\log\left(\frac{\Lambda}{M}\right) - 52 + 2\left(3\gamma - 5\right) - 3\log(3)\right) + 3\Lambda^2M^2 + 6\Lambda^4\right]. \tag{3.27}$$

To reiterate, $\Gamma_{2,1} \sim \Gamma_{2,2} \sim \Lambda^4$, as the counting of superficial degree of divergence would suggest. While we have not explicitly calculated higher than two loop graphs, we would expect the same pattern to continue to hold, *i.e.*, we do not expect larger than quartic divergence in any loop order.

3.5.4 The other 2-loop diagram

After setting the external momenta equal to zero, the Feynman diagram in Fig. 3.2 (right) becomes

$$\Gamma_{2,2b} = \frac{i^2}{2i^5M_P^4}\int\frac{d^4k_1}{(2\pi)^4}\frac{d^4k_2}{(2\pi)^4}\frac{V^2(k_1)V^2(k_1,-\frac{k_1}{2}+k_2,-\frac{k_1}{2}-k_2)}{k_1^6(\frac{k_1}{2}+k_2)^2(\frac{k_1}{2}-k_2)^2e^{3\bar{k}_1^2}e^{\left(\frac{\bar{k}_1}{2}+\bar{k}_2\right)^2}e^{\left(\frac{\bar{k}_1}{2}-\bar{k}_2\right)^2}}, \tag{3.28}$$

where we have assumed symmetrical routing of momenta and the symmetry factor of the diagram is 2. Again, the numerator contains a sum of different exponents, so that the overall integral can be written in the form

$$\Gamma_{2,2b} = \frac{i}{2M_P^4}\int\frac{d^4k_1}{(2\pi)^4}\frac{d^4k_2}{(2\pi)^4}\frac{D^2}{k_1^2(\frac{k_1}{2}+k_2)^2(\frac{k_1}{2}-k_2)^2}\sum_i\mu_i\exp[F_i(k_1,k_2)], \tag{3.29}$$

where F_i's are quadratic polynomials of k_1, k_2, and μ_i are constants which take on the values -2, -1, $+1$, $+2$, similar to the first 2-loop diagram. Also,

$$D = \frac{1}{4}\left(k_1^2 + \left(\frac{k_1}{2}+k_2\right)^2 + \left(\frac{k_1}{2}-k_2\right)^2\right). \tag{3.30}$$

If we change variables $k_1 \to k_1^{'}$, $-\frac{k_1}{2} - k_2 \to k_2^{'}$ (or, equivalently, $k_1 \to k_1^{'}$ and $-\frac{k_1}{2} + k_2 \to k_2^{'}$) in $\Gamma_{2,1}$, we get $\Gamma_{2,2}$, since the Jacobian is 1, that is, (3.29) is

exactly equivalent to (3.19):

$$\Gamma_{2,2b} = \Gamma_{2,2a}. \tag{3.31}$$

Hence, the results for both the 2-loop diagrams are exactly the same. To reiterate, $\Gamma_{2,1} \sim \Gamma_{2,2} \sim \Lambda^4$, which would seem to corroborate the counting of superficial degree of divergence (2.90).

3.6 Arbitrary loop diagrams

The calculations in the earlier subsection supported our naive divergence counting argument in Section 2.6, which suggested that the highest divergence for all 1-loop diagrams should be proportional to Λ^4, and that this divergence should not increase as we go to higher loops. While this agreement is encouraging, merely the fact that the divergence does not increase at higher loops does not ensure renormalisability. To achieve renormalisability, one has to check, for instance, that once the 1-loop subdivergences are removed from a higher-loop diagram, the diagram becomes finite. This requires keeping track of the UV behaviour of the external momenta while performing the various loops. Let us illustrate the point with a few examples.

Consider the 2-loop diagram in Fig. 3.2 (left). This contains a sub-divergent 3-point, 1-loop diagram. If we had found a prescription to make the 1-loop diagram finite (for instance by adding appropriate counterterms as suggested in the previous section [1]), then the 2-loop diagram should really be replaced by Fig. 3.3 (left), where we now have a finite renormalised 3-point function. We then have to perform a loop integral involving the renormalised 1-loop, 3-point function $\Gamma_{3,1r}$:

$$\begin{aligned}\Gamma_{2,2a} &= \frac{i^2}{2i^5 M_P^4} \int \frac{d^4k_1}{(2\pi)^4} \frac{d^4k_2}{(2\pi)^4} \frac{V(k_1)V(k_2)V^2(k_1,k_2,k_3)}{k_1^4 k_2^4 k_3^2 e^{2\bar{k}_1^2+2\bar{k}_2^2+\bar{k}_3^2}} \\ &\to \int \frac{d^4k_1}{(2\pi)^4} \frac{V(k_1)\Gamma_{3,1r}(k_1,-k_1,0)}{k_1^4 e^{2\bar{k}_1^2}},\end{aligned} \tag{3.32}$$

[1] We will see later that the 3-point function is actually finite once we introduce the dressed propagator.

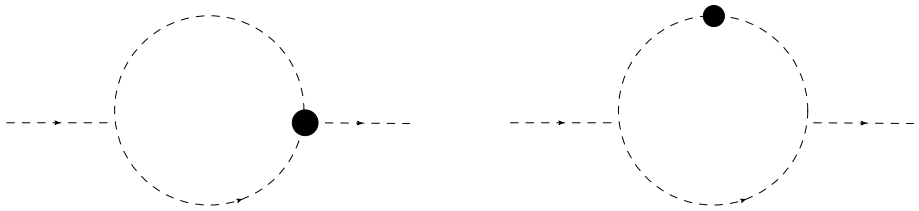

Figure 3.3: Left: 2-loop, 2-point diagram, $\Gamma_{2,2a}$, now containing the renormalised 1-loop 3-point function (dark blob), $\Gamma_{3,1}$. Right: Second 2-loop, 2-point diagram, $\Gamma_{2,2b}$, containing the renormalised 1-loop 2-point function (dark blob), $\Gamma_{2,1}$.

where $k_3 = -k_1 - k_2$. The key question then is whether this integral is finite. A very similar reasoning can be applied to the 2-loop diagram in Fig. 3.2 (right), where one can think of replacing the 2-point 1-loop subdiagram with the renormalised 1-loop, 2-point function $\Gamma_{2,1r}$, see Fig. 3.3 (right), and then perform the remaining loop integral:

$$\Gamma_{2,2b} = \frac{i^2}{2i^5 M_P^4} \int \frac{d^4k_1}{(2\pi)^4} \frac{d^4k_2}{(2\pi)^4} \frac{V^2(k_1)V^2(k_1, -\frac{k_1}{2} + k_2, -\frac{k_1}{2} - k_2)}{k_1^6 (\frac{k_1}{2} + k_2)^2 (\frac{k_1}{2} - k_2)^2 e^{3\bar{k}_1^2 + \left(\frac{\bar{k}_1}{2} + \bar{k}_2\right)^2 + \left(\frac{\bar{k}_1}{2} - \bar{k}_2\right)^2}} \tag{3.33}$$

$$\to \int \frac{d^4k_1}{(2\pi)^4} \frac{V^2(k_1)\Gamma_{2,1r}(k_1, -k_1)}{k_1^6 e^{3\bar{k}_1^2}}. \tag{3.34}$$

Actually, this is a very general prescription, any n-loop diagram can be thought of as a 1-loop integral over a graph containing renormalised vertex corrections and dressed propagators, see Fig. 3.4 (right) for illustration. To prove renormalisability recursively, one should prove that if all loops up to $n-1$ order are finite, then the remaining 1-loop integral remains finite too.

Now, we have already seen from counting arguments in in the previous section that if the vertices and the propagators are enhanced and suppressed respectively by the same exponential factor then a 1-loop diagram remains divergent. This argument can clearly be applied to n-loop graphs when viewed as 1-loop diagrams involving renormalised vertices, and (most importantly) renormalised propagators. What the argument suggests is that to have a chance at renormalisability, the renormalised vertices must be growing less strongly than the renormalised or the "dressed" propagators. In the next section, we are going to compute ex-

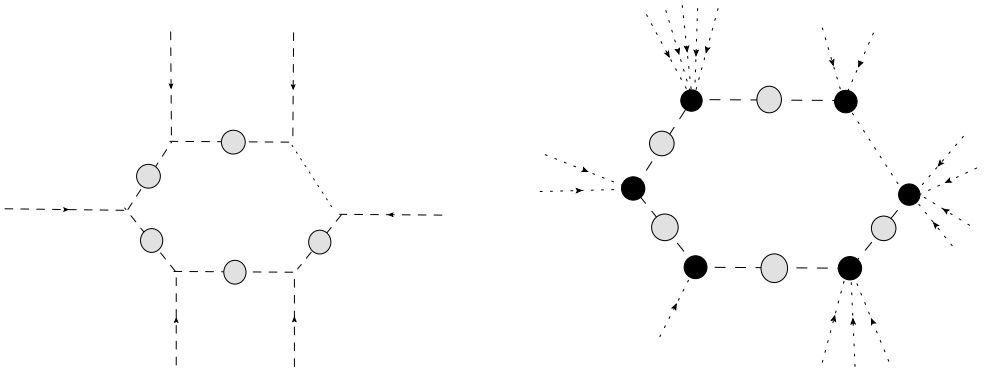

Figure 3.4: Left: N-point diagram with dressed propagators (shaded blobs). The dots indicate an arbitrary number of (bare) vertices and dressed propagators. Right: n-loop, N-point diagram constructed out of lower-loop N_i-point diagrams with loop corrections to the vertices (dark blobs) and dressed propagators (shaded blobs). The internal dots indicate an arbitrary number of renormalised vertex corrections and dressed propagators. The external dots indicate an arbitrary number of external lines.

ternal momentum dependence of the 2-point function at 1-loop, and discuss its ramifications.

3.7 1-loop, 2-point function with arbitrary external momenta

Calculating the dressed propagator amounts to calculating the 2-point function with external momenta. At the 1-loop level with external momenta p, $-p$ (we assume the convention that the external momenta are incoming and sum to zero), and symmetrical routing of momenta, the Feynman integral is given by (see Appendix I.1 for details),

$$\Gamma_{2,1}(p^2) = \frac{i}{2i^2 M_P^2} \int \frac{d^4k}{(2\pi)^4} \frac{V^2(-p, \frac{p}{2}+k, \frac{p}{2}-k)}{(\frac{p}{2}+k)^2(\frac{p}{2}-k)^2 e^{\left(\frac{\bar{p}}{2}+\bar{k}\right)^2} e^{\left(\frac{\bar{p}}{2}-\bar{k}\right)^2}}, \tag{3.35}$$

where

$$V^2\left(-p,\frac{p}{2}+k,\frac{p}{2}-k\right) = i^2C^2\left[1-2e^{\left(\frac{\bar{p}}{2}+\bar{k}\right)^2}-2e^{\left(\frac{\bar{p}}{2}-\bar{k}\right)^2}-2e^{\bar{p}^2}+2e^{\left(\frac{\bar{p}}{2}+\bar{k}\right)^2}e^{\left(\frac{\bar{p}}{2}-\bar{k}\right)^2}\right.$$
$$\left.+\,2e^{\left(\frac{\bar{p}}{2}-\bar{k}\right)^2}e^{\bar{p}^2}+2e^{\bar{p}^2}e^{\left(\frac{\bar{p}}{2}+\bar{k}\right)^2}+e^{2\left(\frac{\bar{p}}{2}+\bar{k}\right)^2}+e^{2\left(\frac{\bar{p}}{2}-\bar{k}\right)^2}+e^{2\bar{p}^2}\right] \tag{3.36}$$

$$= i^2C^2\left[1-2e^{\left(\frac{\bar{p}}{2}+\bar{k}\right)^2}-2e^{\left(\frac{\bar{p}}{2}-\bar{k}\right)^2}-2e^{\bar{p}^2}+4e^{\left(\frac{\bar{p}}{2}+\bar{k}\right)^2}e^{\left(\frac{\bar{p}}{2}-\bar{k}\right)^2}\right.$$
$$+\,2e^{\left(\frac{\bar{p}}{2}-\bar{k}\right)^2}e^{\bar{p}^2}+2e^{\bar{p}^2}e^{\left(\frac{\bar{p}}{2}+\bar{k}\right)^2}+\left(e^{2\left(\frac{\bar{p}}{2}+\bar{k}\right)^2}-e^{\left(\frac{\bar{p}}{2}+\bar{k}\right)^2}e^{\left(\frac{\bar{p}}{2}-\bar{k}\right)^2}\right)$$
$$\left.+\left(e^{2\left(\frac{\bar{p}}{2}-\bar{k}\right)^2}-e^{\left(\frac{\bar{p}}{2}+\bar{k}\right)^2}e^{\left(\frac{\bar{p}}{2}-\bar{k}\right)^2}\right)+e^{2\bar{p}^2}\right] \tag{3.37}$$

and

$$C=\frac{1}{4}\left[p^2+\left(\frac{p}{2}+k\right)^2+\left(\frac{p}{2}-k\right)^2\right]. \tag{3.38}$$

While using a cut-off scheme to regulate the integral is more instructive to see the divergent structure, technically it is much more convenient to use dimensional regularisation, which is what we will employ from here onwards. The integral in (3.35) contains several terms coming from the various sums of exponents that make up the vertex functions. The different integrals arising from the sum in V^2 can be grouped in three ways:

(I) When the integrand contains no exponentials, this comes from the fifth term in (3.37), and gives a divergent result.

(II) When we have a Gaussian damping term present in (3.37). This is the case for all the terms except the fifth, eighth and the ninth terms and gives a convergent answer.

(III) The eighth and the ninth terms in (3.37) give rise to integrals containing the terms $e^{2\bar{p}\cdot\bar{k}}-1$ and $e^{-2\bar{p}\cdot\bar{k}}-1$, respectively, but they are not particularly important for our discussion as will become clear soon. Let us discuss these terms separately now.

3.7.1 Group (I) terms

The divergent integral corresponding to the fifth term can again be calculated straightforwardly using dimensional regularisation (see Appendix J), and one obtains

$$\Gamma_{2,1,i}(p^2) = \frac{ip^4}{128\pi^2 M_P^2}\left(\frac{2}{\epsilon} - \log\left(\frac{p^2}{4\pi M^2}\right) - \gamma + 2\right), \tag{3.39}$$

where $\epsilon = 4 - D$ (D is the dimensionality of spacetime) and γ is the Euler-Mascheroni constant. Let us make a couple of comments: firstly, the $p^2 \to 0$ limit is well defined, *i.e.*, none of the expressions diverge. If it did, that would make the low energy limit ill-defined, ruling out such modifications phenomenologically even as an effective theory. Secondly, the counterterm needed to cancel the divergence is given by

$$\mathcal{L}_{\mathtt{ct}} = -\frac{1}{128\epsilon\pi^2 M_P^2}\int d^4x \left(\phi\Box^2\phi\right), \tag{3.40}$$

or, equivalently,

$$\Gamma_{2,1,\mathtt{ct}}(p^2) = -\frac{ip^4}{64\pi^2 M_P^2}\frac{1}{\epsilon}. \tag{3.41}$$

We observe that the counterterm is not of the same form as the original action given by (2.88). This happens because the symmetry principle we used to write down the action given by (2.88) was not a symmetry of the action, but only that of the field equations.

3.7.2 Group (II) terms

The group (II) type integrals are all convergent due to the presence of the exponential damping factor. They can therefore be evaluated rather straightforwardly

to yield

$$\Gamma_{2,1,ii}(p^2) = \frac{iM^4 e^{-\bar{p}^2}}{512 M_P^2 \pi^2 \bar{p}^2}\Bigg[-2e^{\bar{p}^2}\left(e^{2\bar{p}^2}-1\right)\bar{p}^6 \mathrm{Ei}\left(-\bar{p}^2\right) + \left(e^{\bar{p}^2}-1\right)\Bigg(-2\left(\bar{p}^4+3\bar{p}^2+2\right) + \left(e^{\frac{3\bar{p}^2}{2}} - e^{\frac{\bar{p}^2}{2}}\right)\left(2\bar{p}^4+5\bar{p}^2+4\right) + e^{\bar{p}^2}\left(e^{\bar{p}^2}-1\right)\bar{p}^6 \mathrm{Ei}\left(-\frac{\bar{p}^2}{2}\right) + 2e^{\bar{p}^2}\left(7\left(\bar{p}^4+\bar{p}^2\right)+2\right)\Bigg)\Bigg]. \tag{3.42}$$

Again, the expression is regular as $p^2 \to 0$. This again shows that the theory has a well defined low energy limit. However, to assess the renormalisability of the theory we need to look at the UV behaviour, and especially track any exponential growth. With this in mind, let us look at the various terms that grow as a Gaussian as $p^2 \to \infty$:

$$\begin{aligned}\Gamma_{2,1,ii}(p^2) = \frac{iM^2}{512 M_P^2 \pi^2 p^2}\Bigg[& e^{\frac{3\bar{p}^2}{2}}\left(4M^4+5M^2p^2+2p^4\right) + 2e^{\bar{p}^2}\left(2M^4+7M^2p^2+7p^4\right) \\ & - 2e^{\frac{\bar{p}^2}{2}}\left(4M^4+5M^2p^2+2p^4\right)\Bigg] - \frac{iM^2p^2}{256 M_p^2\pi^2}\Bigg[\left(1-2M^2p^{-2}+8M^4p^{-4}\right)e^{\frac{3\bar{p}^2}{2}} \\ & - 2e^{\frac{\bar{p}^2}{2}} - e^{\bar{p}^2}\Bigg] + \dots\ ,\end{aligned} \tag{3.43}$$

where the $\dots$ indicate subleading terms or terms which are growing at most as a polynomial, and we have used the following relation [123],

$$\lim_{x\to+\infty} x^2 e^{\alpha x^2}\mathrm{Ei}\left(-\alpha x^2\right) = -\frac{1}{\alpha}, \tag{3.44}$$

where α is positive, to obtain the asymptotic behaviour. In particular, as $p^2 \to \infty$, we find

$$\Gamma_{2,1,ii}(p^2) \to \frac{iM^4 e^{\frac{3\bar{p}^2}{2}}}{512 M_P^2\pi^2}\left[9 - 12\bar{p}^{-2} + \dots\right]. \tag{3.45}$$

As we see, the correction to the propagator grows with a larger exponent than the "bare" inverse propagator, which grows as $e^{\bar{p}^2}$ when p^2 is large, and this will be crucial in proving finiteness of the 1-loop diagrams and in our arguments on renormalisability of the theory.

3.7.3 Group (III) terms

For the purpose of completeness, let us also compute the group (III) integrals using dimensional regularisation (see Appendix J for details). We find that the $e^{2\bar{p}\cdot\bar{k}}$ integrals do not give rise to any poles. In fact, we have that (see Appendix J.1)

$$\Gamma_{2,1,iii}(p^2) = 0. \tag{3.46}$$

As we can see, the $\Gamma_{2,1,ii}(p^2)$ term dominates for large momentum, and is therefore going to be the most important for understanding the UV behaviour of the quantum theory.

To summarise, from our preceding calculations in the UV limit we have

$$\Gamma_{2,1}(p^2) = \Gamma_{2,1,i}(p^2) + \Gamma_{2,1,ii}(p^2) + \Gamma_{2,1,iii}(p^2) \approx \frac{9iM^4 e^{3\bar{p}^2/2}}{512M_P^2\pi^2}. \tag{3.47}$$

In other words, the 2-point "vertex" grows more strongly than even the momentum dependence, $\sim e^{\bar{p}^2}$, of the bare 3-point vertex. Also note that the term is finite and therefore it is expected to survive even after we have renormalised the divergent part in the 1-loop 2-point function, which naively looks not helpful at all. For instance, it is easy to see that this leads to an additional divergence in the 2-loop diagram, Fig. 3.3 (right), which contains the 1-loop 2-point subdiagram. In (3.34), since $\Gamma_{2,1r}(k^2)$ goes as $e^{\frac{3\bar{k}^2}{2}}$, the integrand now diverges exponentially as $e^{\frac{\bar{k}^2}{2}}$. This is worse than the power law divergence of 1-loop. As we shall see in the next section, it is precisely this strong exponential dependence which can make all the higher loops finite.

3.8 Dressed propagator & 1-loop integrals

We saw in the earlier section that additional divergences may arise in higher loops from the 1-loop, 2-point functions. However, we know that, in quantum field theory, the 1-loop correction is only the first term in a sequence of graphs, see Figs. 3.5, which can be resummed as a geometric series in the region of con-

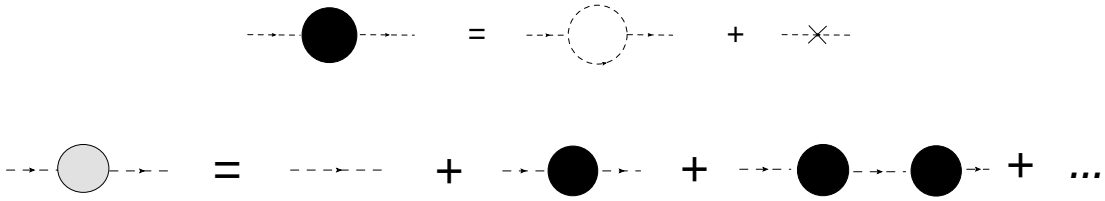

Figure 3.5: Top: The 1-loop, 2-point contribution of 1PI diagrams. The cross denotes a counterterm vertex. Bottom: The dressed propagator as the sum of an infinite geometric series. The dressed propagator is denoted by the shaded blob.

vergence and then analytically continued to the entire momentum space. In other words, the bare propagators need to be replaced by the dressed propagator while performing calculations for higher-point Green's functions or higher loops. Note that no such infinite sequence exists for interaction vertices, the loop contributions simply add to the bare vertex. Thus, a rather remarkable consequence of this resummation will be that for infinite derivative theories the dressed propagators will be more exponentially suppressed than their bare counterparts at large momentum, and therefore going to overwhelm the exponential enhancements coming from the vertices [1]. In particular, we will explicitly see that this will make the UV part of all higher (than two) point 1-loop graphs finite.

The UV part of the 2-loop integrals, and here we will only illustrate the 2-point function, will also become finite. We will argue that it is possible to extend this reasoning to all higher loop graphs. In other words, except for the 1-loop, 2-point function, all graphs in this toy model for quantum gravity converge in the UV.

The 1-loop, 2-point contribution schematically reads (see Fig. 3.5 (top) for a diagrammatic representation):

$$\Gamma_{2,1}(p^2) + \Gamma_{2,1,\mathtt{ct}}(p^2) = \Gamma_{2,1\mathtt{r}}(p^2) = \frac{iM^4}{M_P^2} f(\bar{p}^2), \tag{3.48}$$

[1] This property is more general than just the infinite-derivative theories as finite 1-loop results were also obtained for "local" higher-derivative extensions of gravity [124].

where $\Gamma_{2,1\mathtt{r}}$ is the renormalised 1-loop, 2-point function and

$$f(\bar{p}^2) = \frac{\bar{p}^4}{128\pi^2}\left(-\log\left(\frac{\bar{p}^2}{4\pi}\right) - \gamma + 2\right) + \frac{e^{-\bar{p}^2}}{512\pi^2\bar{p}^2}\Bigg[-2e^{\bar{p}^2}\left(e^{2\bar{p}^2}-1\right)\bar{p}^6\mathrm{Ei}\left(-\bar{p}^2\right) + \left(e^{\bar{p}^2}-1\right)\Bigg(-2\left(\bar{p}^4+3\bar{p}^2+2\right) + \left(e^{\frac{3\bar{p}^2}{2}} - e^{\frac{\bar{p}^2}{2}}\right)\left(2\bar{p}^4+5\bar{p}^2+4\right) + e^{\bar{p}^2}\left(e^{\bar{p}^2}-1\right)\bar{p}^6\mathrm{Ei}\left(-\frac{\bar{p}^2}{2}\right) + 2e^{\bar{p}^2}\left(7\left(\bar{p}^4+\bar{p}^2\right)+2\right)\Bigg)\Bigg]. \tag{3.49}$$

$f(\bar{p}^2)$ is a regular analytic function of $\bar{p}^2$ which grows as $e^{3\bar{p}^2/2}$ as $p^2 \to \infty$. One can observe that $f(\bar{p}^2) \to 0$ as $p^2 \to 0$. Hence, $\Gamma_{2,1\mathtt{r}}(p^2) \to 0$ as $p^2 \to 0$, thereby implying that the renormalised 1-loop, 2-point function has a well defined low-energy limit. The dressed propagator then represents the geometric series of all the graphs with 1-loop, 2-point insertions as shown in Fig. 3.5 (bottom), analytically continued to the entire complex p^2-plane. Mathematically, this is equivalent to replacing the bare propagator, $\Pi(p^2)$, with the dressed propagator, $\widetilde{\Pi}(p^2)$:

$$\widetilde{\Pi}(p^2) = \frac{\Pi(p^2)}{1-\Pi(p^2)\Gamma_{2,1\mathtt{r}}(p^2)} = \frac{-i}{p^2e^{\bar{p}^2} - \frac{M^4}{M_P^2}f\left(\bar{p}^2\right)}, \tag{3.50}$$

where the bare propagator, $\Pi(p^2)$, is given by (3.2). Since in this case $\Pi(p^2)\Gamma_{2,1\mathtt{r}}(p^2)$ grows with large momenta in the UV limit, we have

$$\widetilde{\Pi}(p^2) \to \Gamma^{-1}_{2,1\mathtt{r}}(p^2) \approx \left(9-12\bar{p}^{-2}\right)^{-1} e^{-\frac{3\bar{p}^2}{2}}. \tag{3.51}$$

Clearly, the dressed propagator is more strongly suppressed than the bare propagator. This is a very crucial result that is now going to ensure that the UV contribution of quantum fluctuations for all the other higher-point 1-loop graphs are finite.

Let us now revisit the 1-loop calculations of the N-point diagrams. Once the infinite sum of diagrams leading to the dressed propagators are taken into

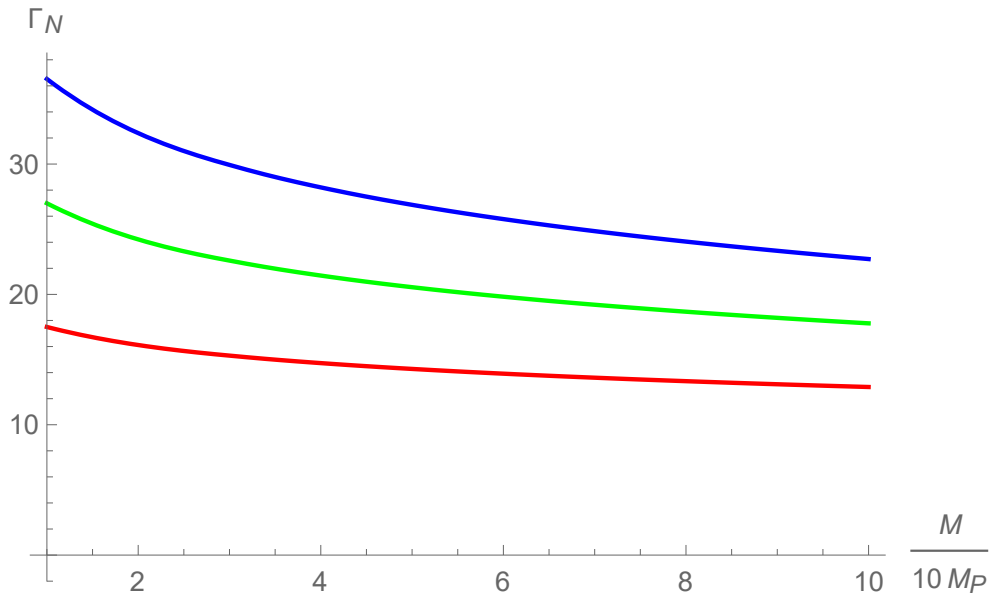

Figure 3.6: A log-plot for 3-point diagrams Γ_3 (in units of iM_P), 4-point diagrams Γ_4 (in units of i) and 5-point diagrams Γ_5 (in units of iM_P^{-1}) where M/M_P ranges from 0.1 to 1. The red, green and blue curves represents Eq. (3.53) for $N = 3, 4$ and 5, respectively.

account, see Fig. 3.4 (left), the UV part of the 1-loop integral reduces to

$$\Gamma_{N,UV} \approx \frac{i}{i^N M_P^N} \int \frac{d^4k}{(2\pi)^4} \frac{V^N(k)}{\left[-\frac{M^4}{M_P^2} f\left(\bar{k}\right)\right]^N} \tag{3.52}$$

$$= \frac{iM^4}{M_P^N} \int \frac{d^4\bar{k}}{(2\pi)^4} \frac{\bar{k}^{2N} e^{N\bar{k}^2}}{\left[\frac{M^2}{M_P^2} f\left(\bar{k}\right)\right]^N}. \tag{3.53}$$

This integral is finite and we have provided numerical plots as a function of M/M_P, see Fig. 3.6. We note that the amplitudes remain well behaved even in the limits $M \ll M_P$ and $M_P \ll M$.

Now if we replace the bare propagators with dressed propagators in the 1-loop, 2-point function with external momenta p & $-p$ while the vertices stay bare, the

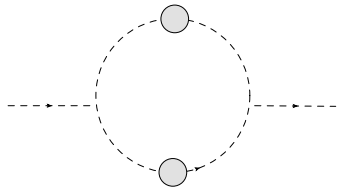

Figure 3.7: The 1-loop, 2-point function with dressed propagators. The shaded blobs denote dressed propagators.

Feynman integral, see Fig. 3.7, is given by

$$\Gamma_{2,1\texttt{dressed}}(p^2) = \frac{1}{2iM_P^2}\int \frac{d^4k}{(2\pi)^4}\frac{V^2(-p,\frac{p}{2}+k,\frac{p}{2}-k)}{\left[(\frac{p}{2}+k)^2 e^{\left(\frac{\bar{p}}{2}+\bar{k}\right)^2} - \frac{M^4}{M_P^2}f\left((\frac{\bar{p}}{2}+\bar{k})^2\right)\right]} \times \frac{1}{\left[(\frac{p}{2}-k)^2 e^{\left(\frac{\bar{p}}{2}-\bar{k}\right)^2} - \frac{M^4}{M_P^2}f\left((\frac{\bar{p}}{2}-\bar{k})^2\right)\right]}. \tag{3.54}$$

As $|k| \to \infty$, the integrand goes as $\sim e^{-k^2}$. Therefore, the integral is convergent since there are no internal loop momentum divergences. On the other hand, we observe that $\Gamma_{2,1\texttt{dressed}}$ goes in terms of external momentum p as $\sim e^{\frac{5\bar{p}^2}{4}}$ for large p^2. We observe that the exponential momentum dependence of $\Gamma_{2,1\texttt{dressed}}$ is less divergent than the exponential momentum dependence of the renormalised 1-loop, 2-point function $\Gamma_{2,1\texttt{r}}(p^2)$.

3.9 UV convergence of 2-loop diagrams

In the previous section we have seen how when we make the transition from the bare to the dressed propagator, the 1-loop diagrams in infinite derivative theories become finite. This means that to renormalise at the 1-loop level, all we have to do is to renormalise the divergence in the 2-point function. This is not very different from the situation in local field theories. For instance, in $\lambda\phi^4$ theory, once the 2-point and 4-point functions are renormalised, all the higher-point Green's functions become finite. We shall see that this procedure can be extended to all loop orders. To that end, let us investigate 2-loop, 2-point Feynman diagrams where the bare propagators have been replaced with dressed propagators. We

Figure 3.8: Left: The 2-loop, 2-point diagram $\Gamma_{2,3a}$. The shaded blobs denote dressed propagators. Right: The 2-loop, 2-point diagram $\Gamma_{2,3b}$. The shaded blobs denote dressed propagators.

shall see that they become finite as opposed to the Λ^4 divergence found in (3.27).

Consider first the Fig. 3.8 (right) that resembles the 1-loop, 2-point Fig. 3.2 (right), except that now the bare propagator has been replaced by the dressed propagator. Again, to determine the finiteness of the graph it is sufficient to focus on the zero external momenta case. The Feynman integral is given by

$$\Gamma_{2,3b} = \frac{i^2}{2i^5 M_P^4}\int \frac{d^4k_1}{(2\pi)^4}\frac{d^4k_2}{(2\pi)^4}\frac{V^2(k_1)V^2(k_1,-\frac{k_1}{2}+k_2,-\frac{k_1}{2}-k_2)}{\left[k_1^2 e^{\bar{k}_1^2}-\frac{M^4}{M_P^2}f\left(\bar{k}_1^2\right)\right]^3\left[(\frac{k_1}{2}+k_2)^2 e^{\left(\frac{\bar{k}_1}{2}+\bar{k}_2\right)^2}-\frac{M^4}{M_P^2}f\left(\left(\frac{\bar{k}_1}{2}+\bar{k}_2\right)^2\right)\right]}$$
$$\times\frac{1}{\left[(\frac{k_1}{2}-k_2)^2 e^{\left(\frac{\bar{k}_1}{2}-\bar{k}_2\right)^2}-\frac{M^4}{M_P^2}f\left(\left(\frac{\bar{k}_1}{2}-\bar{k}_2\right)^2\right)\right]}. \tag{3.55}$$

Making the redefinition $k_1 \to k_1$, $-\frac{k_1}{2}-k_2 \to k_2$ and $k_3 = -k_1-k_2$, we get

$$\Gamma_{2,3b} = \frac{1}{2i^3 M_P^4}\int \frac{d^4k_1}{(2\pi)^4}\frac{d^4k_2}{(2\pi)^4}\frac{V^2(k_1)V^2(k_1,k_2,k_3)}{\left[k_1^2 e^{\bar{k}_1^2}-\frac{M^4}{M_P^2}f\left(\bar{k}_1^2\right)\right]^3\left[k_2^2 e^{\bar{k}_2^2}-\frac{M^4}{M_P^2}f\left(\bar{k}_2^2\right)\right]\left[\bar{k}_3^2 e^{\bar{k}_3^2}-\frac{M^4}{M_P^2}f\left(\bar{k}_3^2\right)\right]}. \tag{3.56}$$

To see whether the integrals are convergent or not, we need to look at large values of $k_1,\ k_2$ where the exponentials dominate. One can check that the integrand goes as

$$\sim \exp\left[-(\frac{k_1}{2}-k_2)^2-\frac{7}{4}k_1^2\right],$$

ensuring that both the k_1 and k_2 integrals are convergent.

The other 2-loop diagram for the 2-point function, see Fig. 3.8 (left), reads as

follows,

$$\Gamma_{2,3a} = \frac{i^2}{2i^5 M_P^4} \int \frac{d^4k_1}{(2\pi)^4} \frac{d^4k_2}{(2\pi)^4} \frac{V(k_1)V(k_2)V^2(k_1,k_2,k_3)}{\left[k_1^2 e^{\bar{k}_1^2} - \frac{M^4}{M_P^2} f\left(\bar{k}_1^2\right)\right]^2 \left[k_2^2 e^{\bar{k}_2^2} - \frac{M^4}{M_P^2} f\left(\bar{k}_2^2\right)\right]^2 \left[k_3^2 e^{\bar{k}_3^2} - \frac{M^4}{M_P^2} f\left(\bar{k}_3^2\right)\right]}, \tag{3.57}$$

where $k_3 = -k_1 - k_2$. The exponential dependence of the integrand as $|k_1|, |k_2| \to \infty$, goes as

$$\sim \exp\left[-\frac{3}{2}\left(k_1 - \frac{k_2}{3}\right)^2 - \frac{4}{3}k_2^2\right],$$

again leading to a convergent integral.

3.10 Higher vertices and prospects for a finite theory

We have just now seen how strong exponential suppression of the dressed propagator can make the 1-loop and 2-loop integrals finite. We believe that this remarkable feature continues to higher loops. The basic reason is that, even for the 1-loop diagrams, the suppression coming from the propagators is stronger than the enhancements coming from the vertices. This ensures two things: first it makes the loops finite, and second the UV growth of the finite diagrams with respect to the external momenta becomes weaker in every subsequent loop. Thus, finiteness of higher loops is guaranteed recursively. We will now sketch heuristic arguments to demonstrate finiteness of the particular set of 2- and 3-point diagrams that can be constructed out of lower-loop 2- and 3-point diagrams, see Fig. 3.9.

The basic approach is the following - in order to understand whether any diagram converges in the UV or not, we only need to keep track of the exponential momentum dependences. We already know that the dressed propagators, represented by the shaded blobs, decay in the UV as $e^{-3\bar{k}^2/2}$. Conservatively, we are therefore going to assume $\widetilde{\Pi}(k^2) \xrightarrow{UV} e^{-3\bar{k}^2/2}$. The 3-point function (represented

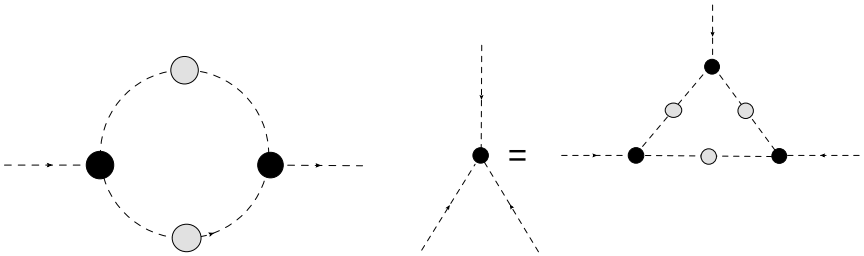

Figure 3.9: Left: 2-point diagram constructed out of lower-loop 2-point & 3-point diagrams. The shaded blobs indicate dressed propagators and the dark blobs indicate renormalised vertex corrections. Right: 3-point diagram constructed out of lower-loop 2-point & 3-point diagrams. The shaded blobs indicate dressed internal propagators and the dark blobs indicate renormalised vertex corrections. The loop order of the dark blob on the left is n while the loop order of the dark blobs on the right is $n-1$. The external momenta are p_1, p_2, p_3 and the internal (that is, inside the loop) momenta are $k+\frac{p_1}{3}-\frac{p_2}{3}$, $k+\frac{p_2}{3}-\frac{p_3}{3}$, $k+\frac{p_3}{3}-\frac{p_1}{3}$.

by the dark blobs) can, on the other hand, be written as

$$\Gamma_3 \xrightarrow{UV} \sum_{\alpha,\beta,\gamma} e^{\alpha\bar{p}_1^2+\beta\bar{p}_2^2+\gamma\bar{p}_3^2} \ , \tag{3.58}$$

with the convention (γ in this section is *not* the Euler-Mascheroni constant)

$$\alpha \geq \beta \geq \gamma, \tag{3.59}$$

where $p_1,\ p_2,\ p_3$ are the three external momenta. This is because once all the lower-loop subdiagrams have been integrated out, what remains are expressions in terms of the corresponding external momenta. Some of these external momenta can then become the internal loop momentum in a subsequent higher loop diagram, see Fig. 3.9 for a pictorial representation of the recursive construction.

The sum over the exponents $\{\alpha,\ \beta,\ \gamma\}$ in (3.58) indicates that there could be many different exponential terms including the permutations needed to symmetrize the vertices over the three internal momenta. We are going to assume that these exponents satisfy certain properties, up to say $(n-1)$-loop order. These conditions will allow us to demonstrate that the loops remain finite. Moreover, we will recursively argue that these properties are also satisfied at the n-th

loop-order.

3.10.1 2-point diagram

First, let us look at the zero external momentum limit. It is easy to see that the most divergent UV part of the 2-point diagram reads

$$\Gamma_{2,n} \longrightarrow \int \frac{d^4k}{(2\pi)^4} \frac{e^{(\alpha_1+\alpha_2+\beta_1+\beta_2)\bar{k}^2}}{e^{3\bar{k}^2}}, \tag{3.60}$$

where k is the loop momentum variable in Fig. 3.9 (left). We have two propagators $e^{\frac{3\bar{k}^2}{2}}$ while the (most divergent UV parts of the) vertex factors originating from lower-loop diagrams are $e^{\alpha_1\bar{k}^2+\beta_1\bar{k}^2}$ and $e^{\alpha_2\bar{k}^2+\beta_2\bar{k}^2}$ (we get no γ_1, γ_2 terms in the exponents, since the external momenta are set equal to zero). Clearly, the integral is finite if

$$\alpha_i + \beta_i < \frac{3}{2}, \tag{3.61}$$

where $i = 1, 2$. One can check that the same condition ensures finiteness of the diagram even when one includes non-zero external momenta.

3.10.2 3-point diagram

First, let us check whether the 3-point diagram (see Fig. 3.9, right) is finite or not for zero external momenta. Again the most divergent UV contribution comes when the momentum associated with exponents, α's and β's, run in the internal loop giving rise to

$$\Gamma_{3,n} \longrightarrow \int \frac{d^4k}{(2\pi)^4} \frac{e^{(\alpha_1+\alpha_2+\alpha_3+\beta_1+\beta_2+\beta_3)\bar{k}^2}}{e^{\frac{9\bar{k}^2}{2}}}, \tag{3.62}$$

where k is the loop momentum variable in Fig. 3.9, right. Similarly to the argument for the 2-point function, we have three propagators $e^{\frac{3\bar{k}^2}{2}}$, while the (most divergent UV parts of the) vertex factors originating from lower-loop diagrams are $e^{\alpha_1\bar{k}^2+\beta_1\bar{k}^2}$, $e^{\alpha_2\bar{k}^2+\beta_2\bar{k}^2}$ and $e^{\alpha_3\bar{k}^2+\beta_3\bar{k}^2}$. Again the integral converges if Eq. (3.61) is valid.

To prove the validity of (3.61), let us try to find out how one can get the largest exponents for the external momenta. First, let us consider how one can get the largest sum of all the exponents, *i.e.*, $\alpha+\beta+\gamma$. Although all the arguments below can be conducted for three different sets of exponents in the three 3-point vertices making up the 1-loop triangle, Fig. 3.9 (right), for simplicity, here we will look at what happens when all the three vertices have the same exponents. Clearly, the best way to obtain the largest exponents for the external momenta is to have the α exponent correspond to the external momenta. For a symmetric distribution of (β,γ) among the internal loops, we get

$$\Gamma_{3,n}\longrightarrow\int\frac{d^4k}{(2\pi)^4}\frac{e^{\alpha^{n-1}(\bar{p}_1^2+\bar{p}_2^2+\bar{p}_3^2)}}{e^{[\frac{3}{2}-\beta^{n-1}-\gamma^{n-1}][3\bar{k}^2+\frac{1}{3}(\bar{p}_1^2+\bar{p}_2^2+\bar{p}_3^2)]}}, \tag{3.63}$$

where p_1, p_2, p_3 are the external momenta for the 1-loop triangle, and the superscript in the α,β,γ indicates that these are coefficients that one obtains from contributions up to $n-1$-loop order (the superscripts are clearly not powers). Before proceeding to obtain the n-th loop coefficients, let us briefly explain how we got (3.63). Assuming symmetrical routing of momenta in the 1-loop triangle, we get the propagators $e^{-\frac{3}{2}\left(\bar{k}+\frac{\bar{p}_1}{3}-\frac{\bar{p}_2}{3}\right)^2}$, $e^{-\frac{3}{2}\left(\bar{k}+\frac{\bar{p}_2}{3}-\frac{\bar{p}_3}{3}\right)^2}$ and $e^{-\frac{3}{2}\left(\bar{k}+\frac{\bar{p}_3}{3}-\frac{\bar{p}_1}{3}\right)^2}$, and the vertex factors $e^{\alpha^{n-1}\bar{p}_1^2+\beta^{n-1}\left(\bar{k}+\frac{\bar{p}_3}{3}-\frac{\bar{p}_1}{3}\right)^2+\gamma^{n-1}\left(\bar{k}+\frac{\bar{p}_1}{3}-\frac{\bar{p}_2}{3}\right)^2}$, $e^{\alpha^{n-1}\bar{p}_2^2+\beta^{n-1}\left(\bar{k}+\frac{\bar{p}_1}{3}-\frac{\bar{p}_2}{3}\right)^2+\gamma^{n-1}\left(\bar{k}+\frac{\bar{p}_2}{3}-\frac{\bar{p}_3}{3}\right)^2}$ and $e^{\alpha^{n-1}\bar{p}_3^2+\beta^{n-1}\left(\bar{k}+\frac{\bar{p}_2}{3}-\frac{\bar{p}_3}{3}\right)^2+\gamma^{n-1}\left(\bar{k}+\frac{\bar{p}_3}{3}-\frac{\bar{p}_1}{3}\right)^2}$. Conservation of momenta then yields (3.63).

By integrating (3.63), we have

$$\alpha^n=\beta^n=\gamma^n=\alpha^{n-1}+\frac{1}{3}(\beta^{n-1}+\gamma^{n-1})-\frac{1}{2}. \tag{3.64}$$

In particular, for the 1-loop, 3-point graph, one has to use the 3-point bare vertices: $\alpha^0=1$ and $\beta^0=\gamma^0=0$. One then obtains

$$\alpha^1=\beta^1=\gamma^1=\frac{1}{2}, \tag{3.65}$$

leading to an overall symmetric vertex $e^{\frac{1}{2}(\bar{p}_1^2+\bar{p}_2^2+\bar{p}_3^2)}$ and $\alpha^1+\beta^1+\gamma^1=\frac{3}{2}$. Since we expect the exponents to decrease as we increase loops, we therefore conjecture

that the sum of exponents satisfies the inequality

$$\alpha^n + \beta^n + \gamma^n \leq \frac{3}{2}. \tag{3.66}$$

From (3.64), we see that this is satisfied provided a further condition is satisfied by the exponents, that is,

$$\alpha^{n-1} + \frac{1}{3}(\beta^{n-1} + \gamma^{n-1}) \leq 1. \tag{3.67}$$

To summarise, so far we have shown that if, up to $n-1$-loop order, (3.67) is satisfied, then, at the n-th loop-order, (3.66) is also satisfied. To complete the recursive proof, we must argue that (3.67) is also satisfied at the n-th loop-order. For the loop contribution we are discussing, we have

$$\alpha^n + \frac{1}{3}(\beta^n + \gamma^n) = \frac{5}{3}\left[\alpha^{n-1} + \frac{1}{3}(\beta^{n-1} + \gamma^{n-1}) - \frac{1}{2}\right] \leq \frac{5}{6} < 1, \tag{3.68}$$

and (3.67) is indeed satisfied.

One may wonder whether there are other ways of distributing the exponents which could violate (3.66). For instance, one can try to maximise α^n by distributing α^{n-1} in two of the vertices to run along the internal loop. However, one can check that (3.67) still remains valid.

The final point is that the sum of the exponents is maximised by distributing the largest exponents to all the external momentum, thereby ensuring that (3.61) follows from (3.66). While we do not yet have a rigorous proof of these above arguments, in all the cases we have looked at so far, the inequalities (3.61), (3.66) and (3.67) seem to hold up.

3.10.3 n-loop, N-point diagrams constructed out of lower-loop, 2- & 3-point diagrams

Now we shall look into the UV finiteness of n-loop, N-point diagrams constructed out of lower-loop, 2- & 3-point diagrams. Let us point out that n-loop, N-point

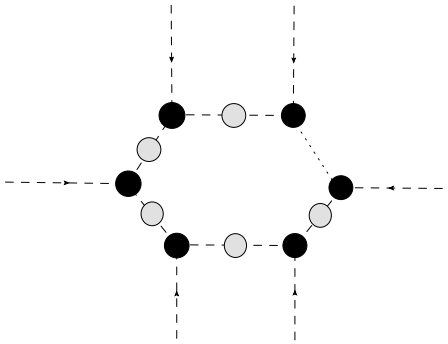

Figure 3.10: n-loop, N-point diagram constructed out of lower-loop 2- & 3-point diagrams with loop corrections to the vertices (dark blobs) and dressed propagators (shaded blobs). The internal dots indicate an arbitrary number of renormalised vertex corrections and dressed propagators.

diagrams constructed out of lower-loop, 2- & 3-point diagrams are one-particle irreducible (1PI) diagrams. We know the following:

- the dressed propagators represented by the shaded blobs decay in the UV as $e^{-3\bar{k}^2/2}$ (see (3.51)).

- the 3-point function represented by the dark blobs (see Figs. 3.9 (right) & 3.10) can be written (after first integrating out the internal loop momentum k^μ in the 1-loop triangle) as

$$\Gamma_3 \xrightarrow{UV} \sum_{\alpha,\beta,\gamma} e^{\alpha\bar{p}_1^2+\beta\bar{p}_2^2+\gamma\bar{p}_3^2}, \tag{3.69}$$

  with the convention (since we assume $p_1+p_2+p_3=0$, terms such as $p_i \cdot p_j$, where $i,j=1,2,3$, can be written as a sum of p_l^2, $l=1,2,3$, terms)

$$\alpha \geq \beta \geq \gamma, \tag{3.70}$$

  where p_1, p_2, p_3 are the three external momenta.

Now one can generalise (3.69) and write the N-point function in the following form (again after first integrating out the internal loop momentum k^μ in the

1-loop N-polygon, see also Appendix K):

$$\Gamma_N \xrightarrow{UV} \sum_{\alpha_l} e^{\sum_{l=1}^{N} \alpha_l \bar{p}_l^2}, \tag{3.71}$$

with the convention

$$\alpha_1 \geq \alpha_2 \geq \cdots \geq \alpha_N, \tag{3.72}$$

where $p_1, p_2, \ldots, p_N$ are the N external momenta.

Now, let us look at the case where the external momenta are arbitrary; we wish to find out how one can get the largest exponents for the external momenta. First, let us consider how one can get the largest sum of all the exponents, *i.e.*, $\sum_{l=1}^{N} \alpha_l$. Even though all the arguments below can be conducted for N different sets of exponents in the N 3-point vertices, see Fig. 3.9 (right), making up the 1-loop N-polygon, see Fig. 3.10, for simplicity, here we will look at what happens when all the N vertices have the same exponents. The best way to obtain the largest exponents for the external momenta is to have the α exponent correspond to the external momenta (we assume a symmetric distribution of (β, γ) among the internal loops and symmetrical routing of momenta in the 1-loop N-polygon). We have that $p_1,\ p_2, \ldots,\ p_N$ are the external momenta for the 1-loop triangle, and the superscript in the $\alpha^{n-1}, \beta^{n-1}, \gamma^{n-1}$ indicates that these are coefficients that one obtains from contributions up to $n-1$-loop order (again, the superscripts are clearly not powers). The internal momenta of the N-point diagram are given

by

$$\begin{aligned}
q_{N-1} &= \frac{1}{N}\left[\sum_{l=1}^{N-2}(lp_l) - p_{N-1}\right], \\
q_N &= \frac{1}{N}\left[\sum_{l=1}^{N-2}(lp_{l+1}) - p_N\right], \\
&\vdots \\
q_{N-3} &= \frac{1}{N}\left[p_{N-1} + 2p_N + \sum_{l=1}^{N-4}((l+2)p_l) - p_{N-3}\right], \\
q_{N-2} &= \frac{1}{N}\left[p_N + \sum_{l=1}^{N-3}((l+1)p_l) - p_{N-2}\right].
\end{aligned} \tag{3.73}$$

That is,

- the dressed propagators are given by $e^{-\frac{3}{2}(\bar{k}+\bar{q}_l)^2}$, $l = 1, \ldots, N$,
- and the vertex factors are of the form $e^{\alpha^{n-1}\bar{p}_l^2 + \beta^{n-1}\left(\bar{k}+\bar{q}_l\right)^2 + \gamma^{n-1}\left(\bar{k}+\bar{q}_{l+1}\right)^2}$.

Hence, conservation of momenta then yields

$$\Gamma_{N,n} \longrightarrow \int \frac{d^4k}{(2\pi)^4} \frac{e^{\alpha^{n-1}(\bar{p}_1^2+\bar{p}_2^2+\cdots+\bar{p}_N^2)}}{e^{[\frac{3}{2}-\beta^{n-1}-\gamma^{n-1}][N\bar{k}^2+c_N(\bar{p}_1^2+\bar{p}_2^2+\cdots+\bar{p}_N^2)]}}, \tag{3.74}$$

where c_N is a coefficient depending on N, the number of external lines, that satisfies $c_N > 0$ for all N (see Appendix K).

- *Internal momentum*: we observe that the integrand in (3.74) is of the form $e^{-s\bar{k}^2}$, where $s > 0$. That is,

$$\beta^{n-1} + \gamma^{n-1} < \frac{3}{2}. \tag{3.75}$$

  Hence, the integral in (3.74) is convergent and the diagram is UV finite with respect to internal loop momentum.

- *External momenta*: by integrating (3.74), we have

$$\alpha_1^n = \alpha_2^n = \cdots = \alpha_N^n = \alpha^{n-1} + c_N(\beta^{n-1} + \gamma^{n-1}) - \frac{3c_N}{2}. \tag{3.76}$$

In particular, for the one-loop, three-point graph, one has to use the 3-point bare vertices: $\alpha^0 = 1$ and $\beta^0 = \gamma^0 = 0$. Using (3.64), one can see that the coefficients α^{n-1}, β^{n-1}, γ^{n-1}, that is, the exponents in the dressed vertices, decrease as the loop-order increases and, at sufficiently high loop-order, become negative. In particular, we have that, for $n = 1$ (n is the loop-order of the three-point dressed vertices),

$$\alpha^1 = \beta^1 = \gamma^1 = \frac{1}{2}, \tag{3.77}$$

for $n = 2$,

$$\alpha^2 = \beta^2 = \gamma^2 = \frac{1}{3}, \tag{3.78}$$

for $n = 3$,

$$\alpha^3 = \beta^3 = \gamma^3 = \frac{1}{18}, \tag{3.79}$$

for $n = 4$,

$$\alpha^4 = \beta^4 = \gamma^4 = -\frac{11}{27}\,. \tag{3.80}$$

We conclude that, for $n \geq 4$, α^n, β^n and γ^n become negative.

Hence, from (3.76) we see that the coefficients $\alpha_1^n,\ \alpha_2^n, \ldots, \alpha_N^n$ also decrease as the loop-order increases and at sufficiently high loop-order become negative. Thus, the external momentum dependences of n-loop, N-point diagrams constructed out of lower-loop, 2- & 3-point diagrams decrease as the loop-order increases and the external momentum divergences are eliminated at sufficiently high loop-order, that is, the exponents in (3.71) corresponding to the external momenta become negative when the loop order is sufficiently large.

Consequently, this class of diagrams are finite in the UV, both with respect to internal loop momentum and at sufficiently high loop-order external momenta

as well. One could also consider the case where the loop-order of the dressed vertices is not the same for all of the dressed vertices, that is, each dressed vertex is of different loop-order. Again the results would be the same as far as UV finiteness with respect to both internal loop momentum and external momenta is concerned.

As a check, when the external momenta tend to zero, it is easy to see that the most divergent UV part of the N-point diagram reads

$$\Gamma_{N,n} \longrightarrow \int \frac{d^4k}{(2\pi)^4} \frac{e^{(\alpha_1+\cdots+\alpha_N+\beta_1+\cdots+\beta_N)\bar{k}^2}}{e^{\frac{3N\bar{k}^2}{2}}}, \tag{3.81}$$

where k is the loop momentum variable in Fig. 3.10. There are N propagators $e^{\frac{3\bar{k}^2}{2}}$ while the (most divergent UV parts of the) vertex factors originating from lower-loop diagrams are $e^{\alpha_1\bar{k}^2+\beta_1\bar{k}^2}$,...,$e^{\alpha_N\bar{k}^2+\beta_N\bar{k}^2}$ (we get no γ_1, γ_2 terms in the exponents, since the external momenta are set equal to zero). Clearly, the integral is finite if

$$\alpha_i + \beta_i < \frac{3}{2}, \tag{3.82}$$

where $i = 1, 2, \ldots, N$.

3.10.4 n-loop, N-point diagrams constructed out of lower-loop, N_i-point diagrams

Now let us look at n-loop, N-point diagrams constructed out of lower-loop, N_i-point diagrams. Let us mention again that n-loop, N-point diagrams constructed out of lower-loop, N_i-point diagrams are the most general one-particle irreducible (1PI) diagrams. Any n-loop diagram can be thought of as a 1-loop integral over a graph containing renormalised vertex corrections and dressed propagators, see Fig. 3.4 (right). At the i-th dressed vertex, we have N_i-2 external lines (excluding the two internal propagators in the n-loop, N-point diagram that are attached to each dressed vertex).

In general, the lower-loop, N_i-point diagrams can be constructed out of N_j-point diagrams whose loop-order is even lower. In turn, the N_j-point diagrams

can be constructed out of N_k-point diagrams whose loop-order is even lower and so on. It can be easily deduced that the basic building blocks of all Feynman diagrams within the framework of our infinite derivative scalar toy model are three-point vertices.

For simplicity, we take all the vertices to have the same exponents. We have m dressed vertices with N_i external lines attached to each dressed vertex; thus,

$$N = \sum_{i=1}^{m} (N_i - 2). \tag{3.83}$$

Regarding the external momenta, we use the following notation:

$$p_i^{'} = \sum_{l=1}^{N_i-2} p_{i_l}, \tag{3.84}$$

where $i = 1, \ldots, m$ and p_{i_l} are the external momenta to the i-th dressed vertex. For each dressed vertex, the N_i-point function can be written as follows,

$$\Gamma_{N_i} \xrightarrow{UV} \sum_{\alpha_{i_l},\beta_i,\gamma_i} e^{\sum_{l=1}^{N_i-2} \alpha_{i_l} \bar{p}_{i_l}^2 + \beta_i \bar{q}_1^2 + \gamma_i \bar{q}_2^2}, \tag{3.85}$$

where q_1 and q_2 are internal propagators in the N-point diagram, with the convention

$$\alpha_{i_1} \geq \alpha_{i_2} \geq \cdots \geq \alpha_{i_{N_i-2}} \geq \beta_i \geq \gamma_i. \tag{3.86}$$

The internal momenta of the N-point diagram are given by

$$\begin{aligned}
q^{'}_{m-1} &= \frac{1}{m}\left[\sum_{l=1}^{m-2}\left(lp^{'}_{l}\right) - p^{'}_{m-1}\right], \\
q^{'}_{m} &= \frac{1}{m}\left[\sum_{l=1}^{m-2}\left(lp^{'}_{l+1}\right) - p^{'}_{m}\right], \\
&\vdots \\
q^{'}_{m-3} &= \frac{1}{m}\left[p^{'}_{m-1} + 2p^{'}_{m} + \sum_{l=1}^{m-4}\left((l+2)p^{'}_{l}\right) - p^{'}_{m-3}\right], \\
q^{'}_{m-2} &= \frac{1}{m}\left[p^{'}_{m} + \sum_{l=1}^{m-3}\left((l+1)p^{'}_{l}\right) - p^{'}_{m-2}\right].
\end{aligned} \tag{3.87}$$

That is,

- the dressed propagators are given by $e^{-\frac{3}{2}(\bar{k}+\bar{q}^{'}_{i})^2}$, $i = 1, \ldots, m$,
- and the vertex factors are of the form $e^{\sum_{l=1}^{N_i-2}\alpha_{i_l}^{n-1}\bar{p}^2_{i_l} + \beta_i^{n-1}\left(\bar{k}+\bar{q}^{'}_{i}\right)^2 + \gamma_i^{n-1}\left(\bar{k}+\bar{q}^{'}_{i+1}\right)^2}$.

Hence, conservation of momenta then yields

$$\Gamma_{N,n} \longrightarrow \int \frac{d^4k}{(2\pi)^4} \frac{e^{\sum_{i=1}^{m}\sum_{l=1}^{N_i-2}\alpha_{i_l}^{n-1}\bar{p}^2_{i_l}}}{e^{[\frac{3m}{2} - \sum_{i=1}^{m}(\beta_i^{n-1}+\gamma_i^{n-1})]\bar{k}^2} e^{\sum_{i=1}^{m}\sum_{l=1}^{N_i-2}[\frac{3}{2}b_{i_l} - \beta_i^{n-1}c_{i_l} - \gamma_i^{n-1}d_{i_l}]\bar{p}^2_{i_l}}}, \tag{3.88}$$

where b_{i_l}, c_{i_l} and d_{i_l} are coefficients depending on i & l and satisfy $b_{i_l}, c_{i_l}, d_{i_l} > 0$ for all values of i and l.

- *Internal momentum*: we observe that the integrand in (3.88) is of the form $e^{-s\bar{k}^2}$, where $s > 0$. That is,

$$\sum_{i=1}^{m}(\beta_i^{n-1} + \gamma_i^{n-1}) < \frac{3m}{2}. \tag{3.89}$$

  Hence, the integral in (3.88) is convergent and the diagram is UV finite with respect to internal loop momentum.

- *External momenta*: by integrating (3.88), we have

$$\alpha_1^n = \alpha_2^n = \cdots = \alpha_N^n = \alpha_{i_l}^{n-1} + c_{i_l}\beta_i^{n-1} + d_{i_l}\gamma_i^{n-1} - \frac{3b_{i_l}}{2}. \tag{3.90}$$

  From Section 3.10.3, one can see that the coefficients $\alpha_{i_l}^{n-1}$, β_i^{n-1}, γ_i^{n-1}, that is, the exponents in the dressed vertices, decrease as the loop-order increases and at sufficiently high loop-order become negative. Hence, from (3.90) we see that the coefficients $\alpha_1^n,\ \alpha_2^n, \ldots, \alpha_N^n$ also decrease as the loop-order increases and at sufficiently high loop-order become negative. Thus, the external momentum dependences of n-loop, N-point diagrams constructed out of lower-loop, N_i-point diagrams decrease as the loop-order increases and the external momentum divergences are eliminated at sufficiently high loop-order, that is, the exponents in (3.85) corresponding to the external momenta become negative when the loop order is sufficiently large.

It should be pointed out that, if each dressed vertex were of different loop-order, we would still obtain the same results regarding UV finiteness with respect to internal loop momentum and external momenta. Moreover, in the limit of vanishing external momenta, again we recover the condition given by (3.82). Hence, n-loop, N-point diagrams constructed out of lower-loop, N_i-point diagrams are finite in the UV, both with respect to internal loop momentum and at sufficiently high loop-order external momenta as well.

3.11 Summary

In this chapter, we have looked into radiative corrections for an infinite derivative scalar field theory toy model resembling the UV properties of infinite derivative gravity. If we expand the infinite derivative gravitational action given by (1.10) around a Minkowski background, we can derive the propagator from the $\mathcal{O}(h^2)$ terms and the vertex factors from the $\mathcal{O}(h^3)$ terms. Moreover, the scalar toy model satisfies a shift-scaling symmetry which determines the opposing momentum dependence of the propagator and vertex factors.

We have written down the Feynman rules for our toy model, that is, the propagator and the vertex factors. Next, we evaluated the 1-loop, 2-point diagram with arbitrary external momenta, which gives rise to a Λ^4 divergence, where Λ is a momentum cutoff. The highest divergence for 2-loop diagrams with vanishing external momenta is Λ^4 as well, meaning that we do not get higher divergences as the loop-order increases. In the 1-loop, 2-point function, we got a $e^{\frac{3\bar{p}^2}{2}}$ external momentum dependence at high energies, which appears as a subdivergence in higher-loop diagrams. This property renders all higher-loop and higher-point diagrams finite after, in place of bare propagators, dressed ones are considered. Specifically, the exponential suppression coming from the dressed propagator is stronger than the exponential enhancement engendered by the vertices. When we replace the bare propagators with dressed propagators in the 1-loop, 2-point function, the corresponding Feynman integrals are convergent. The 1-loop, N-point functions with vanishing external momenta are now finite in the UV; the same holds for 2-loop integrals with zero external momenta. To that end, we have also established the UV finiteness of n-loop, 2- & 3-point diagrams constructed out of lower-loop, 2- & 3-point diagrams.

Generalising, we have shown that, by employing dressed vertices and dressed propagators, n-loop, N-point diagrams constructed out of lower-loop, 2- & 3-point and, in general, N_i-point diagrams are UV finite. This implies that the most general one-particle irreducible (1PI) Feynman diagrams within the framework of infinite-derivative field theories are finite in the UV. Hence, no UV divergences arise and no new counterterm is necessary.

Finally, we have demonstrated that the external momentum dependences of n-loop, N-point diagrams constructed out of lower-loop, 2- & 3-point and, in general, N_i-point diagrams decrease as the loop-order increases and the external momentum divergences are eliminated at sufficiently high loop-order.

Chapter 4

Scattering diagrams

Scattering diagrams play an important role in quantum field theory (QFT). By studying scattering diagrams, one can obtain the scattering matrix element and, ultimately, the cross section. A cross section that blows up at high energies signifies an unphysical theory. Typically, in non-renormalisable theories, the cross section blows up at finite-order [125]. For example, scalar field theories containing more than two derivatives are one such example. Other examples are GR and SUGRA [103]. Besides studying whether the amplitudes are finite or not, there are very interesting applications in cosmology and in formation of microscopic black holes in trans-Plankian scatterings of plane waves [126, 127, 128, 129, 130, 131, 132, 133, 134]. In all these cases, the cross section of a scattering diagram, especially involving gravitons, blows up for large external momenta, *i.e.*, in the UV. On the other hand, string theory has been conjectured to be UV-finite [14, 15]. However, the problem here lies in higher-order corrections in string coupling g_s and α' [1], which would naturally induce corrections beyond the Einstein-Hilbert action. Unfortunately, many of these corrections cannot be computed so easily in a time-dependent cosmological background. Nevertheless, there have been many studies in a fixed background in the context of string scatterings [14, 15, 136, 137, 138, 139, 140]. Indeed, none of these analyses moti-

[1] Infinitely many derivatives are also present in (open) string field theory [20] and in p-adic strings [22]. The non-locality of the invariant string field action was demonstrated in [135]. One would naturally expect them to be present from higher-order α' corrections.

vated from strings or supergravity can probe the region of space-time singularity while neither string theory nor supergravity in its current form can avoid forming a black hole or cosmological singularity. Besides string theory, there are other approaches of quantum gravity, such as loop quantum gravity [16, 17] or the causal set approach [18], where it is possible to set up similar physical problems to study the behaviour at short distances and at small time scales, as well as high-momentum scatterings.

One common thread in all these quantum and semiclassical approaches is the presence of non-locality, where the interactions happen in a finite region of space. It has been conjectured by many that such non-local interactions may ameliorate the UV behaviour of scattering amplitudes, see [63, 65, 90, 91, 126, 131, 132, 138, 139, 141, 142, 143, 144, 145] (see also [66, 67, 68, 70] for finite temperature effects of non-local field theories). It is expected that any such realistic theory of quantum gravity should be able to resolve short-distance and small-timescale singular behaviour present in GR, both in static and in time-dependent backgrounds. Indeed, close to the singularity or close to super-Planckian energies, one would naturally expect higher-derivative corrections to the Einstein-Hilbert action. Such higher-derivative corrections may as well open a door for non-local interactions in a very interesting way.

In this chapter, we shall consider scattering diagrams within the framework of infinite derivative theories. For the purposes of this chapter, we shall work perturbatively about a specific background in Euclidean momentum space.

4.1 Preliminaries

Let us now define the Mandelstam variables s, t and u. We have that (p_1, p_2, p_3, p_4 are the four external momenta in a 4-point scattering diagram)

$$s = -\left(p_1 + p_2\right)^2 = -\left(p_3 + p_4\right)^2 = -E_{\rm CM}^2, \tag{4.1}$$

where $p_1 + p_2 = p_3 + p_4$ and E_{CM} is the total energy in the centre-of-mass frame. Moreover,

$$t = -\left(p_1 - p_3\right)^2 = -\left(p_2 - p_4\right)^2 \tag{4.2}$$

and

$$u = -\left(p_1 - p_4\right)^2 = -\left(p_2 - p_3\right)^2 . \tag{4.3}$$

We have that s, t, u are all negative in Euclidean space and satisfy $s = u + t$. It should be pointed out that massless particles are considered in this chapter.

The total cross section, σ, in the centre-of-mass (CM) frame is given by

$$\sigma = \frac{1}{S} \int_{t_{\min}}^{t_{\max}} dt \; \frac{d\sigma}{dt}, \tag{4.4}$$

where t is given by

$$t = -2E_1E_3 + 2|\mathbf{p}_1||\mathbf{p}_3| \cos\theta. \tag{4.5}$$

When $\cos\theta = -1$, we get $t_{\min}$ and, when $\cos\theta = +1$, we obtain $t_{\max}$ (θ is the angle between $|\mathbf{p}_1|$ and $|\mathbf{p}_3|$). S is the symmetry factor for $n_i^{'}$ identical outgoing particles of type i,

$$S = \prod_i n_i^{'}!, \tag{4.6}$$

and, for two outgoing particles (after we analytically continue to Euclidean space), we have that

$$\frac{d\sigma}{dt} = -\frac{1}{64\pi s|\mathbf{p}_1|^2} |\mathcal{T}|^2, \tag{4.7}$$

where $d\sigma$ is the differential cross section and $\mathcal{T}$ is the scattering matrix element. In the CM frame, we also have

$$|\mathbf{p}_1| = |\mathbf{p}_2| = |\mathbf{p}_3| = |\mathbf{p}_4| = E_1 = E_2 = E_3 = E_4 = \frac{\sqrt{-s}}{2}. \tag{4.8}$$

Furthermore, we have that $t_{\min} = s$ and $t_{\max} = 0$. Since the two outgoing particles are identical, the symmetry factor is $S = 2$. Moreover, in Euclidean space,

$$t = \frac{s}{2}\left(1 - \cos\theta\right) \tag{4.9}$$

and

$$u = \frac{s}{2}\left(1 + \cos\theta\right). \tag{4.10}$$

4.2 Scatterings in scalar field theory with higher derivative interactions

Let us now begin with a simple massless scalar field with a higher-derivative interaction term,

$$S = S_{\texttt{free}} + S_{\texttt{int}}, \tag{4.11}$$

where

$$S_{\texttt{free}} = \frac{1}{2}\int d^4x\,(\phi\Box\phi) \tag{4.12}$$

and

$$S_{\texttt{int}} = \lambda\int d^4x\,(\phi\Box\phi\Box\phi)\,. \tag{4.13}$$

λ is a coupling constant and $\lambda \ll \mathcal{O}(1)$, so that we are within the perturbative limit. We will be working in Euclidean space; hence, the propagator in momentum space is then given by

$$\Pi(k^2) = \frac{-i}{k^2}, \tag{4.14}$$

while the vertex factor is given by

$$\lambda V(k_1, k_2, k_3) = 2i\lambda\left(k_1^2k_2^2 + k_2^2k_3^2 + k_3^2k_1^2\right), \tag{4.15}$$

where

$$k_1 + k_2 + k_3 = 0. \tag{4.16}$$

We can compute the tree-level amplitudes for the $s,\ t,\ u$ channels, see Fig. 4.1,

$$i\mathcal{T}^{\text{s-channel}}_{\text{tree-level}} = -\frac{25}{4}\lambda^2 s^4\left(\frac{i}{s}\right), \tag{4.17}$$

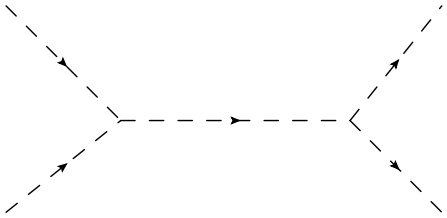

Figure 4.1: The s-channel, tree-level scattering diagram $p_1p_2 \to p_3p_4$.

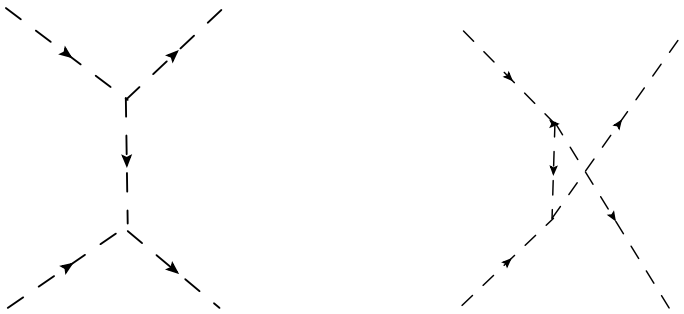

Figure 4.2: Left: The t-channel, tree-level scattering diagram $p_1p_2 \to p_3p_4$. Right: The u-channel, tree-level scattering diagram $p_1p_2 \to p_3p_4$ (it should be pointed out that the two outgoing momenta p_3, p_4 do not cross).

where $s = -(p_1 + p_2)^2$. Similarly, see Fig. 4.2 (left),

$$i\mathcal{T}^{\text{t-channel}}_{\text{tree-level}} = -4\lambda^2 s^2 \left(t + \frac{s}{4}\right)^2 \left(\frac{i}{t}\right) \tag{4.18}$$

and, see Fig. 4.2 (right),

$$i\mathcal{T}^{\text{u-channel}}_{\text{tree-level}} = -4\lambda^2 s^2 \left(u + \frac{s}{4}\right)^2 \left(\frac{i}{u}\right), \tag{4.19}$$

where $t = -(p_1 - p_3)^2$ and $u = -(p_1 - p_4)^2$. Hence, the total amplitude is given by:

$$\mathcal{T}_{\text{tree-level}} = -4\lambda^2 s^2 \left(\frac{\left(\frac{5s}{4}\right)^2}{s} + \frac{\left(t + \frac{s}{4}\right)^2}{t} + \frac{\left(u + \frac{s}{4}\right)^2}{u} \right). \tag{4.20}$$

Since the scattering matrix element $\mathcal{T}_{\text{tree-level}}$ in (4.20) blows up as $s \to -\infty$, the total cross section $\sigma_{\text{tree-level}}$ in the centre-of-mass (CM) frame also blows up as $s \to -\infty$.

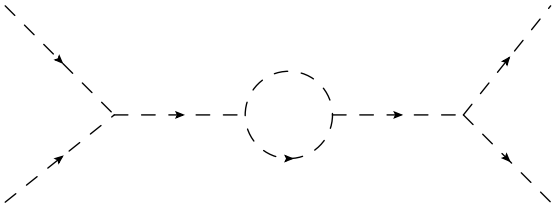

Figure 4.3: The s-channel, 1-loop scattering diagram $p_1p_2 \to p_3p_4$.

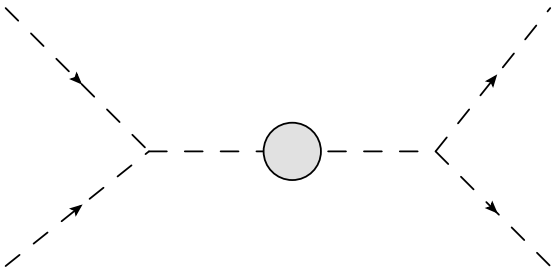

Figure 4.4: The s-channel, scattering diagram $p_1p_2 \to p_3p_4$ in which the bare propagator is replaced by the dressed propagator. The shaded blob indicates a dressed propagator.

4.2.1 Dressing the propagator

Since the tree-level amplitude blows up, we should now study the 1-loop, 2-point function in the propagator for the above interaction, see (4.11). We can compute the 1-loop, 2-point function with arbitrary external momentum, p. Therefore, regarding the 1-loop, 2-point function with external momenta p, $-p$ and symmetrical routing of momenta, we have that the 1-loop, 2-point function, $\Gamma_{2,1}(p^2)$, is given by

$$\begin{aligned}\Gamma_{2,1}(p^2) &= \frac{i\lambda^2}{2}\int^{\Lambda}\frac{d^4k}{(2\pi)^4}\frac{4\left[p^2(\frac{p}{2}-k)^2+p^2(\frac{p}{2}+k)^2+(\frac{p}{2}+k)^2(\frac{p}{2}-k)^2\right]^2}{(\frac{p}{2}-k)^2(\frac{p}{2}+k)^2}\\ &= \frac{i\lambda^2}{2}\int_0^{\Lambda}d\mathbf{k}\int_{-1}^{1}dx\frac{4\pi\mathbf{k}^3\sqrt{1-x^2}}{(2\pi)^4}\frac{4\left[p^2(\frac{p}{2}-k)^2+p^2(\frac{p}{2}+k)^2+(\frac{p}{2}+k)^2(\frac{p}{2}-k)^2\right]^2}{(\frac{p}{2}-k)^2(\frac{p}{2}+k)^2}\\ &= i\lambda^2\left(-\frac{p^8}{48\pi^2}+\frac{\Lambda^2p^6}{8\pi^2}+\frac{81\Lambda^4p^4}{256\pi^2}+\frac{17\Lambda^6p^2}{96\pi^2}+\frac{\Lambda^8}{32\pi^2}\right),\end{aligned} \tag{4.21}$$

where k is the internal loop momentum, x is the cosine of the angle between p and k ($p\cdot k = \mathbf{pk}x$, where $\mathbf{p}$ and $\mathbf{k}$ are the norms of p and k in Euclidean

space) and Λ is a hard cutoff. The counterterm, which is needed to cancel the divergences denoted by powers of Λ in (4.21), and which should be added to the action in (4.11), is given by

$$S_{\mathtt{ct}} = \frac{\lambda^2\Lambda^2}{16\pi^2}\int d^4x\left(\phi\Box^3\phi - \frac{81\Lambda^2}{32}\phi\Box^2\phi + \frac{17\Lambda^4}{12}\phi\Box\phi - \frac{\Lambda^6}{4}\phi^2\right), \tag{4.22}$$

which yields

$$\Gamma_{2,1,\mathtt{ct}}(p^2) = -\frac{i\lambda^2\Lambda^2}{8\pi^2}\left(p^6 + \frac{81\Lambda^2p^4}{32} + \frac{17\Lambda^4p^2}{12} + \frac{\Lambda^6}{4}\right). \tag{4.23}$$

Thus, the renormalised 1-loop, 2-point function, see Fig. 3.5 (top), is

$$\Gamma_{2,1\mathtt{r}}(p^2) = \Gamma_{2,1}(p^2) + \Gamma_{2,1,\mathtt{ct}}(p^2) = -\frac{i\lambda^2p^8}{48\pi^2}. \tag{4.24}$$

We observe that the maximum power of p appearing in the renormalised 1-loop, 2-point function with arbitrary external momenta, see (4.24), is p^8. Hence, in the UV, *i.e.*, in the limit $s \to -\infty$, $\Gamma_{2,1\mathtt{r}}(-s) \propto (p_1+p_2)^8 = s^4$, where $\Gamma_{2,1\mathtt{r}}$ is the renormalised 1-loop, 2-point function. Since

$$\begin{aligned} i\mathcal{T}_{1-\text{loop}} &= \lambda^2V(p_1,p_2,-p_1-p_2)V(-p_3,-p_4,p_1+p_2)\left(\frac{i}{s}\right)^2\Gamma_{2,1\mathtt{r}}(-s) \\ &+ \lambda^2V(p_1,-p_3,p_3-p_1)V(p_2,-p_4,p_1-p_3)\left(\frac{i}{t}\right)^2\Gamma_{2,1\mathtt{r}}(-t) \\ &+ \lambda^2V(p_1,-p_4,p_4-p_1)V(p_2,-p_3,p_1-p_4)\left(\frac{i}{u}\right)^2\Gamma_{2,1\mathtt{r}}(-u), \end{aligned} \tag{4.25}$$

the s-channel of $\mathcal{T}_{1-\text{loop}}$ (an s-channel diagram having a 1-loop subdiagram) goes as $s^2s^2s^{-2}s^4 = s^6$ when $s \to -\infty$, see Fig. 4.3 (the two bare propagators go as $1/s$ each while the two bare vertices go as s^2 each). Hence, as $s \to -\infty$, $\mathcal{T}^{\text{s-channel}}_{1-\text{loop}}$ diverges. $\mathcal{T}^{\text{t-channel}}_{1-\text{loop}}$ (a t-channel diagram having a 1-loop subdiagram) and $\mathcal{T}^{\text{u-channel}}_{1-\text{loop}}$ (a u-channel diagram having a 1-loop subdiagram) also diverge except for $\theta = 0$ and $\theta = \pi$, respectively.

Now what if we had an infinite series of loops in the scattering diagrams, see

Fig. 3.5 (bottom), that is, if we had replaced the bare propagator with the *dressed propagator*? As we shall see below, the external momentum dependence of the 1-loop, 2-point function shall actually determine the UV behaviour of the dressed propagator.

The dressed propagator, see Fig. 3.5 (bottom), represents the geometric series of all the graphs with 1-loop, 2-point insertions, analytically continued to the entire complex p^2-plane. Mathematically, the dressed propagator, $\widetilde{\Pi}(p^2)$, is given by [100]

$$\widetilde{\Pi}(p^2) = \frac{\Pi(p^2)}{1 - \Pi(p^2)\Gamma_{2,1\mathbf{r}}(p^2)}. \tag{4.26}$$

Hence, for our example, we have

$$\begin{aligned}\widetilde{\Pi}(p^2) &= \frac{-\frac{i}{p^2}}{1 - \left(-\frac{i}{p^2}\right)\left(-\frac{i\lambda^2 p^8}{48\pi^2}\right)} \\ &= \frac{-i}{p^2 + \frac{\lambda^2 p^8}{48\pi^2}}.\end{aligned} \tag{4.27}$$

When p^2 is large, p^8 dominates p^2 in the denominator of (4.27), and we have

$$\widetilde{\Pi}(p^2) \approx -\frac{48\pi^2 i}{\lambda^2 p^8}. \tag{4.28}$$

Since

$$\begin{aligned}i\mathcal{T}_{\text{dressed}} &= \lambda^2 V(p_1, p_2, -p_1 - p_2) V(-p_3, -p_4, p_1 + p_2)\widetilde{\Pi}(-s) \\ &+ \lambda^2 V(p_1, -p_3, p_3 - p_1) V(p_2, -p_4, p_1 - p_3)\widetilde{\Pi}(-t) \\ &+ \lambda^2 V(p_1, -p_4, p_4 - p_1) V(p_2, -p_3, p_1 - p_4)\widetilde{\Pi}(-u),\end{aligned} \tag{4.29}$$

then, if we replace the bare propagator with the dressed propagator in the tree-

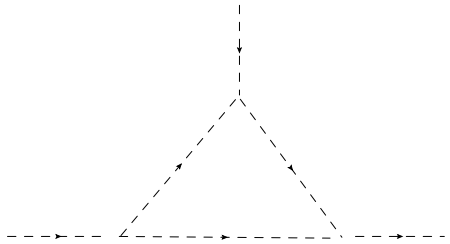

Figure 4.5: 1-loop, 3-point diagram with bare vertices and bare internal propagators and symmetrical routing of momenta. The external momenta are p_1, p_2, p_3 and the internal (that is, inside the loop) momenta are $k + \frac{p_1}{3} - \frac{p_2}{3}$, $k + \frac{p_2}{3} - \frac{p_3}{3}$, $k + \frac{p_3}{3} - \frac{p_1}{3}$.

level scattering diagrams, see Fig. 4.4, we will have

$$\mathcal{T}^{\text{s-channel}}_{\text{dressed}} = -\frac{25}{4}\lambda^2 \frac{s^3}{1 - \frac{\lambda^2 s^3}{48\pi^2}}, \tag{4.30}$$

$$\mathcal{T}^{\text{t-channel}}_{\text{dressed}} = -4\lambda^2 \left(\frac{3s}{4} - \frac{s}{2}\cos\theta\right)^2 \frac{2s}{(1-\cos\theta)\left[1 - \frac{\lambda^2 s^3 (1-\cos\theta)^3}{384\pi^2}\right]}, \tag{4.31}$$

$$\mathcal{T}^{\text{u-channel}}_{\text{dressed}} = -4\lambda^2 \left(\frac{3s}{4} + \frac{s}{2}\cos\theta\right)^2 \frac{2s}{(1+\cos\theta)\left[1 - \frac{\lambda^2 s^3 (1+\cos\theta)^3}{384\pi^2}\right]}. \tag{4.32}$$

Hence, we can make the following observations:

- $\mathcal{T}^{\text{s-channel}}_{\text{dressed}}$ does not blow up as $s \to -\infty$.
- $\mathcal{T}^{\text{t-channel}}_{\text{dressed}}$ blows up as $s \to -\infty$ when $\cos(\theta) = 1 \Rightarrow \theta = 0$.
- Similarly, $\mathcal{T}^{\text{u-channel}}_{\text{dressed}}$ blows up as $s \to -\infty$ when $\cos(\theta) = -1 \Rightarrow \theta = \pi$.

Since we have that $\mathcal{T}_{\text{dressed}} = \mathcal{T}^{\text{s-channel}}_{\text{dressed}} + \mathcal{T}^{\text{t-channel}}_{\text{dressed}} + \mathcal{T}^{\text{u-channel}}_{\text{dressed}}$, one can verify that the total cross section σ_{dressed} corresponding to $\mathcal{T}_{\text{dressed}}$ blows up as $s \to -\infty$. To summarise, the dressed propagator is not sufficient to prevent the scattering diagram from blowing up as $s \to -\infty$ since the polynomial suppression coming from the dressed propagator cannot overcome the polynomial enhancement originating from the two bare vertices in Fig. 4.4. In Section 4.2.2, we shall dress the vertices to see whether we can eliminate the external momentum divergences of the scattering diagrams.

As a prelude to Section 4.2.2, suppose we consider a 1-loop, 3-point diagram, see Fig. 4.5, with external momenta p_1, p_2 and p_3 (we assume that the propagators and the vertices are bare), and symmetrical routing of momenta. Then the propagators in the 1-loop triangle are given by

$$-i\left(k+\frac{p_1}{3}-\frac{p_2}{3}\right)^{-2},\ -i\left(k+\frac{p_2}{3}-\frac{p_3}{3}\right)^{-2},\ -i\left(k+\frac{p_3}{3}-\frac{p_1}{3}\right)^{-2},$$

and the vertex factors are given by

$$2i\lambda\left(p_2^2\left(k+\frac{p_1}{3}-\frac{p_2}{3}\right)^2+p_2^2\left(k+\frac{p_2}{3}-\frac{p_3}{3}\right)^2+\left(k+\frac{p_1}{3}-\frac{p_2}{3}\right)^2\left(k+\frac{p_2}{3}-\frac{p_3}{3}\right)^2\right),$$
$$2i\lambda\left(p_3^2\left(k+\frac{p_2}{3}-\frac{p_3}{3}\right)^2+p_3^2\left(k+\frac{p_3}{3}-\frac{p_1}{3}\right)^2+\left(k+\frac{p_2}{3}-\frac{p_3}{3}\right)^2\left(k+\frac{p_3}{3}-\frac{p_1}{3}\right)^2\right),$$
$$2i\lambda\left(p_1^2\left(k+\frac{p_3}{3}-\frac{p_1}{3}\right)^2+p_1^2\left(k+\frac{p_1}{3}-\frac{p_2}{3}\right)^2+\left(k+\frac{p_3}{3}-\frac{p_1}{3}\right)^2\left(k+\frac{p_1}{3}-\frac{p_2}{3}\right)^2\right).$$

Hence, the 1-loop, 3-point diagram, $\Gamma_{3,1}(p^2)$, will be given by

$$\begin{aligned}\Gamma_{3,1}(p^2)=i\lambda^3\int^{\Lambda}\frac{d^4k}{(2\pi)^4}\Bigg[&\frac{8}{\left(k+\frac{p_1}{3}-\frac{p_2}{3}\right)^2\left(k+\frac{p_2}{3}-\frac{p_3}{3}\right)^2\left(k+\frac{p_3}{3}-\frac{p_1}{3}\right)^2}\\&\times\left(p_2^2\left(k+\frac{p_1}{3}-\frac{p_2}{3}\right)^2+p_2^2\left(k+\frac{p_2}{3}-\frac{p_3}{3}\right)^2+\left(k+\frac{p_1}{3}-\frac{p_2}{3}\right)^2\left(k+\frac{p_2}{3}-\frac{p_3}{3}\right)^2\right)\\&\times\left(p_3^2\left(k+\frac{p_2}{3}-\frac{p_3}{3}\right)^2+p_3^2\left(k+\frac{p_3}{3}-\frac{p_1}{3}\right)^2+\left(k+\frac{p_2}{3}-\frac{p_3}{3}\right)^2\left(k+\frac{p_3}{3}-\frac{p_1}{3}\right)^2\right)\\&\times\left(p_1^2\left(k+\frac{p_3}{3}-\frac{p_1}{3}\right)^2+p_1^2\left(k+\frac{p_1}{3}-\frac{p_2}{3}\right)^2+\left(k+\frac{p_3}{3}-\frac{p_1}{3}\right)^2\left(k+\frac{p_1}{3}-\frac{p_2}{3}\right)^2\right)\Bigg].\end{aligned}\tag{4.33}$$

After integration with respect to the internal loop momentum k and renormalisation of the loop integral divergences, *i.e.*, the terms involving powers of Λ (Λ is a hard cutoff), by adding appropriate counterterms involving powers of Λ to the action so that no powers of Λ remain in the renormalised action, we are left with a polynomial function of the three external momenta p_1, p_2, p_3, that is, we have an expression of the form $\sum_{\alpha,\beta,\gamma}p_1^{2\alpha}p_2^{2\beta}p_3^{2\gamma}$, where α,β,γ are parameters. We will

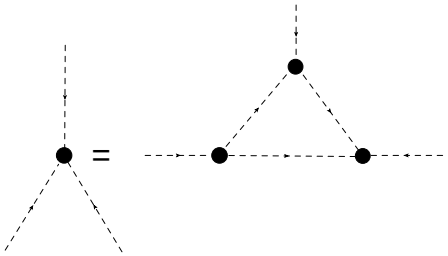

Figure 4.6: 3-point diagram constructed out of lower-loop 2-point & 3-point diagrams. The dark blobs indicate renormalised vertex corrections and the dashed lines inside the triangle denote bare internal propagators. The loop order of the dark blob on the left is n while the loop order of the dark blobs on the right is $n-1$. The external momenta are p_1, p_2, p_3 and the internal (that is, inside the loop) momenta are $k+\frac{p_1}{3}-\frac{p_2}{3}$, $k+\frac{p_2}{3}-\frac{p_3}{3}$, $k+\frac{p_3}{3}-\frac{p_1}{3}$.

require these computations in the following subsection.

4.2.2 Dressing the vertices by making vertex loop corrections to the bare vertices

Based on the results of Section 4.2.1, suppose we want to dress the vertices by making renormalised vertex loop corrections to the bare vertices at the left- and right-ends of the scattering diagrams, see Fig. 4.6. As we saw in (4.33), both the bare propagators and the bare vertices can be written in terms of powers of momenta. After integration with respect to the internal loop momentum k, we obtain a polynomial expression involving powers of the external momenta p_1, p_2, p_3. As the loop-order increases, the 3-point function can still be written as a polynomial function of the external momenta; this happens because, as previously, the (bare) propagators are polynomials in momenta while the (dressed) vertices are also polynomials in momenta. Therefore, we expect the external momentum dependence of the 3-point function, see Fig 4.6, in the UV limit, *i.e.*, as $p_i^2 \to \infty$, where $i=1,2,3$, in terms of the three external momenta, p_1, p_2, p_3, to follow as:

$$\Gamma_3 \xrightarrow{UV} \sum_{\alpha,\beta,\gamma} p_1^{2\alpha} p_2^{2\beta} p_3^{2\gamma}, \tag{4.34}$$

with the convention

$$\alpha \geq \beta \geq \gamma. \tag{4.35}$$

The reason we expect the external momentum dependence of 3-point function to be given by (4.34) is that, once all the (lower-) loop subdiagrams have been integrated out, what remains are polynomial expressions in terms of the corresponding external momenta. Some of these external momenta can then become the internal loop momentum in a subsequent higher-loop diagram.

First, let us consider how one can get the largest sum of all the exponents, *i.e.*, $\alpha + \beta + \gamma$. Although all the arguments below can be conducted for three different sets of exponents in the three 3-point vertices making up the 1-loop triangle, see Fig. 4.6, for simplicity, here we will look at what happens when all the three vertices have the same exponents.

Clearly, the best way to obtain the largest exponents for the external momenta is to have the α exponent correspond to the external momenta. Assuming a symmetric distribution of (β, γ) among the internal loops and considering the n-loop, 3-point diagram with symmetrical routing of momenta, see Fig. 4.6, the propagators in the 1-loop triangle are given by

$$-i\left(k + \frac{p_1}{3} - \frac{p_2}{3}\right)^{-2},\ -i\left(k + \frac{p_2}{3} - \frac{p_3}{3}\right)^{-2},\ -i\left(k + \frac{p_3}{3} - \frac{p_1}{3}\right)^{-2},$$

and the vertex factors are (the superscripts in α^{n-1}, β^{n-1}, γ^{n-1} denote the loop-order; clearly, they are not powers)

$$\begin{aligned}
&ip_1^{2\alpha^{n-1}}\left(k + \frac{p_3}{3} - \frac{p_1}{3}\right)^{2\beta^{n-1}}\left(k + \frac{p_1}{3} - \frac{p_2}{3}\right)^{2\gamma^{n-1}},\\
&ip_2^{2\alpha^{n-1}}\left(k + \frac{p_1}{3} - \frac{p_2}{3}\right)^{2\beta^{n-1}}\left(k + \frac{p_2}{3} - \frac{p_3}{3}\right)^{2\gamma^{n-1}},\\
&ip_3^{2\alpha^{n-1}}\left(k + \frac{p_2}{3} - \frac{p_3}{3}\right)^{2\beta^{n-1}}\left(k + \frac{p_3}{3} - \frac{p_1}{3}\right)^{2\gamma^{n-1}}.
\end{aligned}$$

Conservation of momenta then yields, in the UV, *i.e.*, as $p_i^2 \to \infty$, where

$i = 1, 2, 3$, and $\Gamma_{3,n}$ is the n-loop, 3-point function,

$$\Gamma_{3,n} \longrightarrow \int \frac{\mathrm{d}^4 k}{(2\pi)^4} \left[\frac{p_1^{2\alpha^{n-1}} p_2^{2\alpha^{n-1}} p_3^{2\alpha^{n-1}}}{\left(k + \frac{p_1}{3} - \frac{p_2}{3}\right)^2 \left(k + \frac{p_2}{3} - \frac{p_3}{3}\right)^2 \left(k + \frac{p_3}{3} - \frac{p_1}{3}\right)^2} \right.$$
$$\left. \times \left(k + \frac{p_1}{3} - \frac{p_2}{3}\right)^{2(\beta^{n-1}+\gamma^{n-1})} \left(k + \frac{p_2}{3} - \frac{p_3}{3}\right)^{2(\beta^{n-1}+\gamma^{n-1})} \left(k + \frac{p_3}{3} - \frac{p_1}{3}\right)^{2(\beta^{n-1}+\gamma^{n-1})} \right], \tag{4.36}$$

where p_1, p_2, p_3 are the external momenta for the 1-loop triangle and the superscript in the α, β, γ indicates that these are coefficients that one obtains from contributions up to $n-1$ loop level. Now, let us proceed to obtain the n-th loop coefficients. We obtain from (4.36) that

$$\alpha^n = \beta^n = \gamma^n = \alpha^{n-1} + 2(\beta^{n-1} + \gamma^{n-1}). \tag{4.37}$$

For 3-point bare vertices, we have now $\alpha^0 = \beta^0 = 1$ and $\gamma^0 = 0$. As n increases, α^n, β^n and γ^n increase; this means that, as the number of loops increases, the external momentum dependences of the dressed vertices become larger and larger as the external momenta become larger.

If we now dress the vertices by making renormalised vertex loop corrections to the bare vertices at the left- and right-ends of the tree-level scattering diagrams, we will have, see Fig. 4.7 (for $n \geq 1$, $\alpha^n = \beta^n = \gamma^n$),

$$\mathcal{T}^{\mathrm{s-channel}}_{\text{vertex corrections}} \sim s^{2\alpha^n} \left(\frac{s}{2}\right)^{4\alpha^n} \frac{1}{s}, \tag{4.38}$$

$$\mathcal{T}^{\mathrm{t-channel}}_{\text{vertex corrections}} \sim t^{2\alpha^n} \left(\frac{s}{2}\right)^{4\alpha^n} \frac{1}{t} = \left[\frac{s}{2}(1 - \cos\theta)\right]^{2\alpha^n - 1} \left(\frac{s}{2}\right)^{4\alpha^n}, \tag{4.39}$$

$$\mathcal{T}^{\mathrm{u-channel}}_{\text{vertex corrections}} \sim u^{2\alpha^n} \left(\frac{s}{2}\right)^{4\alpha^n} \frac{1}{u} = \left[\frac{s}{2}(1 + \cos\theta)\right]^{2\alpha^n - 1} \left(\frac{s}{2}\right)^{4\alpha^n}. \tag{4.40}$$

Since $\alpha^0 = \beta^0 = 1$ and $\gamma^0 = 0$, using (4.37), we can see that $\alpha^1 = 3$; therefore, $\alpha^n \geq 3$ for $n \geq 1$. Hence, we can make the following observations from the above expressions:

- $\mathcal{T}^{\mathrm{s-channel}}_{\text{vertex corrections}}$ blows up as $s \to -\infty$.

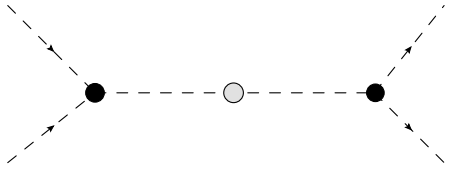

Figure 4.7: An s-channel scattering diagram $p_1p_2 \to p_3p_4$. The shaded blob indicates a dressed propagator and the dark blobs indicate renormalised vertex corrections.

- $\mathcal{T}^{\text{t-channel}}_{\text{vertex corrections}}$ blows up as $s \to -\infty$ except when $\cos(\theta) = 1 \Rightarrow \theta = 0$.
- Similarly, $\mathcal{T}^{\text{u-channel}}_{\text{vertex corrections}}$ blows up as $s \to -\infty$ except when $\cos(\theta) = -1 \Rightarrow \theta = \pi$.

Thus, one can check that the cross section $\sigma_{\text{dressed vertices}}$ corresponding to $\mathcal{T}_{\text{vertex corrections}} = \mathcal{T}^{\text{s-channel}}_{\text{vertex corrections}} + \mathcal{T}^{\text{t-channel}}_{\text{vertex corrections}} + \mathcal{T}^{\text{u-channel}}_{\text{vertex corrections}}$ blows up as $s \to -\infty$.

We see that dressing the vertices by making just vertex loop corrections to the bare vertices does not ameliorate the external momentum growth of scattering diagrams in the UV in our example, see (4.11). In fact, it makes the growth increase. In the next subsection, we shall dress the vertices by making both propagator and vertex loop corrections to the bare vertices at the left- and right-ends of the scattering diagrams.

4.2.3 Dressing the vertices by making propagator & vertex loop corrections to the bare vertices

In this subsection, we shall dress the vertices by making renormalised propagator and vertex loop corrections to the bare vertices at the left- and right-ends of the scattering diagrams, see Fig. 3.9 (right). Again, we expect the external momentum dependence of the 3-point function to be given in the UV limit, *i.e.*, as $p_i^2 \to \infty$, where $i = 1, 2, 3$, by (4.34).

As previously, the best way to obtain the largest exponents for the external momenta is to have the α exponent correspond to the external momenta. Assuming a symmetric distribution of (β, γ) among the internal loops and considering

the n-loop, 3-point diagram with symmetrical routing of momenta, see Fig. 3.9 (right), the dressed propagators in the 1-loop triangle are

$$-i\left(k+\frac{p_1}{3}-\frac{p_2}{3}\right)^{-8},\ -i\left(k+\frac{p_2}{3}-\frac{p_3}{3}\right)^{-8},\ -i\left(k+\frac{p_3}{3}-\frac{p_1}{3}\right)^{-8},$$

while the vertex factors are

$$\begin{aligned}
&ip_1^{2\alpha^{n-1}}\left(k+\frac{p_3}{3}-\frac{p_1}{3}\right)^{2\beta^{n-1}}\left(k+\frac{p_1}{3}-\frac{p_2}{3}\right)^{2\gamma^{n-1}},\\
&ip_2^{2\alpha^{n-1}}\left(k+\frac{p_1}{3}-\frac{p_2}{3}\right)^{2\beta^{n-1}}\left(k+\frac{p_2}{3}-\frac{p_3}{3}\right)^{2\gamma^{n-1}},\\
&ip_3^{2\alpha^{n-1}}\left(k+\frac{p_2}{3}-\frac{p_3}{3}\right)^{2\beta^{n-1}}\left(k+\frac{p_3}{3}-\frac{p_1}{3}\right)^{2\gamma^{n-1}}.
\end{aligned}$$

Conservation of momenta then yields, in the UV, *i.e.*, as $p_i^2\to\infty$, where $i=1,2,3$,

$$\begin{aligned}
\Gamma_{3,n}\longrightarrow\int\frac{\mathrm{d}^4k}{(2\pi)^4}\Bigg[&\frac{p_1^{2\alpha^{n-1}}p_2^{2\alpha^{n-1}}p_3^{2\alpha^{n-1}}}{\left(k+\frac{p_1}{3}-\frac{p_2}{3}\right)^8\left(k+\frac{p_2}{3}-\frac{p_3}{3}\right)^8\left(k+\frac{p_3}{3}-\frac{p_1}{3}\right)^8}\\
&\times\left(k+\frac{p_1}{3}-\frac{p_2}{3}\right)^{2(\beta^{n-1}+\gamma^{n-1})}\left(k+\frac{p_2}{3}-\frac{p_3}{3}\right)^{2(\beta^{n-1}+\gamma^{n-1})}\left(k+\frac{p_3}{3}-\frac{p_1}{3}\right)^{2(\beta^{n-1}+\gamma^{n-1})}\Bigg],
\end{aligned}\tag{4.41}$$

where p_1, p_2, p_3 are the external momenta for the 1-loop triangle and the superscript in the α,β,γ indicates that these are coefficients that one obtains from contributions up to $n-1$ loop level. Now, let us proceed to obtain the n-th loop coefficients by inspecting (4.41), we have

$$\alpha^n=\beta^n=\gamma^n=\alpha^{n-1}+2(\beta^{n-1}+\gamma^{n-1}).\tag{4.42}$$

For the 3-point bare vertices, we have that $\alpha^0=\beta^0=1$ and $\gamma^0=0$. As n increases, α^n, β^n and γ^n increase; this means that, as the number of loops increases, the external momentum growth of the dressed vertices increases.

If we now dress the vertices by making renormalised propagator and vertex loop corrections to the bare vertices at the left- and right-ends of the tree-level

scattering diagrams, see Fig. 4.7, we obtain, as $s \to -\infty$,

$$\mathcal{T}^{\text{s-channel}}_{\text{both corrections}} \sim s^{2\alpha^n} \left(\frac{s}{2}\right)^{4\alpha^n} \frac{1}{s^4}, \tag{4.43}$$

$$\mathcal{T}^{\text{t-channel}}_{\text{both corrections}} \sim t^{2\alpha^n} \left(\frac{s}{2}\right)^{4\alpha^n} \frac{1}{t^4} = \left[\frac{s}{2}(1-\cos\theta)\right]^{2\alpha^n-4} \left(\frac{s}{2}\right)^{4\alpha^n}, \tag{4.44}$$

$$\mathcal{T}^{\text{u-channel}}_{\text{both corrections}} \sim u^{2\alpha^n} \left(\frac{s}{2}\right)^{4\alpha^n} \frac{1}{u^4} = \left[\frac{s}{2}(1+\cos\theta)\right]^{2\alpha^n-4} \left(\frac{s}{2}\right)^{4\alpha^n}. \tag{4.45}$$

Since $\alpha^n \geq 3$ for $n \geq 1$, we can make the following observations:

- $\mathcal{T}^{\text{s-channel}}_{\text{both corrections}}$ blows up as $s \to -\infty$.
- $\mathcal{T}^{\text{t-channel}}_{\text{both corrections}}$ blows up as $s \to -\infty$ except when $\cos(\theta) = 1 \Rightarrow \theta = 0$.
- Similarly, $\mathcal{T}^{\text{u-channel}}_{\text{both corrections}}$ blows up as $s \to -\infty$ except when $\cos(\theta) = -1 \Rightarrow \theta = \pi$.

Thus, one can check that the cross section $\sigma_{\text{both corrections}}$ corresponding to $\mathcal{T}_{\text{both corrections}} = \mathcal{T}^{\text{s-channel}}_{\text{both corrections}} + \mathcal{T}^{\text{t-channel}}_{\text{both corrections}} + \mathcal{T}^{\text{u-channel}}_{\text{both corrections}}$ blows up as $s \to -\infty$.

We see that dressing the vertices by making propagator and vertex loop corrections to the bare vertices cannot ameliorate the UV external momentum growth of scattering diagrams in our toy model example given by (4.11). This motivates us to consider something very different; in the following section, we shall not consider a finite-order, higher-derivative theory, but an infinite-derivative massless scalar field theory with cubic interaction in ϕ. Both the free and interaction parts of the action will contain infinite derivatives.

4.3 Scatterings in infinite derivative theory

We saw in Section 4.2 that, within the context of a finite-order higher-derivative scalar toy model, we cannot tame the UV external momentum growth appearing in scattering diagrams. In particular, we need to "soften" the external momentum contributions coming from the dressed vertices; as we saw in Sections 4.2.2 & 4.2.3, dressing the vertices in a finite-order higher-derivative toy

model cannot help us tame the external momentum growth of the scattering diagrams. Since this is not possible for a finite-order higher-derivative toy model, we shall examine an infinite derivative scalar toy model. Therefore, let us consider the following action, which has a cubic interaction where $\lambda \ll \mathcal{O}(1)$, and treat it perturbatively:

$$S = \int d^4x \left[\frac{1}{2}\phi\Box a(\bar{\Box})\phi + \lambda\phi\Box\phi a(\bar{\Box})\phi\right]. \tag{4.46}$$

Now, let us demand that the propagator for free action retains *only* the massless scalar degree of freedom. In which case, we assume that the kinetic term obtains an *entire function* correction. For simplicity, we take such a function to be Gaussian:

$$a(\bar{\Box}) = e^{-\bar{\Box}}, \tag{4.47}$$

where $\bar{\Box} \equiv \Box/M^2$and M is the mass scale at which the non-local modifications become important. When a is an entire function having no zeroes, the infinite derivative theory can be made ghost-free [56, 87]. Such a choice of $a(\bar{\Box})$ is also well motivated by p-adic strings [22]. The propagator in momentum space is then given in Euclidean space by

$$\Pi(k^2) = \frac{-i}{k^2 e^{\bar{k}^2}}, \tag{4.48}$$

where barred 4-momentum vectors denote $\bar{k} = k/M$. The vertex factor for three incoming momenta $k_1,\ k_2,\ k_3$ satisfying the following conservation law,

$$k_1 + k_2 + k_3 = 0, \tag{4.49}$$

is given by

$$\lambda V(k_1, k_2, k_3) = -i\lambda\left[k_1^2(e^{\bar{k}_2^2} + e^{\bar{k}_3^2}) + k_2^2(e^{\bar{k}_3^2} + e^{\bar{k}_1^2}) + k_3^2(e^{\bar{k}_1^2} + e^{\bar{k}_2^2})\right]. \tag{4.50}$$

We can compute the tree-level s, t, u channels in the CM frame and we obtain

$$i\mathcal{T}^{\text{s-channel}}_{\text{tree-level}} = -\lambda^2 s^2 \left[3e^{-s/2M^2} + e^{-s/M^2}\right]^2 \left(\frac{i}{se^{-s/M^2}}\right), \tag{4.51}$$

$$i\mathcal{T}^{\text{t-channel}}_{\text{tree-level}} = -\lambda^2 \left[(s+2t)e^{-s/2M^2} + se^{-t/M^2}\right]^2 \left(\frac{i}{te^{-t/M^2}}\right), \tag{4.52}$$

$$i\mathcal{T}^{\text{u-channel}}_{\text{tree-level}} = -\lambda^2 \left[(s+2u)e^{-s/2M^2} + se^{-u/M^2}\right]^2 \left(\frac{i}{ue^{-u/M^2}}\right). \tag{4.53}$$

We note that, as $s \to -\infty$, $\mathcal{T}_{\text{tree-level}} = \mathcal{T}^{\text{s-channel}}_{\text{tree-level}} + \mathcal{T}^{\text{t-channel}}_{\text{tree-level}} + \mathcal{T}^{\text{u-channel}}_{\text{tree-level}}$ blows up.

Now, in order to compute the dressed propagator, we have, first, to write down the 1-loop, 2-point function with external momenta p and $-p$. We have

$$\begin{aligned}\Gamma_{2,1}(p^2) = \frac{i\lambda^2}{2}\int \frac{d^4k}{(2\pi)^4} &\frac{1}{(\frac{p}{2}+k)^2(\frac{p}{2}-k)^2 e^{(\frac{\bar{p}}{2}+\bar{k})^2} e^{(\frac{\bar{p}}{2}-\bar{k})^2}} \\ &\times \left[p^2(e^{(\frac{\bar{p}}{2}+\bar{k})^2} + e^{(\frac{\bar{p}}{2}-\bar{k})^2}) + (\frac{p}{2}+k)^2(e^{\bar{p}^2} + e^{(\frac{\bar{p}}{2}-\bar{k})^2}) + (\frac{p}{2}-k)^2(e^{\bar{p}^2} + e^{(\frac{\bar{p}}{2}+\bar{k})^2})\right]^2.\end{aligned} \tag{4.54}$$

After renormalising the divergent (in terms of the internal loop momentum k^μ) terms [1], we have that the most divergent part (in terms of the external momentum p^μ) of the 1-loop, 2-point function is given by (see also (3.48) & (3.49))

$$\frac{i\lambda^2 M^4 e^{\frac{3\bar{p}^2}{2}}(4M^2+p^2)}{32\pi^2 p^2}.$$

Thus, the renormalised 1-loop, 2-point function goes as $(1+4\bar{p}^{-2})e^{\frac{3\bar{p}^2}{2}}$ when p^2 is large.

As $s \to -\infty$, the renormalised 1-loop, 2-point function $\Gamma_{2,1\text{r}}(-s)$ goes as

[1] Within the context of dimensional regularisation, we obtain an ϵ^{-1} pole, where $\epsilon = 4 - D$ and D is the dimensionality of spacetime.

$e^{-\frac{3s}{2M^2}}$. Since

$$\begin{aligned} i\mathcal{T}_{1-\text{loop}} &= \lambda^2 V(p_1, p_2, -p_1-p_2)V(-p_3, -p_4, p_1+p_2)\left(\frac{i}{se^{-s/M^2}}\right)^2 \Gamma_{2,1\mathbf{r}}(-s) \\ &+ \lambda^2 V(p_1, -p_3, p_3-p_1)V(p_2, -p_4, p_1-p_3)\left(\frac{i}{te^{-t/M^2}}\right)^2 \Gamma_{2,1\mathbf{r}}(-t) \\ &+ \lambda^2 V(p_1, -p_4, p_4-p_1)V(p_2, -p_3, p_1-p_4)\left(\frac{i}{ue^{-u/M^2}}\right)^2 \Gamma_{2,1\mathbf{r}}(-u), \end{aligned} \tag{4.55}$$

we have that the s-channel of $\mathcal{T}_{1-\text{loop}}$, see again Fig. 4.3, goes as $e^{-\frac{2s}{M^2}} e^{\frac{2s}{M^2}} e^{-\frac{3s}{2M^2}} = e^{-\frac{3s}{2M^2}}$ when $s \to -\infty$. Hence, as $s \to -\infty$, $\mathcal{T}_{1-\text{loop}}^{\text{s-channel}}$ diverges. $\mathcal{T}_{1-\text{loop}}^{\text{t-channel}}$ and $\mathcal{T}_{1-\text{loop}}^{\text{u-channel}}$ also diverge as $s \to -\infty$.

4.3.1 Dressing the propagator

Since, for large p^2, the dressed propagator goes as

$$\widetilde{\Pi}(p^2) \approx (1 + 4\bar{p}^{-2})^{-1} e^{-\frac{3\bar{p}^2}{2}}, \tag{4.56}$$

we observe that the dressed propagator is more strongly exponentially suppressed than the bare propagator.

Since

$$\begin{aligned} i\mathcal{T}_{\text{dressed}} &= \lambda^2 V(p_1, p_2, -p_1-p_2)V(-p_3, -p_4, p_1+p_2)\widetilde{\Pi}(-s) \\ &+ \lambda^2 V(p_1, -p_3, p_3-p_1)V(p_2, -p_4, p_1-p_3)\widetilde{\Pi}(-t) \\ &+ \lambda^2 V(p_1, -p_4, p_4-p_1)V(p_2, -p_3, p_1-p_4)\widetilde{\Pi}(-u), \end{aligned} \tag{4.57}$$

then, if we now replace the bare propagator with the dressed propagator in the

tree-level scattering diagrams, see Fig. 4.4 (bottom), we will have, as $s \to -\infty$,

$$\mathcal{T}^{\text{s-channel}}_{\text{dressed}} \sim \left[3e^{-\frac{s}{2M^2}} + e^{-\frac{s}{M^2}}\right]^2 e^{\frac{3s}{2M^2}} \sim e^{-\frac{s}{2M^2}}, \tag{4.58}$$

$$\mathcal{T}^{\text{t-channel}}_{\text{dressed}} \sim \left[(s+2t)e^{-\frac{s}{2M^2}} + se^{-\frac{t}{M^2}}\right]^2 e^{\frac{3t}{2M^2}} = \left[s(2-\cos\theta)e^{-\frac{s}{2M^2}} + se^{-\frac{s(1-\cos\theta)}{2M^2}}\right]^2 e^{\frac{3s(1-\cos\theta)}{4M^2}}, \tag{4.59}$$

$$\mathcal{T}^{\text{u-channel}}_{\text{dressed}} \sim \left[(s+2u)e^{-\frac{s}{2M^2}} + se^{-\frac{u}{M^2}}\right]^2 e^{\frac{3u}{2M^2}} = \left[s(2+\cos\theta)e^{-\frac{s}{2M^2}} + se^{-\frac{s(1+\cos\theta)}{2M^2}}\right]^2 e^{\frac{3s(1+\cos\theta)}{4M^2}}. \tag{4.60}$$

Hence, we can make the following observations:

- $\mathcal{T}^{\text{s-channel}}_{\text{dressed}}$ blows up as $s \to -\infty$.
- $\mathcal{T}^{\text{t-channel}}_{\text{dressed}}$ blows up as $s \to -\infty$ for all values of θ.
- $\mathcal{T}^{\text{u-channel}}_{\text{dressed}}$ blows up as $s \to -\infty$ for all values of θ.

Since $\mathcal{T}_{\text{dressed}} = \mathcal{T}^{\text{s-channel}}_{\text{dressed}} + \mathcal{T}^{\text{t-channel}}_{\text{dressed}} + \mathcal{T}^{\text{u-channel}}_{\text{dressed}}$, one can verify that the total cross section σ_{dressed} corresponding to $\mathcal{T}_{\text{dressed}}$ blows up as $s \to -\infty$. We also observe that the external momentum dependence of $\mathcal{T}_{\text{dressed}}$ exhibits less growth for large external momenta as compared to the external momentum dependence of $\mathcal{T}_{\text{tree-level}}$ (or $\mathcal{T}_{1-\text{loop}}$).

To conclude, the use of the dressed propagator ameliorates the external momentum growth of the scattering diagrams, but this is not sufficient by itself. In Section 4.3.2, we shall dress the vertices to see whether we can eliminate the external momentum growth of the scattering diagrams.

4.3.2 Dressing the vertices by making vertex loop corrections to the bare vertices

In this subsection, we shall dress the vertices by making renormalised vertex loop corrections to the bare vertices at the left- and right-ends of the scattering diagrams, see Fig. 4.6. We have that both the bare propagators and the bare vertices can be written as exponentials in momenta; after integration with respect to the internal loop momentum k, we obtain an exponential expression where the

exponents are in terms of the external momenta p_1, p_2, p_3. As the loop-order increases, the 3-point function can still be written as an exponential function of the external momenta; this happens because, as previously, the (bare) propagators are exponentials in momenta while the (dressed) vertices are also exponentials in momenta. Thus, in the UV limit, *i.e.*, as $p_i^2 \to \infty$, where $i = 1, 2, 3$, the 3-point function, again see Fig. 4.6, can be written as

$$\Gamma_3 \xrightarrow{UV} \sum_{\alpha,\beta,\gamma} e^{\alpha\bar{p}_1^2+\beta\bar{p}_2^2+\gamma\bar{p}_3^2}, \tag{4.61}$$

with the convention

$$\alpha \geq \beta \geq \gamma, \tag{4.62}$$

where p_1, p_2, p_3 are the three external momenta. The reason we expect the external momentum dependence of the 3-point function to be given by (4.61) is that, once all the lower-loop subdiagrams have been integrated out, what remains are exponential expressions in terms of the three external momenta p_1, p_2, p_3.

The best way to obtain the largest exponents for the external momenta is to have the α exponent correspond to the external momenta. Assuming a symmetric distribution of (β, γ) among the internal loops and considering the n-loop, 3-point diagram with symmetrical routing of momenta, see Fig. 4.6, the propagators in the 1-loop triangle are given by

$$e^{-\left(\bar{k}+\frac{\bar{p}_1}{3}-\frac{\bar{p}_2}{3}\right)^2},\ e^{-\left(\bar{k}+\frac{\bar{p}_2}{3}-\frac{\bar{p}_3}{3}\right)^2},\ e^{-\left(\bar{k}+\frac{\bar{p}_3}{3}-\frac{\bar{p}_1}{3}\right)^2},$$

and the vertex factors are (the superscripts on α^{n-1}, β^{n-1}, γ^{n-1} are clearly not powers)

$$\begin{aligned}
&e^{\alpha^{n-1}\bar{p}_1^2+\beta^{n-1}\left(\bar{k}+\frac{\bar{p}_3}{3}-\frac{\bar{p}_1}{3}\right)^2+\gamma^{n-1}\left(\bar{k}+\frac{\bar{p}_1}{3}-\frac{\bar{p}_2}{3}\right)^2},\\
&e^{\alpha^{n-1}\bar{p}_2^2+\beta^{n-1}\left(\bar{k}+\frac{\bar{p}_1}{3}-\frac{\bar{p}_2}{3}\right)^2+\gamma^{n-1}\left(\bar{k}+\frac{\bar{p}_2}{3}-\frac{\bar{p}_3}{3}\right)^2},\\
&e^{\alpha^{n-1}\bar{p}_3^2+\beta^{n-1}\left(\bar{k}+\frac{\bar{p}_2}{3}-\frac{\bar{p}_3}{3}\right)^2+\gamma^{n-1}\left(\bar{k}+\frac{\bar{p}_3}{3}-\frac{\bar{p}_1}{3}\right)^2}.
\end{aligned}$$

Conservation of momenta then yields, in the UV, *i.e.*, as $p_i^2 \to \infty$, where

$i = 1, 2, 3$, and $\Gamma_{3,n}$ is the n-loop, 3-point function,

$$\Gamma_{3,n} \longrightarrow \int \frac{d^4k}{(2\pi)^4} \left[\frac{e^{\alpha^{n-1}\bar{p}_1^2 + \beta^{n-1}\left(\bar{k}+\frac{\bar{p}_3}{3}-\frac{\bar{p}_1}{3}\right)^2 + \gamma^{n-1}\left(\bar{k}+\frac{\bar{p}_1}{3}-\frac{\bar{p}_2}{3}\right)^2}}{e^{-\left(\bar{k}+\frac{\bar{p}_1}{3}-\frac{\bar{p}_2}{3}\right)^2} e^{-\left(\bar{k}+\frac{\bar{p}_2}{3}-\frac{\bar{p}_3}{3}\right)^2} e^{-\left(\bar{k}+\frac{\bar{p}_3}{3}-\frac{\bar{p}_1}{3}\right)^2}} \right.$$
$$\left. \times \; e^{\alpha^{n-1}\bar{p}_2^2 + \beta^{n-1}\left(\bar{k}+\frac{\bar{p}_1}{3}-\frac{\bar{p}_2}{3}\right)^2 + \gamma^{n-1}\left(\bar{k}+\frac{\bar{p}_2}{3}-\frac{\bar{p}_3}{3}\right)^2} e^{\alpha^{n-1}\bar{p}_3^2 + \beta^{n-1}\left(\bar{k}+\frac{\bar{p}_2}{3}-\frac{\bar{p}_3}{3}\right)^2 + \gamma^{n-1}\left(\bar{k}+\frac{\bar{p}_3}{3}-\frac{\bar{p}_1}{3}\right)^2} \right]$$
$$= \int \frac{d^4k}{(2\pi)^4} \frac{e^{\alpha^{n-1}(\bar{p}_1^2+\bar{p}_2^2+\bar{p}_3^2)}}{e^{[1-\beta^{n-1}-\gamma^{n-1}][3\bar{k}^2+\frac{1}{3}(\bar{p}_1^2+\bar{p}_2^2+\bar{p}_3^2)]}}, \tag{4.63}$$

where p_1, p_2, p_3 are the external momenta for the 1-loop triangle, and the superscript in the α, β, γ indicates that these are coefficients that one obtains from contributions up to $n-1$ loop level.

Integrating (4.63) with respect to the loop momentum k and reminding ourselves that α^n, β^n and γ^n are the coefficients of $\bar{p}_1^2$, $\bar{p}_2^2$ and $\bar{p}_3^2$, respectively, appearing in the exponentials in (4.61), we have

$$\alpha^n = \beta^n = \gamma^n = \alpha^{n-1} + \frac{1}{3}(\beta^{n-1} + \gamma^{n-1}) - \frac{1}{3}. \tag{4.64}$$

In particular, for the 1-loop, 3-point graph, one has to use the 3-point bare vertices (see (4.50)): $\alpha^0 = 1$ and $\beta^0 = \gamma^0 = 0$. One then obtains

$$\alpha^1 = \beta^1 = \gamma^1 = \frac{2}{3}, \tag{4.65}$$

leading to an overall symmetric vertex: $e^{\frac{2}{3}(\bar{p}_1^2+\bar{p}_2^2+\bar{p}_3^2)}$ and $\alpha^1 + \beta^1 + \gamma^1 = 2$. We observe that, as n increases, α^n, β^n and γ^n increase; this means that, as the number of loops increases, the external momentum contributions of the dressed vertices become larger and larger.

We conclude that dressing the vertices by considering just vertex loop corrections to the bare vertices does not ameliorate the external momentum growth of scattering diagrams in the UV in our toy model example given by (4.46); in fact, it makes that growth increase. In the next subsection, we shall dress the vertices by considering both propagator and vertex loop corrections to the bare vertices.

4.3.3 Dressing the vertices by making propagator & vertex loop corrections to the bare vertices

As our next step, let us now consider $\mathcal{T}_{\text{dressed}}$ [1]. We know that $\mathcal{T}_{\text{dressed}}$ diverges as $s \to -\infty$. Let us now dress the vertices by making renormalised propagator and vertex loop corrections to the bare vertices at the left- and right-ends of the diagram. Regarding the dressed propagator, we have $\widetilde{\Pi}(p^2) \xrightarrow{UV} e^{-3\bar{p}^2/2}$. Therefore, following the prescription given in Section 4.3.2, the three-point function can again be written as an exponential function of the external momenta; this happens because, as previously, the (dressed) propagators are exponentials in momenta while the (dressed) vertices are also exponentials in momenta. Hence, in the UV limit, *i.e.*, as $p_i^2 \to \infty$, where $i = 1, 2, 3$, the 3-point function Γ_3, see Fig. 3.9 (right), is again given by (4.61). As previously, the best way to obtain the largest exponents for the external momenta is to have the α exponent correspond to the external momenta. Assuming a symmetric distribution of (β, γ) among the internal loops and considering the n-loop, 3-point diagram with symmetrical routing of momenta, see Fig. 3.9 (right), the propagators in the 1-loop triangle are given by

$$e^{-\frac{3}{2}\left(\bar{k}+\frac{\bar{p}_1}{3}-\frac{\bar{p}_2}{3}\right)^2},\ e^{-\frac{3}{2}\left(\bar{k}+\frac{\bar{p}_2}{3}-\frac{\bar{p}_3}{3}\right)^2},\ e^{-\frac{3}{2}\left(\bar{k}+\frac{\bar{p}_3}{3}-\frac{\bar{p}_1}{3}\right)^2},$$

and the vertex factors are

$$e^{\alpha^{n-1}\bar{p}_1^2+\beta^{n-1}\left(\bar{k}+\frac{\bar{p}_3}{3}-\frac{\bar{p}_1}{3}\right)^2+\gamma^{n-1}\left(\bar{k}+\frac{\bar{p}_1}{3}-\frac{\bar{p}_2}{3}\right)^2},$$
$$e^{\alpha^{n-1}\bar{p}_2^2+\beta^{n-1}\left(\bar{k}+\frac{\bar{p}_1}{3}-\frac{\bar{p}_2}{3}\right)^2+\gamma^{n-1}\left(\bar{k}+\frac{\bar{p}_2}{3}-\frac{\bar{p}_3}{3}\right)^2},$$
$$e^{\alpha^{n-1}\bar{p}_3^2+\beta^{n-1}\left(\bar{k}+\frac{\bar{p}_2}{3}-\frac{\bar{p}_3}{3}\right)^2+\gamma^{n-1}\left(\bar{k}+\frac{\bar{p}_3}{3}-\frac{\bar{p}_1}{3}\right)^2}.$$

[1] We could equally well consider $\mathcal{T}_{\text{tree-level}}$, $\mathcal{T}_{1-\text{loop}}$, etc. By making renormalised propagator & vertex loop corrections to the bare vertices at the left- and right-ends of the scattering diagram under consideration, the external momentum growth would be eliminated at sufficiently high loop order.

In the UV, *i.e.*, as $p_i^2 \to \infty$, where $i = 1, 2, 3$, conservation of momenta gives

$$\begin{aligned}\Gamma_{3,n} \longrightarrow & \int \frac{d^4k}{(2\pi)^4} \frac{e^{\alpha^{n-1}\bar{p}_1^2+\beta^{n-1}\left(\bar{k}+\frac{\bar{p}_3}{3}-\frac{\bar{p}_1}{3}\right)^2+\gamma^{n-1}\left(\bar{k}+\frac{\bar{p}_1}{3}-\frac{\bar{p}_2}{3}\right)^2}}{e^{-\frac{3}{2}\left(\bar{k}+\frac{\bar{p}_1}{3}-\frac{\bar{p}_2}{3}\right)^2} e^{-\frac{3}{2}\left(\bar{k}+\frac{\bar{p}_2}{3}-\frac{\bar{p}_3}{3}\right)^2} e^{-\frac{3}{2}\left(\bar{k}+\frac{\bar{p}_3}{3}-\frac{\bar{p}_1}{3}\right)^2}} \\ & \times e^{\alpha^{n-1}\bar{p}_2^2+\beta^{n-1}\left(\bar{k}+\frac{\bar{p}_1}{3}-\frac{\bar{p}_2}{3}\right)^2+\gamma^{n-1}\left(\bar{k}+\frac{\bar{p}_2}{3}-\frac{\bar{p}_3}{3}\right)^2} e^{\alpha^{n-1}\bar{p}_3^2+\beta^{n-1}\left(\bar{k}+\frac{\bar{p}_2}{3}-\frac{\bar{p}_3}{3}\right)^2+\gamma^{n-1}\left(\bar{k}+\frac{\bar{p}_3}{3}-\frac{\bar{p}_1}{3}\right)^2} \\ & = \int \frac{d^4k}{(2\pi)^4} \frac{e^{\alpha^{n-1}(\bar{p}_1^2+\bar{p}_2^2+\bar{p}_3^2)}}{e^{[\frac{3}{2}-\beta^{n-1}-\gamma^{n-1}][3\bar{k}^2+\frac{1}{3}(\bar{p}_1^2+\bar{p}_2^2+\bar{p}_3^2)]}}, \end{aligned} \tag{4.66}$$

where p_1, p_2, p_3 are the external momenta for the 1-loop triangle, and the superscript in the α, β, γ indicates that these are coefficients that one obtains from contributions up to $n-1$ loop level.

Using the results of Sections 3.10.2 & 3.10.3, we conclude that α^n, β^n and γ^n become negative for $n \geq 4$. The fact that α^n, β^n and γ^n become negative for sufficiently large n should be emphasised since it is precisely this negativity which eliminates the external momentum growth of the scattering diagrams in the UV.

For $n = 4$, we have the following results:

- We find that the largest external momentum contribution of the s-channel, see Fig. 4.7, goes as
$$e^{\frac{44s}{27M^2}} e^{\frac{3s}{2M^2}} = e^{\frac{169s}{54M^2}}, \tag{4.67}$$
which tends to 0 as $s \to -\infty$.

- Regarding the t-channel, the largest external momentum contribution goes as
$$e^{\frac{22t}{27M^2}} e^{\frac{22s}{27M^2}} e^{\frac{3t}{2M^2}} = e^{\frac{s(213-125\cos\theta)}{108M^2}}, \tag{4.68}$$
which, again, tends to 0 as $s \to -\infty$ for all values of θ.

- Regarding the u-channel, the largest external momentum contribution goes as
$$e^{\frac{22u}{27M^2}} e^{\frac{22s}{27M^2}} e^{\frac{3u}{2M^2}} = e^{\frac{s(213+125\cos\theta)}{108M^2}}, \tag{4.69}$$
which, again, tends to 0 as $s \to -\infty$ for all values of θ. Hence, for sufficiently large n (specifically, for $n \geq 4$), there is no exponential growth for the s-, t- and u-channels as $s \to -\infty$.

Let us also point out that we do not have to worry about polynomial growth in s since any polynomial functions of s will be multiplied by exponential functions of s and their product will tend to 0 as $s \to -\infty$, keeping in mind that exponential functions always dominate polynomial ones at large values.

Dressing the vertices by making *both* propagator and vertex loop corrections to the bare vertices ameliorates and, in fact, completely eliminates, for sufficiently large n, the external momentum growth of the scattering diagrams in the UV. In the next section, we will study an infinite derivative scalar toy model inspired by an infinite derivative theory of gravity.

4.4 Scatterings in the context of infinite derivative theories of gravity

Inspired by the results of previous section, let us now investigate scattering diagrams in the context of infinite derivative theories of gravity. Our scalar *toy model* action is now given by (2.88).

Now, we can compute the s, t, u-channels, tree-level scattering diagram $p_1p_2 \to p_3p_4$, see Fig. 4.1, as follows,

$$i\mathcal{T}^{\rm s-channel}_{\rm tree-level} = \frac{1}{M_P^2}V(p_1,p_2,-p_1-p_2)V(-p_3,-p_4,p_1+p_2)\left(\frac{i}{se^{-s/M^2}}\right), \quad (4.70)$$

$$i\mathcal{T}^{\rm t-channel}_{\rm tree-level} = \frac{1}{M_P^2}V(p_1,-p_3,p_3-p_1)V(p_2,-p_4,p_4-p_2)\left(\frac{i}{te^{-t/M^2}}\right), \quad (4.71)$$

$$i\mathcal{T}^{\rm u-channel}_{\rm tree-level} = \frac{1}{M_P^2}V(p_1,-p_4,p_4-p_1)V(p_2,-p_3,p_3-p_2)\left(\frac{i}{ue^{-u/M^2}}\right). \quad (4.72)$$

Therefore, we have

$$\begin{aligned}\mathcal{T}_{\text{tree-level}} = & \frac{1}{16M_P^2\left(p_1+p_2\right)^2 e^{(\bar{p}_1+\bar{p}_2)^2}}\left[p_1^2+p_2^2+(p_1+p_2)^2\right]\left[p_3^2+p_4^2+(p_1+p_2)^2\right] \\ & \times\left[1-e^{\bar{p}_1^2}-e^{\bar{p}_2^2}-e^{(\bar{p}_1+\bar{p}_2)^2}\right]\left[1-e^{\bar{p}_3^2}-e^{\bar{p}_4^2}-e^{(\bar{p}_1+\bar{p}_2)^2}\right] \\ & +(p_2\leftrightarrow -p_3) \\ & +(p_2\leftrightarrow -p_4). \end{aligned} \tag{4.73}$$

In the CM frame, we obtain

$$\begin{aligned}\mathcal{T}_{\text{tree-level}} = & -\frac{1}{16M_P^2 s e^{-\frac{s}{M^2}}}(-2s)^2\left(1-2e^{-\frac{s}{2M^2}}-e^{-\frac{s}{M^2}}\right)^2 \\ & -\frac{1}{16M_P^2 t e^{-\frac{t}{M^2}}}(-s-t)^2\left(1-2e^{-\frac{s}{2M^2}}-e^{-\frac{t}{M^2}}\right)^2 \\ & -\frac{1}{16M_P^2 u e^{-\frac{u}{M^2}}}(-s-u)^2\left(1-2e^{-\frac{s}{2M^2}}-e^{-\frac{u}{M^2}}\right)^2. \end{aligned} \tag{4.74}$$

Let us again point out that s, t, u are all negative in Euclidean space and satisfy $s=u+t$. Clearly, the cross section $\sigma_{\text{tree-level}}$ corresponding to $\mathcal{T}_{\text{tree-level}}$ blows up as $s\to-\infty$ since $|\mathcal{T}|^2$ diverges in that limit.

Regarding the renormalised 1-loop, 2-point function, $\Gamma_{2,1\mathtt{r}}$, with external momenta $p,-p$, we have $\Gamma_{2,1\mathtt{r}}=\frac{iM^4}{M_P^2}f(\bar{p}^2)$, where $f(\bar{p}^2)$ is given by (3.49).

Thus, regarding the 1-loop scattering diagram, see Fig. 4.3, we obtain

$$\begin{aligned}\mathcal{T}_{1-\text{loop}} = & V(p_1,p_2,-p_1-p_2)V(-p_3,-p_4,p_1+p_2)\left(\frac{i}{se^{-s/M^2}}\right)^2\frac{M^4}{M_P^4}f(-s) \\ & +V(p_1,-p_3,p_3-p_1)V(p_2,-p_4,p_1-p_3)\left(\frac{i}{te^{-t/M^2}}\right)^2\frac{M^4}{M_P^4}f(-t) \\ & +V(p_1,-p_4,p_4-p_1)V(p_2,-p_3,p_1-p_4)\left(\frac{i}{ue^{-u/M^2}}\right)^2\frac{M^4}{M_P^4}f(-u), \end{aligned} \tag{4.75}$$

where $\Gamma_{2,1\mathtt{r}}=\frac{iM^4}{M_P^2}f(-s)$. Let us mention again that $f(\bar{p}^2)$ is a regular analytic function of $\bar{p}^2$ which grows as $e^{\frac{3\bar{p}^2}{2}}$ as $\bar{p}^2\to\infty$.

As $s\to-\infty$, $\Gamma_{2,1\mathtt{r}}(-s)$ (and $f(-s)$) goes as $e^{-\frac{3s}{2M^2}}$. The s-channel of $\mathcal{T}_{1-\text{loop}}$

goes as $e^{-\frac{2s}{M^2}}e^{\frac{2s}{M^2}}e^{-\frac{3s}{2M^2}} = e^{-\frac{3s}{2M^2}}$ when $s \to -\infty$. As $s \to -\infty$, $\mathcal{T}^{\text{s-channel}}_{\text{1-loop}}$ diverges. $\mathcal{T}^{\text{t-channel}}_{\text{1-loop}}$ and $\mathcal{T}^{\text{u-channel}}_{\text{1-loop}}$ also diverge.

4.4.1 Dressing the propagator and the vertices

Now if we replace the bare propagator with the dressed propagator in the tree-level scattering diagrams, see Fig. 4.4 (bottom), we obtain

$$\begin{aligned}\mathcal{T}_{\text{dressed}} = {} & V(p_1, p_2, -p_1 - p_2)V(-p_3, -p_4, p_1 + p_2)\left(\frac{1}{M_P^2 s e^{-s/M^2} + M^4 f(-s)}\right) \\ & + V(p_1, -p_3, p_3 - p_1)V(p_2, -p_4, p_1 - p_3)\left(\frac{1}{M_P^2 t e^{-t/M^2} + M^4 f(-t)}\right) \\ & + V(p_1, -p_4, p_4 - p_1)V(p_2, -p_3, p_1 - p_4)\left(\frac{1}{M_P^2 u e^{-u/M^2} + M^4 f(-u)}\right),\end{aligned} \tag{4.76}$$

where, as $s \to -\infty$, $f(-s)$ goes as $e^{-\frac{3s}{2M^2}}$. An explicit computation, see Fig. 4.4, gives us, as $s \to -\infty$,

$$\mathcal{T}^{\text{s-channel}}_{\text{dressed}} \sim \left[2e^{-\frac{s}{2M^2}} + e^{-\frac{s}{M^2}} - 1\right]^2 e^{\frac{3s}{2M^2}} \sim e^{-\frac{s}{2M^2}}, \tag{4.77}$$

$$\mathcal{T}^{\text{t-channel}}_{\text{dressed}} \sim \left[2e^{-\frac{s}{2M^2}} + e^{-\frac{t}{M^2}} - 1\right]^2 e^{\frac{3t}{2M^2}} = \left[2e^{-\frac{s}{2M^2}} + e^{-\frac{s(1-\cos\theta)}{2M^2}} - 1\right]^2 e^{\frac{3s(1-\cos\theta)}{4M^2}}, \tag{4.78}$$

$$\mathcal{T}^{\text{u-channel}}_{\text{dressed}} \sim \left[2e^{-\frac{s}{2M^2}} + e^{-\frac{u}{M^2}} - 1\right]^2 e^{\frac{3u}{2M^2}} = \left[2e^{-\frac{s}{2M^2}} + e^{-\frac{s(1+\cos\theta)}{2M^2}} - 1\right]^2 e^{\frac{3s(1+\cos\theta)}{4M^2}}. \tag{4.79}$$

Hence, we can make the following observations:

- $\mathcal{T}^{\text{s-channel}}_{\text{dressed}}$ blows up as $s \to -\infty$.
- $\mathcal{T}^{\text{t-channel}}_{\text{dressed}}$ blows up as $s \to -\infty$ for all values of θ.
- $\mathcal{T}^{\text{u-channel}}_{\text{dressed}}$ blows up as $s \to -\infty$ for all values of θ.

Since $\mathcal{T}_{\text{dressed}} = \mathcal{T}^{\text{s-channel}}_{\text{dressed}} + \mathcal{T}^{\text{t-channel}}_{\text{dressed}} + \mathcal{T}^{\text{u-channel}}_{\text{dressed}}$, one can verify that the total cross section σ_{dressed} corresponding to $\mathcal{T}_{\text{dressed}}$ blows up as $s \to -\infty$. We

also observe that the external momentum dependence of $\mathcal{T}_{\text{dressed}}$ grows less for large external momenta as compared to the external momentum dependence of $\mathcal{T}_{\text{tree-level}}$ (or $\mathcal{T}_{1-\text{loop}}$). Hence, the use of the dressed propagator ameliorates the external momentum growth of the scattering diagrams, but it is not sufficient by itself.

To see whether we can eliminate the external momentum growth of the scattering diagrams, we will dress the vertices by making renormalised vertex loop corrections to the bare vertices at the left- and right-ends of the scattering diagrams, see Fig. 4.6. Using (3.64) again, we observe that the coefficients α^n, β^n and γ^n increase as n increases; thus, dressing the vertices by keeping the propagators bare and making just vertex loop corrections to the bare vertices at the left- and right-ends of the scattering diagrams cannot tame the external momentum growth of the scattering diagrams.

For that reason, and as an example, we will now dress the bare vertices at the left- and right-ends of the scattering diagram whose scattering matrix element is $\mathcal{T}_{\text{dressed}}$ by making *both* propagator and vertex loop corrections to the said vertices, see Fig. 3.9 (right). Employing (3.64) one more time, α^n, β^n and γ^n become negative for $n \geq 4$.

For $n = 4$, we have the following conclusions:

- As in Section 4.3.3, the largest external momentum contribution of the s-channel, see Fig. 4.7, goes as

$$e^{\frac{44s}{27M^2}} e^{\frac{3s}{2M^2}} = e^{\frac{169s}{54M^2}}, \tag{4.80}$$

  which tends to 0 as $s \to -\infty$.

- The largest external momentum contribution of the t-channel goes as

$$e^{\frac{22t}{27M^2}} e^{\frac{22s}{27M^2}} e^{\frac{3t}{2M^2}} = e^{\frac{s(213-125\cos\theta)}{108M^2}}, \tag{4.81}$$

  which, again, tends to 0 as $s \to -\infty$ for all values of θ.

- The largest external momentum contribution of the u-channel goes as

$$e^{\frac{22u}{27M^2}} e^{\frac{22s}{27M^2}} e^{\frac{3u}{2M^2}} = e^{\frac{s(213+125\cos\theta)}{108M^2}}, \tag{4.82}$$

  which, again, tends to 0 as $s \to -\infty$ for all values of θ. Hence, for sufficiently large n (specifically, for $n \geq 4$), there is no exponential growth for the s-, t- and u-channels as $s \to -\infty$. The external momentum growth of $\mathcal{T}_{\text{tree-level}}$, $\mathcal{T}_{1-\text{loop}}$ etc. would also be eliminated following this prescription at sufficiently high loop order.

We observe that, for sufficiently large n, dressing the vertices by making both propagator and vertex loop corrections to the bare vertices at the left- and right-ends of the scattering diagrams makes the external momentum dependence of any scattering diagram convergent in the UV. By considering renormalised propagator and vertex loop corrections to the bare vertices, we can eliminate the external momentum growth appearing in scattering diagrams in the regime of large external momenta, *i.e.*, as $s \to -\infty$. In contrast, dressing the vertices by considering just vertex loop corrections to the bare vertices is not sufficient. Thus, dressing the vertices by making both propagator and vertex loop corrections to the bare vertices is essential to taming the external momentum growth of scattering diagrams in the UV and, as a result, we expect the cross sections of those diagrams to be finite.

4.5 Summary

In this chapter, we have investigated the external momentum dependence of scattering diagrams within the framework of infinite derivative field theories and gravity. For a finite-order, higher-derivative scalar field theory, the cross section of tree-level scattering diagrams blows up at large external momenta. If we dress the propagators and the vertices by making propagator and vertex loop corrections to the bare vertices of the scattering diagrams, the external momentum growth can still not be tamed. We observe that dressing the propagators somewhat softens the external momentum growth.

Subsequently, we have investigated a scalar field theory with infinite derivative kinetic and interaction terms. The propagators are exponentially suppressed while the vertices are exponentially enhanced. We have obtained that the corresponding tree-level cross section blows up when the external momenta are large. Only if we dress the propagators and the vertices by making renormalised propagator and vertex loop corrections to the bare vertices at sufficiently high loop-order (the loop-order n being greater than or equal to four) can the cross section be made finite in the UV. As the loop-order increases, the dressed vertices give rise to negative exponents so that scattering amplitudes are ameliorated at high energies. Hence, the cross section does not blow up in the UV.

Finally, we have looked into high-energy scattering diagrams in a scalar toy model motivated by infinite derivative gravity. In particular, we have established that dressing the vertices and the propagators indeed gives rise to a finite cross section.

Chapter 5

Hamiltonian analysis

In this chapter, we shall perform a Hamiltonian analysis on an infinite derivative gravitational theory (IDG) and compute the number of relevant degrees of freedom. Due to technical complexities, we shall not perform a Hamiltonian analysis on the infinite derivative gravitational action given by (1.10) but on a simpler infinite derivative gravitational action containing only the Ricci scalar, which was given in [41].

Hamiltonian analysis provides a framework whereby the stability/instability and boundedness/unboundedness of the corresponding theory can be investigated. Finite-order, higher-derivative theories (that is, theories containing more than two derivatives) usually suffer from the Ostrogradsky instability [104, 105]. As the IDG action includes infinitely many covariant derivatives, there is no highest momentum operator and, consequently, Ostrogradsky analysis is not particularly useful. In this chapter, the Hamiltonian density for the IDG action shall be written down explicitly. Consequently, we shall discuss how to define *primary* and *secondary constraints*, how to deduce *first-class* and *second-class constraints*, how to identify the relevant dynamical degrees of freedom, etc; one may consult [146, 147, 148, 149].

In the late 1950s, Richard Arnowitt, Stanley Deser and Charles W. Misner (ADM) [150, 151] formulated the 3+1 decomposition. In the 3+1 decomposition, one can decompose four-dimensional spacetime such that a generic region $\mathcal{M}$ of

the spacetime manifold is foliated into a family of spacelike hypersurfaces Σ_t, one for each instant in time.

It is vital that the *first-class* and *second-class constraints* be identified. If the Poisson bracket of a constraint with all other constraints, including itself, is equal to zero, then it is a *first-class constraint*; otherwise, it is a *second-class constraint*. First, we shall study a scalar field theory toy model containing infinitely many derivatives. Subsequently, we shall consider the IDG action. We shall explicitly illustrate and contrast cases where the IDG action possesses infinitely many or finitely many degrees of freedom.

5.1 Preliminaries

Let us suppose we have an action that depends on time evolution. We can write down the equations of motion by imposing the stationary conditions on the action and then use the variational method. We start off with the following action,

$$I = \int dt\ \mathcal{L}(q^i, \dot{q}^i). \tag{5.1}$$

The above action is expressed as a time integral and $\mathcal{L}$ is the Lagrangian density depending on the position q^i and the velocity $\dot{q}^i$ [1]. The variation of the action leads to the equations of motion known as Euler-Lagrange equation, (we assume that $\mathcal{L}$ does not depend explicitly on time)

$$\frac{d}{dt}\left(\frac{\partial \mathcal{L}}{\partial \dot{q}^i}\right) - \frac{\partial \mathcal{L}}{\partial q^i} = 0, \tag{5.2}$$

we can expand the above expression and write

$$\ddot{q}^j \frac{\partial^2 \mathcal{L}}{\partial \dot{q}^i \partial \dot{q}_i} = \frac{\partial \mathcal{L}}{\partial q_j} - \dot{q}^j \frac{\partial^2 \mathcal{L}}{\partial q_i \partial \dot{q}^i}, \tag{5.3}$$

[1] The *phase space* is composed of all positions and velocities together while the *configuration space* consists of positions only.

the above equation yields an acceleration, $\ddot{q}^j$, which can be uniquely calculated from position and velocity at a given time if and only if $\frac{\partial^2 \mathcal{L}}{\partial \dot{q}^i \partial \dot{q}_i}$ is invertible. In other words, if the determinant of the matrix $\frac{\partial^2 \mathcal{L}}{\partial \dot{q}^i \partial \dot{q}_i}$ is not equal to zero, *i.e.*, it is non-vanishing, then the theory is called *non-degenerate*. However, if the determinant is zero, then the acceleration can *not* be uniquely determined by position and the velocity. The latter system is called *singular* and leads to *constraints* in the phase space, see [149, 152, 153].

5.1.1 Constraints for a singular system

In order to formulate the Hamiltonian, we need to first define the canonical momenta,

$$p_i = \frac{\partial \mathcal{L}}{\partial \dot{q}^i}. \tag{5.4}$$

The non-invertible matrix $\frac{\partial^2 \mathcal{L}}{\partial \dot{q}^i \partial \dot{q}_i}$ indicates that not all the velocities can be written in terms of the canonical momenta, in other words, not all the momenta are independent, and there are some relations between the canonical coordinates [146, 147, 148, 149, 152] such as

$$\varphi(q^i,\ p_i) = 0 \iff \texttt{primary constraints}, \tag{5.5}$$

known as *primary constraints*. For instance, if we have *vanishing canonical momenta*, then we have *primary constraints*. The primary constraints hold without using the equations of motion. The primary constraints define a submanifold smoothly embedded in a phase space, which is also known as the *primary constraint surface*, Γ_p. We can now define the Hamiltonian density as

$$\mathcal{H} = p_i \dot{q}^i - \mathcal{L}. \tag{5.6}$$

If the theory admits primary constraints, we will have to redefine the Hamiltonian density and write the *total* Hamiltonian density as follows [149],

$$\mathcal{H}_{tot} = \mathcal{H} + \lambda^a(q^i, p_i)\varphi_a(q^i, p_i), \tag{5.7}$$

where $\lambda^a(q^i, p_i)$ is called the *Lagrange multiplier* and $\varphi_a(q^i, p_i)$ are linear combinations of the primary constraints [1]. The Hamiltonian equations of motion,

$$\dot{p}_i = -\frac{\delta \mathcal{H}_{tot}}{\delta q^i} = \{q_i, \mathcal{H}_{tot}\}, \tag{5.8}$$

$$\dot{q}^i = -\frac{\delta \mathcal{H}_{tot}}{\delta p_i} = \{p^i, \mathcal{H}_{tot}\}, \tag{5.9}$$

are the time evolutions in which the Hamiltonian density remains invariant under arbitrary variations of δp_i, δq^i and $\delta\lambda$.

As a result, the Hamiltonian equations of motion can be expressed in terms of the Poisson bracket. In general, for canonical coordinates (q^i, p_i) on the phase space, the Poisson bracket for two given functions $f(q^i, p_i)$ and $g(q^i, p_i)$ can be defined as

$$\{f, g\} = \sum_{i=1}^{n} \Big(\frac{\partial f}{\partial q^i} \frac{\partial g}{\partial p_i} - \frac{\partial f}{\partial p_i} \frac{\partial g}{\partial q^i} \Big), \tag{5.10}$$

where q^i are the generalised coordinates and p_i are the generalised conjugate momenta while f and g are functions of the phase space coordinates. Moreover, i indicates the number of the phase space variables.

Now, any quantity is *weakly* vanishing when it is numerically restricted to be zero on a submanifold Γ of the phase space, but does not vanish throughout the phase space. In other words, a function $F(q^i, p_i)$ defined in a neighbourhood of Γ is called *weakly zero*, if

$$F(q^i, p_i)|_\Gamma = 0 \Longleftrightarrow F(q^i, p_i) \approx 0, \tag{5.11}$$

where Γ is the *constraint surface* defined on a submanifold of the phase space. Note that the notation "$\approx$" indicates that the quantity is *weakly* vanishing; this

[1] We should point out that the total Hamiltonian density is the sum of the canonical Hamiltonian density and terms which are products of Lagrange multipliers and the primary constraints. The time evolution of the primary constraints, should it be equal to zero, gives the *secondary constraints* and those secondary constraints are evaluated by computing the Poisson bracket of the *primary constraints* and the total Hamiltonian density. In the literature, one may also come across the *extended* Hamiltonian density, which is the sum of the canonical Hamiltonian density and terms which are products of Lagrange multipliers and the first-class constraints, see [153].

is standard terminology denoting that $F(q^i, p_i)$ shall vanish on the constraint surface, Γ, but not necessarily throughout the phase space.

When a theory admits primary constraints, we must ensure that the theory is consistent by essentially checking whether the primary constraints are preserved under time evolution or not. In other words, we demand that, on the constraint surface Γ_p (let us note that Γ_p is a smooth submanifold of the phase space determined by the *primary* constraints; in order to denote equality on Γ_p, we shall use the "$\approx$" notation),

$$\dot{\varphi}|_{\Gamma_p} = \{\varphi, \mathcal{H}_{tot}\}|_{\Gamma_p} = 0 \Longleftrightarrow \dot{\varphi} = \{\varphi, \mathcal{H}_{tot}\} \approx 0. \tag{5.12}$$

That is,

$$\dot{\varphi} = \{\varphi, \mathcal{H}_{tot}\} \approx 0 \Longrightarrow \texttt{secondary constraint}. \tag{5.13}$$

Demanding that (5.12) be (not identically) zero on the constraint surface Γ_p yields a *secondary constraint* [146, 154] and the theory is consistent (if (5.12) is identically zero or fixes a Lagrange multiplier, then there will be no secondary constraints). One can now define Γ_1, where Γ_1 is a smooth submanifold of the phase space determined by the *primary* & *secondary* constraints: $\Gamma_1 \subseteq \Gamma_p$. We can verify whether the theory is consistent by checking if the secondary constraints are preserved under time evolution or not. A theory can also admit *tertiary constraints*, and so on and so forth [153].

Note that $\mathcal{H}_{tot}$ is the total Hamiltonian density defined by (5.7). To summarise, if a canonical momentum is vanishing, we have a primary constraint, while *enforcing* that the time evolution of the primary constraint vanishes on the constraint surface, Γ_1, gives rise to a secondary constraint.

5.1.2 First-class and second-class constraints

Any theory that can be formulated in Hamiltonian formalism gives rise to Hamiltonian constraints. Constraints in the context of Hamiltonian formulation can be thought of as reparameterisation [1]. The most important step in Hamiltonian

[1]For example, in the case of gravity, constraints are obtained by using the ADM formalism, that is, reparameterising the theory under spatial and time coordinates. Hamiltonian

analysis is the classification of the constraints. By definition, we call a constraint $f(q^i, p_i)$ to be *first-class* if its Poisson brackets with all other constraints vanish *weakly*. A function which is not *first-class* is called *second-class* [1]. On the constraint surface Γ_1, this is mathematically expressed as

$$\{f(q^i, p_i), \varphi\}|_{\Gamma_1} \approx 0 \Longrightarrow \texttt{first} - \texttt{class}, \tag{5.14}$$

$$\{f(q^i, p_i), \varphi\}|_{\Gamma_1} \not\approx 0 \Longrightarrow \texttt{second} - \texttt{class}. \tag{5.15}$$

We should point out that we use the "$\approx$" sign as we are interested in whether the Poisson brackets of $f(q^i, p_i)$ with all other constraints vanish on the constraint surface Γ_1 or not. Determining whether they vanish globally, *i.e.*, throughout the phase space, is not necessary for our purposes.

5.1.3 Counting the degrees of freedom

After evaluating the number of first-class and/or second-class constraints, we can use the following formula to count the number of the physical degrees of freedom [153]:

$$\mathcal{N} = \frac{1}{2}(2\mathcal{A} - \mathcal{B} - 2\mathcal{C}), \tag{5.16}$$

where

- $\mathcal{N}$ = number of physical degrees of freedom,
- $\mathcal{A}$ = number of *configuration space variables*,
- $\mathcal{B}$ = number of *second-class constraints*,
- $\mathcal{C}$ = number of *first-class constraints*.

constraints generate time diffeomorphisms [155].

[1] One should mention that the *primary/secondary* and *first-class/second-class* classifications overlap. A *primary constraint* can be *first-class or second-class* and a *secondary constraint* can also be *first-class* or *second-class*.

5.2 Infinite derivative scalar field theory

In this section, and before moving on to gravity, we are going to consider a Lagrangian which is constructed from an infinite number of d'Alembertian operators; in other words, we can have an action of the following form (in Minkowski spacetime)

$$I = \int d^4x \left(\phi \mathcal{F}(\bar{\Box})\phi\right) \tag{5.17}$$

where

$$\mathcal{F}(\bar{\Box}) = \sum_{n=0}^{\infty} f_n \bar{\Box}^n \tag{5.18}$$

and the f_n's are constants. For the above action, one would require a rather more elaborate approach [156], which we follow here by first writing an equivalent action of the form,

$$I_{eqv} = \int d^4x \left(A\mathcal{F}(\bar{\Box})A\right), \tag{5.19}$$

where the auxiliary field, A, is introduced as an equivalent scalar field to ϕ. This means that the equations of the motion for both actions (I and I_{eqv}) are equivalent.

In order to eliminate the contributions of $\bar{\Box}A$, $\bar{\Box}^2A$ and so on [1] (one can see (5.25) & (5.57) for this approach applied to higher powers of $\bar{\Box}$), we are going to introduce two auxiliary fields χ_n and η_n, where the χ_n's are dimensionless and the η_n's have mass dimension 2 (this can be seen by parameterising $\bar{\Box}A$, $\bar{\Box}^2A$, ...). We show few steps here by taking a simple example.

- Suppose our action is built by one box only, then

$$I_{eqv} = \int d^4x \left(A\bar{\Box}A\right). \tag{5.20}$$

To eliminate $\bar{\Box}A$ in the term $A\bar{\Box}A$, we wish to add the following term in

[1] When considering higher powers of $\bar{\Box}$, one can see that the use of auxiliary fields simplifies the Hamiltonian analysis and precludes the introduction of higher time-derivatives of A.

the above action,

$$\int d^4x\ \chi_1 A(\eta_1 - \bar{\Box}A) = \int d^4x\ [\chi_1 A\eta_1 + \eta^{\mu\nu}(\partial_\mu\chi_1 A\partial_\nu A + \chi_1\partial_\mu A\partial_\nu A)]\,. \tag{5.21}$$

It should be pointed out that the right-hand side of (5.21) can be derived as follows,

$$\begin{aligned}\chi_1 A(\eta_1 - \Box A) &= \chi_1 A\eta_1 - \chi_1 A\Box A \\ &= \chi_1 A\eta_1 - \eta^{\mu\nu}\chi_1 A\partial_\mu\partial_\nu A \\ &= \chi_1 A\eta_1 - \eta^{\mu\nu}\partial_\mu(\chi_1 A\partial_\nu A) + \eta^{\mu\nu}\partial_\mu\chi_1 A\partial_\nu A + \eta^{\mu\nu}\chi_1\partial_\mu A\partial_\nu A \\ &= \chi_1 A\eta_1 + \eta^{\mu\nu}\partial_\mu\chi_1 A\partial_\nu A + \eta^{\mu\nu}\chi_1\partial_\mu A\partial_\nu A. \end{aligned} \tag{5.22}$$

Let us note that we have dropped total derivative terms and that we have absorbed the powers of M^{-2} into χ_1 while the mass dimension of η_1 has been modified accordingly; as a result, the d'Alembertian operator is not barred. Hence, we have

$$I_{eqv} = \int d^4x\ \left(\chi_1 A\eta_1 + \chi_1 A(\eta_1 - \bar{\Box}A)\right). \tag{5.23}$$

By solving the equation of motion for χ_1, we obtain

$$\eta_1 = \bar{\Box}A, \tag{5.24}$$

and, therefore, (5.20) and (5.23) are equivalent.

Similarly, in order to eliminate the terms $A\bar{\Box}^n A$ and so on, we have to repeat the same procedure up to $\bar{\Box}^n$. For example, in order to eliminate the term $A\bar{\Box}^2 A$, we add the term

$$\frac{1}{2}\int d^4x\sqrt{-g}\chi_2 A(\eta_2 - \bar{\Box}\eta_1) = \frac{1}{2}\int d^4x\sqrt{-g}\,[\chi_2 A\eta_2 + g^{\mu\nu}(\partial_\mu\chi_2 A\partial_\nu\eta_1 + \chi_2\partial_\mu A\partial_\nu\eta_1)]\,. \tag{5.25}$$

Solving the equation of motion for χ_2 yields $\eta_2 = \bar{\Box}\eta_1 = \bar{\Box}^2 A$. Hence, one can establish this by solving the equation of motion for the χ_n's, which yields, for

$n \geq 2$,

$$\eta_n = \bar{\Box}\eta_{n-1} = \bar{\Box}^n A. \tag{5.26}$$

Now, we can rewrite the action given by (5.19) as follows,

$$I_{eqv} = \int d^4x \left\{ A(f_0 A + \sum_{n=1}^{\infty} f_n \eta_n) + \chi_1 A(\eta_1 - \Box A) + \sum_{l=2}^{\infty} \chi_l A(\eta_l - \Box \eta_{l-1}) \right\} \tag{5.27}$$

$$\begin{aligned} &= \int d^4x \Bigg\{ A(f_0 A + \sum_{n=1}^{\infty} f_n \eta_n) + \sum_{l=1}^{\infty} A\chi_l \eta_l \\ &+ \eta^{00}(A\partial_0\chi_1\partial_0 A + \chi_1\partial_0 A\partial_0 A) + \eta^{ij}(A\partial_i\chi_1\partial_j A + \chi_1\partial_i A\partial_j A) \\ &+ \eta^{00}\sum_{l=2}^{\infty}(A\partial_0\chi_l\partial_0\eta_{l-1} + \chi_l\partial_0 A\partial_0\eta_{l-1}) + \eta^{ij}\sum_{l=2}^{\infty}(A\partial_i\chi_l\partial_j\eta_{l-1} + \chi_l\partial_i A\partial_j\eta_{l-1}) \Bigg\}. \end{aligned} \tag{5.28}$$

where we have absorbed the powers of M^{-2} into the f_n's (see (5.18)) & χ_n's and the mass dimension of the η_n's has been modified accordingly. Hence, the box operator is not barred. We also decomposed the d'Alembertian operator to its components on the Minkowski background: $\Box = \eta^{\mu\nu}\partial_\mu\partial_\nu = \eta^{00}\partial_0\partial_0 + \eta^{ij}\partial_i\partial_j$, where the zeroth component is the time coordinate and $\{i,\ j\}$ are the spatial coordinates running from 1 to 3. The conjugate momenta for the above action are given by

$$p_A = \frac{\partial \mathcal{L}}{\partial \dot{A}} = \Big[-(A\partial_0\chi_1 + \chi_1\partial_0 A) - \sum_{l=2}^{\infty}(\chi_l\partial_0\eta_{l-1}) \Big], \tag{5.29}$$

$$p_{\chi_1} = \frac{\partial \mathcal{L}}{\partial \dot{\chi}_1} = -A\partial_0 A, \tag{5.30}$$

$$p_{\chi_l} = \frac{\partial \mathcal{L}}{\partial \dot{\chi}_l} = -(A\partial_0\eta_{l-1}), \tag{5.31}$$

$$p_{\eta_{l-1}} = \frac{\partial \mathcal{L}}{\partial \dot{\eta}_{l-1}} = -(A\partial_0\chi_l + \chi_l\partial_0 A). \tag{5.32}$$

where $\dot{A} \equiv \partial_0 A$. Therefore, the Hamiltonian density is given by

$$\begin{aligned}\mathcal{H} &= p_A\dot{A} + p_{\chi_1}\dot{\chi}_1 + \sum_{l=2}^{\infty}\left(p_{\chi_l}\dot{\chi}_l + p_{\eta_{l-1}}\dot{\eta}_{l-1}\right) - \mathcal{L} \\ &= A(f_0 A + \sum_{n=1}^{\infty} f_n\eta_n) - \sum_{l=1}^{\infty} A\chi_l\eta_l - (\eta^{\mu\nu}A\partial_\mu\chi_1\partial_\nu A + g^{ij}\chi_1\partial_i A\partial_j A) \\ &- \eta^{\mu\nu}\sum_{l=2}^{\infty}(A\partial_\mu\chi_l\partial_\nu\eta_{l-1} + \chi_l\partial_\mu A\partial_\nu\eta_{l-1}). \end{aligned} \tag{5.33}$$

Let us now consider the first line of (5.27), before integrating by parts. We see that we have terms of the form

$$\chi_1 A(\eta_1 - \Box A)$$

and

$$\chi_l A(\eta_l - \Box\eta_{l-1}), \quad \text{for} \quad l \geq 2.$$

Moreover, we know that solving the equations of motion for χ_n leads to $\eta_n = \Box^n A$. Therefore, we can conclude that the χ_n's are the Lagrange multipliers and, as a result, are not dynamical. Hence, we obtain from the equations of motion the following primary constraints:

$$\begin{aligned}\varphi_1 &= \eta_1 - \Box A \approx 0, \\ &\vdots \\ \varphi_l &= \eta_l - \Box\eta_{l-1} \approx 0. \end{aligned} \tag{5.34}$$

In other words, since the χ_n's are Lagrange multipliers, φ_1 and φ_l's are primary constraints. The time evolutions of the φ_n's fix the corresponding Lagrange multipliers λ^{φ_n} (φ_n is an index rather than a power) in the total Hamiltonian (when we add the terms $\lambda^{\varphi_n}\varphi_n$ to the Hamiltonian density $\mathcal{H}$); therefore, the φ_n's do not induce secondary constraints. As a result, to classify the above constraints,

we will need to show that the Poisson bracket given by (5.10) vanishes weakly:

$$\{\varphi_m, \varphi_n\}|_{\Gamma_p} = 0, \tag{5.35}$$

so that the φ_n's can be classified as first-class constraints. It is trivial to show that, for this case, there is no second-class constraint, *i.e.*, $\mathcal{B} = 0$ ($\mathcal{B}$ is the number of second-class constraints), as we do not have $\{\varphi_m, \varphi_n\} \not\approx 0$. That is, the φ_n's are primary, first-class constraints. In our case, the number of phase space variables is given by

$$2\mathcal{A} \equiv 2 \times \left\{ (A, p_A), \underbrace{(\eta_1, p_{\eta_1}), (\eta_2, p_{\eta_2}), \cdots}_{n=1,\ 2,\ 3, \cdots \infty} \right\} = 2 \times (1 + \infty) = \infty. \tag{5.36}$$

where the brackets denote a set with infinitely many terms (each pair (A, p_A), (η_1, p_{η_1}), etc is an element of the set). For each pair (η_n, p_{η_n}), we have assigned one variable, which is multiplied by a factor of 2, since we are dealing with field-conjugate momentum pairs in the phase space. In the next section, we will fix the form of $\mathcal{F}(\bar{\Box})$ to estimate the number of first-class constraints, *i.e.*, $\mathcal{C}$ and, hence, the number of degrees of freedom. Let us also mention that the choice of $\mathcal{F}(\bar{\Box})$ will determine the number of solutions of the equation of motion for A and, consequently, these solutions can be interpreted as first-class constraints which will determine the number of physical degrees of freedom, *i.e.*, whether the number of degrees of freedom is finite or infinite shall depend on the number of solutions to the equation of motion for A.

5.2.1 Gaussian kinetic term and propagator

Let us now consider an example of an infinite derivative scalar field theory, but with a Gaussian kinetic term in (5.17), *i.e.*, the exponential of an entire function,

$$I_{eqv} = \int d^4x\ A \left(\Box e^{-\bar{\Box}} \right) A. \tag{5.37}$$

For the above action, the equation of motion for A is given by

$$2\left(\Box e^{-\bar{\Box}}\right)A = 0. \tag{5.38}$$

We observe that there are finitely many solutions; hence, there are also finitely many degrees of freedom [1]. In momentum space, we obtain the following solution,

$$k^2 = 0, \tag{5.39}$$

and the propagator will be as follows [56, 87],

$$\Pi(\bar{k}^2) \sim \frac{1}{k^2}e^{-\bar{k}^2}, \tag{5.40}$$

where we have used the fact that, in momentum space, $\Box \to -k^2$ and that $\bar{k} \equiv k/M$. There are some interesting properties to note about this propagator:

- The propagator is suppressed by the *exponential of an entire function*, which has no zeroes or poles. Therefore, the only dynamical pole resides at $k^2 = 0$, *i.e.*, the massless pole in the propagator. Thus, the number of degrees of freedom is $\mathcal{N} = 1$. Consequently, the sole dynamical degree of freedom is the massless scalar field and there are no new dynamical degrees of freedom. Furthermore, the propagator is suppressed in the UV [100].

- The propagator contains no *ghosts*, which usually plague higher-derivative theories. By virtue of this, there is no analogue of the Ostrogradsky instability at a classical level. Given the background equation, one can indeed understand the stability of the solution. Such studies have been performed for IDG theories in a cosmological setting [42, 43].

The action given by (5.37) can now be recast in terms of an equivalent action

[1] Note that, for an infinite derivative action of the form $I_{eqv} = \int d^4x \left(A\cos(\bar{\Box})A\right)$, we would have infinitely many solutions and, hence, infinitely many degrees of freedom.

as follows,

$$I_{eqv} = \int d^4x \left[A \sum_{n=0}^{\infty} \frac{(-1)^n}{n! M^{2n}} \eta_{n+1} + \chi_1 A(\eta_1 - \Box A) + \sum_{l=2}^{\infty} \chi_l A(\eta_l - \Box \eta_{l-1}) \right]. \tag{5.41}$$

We can now compute the number of the physical degrees of freedom. Note that the determinant of the phase-space dependent matrix $A_{mn} = \{\varphi_m, \varphi_n\} \neq 0$, so the φ_n's do not induce further constraints, such as secondary constraints. Therefore [1],

$$\begin{aligned} 2\mathcal{A} &\equiv 2 \times \left\{ (A, p_A), \underbrace{(\eta_1, p_{\eta_1}), (\eta_2, p_{\eta_2}), \dots}_{n=1,\ 2,\ 3, \cdots \infty} \right\} = 2 \times (1 + \infty) = \infty, \\ \mathcal{B} &= 0, \\ 2\mathcal{C} &\equiv 2 \times (\varphi_n) = 2 \times (\infty) = \infty, \\ \mathcal{N} &= \frac{1}{2}(2\mathcal{A} - \mathcal{B} - 2\mathcal{C}) = \frac{1}{2}(2 - 0) = 1, \end{aligned} \tag{5.42}$$

since there is a one-to-one correspondence between each pair (η_n, p_{η_n}) and φ_n. As expected, the conclusion of this analysis yields exactly the same dynamical degrees of freedom as that of the Lagrangian formulation. The coefficients f_n of $\mathcal{F}(\bar{\Box})$ are all fixed by the form of $\Box e^{-\bar{\Box}}$.

5.3 ADM formalism

We shall take a simple infinite derivative action [41] and study the Hamiltonian density and degrees of freedom, but before that we briefly recap the ADM formalism for gravity as we will require this for further development.

One of the important concepts in GR is diffeomorphism invariance, *i.e.*, when one transforms coordinates at given space-time points, the physics remains unchanged. As a result of this, one concludes that diffeomorphism is a local trans-

[1] In this case and hereafter in this chapter, one should, in principle, also include the $k^2 = 0$ solution when counting the number of degrees of freedom. This can be written in position space as $\Box A = 0$. Since $\Box A$ is already parameterised as η_1, the counting of number of degrees of freedom is not affected.

formation. In Hamiltonian formalism, we have to specify the direction of time. A very useful approach to do this is ADM decomposition [150, 151]. Such a decomposition allows one to choose a specific time direction without violating the diffeomorphism invariance. In other words, choosing the time direction is nothing but a gauge redundancy, ensuring that diffeomorphism is a local transformation. We assume that the manifold $\mathcal{M}$ is a time orientable spacetime, which can be foliated by a family of spacelike hypersurfaces Σ_t at which the time is fixed to be constant: $t = x^0$. We then introduce an induced metric on the hypersurface as follows,

$$h_{ij} \equiv g_{ij}|_t, \tag{5.43}$$

where the Latin indices run from 1 to 3 for spatial coordinates.

Within the framework of the 3+1 formalism, the line element is parameterised as follows,

$$ds^2 = -N^2 dt^2 + h_{ij}(dx^i + N^i dt)(dx^j + N^j dt), \tag{5.44}$$

where N is the *lapse function* and N^i is the *shift vector* and are given by

$$N = \frac{1}{\sqrt{-g^{00}}}, \quad N^i = -\frac{g^{0i}}{g^{00}}. \tag{5.45}$$

In terms of metric variables, we have

$$\begin{aligned} &g_{00} = -N^2 + h_{ij}N^i N^j, \qquad g_{0i} = N_i, \qquad g_{ij} = h_{ij}\,, \\ &g^{00} = -N^{-2}, \qquad g^{0i} = \frac{N^i}{N^2}, \qquad g^{ij} = h^{ij} - \frac{N^i N^j}{N^2}. \end{aligned} \tag{5.46}$$

Furthermore, we have a timelike vector n^μ, *i.e.*, the vector normal to the hypersurface in (5.44), which takes the following form:

$$n_i = 0, \quad n^i = -\frac{N^i}{N}, \quad n_0 = -N, \quad n^0 = N^{-1}. \tag{5.47}$$

From (5.44), we also get $\sqrt{-g} = N\sqrt{h}$.

In addition, we are going to introduce a covariant derivative associated with

the induced metric h_{ij}:

$$D_i \equiv e_i^\mu \nabla_\mu. \tag{5.48}$$

We will define the extrinsic curvature as follows,

$$K_{ij} \equiv \nabla_i n_j = -\frac{1}{2N}\left(D_i N_j + D_j N_i - \partial_t h_{ij}\right). \tag{5.49}$$

It is well known that the Riemannian curvatures can be written in terms of the $3+1$ variables. In the case of scalar curvature, we have [151]

$$R = K_{ij}K^{ij} - K^2 + \mathcal{R} + \frac{2}{\sqrt{-g}}\partial_\mu(\sqrt{-g}n^\mu K) - \frac{2}{N\sqrt{h}}\partial_i(\sqrt{h}h^{ij}\partial_j N), \tag{5.50}$$

where $K = h^{ij}K_{ij}$ is the trace of the extrinsic curvature and $\mathcal{R}$ is scalar curvature calculated using the induced metric h_{ij} [1].

One may calculate each term in (5.50) using the extrinsic curvature and (5.47). The decomposition of the d'Alembertian operator can be expressed as follows,

$$\begin{aligned}\Box &= g^{\mu\nu}\nabla_\mu\nabla_\nu = (h^{\mu\nu} + \varepsilon n^\mu n^\nu)\nabla_\mu\nabla_\nu = (h^{ij}e_i^\mu e_j^\nu - n^\mu n^\nu)\nabla_\mu\nabla_\nu \\ &= h^{ij}D_iD_j - n^\nu\nabla_{\mathbf{n}}\nabla_\nu = \Box_{hyp} - n^\nu\nabla_{\mathbf{n}}\nabla_\nu,\end{aligned} \tag{5.51}$$

where $\Box_{hyp} = h^{ij}D_iD_j$. Moreover, we have used the completeness relation for a spacelike hypersurface, *i.e.*, $\varepsilon = -1$, and we have defined $\nabla_{\mathbf{n}} = n^\mu\nabla_\mu$.

5.3.1 ADM decomposition

Let us now introduce the IDG action. We shall restrict ourselves to an action containing the Ricci scalar [41]:

$$S = \frac{1}{2}\int d^4x\sqrt{-g}\left[M_P^2 R + R\mathcal{F}(\bar{\Box})R\right], \tag{5.52}$$

[1] We note that Greek indices are four-dimensional while Latin indices are spatial and three-dimensional.

where $\mathcal{F}(\bar{\Box}) = \sum_{n=0}^{\infty} f_n \bar{\Box}^n$ and M_P is the four-dimensional Planck mass scale given by $M_P^2 = (8\pi G_N^{(4)})^{-1}$ while $G_N^{(4)}$ is Newton's gravitational constant in four dimensions. The first term is the Einstein-Hilbert term, with R being the scalar curvature in four dimensions, and the second term is the infinite derivative modification to the action, where $\bar{\Box} \equiv \Box/M^2$ since $\Box$ has mass dimension 2 and $\mathcal{F}(\bar{\Box})$ shall be dimensionless. Note that $\Box$ is the four-dimensional d'Alembertian operator given by $\Box = g^{\mu\nu}\nabla_\mu\nabla_\nu$. Moreover, the f_n's are the dimensionless coefficients of the series expansion.

5.3.2 Equivalent action and decomposition

Now that the fundamentals of the $3+1$ decomposition have been established, we rewrite the action given by (5.52) in its equivalent form. We start off by writing an equivalent action [41] as follows,

$$S_{eqv} = \frac{1}{2}\int d^4x\sqrt{-g}\left[M_P^2 A + A\mathcal{F}(\bar{\Box})A + B(R-A)\right], \tag{5.53}$$

where we have introduced two scalar fields A and B with mass dimension two. Solving the equations of motion for scalar field B results in $A = R$. The equations of motion for the original action given by (5.52) are equivalent to the equations of motion for the action given by (5.53):

$$\delta S_{eqv} = \frac{1}{2}\delta\left\{\sqrt{-g}\left[M_P^2 A + A\mathcal{F}(\bar{\Box})A + B(R-A)\right]\right\} = 0 \Rightarrow R = A. \tag{5.54}$$

Following the steps in Section 5.2, we expand $\mathcal{F}(\bar{\Box})A$ using (5.52):

$$\mathcal{F}(\bar{\Box})A = \sum_{n=0}^{\infty} f_n\bar{\Box}^n A = f_0 A + f_1\bar{\Box}A + f_2\bar{\Box}^2 A + f_3\bar{\Box}^3 A + \dots \tag{5.55}$$

As before, in order to eliminate $\bar{\Box}A$, $\bar{\Box}^2 A, \cdots$, we will introduce two new auxiliary fields χ_n and η_n with the χ_n's being dimensionless and the η_n's being of mass dimension two.

- As an example, in order to eliminate $\bar{\Box}A$ in $A\bar{\Box}A$, we must add the following terms to (5.53):

$$\begin{aligned}\frac{1}{2}\int d^4x\sqrt{-g}\chi_1 A(\eta_1-\bar{\Box}A) &= \frac{1}{2}\int d^4x\sqrt{-g}\left[\chi_1 A\eta_1-\chi_1 A\Box A\right]\\ &= \frac{1}{2}\int d^4x\sqrt{-g}\left[\chi_1 A\eta_1-g^{\mu\nu}\chi_1 A\partial_\mu\partial_\nu A\right]\\ &= \frac{1}{2}\int d^4x\sqrt{-g}\left[\chi_1 A\eta_1-g^{\mu\nu}\partial_\mu(\chi_1 A\partial_\nu A)+g^{\mu\nu}\partial_\mu\chi_1 A\partial_\nu A\right.\\ &\left.+\, g^{\mu\nu}\chi_1\partial_\mu A\partial_\nu A\right]\\ &= \frac{1}{2}\int d^4x\sqrt{-g}\left[\chi_1 A\eta_1+g^{\mu\nu}\partial_\mu\chi_1 A\partial_\nu A+g^{\mu\nu}\chi_1\partial_\mu A\partial_\nu A\right]\\ &= \frac{1}{2}\int d^4x\sqrt{-g}\left[\chi_1 A\eta_1+g^{\mu\nu}(\partial_\mu\chi_1 A\partial_\nu A+\chi_1\partial_\mu A\partial_\nu A)\right],\end{aligned} \tag{5.56}$$

  where we have integrated by parts where appropriate. Solving the equation of motion for χ_1 yields $\eta_1=\bar{\Box}A$.

- For instance, in order to eliminate the term $A\bar{\Box}^2A$, we add the term

$$\frac{1}{2}\int d^4x\sqrt{-g}\chi_2 A(\eta_2-\bar{\Box}\eta_1)=\frac{1}{2}\int d^4x\sqrt{-g}\left[\chi_2 A\eta_2+g^{\mu\nu}(\partial_\mu\chi_2 A\partial_\nu\eta_1+\chi_2\partial_\mu A\partial_\nu\eta_1)\right]. \tag{5.57}$$

  Solving the equation of motion for χ_2 yields $\eta_2=\bar{\Box}\eta_1=\bar{\Box}^2A$.

Similarly, in order to eliminate the terms $A\bar{\Box}^nA$ and so on, we have to repeat the same procedure up to $\bar{\Box}^n$. Again, we have shown that by solving the equations of motion for χ_n, we obtain, for $n\geq 2$,

$$\eta_n=\bar{\Box}\eta_{n-1}=\bar{\Box}^nA. \tag{5.58}$$

Employing the above steps, we can rewrite the action given by (5.53) as

follows:

$$
\begin{aligned}
S_{eqv} = \frac{1}{2}\int d^4x\sqrt{-g}\Bigg\{ & A(M_P^2 + f_0 A + \sum_{n=1}^{\infty} f_n\eta_n) + B(R-A) + \chi_1 A(\eta_1 - \Box A) \\
& + \sum_{l=2}^{\infty}\chi_l A(\eta_l - \Box\eta_{l-1})\Bigg\} \\
= \frac{1}{2}\int d^4x\sqrt{-g}\Bigg\{ & A(M_P^2 + f_0 A + \sum_{n=1}^{\infty} f_n\eta_n) + B(R-A) \\
& + g^{\mu\nu}(A\partial_\mu\chi_1\partial_\nu A + \chi_1\partial_\mu A\partial_\nu A) + g^{\mu\nu}\sum_{l=2}^{\infty}(A\partial_\mu\chi_l\partial_\nu\eta_{l-1} + \chi_l\partial_\mu A\partial_\nu\eta_{l-1}) \\
& + \sum_{l=1}^{\infty} A\chi_l\eta_l\Bigg\},
\end{aligned}
\tag{5.59}
$$

where we have absorbed the powers of M^{-2} into the f_n's and χ_n's while the mass dimension of the η_n's has been modified accordingly; hence, the box operator is not barred.

Note that the gravitational part of the action is simplified. In order to perform the ADM decomposition, let us first look at the $B(R-A)$ term. Using (5.50), we can write

$$
B(R-A) = B\Big(K_{ij}K^{ij} - K^2 + \mathcal{R} - A\Big) + B\frac{2}{\sqrt{-g}}\partial_\mu(\sqrt{-g}n^\mu K) - B\frac{2}{N\sqrt{h}}\partial_i(\sqrt{h}h^{ij}\partial_j N) \tag{5.60}
$$

$$
= B\Big(K_{ij}K^{ij} - K^2 + \mathcal{R} - A\Big) - 2\left(\nabla_{\mathbf{n}}B\right)K - \frac{2}{\sqrt{h}}\partial_j(\partial_i(B)\sqrt{h}h^{ij}), \tag{5.61}
$$

since (boundary terms are discarded while the integration measure is $\sqrt{-g}d^4x$)

$$\begin{aligned}\int d^4x\sqrt{-g}\left[B\frac{2}{\sqrt{-g}}\partial_\mu(\sqrt{-g}n^\mu K)\right] &= \int d^4x\sqrt{-g}\Bigg\{\nabla_\mu\Big[B\frac{2}{\sqrt{-g}}(\sqrt{-g}n^\mu K)\Big] \\ &\quad - (\nabla_\mu B)\frac{2}{\sqrt{-g}}(\sqrt{-g}n^\mu K)\Bigg\} \\ &= \int d^4x\sqrt{-g}\Big\{\nabla_\mu\Big[2Bn^\mu K\Big] - 2(\nabla_\mu B)n^\mu K\Big\} \\ &= \int d^4x\sqrt{-g}\left[-2n^\mu(\nabla_\mu B)K\right] \\ &= \int d^4x\sqrt{-g}\left[-2\left(\nabla_{\mathbf{n}}B\right)K\right] \end{aligned} \tag{5.62}$$

and (again, boundary terms are discarded while the integration measure is $\sqrt{h}d^3x$)

$$\begin{aligned}\int d^3x\sqrt{h}\left[-B\frac{2}{N\sqrt{h}}\partial_i(\sqrt{h}h^{ij}\partial_j N)\right] &= \int d^3x\sqrt{h}\Bigg\{-\frac{2}{N\sqrt{h}}\partial_i(B(\sqrt{h}h^{ij}\partial_j N)) \\ &\quad + \frac{2}{N\sqrt{h}}\partial_i(B)\sqrt{h}h^{ij}\partial_j N\Bigg\} \\ &= \int d^3x\sqrt{h}\left[\frac{2}{N\sqrt{h}}\partial_i(B)\sqrt{h}h^{ij}\partial_j N\right] \\ &= \int d^3x\sqrt{h}\Bigg\{\frac{2}{N\sqrt{h}}\partial_j(\partial_i(B)\sqrt{h}h^{ij}N) \\ &\quad - \frac{2}{\sqrt{h}}\partial_j(\partial_i(B)\sqrt{h}h^{ij})\Bigg\} \\ &= \int d^3x\sqrt{h}\left[-\frac{2}{\sqrt{h}}\partial_j(\partial_i(B)\sqrt{h}h^{ij})\right]. \end{aligned} \tag{5.63}$$

We have used $n^\mu\nabla_\mu \equiv \nabla_{\mathbf{n}}$ and dropped the total derivatives. Furthermore, we can use the decomposition of the d'Alembertian operator, which is given by (5.51). Moreover, we have $\sqrt{-g} = N\sqrt{h}$. Hence, the decomposition of (5.59) becomes

as follows,

$$
\begin{aligned}
S'_{eqv} = \frac{1}{2}\int d^3x\ N\sqrt{h}\Bigg\{ & A(M_P^2 + f_0 A + \sum_{n=1}^{\infty} f_n\eta_n) + B\Big(K_{ij}K^{ij} - K^2 + \mathcal{R} - A\Big) \\
& - 2\nabla_{\mathbf{n}}BK - \frac{2}{\sqrt{h}}\partial_j(\partial_i(B)\sqrt{h}h^{ij}) \\
& + h^{ij}(A\partial_i\chi_1\partial_j A + \chi_1\partial_i A\partial_j A) - (A\nabla_{\mathbf{n}}\chi_1\nabla_{\mathbf{n}}A + \chi_1\nabla_{\mathbf{n}}A\nabla_{\mathbf{n}}A) \\
& + h^{ij}\sum_{l=2}^{\infty}(A\partial_i\chi_l\partial_j\eta_{l-1} + \chi_l\partial_i A\partial_j\eta_{l-1}) - \sum_{l=2}^{\infty}(A\nabla_{\mathbf{n}}\chi_l\nabla_{\mathbf{n}}\eta_{l-1} + \chi_l\nabla_{\mathbf{n}}A\nabla_{\mathbf{n}}\eta_{l-1}) \\
& + \sum_{l=1}^{\infty} A\chi_l\eta_l\Bigg\},
\end{aligned}
\tag{5.64}
$$

where the Latin indices are spatial and run from 1 to 3. Note that the χ fields were introduced to parameterise the contribution of $\bar{\Box}A$, $\bar{\Box}^2A$, ..., and so on. Therefore, A and η are auxiliary fields, signifying that the χ fields are of no intrinsic value and, therefore, are Lagrange multipliers when counting the number of phase space variables.

The same can not be concluded regarding the B field, as it is introduced to obtain equivalence between the scalar curvature, R, and A. Since the B field is coupled to R and the Riemannian curvature is physical, we must count B as a phase space variable. As we shall see later in our Hamiltonian analysis, this is a crucial point in order to count the number of physical degrees of freedom correctly. To summarise, as we shall see below, the B field is not a Lagrange multiplier, while the χ fields are.

5.3.3 $f(R)$ gravity

The action of $f(R)$ gravity is given by (1.7), where $f(R)$ is a function of the scalar curvature. The equivalent action for (1.7) is given by

$$
S = \frac{1}{2}\int d^4x\sqrt{-g}\,(f(A) + B(R - A))\,. \tag{5.65}
$$

Solving the equations of motion for B yields $R = A$; hence, it is clear that the above action is equivalent to (1.7). Using (5.61), we can decompose the action as follows,

$$S' = \frac{1}{2}\int d^3x\ N\sqrt{h}\Big(f(A) + B\Big(K_{ij}K^{ij} - K^2 + \mathcal{R} - A\Big) - 2\left(\nabla_{\mathbf{n}}B\right)K - \frac{2}{\sqrt{h}}\partial_j(\partial_i(B)\sqrt{h}h^{ij})\Big). \tag{5.66}$$

Now that the above action is expressed in terms of (h_{ab}, N, N^i, B, A) and their time and space derivatives. We can proceed with the Hamiltonian analysis and write down the momentum conjugate to each of these variables:

$$\pi^{ij} = \frac{\partial\mathcal{L}}{\partial\dot{h}_{ij}} = \sqrt{h}B(K^{ij} - h^{ij}K) - \sqrt{h}\nabla_{\mathbf{n}}Bh^{ij}, \quad p_B = \frac{\partial\mathcal{L}}{\partial\dot{B}} = -2\sqrt{h}K,$$
$$p_A = \frac{\partial\mathcal{L}}{\partial\dot{A}} \approx 0, \quad \pi_N = \frac{\partial\mathcal{L}}{\partial\dot{N}} \approx 0, \quad \pi_i = \frac{\partial\mathcal{L}}{\partial\dot{N}^i} \approx 0, \tag{5.67}$$

where $\dot{A} \equiv \partial_0 A$ is the time derivative of the variable. We have used the "$\approx$" sign in (5.67) to show that $(p_A,\ \pi_N,\ \pi_i)$ are primary constraints satisfied on the constraint surface:

$$\Gamma_p = (p_A \approx 0,\ \pi_N \approx 0,\ \pi_i \approx 0). \tag{5.68}$$

Γ_p is defined by the aforementioned primary constraints. For our purposes, whether the primary constraints vanish globally (which they do), *i.e.*, throughout the phase space, is irrelevant. Note that the Lagrangian density, $\mathcal{L}$, does not contain $\dot{A}$, $\dot{N}$ or $\dot{N}^i$; therefore, their conjugate momenta vanish identically.

We can define the Hamiltonian density as follows [1],

$$\mathcal{H} = \pi^{ij}\dot{h}_{ij} + p_B\dot{B} - \mathcal{L} \tag{5.69}$$
$$\equiv N\mathcal{H}_N + N^i\mathcal{H}_i, \tag{5.70}$$

[1]We should note that, in [156], the notation $\mathcal{H}_T$ is used for the quantity $\delta\mathcal{H}/\delta N$ which we denote by $\mathcal{H}_N$, *i.e.*, the variational derivative of the canonical Hamiltonian density $\mathcal{H}$ with respect to the lapse function N. In the literature, the notation $\mathcal{H}_T$ is, sometimes, used to refer to the total Hamiltonian density; in [156], the notation $\mathcal{H}_T$ does *not* refer to the total Hamiltonian density. In this chapter, we use the notation $\mathcal{H}_{tot}$ for the total Hamiltonian density.

where $\mathcal{H}_N = \dot{\pi}_N$ and $\mathcal{H}_i = \dot{\pi}_i$. Using (5.69), we can write ($\pi \equiv h^{ij}\pi_{ij}$)

$$\begin{aligned}\mathcal{H}_N = &\frac{1}{\sqrt{h}B}\pi^{ij}h_{ik}h_{jl}\pi^{kl} - \frac{1}{3\sqrt{h}B}\pi^2 - \frac{\pi p_B}{3\sqrt{h}} + \frac{B}{6\sqrt{h}}p_B^2 \\ &- \sqrt{h}BR + \sqrt{h}BA + 2\partial_j[\sqrt{h}h^{ij}\partial_i]B + f(A)\end{aligned} \tag{5.71}$$

and

$$\mathcal{H}_i = -2h_{ik}\nabla_l\pi^{kl} + p_B\partial_i B. \tag{5.72}$$

Therefore, the total Hamiltonian can be written as

$$H_{tot} = \int d^3x\ \mathcal{H} \tag{5.73}$$

$$= \int d^3x \left(N\mathcal{H}_N + N^i\mathcal{H}_i + \lambda^A p_A + \lambda^N\pi_N + \lambda^i\pi_i\right), \tag{5.74}$$

where $\lambda^A, \lambda^N, \lambda^i$ are Lagrange multipliers.

5.3.4 Classification of constraints for $f(R)$ gravity

Having vanishing conjugate momenta means we can not express $\dot{A}$, $\dot{N}$ and $\dot{N}^i$ as functions of their conjugate momenta and hence $p_A \approx 0$, $\pi_N \approx 0$ and $\pi_i \approx 0$ are primary constraints, see (5.67). To ensure the consistency of the primary constraints so that they are preserved under time evolution generated by the total Hamiltonian H_{tot}, we need to employ the Hamiltonian field equations and *enforce* that $\mathcal{H}_N$ and $\mathcal{H}_i$ be zero on the constraint surface Γ_p,

$$\dot{\pi}_N = -\frac{\delta\mathcal{H}_{tot}}{\delta N} = \mathcal{H}_N \approx 0, \quad \dot{\pi}_i = -\frac{\delta\mathcal{H}_{tot}}{\delta N^i} = \mathcal{H}_i \approx 0, \tag{5.75}$$

so that $\mathcal{H}_N \approx 0$ and $H_i \approx 0$, indicating that they are secondary constraints.

Let us also note that Γ_1 is a smooth submanifold of the phase space determined by the primary and secondary constraints; hereafter in this section, we shall exclusively use the "$\approx$" notation to denote equality on Γ_1. It is usual to call $\mathcal{H}_N$ the *Hamiltonian constraint* and $\mathcal{H}_i$ the *diffeomorphism constraint*. Note that $\mathcal{H}_N$

and $\mathcal{H}_i$ are weakly vanishing *only* on the constraint surface; this is why the right-hand sides of (5.71) and (5.72) are not *identically* zero. If $\dot{\pi}_N = \mathcal{H}_N$ and $\dot{\pi}_i = \mathcal{H}_i$ were *identically* zero, then there would be no *secondary constraints*.

Furthermore, we are going to define G_A and *demand* that G_A be weakly zero on the constraint surface Γ_1:

$$G_A = \partial_t p_A = \{p_A, \mathcal{H}_{tot}\} = -\frac{\delta \mathcal{H}_{tot}}{\delta A} = -\sqrt{h}N(B + f'(A)) \approx 0\,, \tag{5.76}$$

which will act as a secondary constraint corresponding to the primary constraint $p_A \approx 0$. Hence,

$$\Gamma_1 = (p_A \approx 0,\ \pi_N \approx 0,\ \pi_i \approx 0,\ G_A \approx 0,\ \mathcal{H}_N \approx 0,\ \mathcal{H}_i \approx 0). \tag{5.77}$$

Following the definition of the Poisson bracket in (5.10), we can see that the constraints $\mathcal{H}_N$ and $\mathcal{H}_i$ are preserved under time evolution, *i.e.*, $\dot{\mathcal{H}}_N = \{\mathcal{H}_N, \mathcal{H}_{tot}\}|_{\Gamma_1} = 0$ and $\dot{\mathcal{H}}_i = \{\mathcal{H}_i, \mathcal{H}_{tot}\}|_{\Gamma_1} = 0$, also fixing the Lagrange multipliers λ^N and λ^i. That is, the expressions for $\dot{\mathcal{H}}_N$ and $\dot{\mathcal{H}}_i$ include the Lagrange multipliers λ^N and λ^i; thus, we can solve the relations $\dot{\mathcal{H}}_N \approx 0$ and $\dot{\mathcal{H}}_i \approx 0$ for λ^N and λ^i, respectively, and compute the values of the Lagrange multipliers. Therefore, we have no further constraints, such as *tertiary* ones and so on. We will check the same for G_A, *i.e.*, that the time evolution of G_A defined in the phase space should also vanish on the constraint surface Γ_1:

$$\dot{G}_A \equiv \{G_A, \mathcal{H}_{tot}\} \tag{5.78}$$

$$= N\left\{\frac{N}{3}\Big(2\pi - 2Bp_B\Big) - 2\sqrt{h}N^i\partial_i B - \sqrt{h}f''(A)\lambda^A\right\} \approx 0. \tag{5.79}$$

The role of (5.78) is to fix the value of the Lagrange multiplier λ^A as long as $f''(A) \neq 0$. We demand that $f''(A) \neq 0$ so as to avoid *tertiary constraints*. As a result, there are no tertiary constraints corresponding to G_A. The next step in our Hamiltonian analysis is to classify the constraints.

As shown above, we have three primary constraints for $f(R)$ gravity. They

are

$$\pi_N \approx 0,\ \pi_i \approx 0,\ p_A \approx 0. \tag{5.80}$$

We also have three secondary constraints:

$$\mathcal{H}_N \approx 0,\ \mathcal{H}_i \approx 0,\ G_A \approx 0. \tag{5.81}$$

Following the definition of the Poisson bracket in (5.10), we have

$$\begin{aligned}\{\pi_N, \pi_i\} = &\left(\frac{\delta\pi_N}{\delta N}\frac{\delta\pi_i}{\delta\pi_N} - \frac{\delta\pi_N}{\delta\pi_N}\frac{\delta\pi_i}{\delta N}\right) + \left(\frac{\delta\pi_N}{\delta N^i}\frac{\delta\pi_i}{\delta\pi_i} - \frac{\delta\pi_N}{\delta\pi_i}\frac{\delta\pi_i}{\delta N^i}\right) \\ &+ \left(\frac{\delta\pi_N}{\delta h_{ij}}\frac{\delta\pi_i}{\delta\pi^{ij}} - \frac{\delta\pi_N}{\delta\pi^{ij}}\frac{\delta\pi_i}{\delta h_{ij}}\right) + \left(\frac{\delta\pi_N}{\delta A}\frac{\delta\pi_i}{\delta p_A} - \frac{\delta\pi_N}{\delta p_A}\frac{\delta\pi_i}{\delta A}\right) \\ &+ \left(\frac{\delta\pi_N}{\delta B}\frac{\delta\pi_i}{\delta p_B} - \frac{\delta\pi_N}{\delta p_B}\frac{\delta\pi_i}{\delta B}\right) \approx 0.\end{aligned} \tag{5.82}$$

Similarly, we can show that

$$\begin{aligned}&\{\pi_N, \pi_N\} = \{\pi_N, \pi_i\} = \{\pi_N, p_A\} = \{\pi_N, \mathcal{H}_N\} = \{\pi_N, \mathcal{H}_i\} = \{\pi_N, G_A\} \approx 0 \\ &\{\pi_i, \pi_i\} = \{\pi_i, p_A\} = \{\pi_i, \mathcal{H}_N\} = \{\pi_i, \mathcal{H}_i\} = \{\pi_i, G_A\} \approx 0 \\ &\{p_A, p_A\} = \{p_A, \mathcal{H}_N\} = \{p_A, \mathcal{H}_i\} \approx 0 \\ &\{\mathcal{H}_N, \mathcal{H}_N\} = \{\mathcal{H}_N, \mathcal{H}_i\} = \{\mathcal{H}_N, G_A\} \approx 0 \\ &\{\mathcal{H}_i, \mathcal{H}_i\} = \{\mathcal{H}_i, G_A\} \approx 0 \\ &\{G_A, G_A\} \approx 0.\end{aligned} \tag{5.83}$$

The only non-vanishing Poisson bracket on Γ_1 is

$$\{p_A, G_A\} = -\frac{\delta p_A}{\delta p_A}\frac{\delta G_A}{\delta A} = -\frac{\delta G_A}{\delta A} = -\sqrt{h}Nf''(A) \not\approx 0. \tag{5.84}$$

Having $\{p_A, G_A\} \neq 0$ for $f''(A) \neq 0$ means that both p_A and G_A are second-class constraints. The rest of the constraints $(\pi_N, \pi_i, \mathcal{H}_N, \mathcal{H}_i)$ are first-class constraints.

5.3.5 Number of physical degrees of freedom for $f(R)$ gravity

Having identified the primary and secondary constraints and categorised them into first-class and second-class constraints [1], we can use (5.16) to count the number of physical degrees of freedom. For $f(R)$ gravity, we have

$$\begin{aligned} 2\mathcal{A} &= 2 \times \{(h_{ij}, \pi^{ij}), (N, \pi_N), (N^i, \pi_i), (A, p_A), (B, p_B)\} \\ &= 2(6 + 1 + 3 + 1 + 1) = 24, \\ \mathcal{B} &= (p_A, G_A) = (1 + 1) = 2, \\ 2\mathcal{C} &= 2 \times (\pi_N, \pi_i, \mathcal{H}_N, H_i) = 2(1 + 3 + 1 + 3) = 16, \\ \mathcal{N} &= \frac{1}{2}(24 - 2 - 16) = 3. \end{aligned} \tag{5.85}$$

Hence, $f(R)$ gravity has three physical degrees of freedom in four dimensions, including the physical degrees of freedom for a massless graviton and also an extra scalar degree of freedom [2].

From the Lagrangian perspective, one can study the propagator for $f(R)$ theory of gravity. The graviton propagator in such a theory can be computed in terms of the spin-2 and spin-0 components [3]. Let us now briefly discuss a few cases of interest:

- Number of degrees of freedom for $f(R) = M_P^2 R + \alpha_0 R^2$:
  In this case (α_0 is a constant), we have

$$\{p_A, G_A\} = -\sqrt{h} N f''(A) = -2\sqrt{h} N \not\approx 0. \tag{5.86}$$

[1] Having *first-class and second-class constraints* means there are no arbitrary functions in the Hamiltonian. Indeed, a set of canonical variables that satisfies the constraint equations determines the physical state.

[2] We may note that the Latin indices run from 1 to 3 and are spatial. Moreover, the (h_{ij}, π^{ij}) pair is symmetric; therefore, there are six independent components.

[3] The propagator for $f(R)$ theory of gravity can be recast in four dimensions as (2.49), where P^2 and P_s^0 are the spin projector operators while a and c are functions of k^2. When $a = c$, we recover the propagator for the Einstein-Hilbert action. For $f(R)$ gravity, $a \neq c$, which yields one extra scalar degrees of freedom. This degree of freedom is nothing but the Brans-Dicke scalar [87].

The other Poisson brackets remain zero on the constraint surface Γ_1 and, hence, we are left with 3 physical degrees of freedom.

- Number of degrees of freedom for $f(R) = M_P^2 R$:
  For the Einstein-Hilbert action, $f(R)$ is simply

$$f(R) = M_P^2 R, \tag{5.87}$$

for which

$$\{p_A, G_A\} = -\sqrt{h} N f''(A) \approx 0. \tag{5.88}$$

Therefore, in this case, both p_A and G_A are first-class constraints. Hence, counting the degrees of freedom yields

$$\begin{aligned} 2\mathcal{A} &\equiv 2 \times \{(h_{ij}, \pi^{ij}), (N, \pi_N), (N^i, \pi_i), (A, p_A), (B, p_B)\} = 2(6+1+3+1+1) = 24, \\ \mathcal{B} &= 0, \\ 2\mathcal{C} &\equiv 2 \times (\pi_N, \pi_i, \mathcal{H}_N, H_i, p_A, G_A) = 2(1+3+1+3+1+1) = 20, \\ \mathcal{N} &= \frac{1}{2}(24 - 0 - 20) = 2, \end{aligned} \tag{5.89}$$

which gives the degrees of freedom for a massless spin-2 graviton.

5.4 Infinite derivative gravity (IDG)

5.4.1 Constraints for IDG

The action and the ADM decomposition of IDG has been explained explicitly in Section 5.3.2. In this section, we will focus on the Hamiltonian analysis for the action given by (5.52). The first step is to consider (5.64) and write down the

conjugate momenta:

$$\pi_N = \frac{\partial \mathcal{L}}{\partial \dot{N}} \approx 0, \quad \pi_i = \frac{\partial \mathcal{L}}{\partial \dot{N}^i} \approx 0, \quad \pi^{ij} = \frac{\partial \mathcal{L}}{\partial \dot{h}_{ij}} = \sqrt{h}B(K^{ij} - h^{ij}K) - \sqrt{h}\nabla_{\mathbf{n}} B h^{ij},$$
$$p_A = \frac{\partial \mathcal{L}}{\partial \dot{A}} = \sqrt{h}\Big[- (A\nabla_{\mathbf{n}}\chi_1 + \chi_1 \nabla_{\mathbf{n}} A) - \sum_{l=2}^{\infty} (\chi_l \nabla_{\mathbf{n}} \eta_{l-1})\Big], \quad p_B = \frac{\partial \mathcal{L}}{\partial \dot{B}} = -2\sqrt{h}K,$$
$$p_{\chi_1} = \frac{\partial \mathcal{L}}{\partial \dot{\chi}_1} = -\sqrt{h}A\nabla_{\mathbf{n}} A, \quad p_{\chi_l} = \frac{\partial \mathcal{L}}{\partial \dot{\chi}_l} = -\sqrt{h}(A\nabla_{\mathbf{n}}\eta_{l-1}),$$
$$p_{\eta_{l-1}} = \frac{\partial \mathcal{L}}{\partial \dot{\eta}_{l-1}} = -\sqrt{h}(A\nabla_{\mathbf{n}}\chi_l + \chi_l \nabla_{\mathbf{n}} A). \tag{5.90}$$

As we can see, the time derivatives of the lapse, *i.e.*, $\dot{N}$, and the shift function, $\dot{N}^i$, are absent. Therefore, we have two primary constraints:

$$\pi_N \approx 0, \ \pi_i \approx 0. \tag{5.91}$$

The total Hamiltonian is given by

$$H_{tot} = \int d^3x \ \mathcal{H} \tag{5.92}$$
$$= \int d^3x \left(N\mathcal{H}_N + N^i \mathcal{H}_i + \lambda^N \pi_N + \lambda^i \pi_i \right), \tag{5.93}$$

where λ^N & λ^i are Lagrange multipliers while the Hamiltonian density is given by

$$\mathcal{H} = \pi^{ij}\dot{h}_{ij} + p_A \dot{A} + p_B \dot{B} + p_{\chi_1}\dot{\chi}_1 + p_{\chi_l}\dot{\chi}_l + p_{\eta_{l-1}}\dot{\eta}_{l-1} - \mathcal{L} \tag{5.94}$$
$$= N\mathcal{H}_N + N^i \mathcal{H}_i \,. \tag{5.95}$$

Using the above equation, we obtain

$$\begin{aligned}\mathcal{H}_N &= \frac{1}{\sqrt{h}B}\pi^{ij}h_{ik}h_{jl}\pi^{kl} - \frac{1}{3\sqrt{h}B}\pi^2 - \frac{\pi p_B}{3\sqrt{h}} \\ &+\frac{B}{6\sqrt{h}}p_B^2 - \sqrt{h}BR + \sqrt{h}BA + 2\partial_j[\sqrt{h}h^{ij}\partial_i]B \\ &-\frac{1}{A\sqrt{h}}p_{\chi_1}(p_A - \frac{\chi_1}{A}p_{\chi_1}) - \frac{1}{A\sqrt{h}}\sum_{l=2}^{n}p_{\chi_l}(p_{\eta_{l-1}} - \frac{\chi_l}{A}p_{\chi_1}) \\ &-\sqrt{h}\sum_{l=1}^{n}A\chi_l\eta_l - \sqrt{h}\frac{1}{2}A(M_p^2 + f_0A + \sum_{n=1}^{\infty}f_n\eta_n) \\ &-\sqrt{h}h^{ij}(A\partial_i\chi_1\partial_jA + \chi_1\partial_iA\partial_jA) - \sqrt{h}h^{ij}\sum_{l=2}^{n}(A\partial_i\chi_l\partial_j\eta_{l-1} + \chi_l\partial_iA\partial_j\eta_{l-1})\end{aligned} \tag{5.96}$$

and

$$\mathcal{H}_i = -2h_{ik}\nabla_l\pi^{kl} + p_A\partial_iA + p_{\chi_1}\partial_i\chi_1 + p_B\partial_iB + \sum_{l=2}^{n}(p_{\chi_l}\partial_i\chi_l + p_{\eta_{l-1}}\partial_i\eta_{l-1}). \tag{5.97}$$

Enforcing that $\mathcal{H}_N$ and $\mathcal{H}_i$ be zero on the constraint surface Γ_p, we get

$$\dot{\pi}_N = -\frac{\delta\mathcal{H}_{tot}}{\delta N} = \mathcal{H}_N \approx 0, \qquad \dot{\pi}_i = -\frac{\delta\mathcal{H}_{tot}}{\delta N^i} = \mathcal{H}_i \approx 0. \tag{5.98}$$

We can also show that, on the constraint surface Γ_1, the time evolutions $\dot{\mathcal{H}}_N = \{\mathcal{H}_N, \mathcal{H}_{tot}\} \approx 0$ and $\dot{\mathcal{H}}_i = \{\mathcal{H}_i, \mathcal{H}_{tot}\} \approx 0$ fix the Lagrange multipliers λ^N and λ^i, and there will be no *tertiary constraints*.

5.4.2 Classifications of constraints for IDG

As we have explained earlier, primary and secondary constraints can be classified into first-class or second-class constraints. This is derived by calculating the Poisson brackets constructed out of the constraints between themselves and each other. Vanishing Poisson brackets indicate a first-class constraint and non-vanishing Poisson brackets means we have a second-class constraint.

For an IDG action, we have two primary constraints: $\pi_N \approx 0$ and $\pi_i \approx 0$, and

two secondary constraints: $\mathcal{H}_N \approx 0$, $H_i \approx 0$. Therefore, we can determine the classification of the constraints as follows,

$$\begin{aligned}\{\pi_N, \pi_i\} = &\left(\frac{\delta\pi_N}{\delta N}\frac{\delta\pi_i}{\delta\pi_N} - \frac{\delta\pi_N}{\delta\pi_N}\frac{\delta\pi_i}{\delta N}\right) + \left(\frac{\delta\pi_N}{\delta N^i}\frac{\delta\pi_i}{\delta\pi_i} - \frac{\delta\pi_N}{\delta\pi_i}\frac{\delta\pi_i}{\delta N^i}\right) + \left(\frac{\delta\pi_N}{\delta h_{ij}}\frac{\delta\pi_i}{\delta\pi^{ij}} - \frac{\delta\pi_N}{\delta\pi^{ij}}\frac{\delta\pi_i}{\delta h_{ij}}\right) \\ &+ \left(\frac{\delta\pi_N}{\delta A}\frac{\delta\pi_i}{\delta p_A} - \frac{\delta\pi_N}{\delta p_A}\frac{\delta\pi_i}{\delta A}\right) + \left(\frac{\delta\pi_N}{\delta B}\frac{\delta\pi_i}{\delta p_B} - \frac{\delta\pi_N}{\delta p_B}\frac{\delta\pi_i}{\delta B}\right) + \left(\frac{\delta\pi_N}{\delta\chi_1}\frac{\delta\pi_i}{\delta p_{\chi_1}} - \frac{\delta\pi_N}{\delta p_{\chi_1}}\frac{\delta\pi_i}{\delta\chi_1}\right) \\ &+ \left(\frac{\delta\pi_N}{\delta\chi_l}\frac{\delta\pi_i}{\delta p_{\chi_l}} - \frac{\delta\pi_N}{\delta p_{\chi_l}}\frac{\delta\pi_i}{\delta\chi_l}\right) + \left(\frac{\delta\pi_N}{\delta\eta_{l-1}}\frac{\delta\pi_i}{\delta p_{\eta_{l-1}}} - \frac{\delta\pi_N}{\delta p_{\eta_{l-1}}}\frac{\delta\pi_i}{\delta\eta_{l-1}}\right) \approx 0. \quad (5.99)\end{aligned}$$

In a similar manner, we can show that

$$\begin{aligned}&\{\pi_N, \pi_N\} = \{\pi_N, \pi_i\} = \{\pi_N, \mathcal{H}_N\} = \{\pi_N, \mathcal{H}_i\} \approx 0 \\ &\{\pi_i, \pi_i\} = \{\pi_i, \mathcal{H}_N\} = \{\pi_i, \mathcal{H}_i\} \approx 0 \\ &\{\mathcal{H}_N, \mathcal{H}_N\} = \{\mathcal{H}_N, \mathcal{H}_i\} \approx 0 \\ &\{\mathcal{H}_i, \mathcal{H}_i\} \approx 0. \quad (5.100)\end{aligned}$$

Therefore, all of $(\pi_N, \pi_i, \mathcal{H}_N, \mathcal{H}_i)$ are first-class constraints. We can establish that solving the equations of motion for χ_n yields

$$\eta_1 = \Box A, \quad \cdots, \quad \eta_l = \Box\eta_{l-1} = \Box^l A, \quad (5.101)$$

for $l \geq 2$. Therefore, we conclude that the χ_n's are Lagrange multipliers, which yield the following primary constraints from the equations of motion:

$$\begin{aligned}\Xi_1 &= \eta_1 - \Box A = 0, \\ \Xi_l &= \eta_l - \Box\eta_{l-1} = 0, \quad (5.102)\end{aligned}$$

where $l \geq 2$. In fact, it is sufficient to say that $\eta_1 - \Box A \approx 0$ and $\eta_l - \Box\eta_{l-1} \approx 0$ on a constraint surface spanned by primary and secondary constraints, *i.e.*, $(\pi_N \approx$

$0,\ \pi_i \approx 0,\ \mathcal{H}_N \approx 0,\ \mathcal{H}_i \approx 0,\ \Xi_n \approx 0$). As a result, we can show that we have

$$\{\Xi_n, \pi_N\} = \{\Xi_n, \pi_i\} = \{\Xi_n, \mathcal{H}_N\} = \{\Xi_n, \mathcal{H}_i\} = \{\Xi_m, \Xi_n\} \approx 0, \tag{5.103}$$

where we have employed the $\approx$ notation, which is a sufficient condition to be satisfied on the constraint surface defined by $\Gamma_1 = (\pi_N \approx 0,\ \pi_i \approx 0,\ \mathcal{H}_N \approx 0,\ \mathcal{H}_i \approx 0,\ \Xi_n \approx 0)$, signifying that the Ξ_n's are first-class constraints. We should point out that we have checked that the Poisson brackets of all possible pairs among the constraints vanish on the constraint surface Γ_1; as a result, there are no second-class constraints.

5.5 Physical degrees of freedom for IDG

We can again use (5.16) to compute the degrees of freedom for the IDG action given by (5.52). First, let us establish the number of the configuration space variables, $\mathcal{A}$. Since the auxiliary field χ_n are Lagrange multipliers, they are not dynamical so are redundant, as we have mentioned earlier. In contrast, we have to count the (B, p_B) pair in the phase space as B contains intrinsic value. For the IDG action given by (5.52), we have

$$\begin{aligned} 2\mathcal{A} &\equiv 2 \times \Big\{ (h_{ij}, \pi^{ij}), (N, \pi_N), (N^i, \pi_i), (B, p_B), (A, p_A), \underbrace{(\eta_1, p_{\eta_1}), (\eta_2, p_{\eta_2}), \cdots}_{n=1,\ 2,\ 3, \cdots \infty} \Big\} \\ &= 2 \times (6 + 1 + 3 + 1 + 1 + \infty) = \infty, \end{aligned} \tag{5.104}$$

For each pair (η_n, p_{η_n}), we have assigned one variable, which is multiplied by a factor of 2 since we are dealing with field-conjugate momentum pairs in the phase space. Moreover, as we have found from the Poisson brackets of all possible pairs among the constraints, the number of the second-class constraints, $\mathcal{B}$, is equal to zero. In the next subsections, we will show that the *correct* number of the *first-class constraints* depends on the choice of $\mathcal{F}(\bar{\Box})$.

5.5.1 Choice of $\mathcal{F}(\bar{\Box})$

In this subsection, we will focus on choosing $\mathcal{F}(\bar{\Box})$ appropriately for the action given by (5.52) (on a flat background). From the Lagrangian point of view, one could analyse the propagator of the action given by (5.52). It was found in [41, 56] that $\mathcal{F}(\bar{\Box})$ can be written in the following form:

$$\mathcal{F}(\bar{\Box}) = M_P^2 \frac{c(\bar{\Box}) - 1}{\Box}. \tag{5.105}$$

The choice of $c(\bar{\Box})$ determines how many roots we have and how many poles are present in the graviton propagator, see [41, 56, 87]. Here, we will consider two choices of $c(\bar{\Box})$, one of which has infinitely many roots, and therefore infinite poles in the propagator. For instance, we can choose

$$c(\bar{\Box}) = \cos(\bar{\Box}). \tag{5.106}$$

Then the equivalent action would be written as follows,

$$S_{eqv} = \frac{1}{2}\int d^4x\sqrt{-g}\left[M_P^2\left(A + A\big(\frac{\cos(\bar{\Box}) - 1}{\Box}\big)A\right) + B(R - A)\right]. \tag{5.107}$$

By solving the equations of motion for A, and subsequently solving for $\cos(\bar{\Box})$, we get

$$\cos(\bar{k}^2) = 1 - \frac{k^2(BM_P^{-2} - 1)}{2A}, \tag{5.108}$$

where, going to momentum space, we have $\Box \to -k^2$ (around Minkowski space). We also have that $\bar{k} \equiv k/M$ while B has mass dimension 2. From (L.6) in Appendix L, we have that

$$B = M_P^2\left(1 + \frac{4A}{3k^2}\right). \tag{5.109}$$

Therefore, solving $\cos(\bar{k}^2) = \frac{1}{3}$ yields infinitely many solutions. We observe that there is an infinite number of solutions; hence, there are also infinitely many degrees of freedom. Thus, we have got infinitely many solutions, which can be

written schematically as follows (the a_i's are parameters),

$$\begin{aligned}
\Psi_1 &= \Box A + a_1 A = 0, \\
\Psi_2 &= \Box A + a_2 A = 0, \\
\Psi_3 &= \Box A + a_3 A = 0, \\
&\vdots
\end{aligned} \tag{5.110}$$

or, in momentum space,

$$\begin{aligned}
-Ak^2 + Aa_1 = 0 \Rightarrow k^2 = a_1, \\
-Ak^2 + Aa_2 = 0 \Rightarrow k^2 = a_2, \\
-Ak^2 + Aa_3 = 0 \Rightarrow k^2 = a_3, \\
\vdots
\end{aligned} \tag{5.111}$$

Now, acting the $\Box$ operators on (5.110), we can write

$$\begin{aligned}
\Box\Psi_2 &= \Box^2 A + a_2 \Box A, \\
\Box^2\Psi_3 &= \Box^3 A + a_3 \Box^2 A, \\
&\vdots \\
\Box^{n-1}\Psi_n &= \Box^n A + a_n \Box^{n-1} A, \\
&\vdots
\end{aligned} \tag{5.112}$$

Following the prescription in Section 5.3.2, we can parameterise the terms of the form $\Box A$, $\Box^2 A$, etc, by employing the auxiliary fields χ_l, η_l, for $l \geq 1$. Therefore, we can write the solutions $\Psi_n^{'}$ as follows [1] (we should point out that we have acted the operator $\Box$ on Ψ_2, the operator $\Box^2$ on Ψ_3, etc, in order to obtain $\Psi_2^{'}$,

[1] For the sake of convenience, we have introduced the notation $\Psi_n^{'}$.

$\Psi_3^{'}$, etc, respectively):

$$\begin{aligned}
&\Psi_1^{'} = \eta_1 + a_1 A = 0,\\
&\Psi_2^{'} = \eta_2 + a_2\eta_1 = 0,\\
&\Psi_3^{'} = \eta_3 + a_3\eta_2 = 0.\\
&\vdots
\end{aligned} \tag{5.113}$$

As a result, we can rewrite the term $A + M_P^{-2} A\mathcal{F}(\bar{\Box})A$ as follows,

$$A + M_P^{-2} A\mathcal{F}(\bar{\Box})A = a_0 \Psi_1^{'} \prod_{n=2}^{\infty} \Box^{-n+1}\Psi_n^{'}. \tag{5.114}$$

Now, absorbing the powers of M^{-2} into the coefficients where appropriate (the ϕ_n auxiliary fields in (5.115) act as Lagrange multipliers while taking the equations of motion for ϕ_n yields $\psi_n = \Box^{-n+1}\Psi_n^{'}$),

$$\begin{aligned}
S_{eqv} = \frac{1}{2}\int d^4x\sqrt{-g}\Big[& M_P^2 a_0 \prod_{n=1}^{\infty}\psi_n + B(R-A) + \chi_1 A(\eta_1 - \Box A)\\
& + \sum_{l=2}^{\infty}\chi_l A(\eta_l - \Box\eta_{l-1}) + \phi_1(\psi_1 - \Psi_1^{'}) + \sum_{n=2}^{\infty}\phi_n\big(\psi_n - \Box^{-n+1}\Psi_n^{'}\big)\Big],
\end{aligned} \tag{5.115}$$

where a_0 is a constant. Let us define $\Phi_1 = \psi_1 - \Psi_1^{'}$ and, for $n \geq 2$, $\Phi_n = \psi_n - \Box^{-n+1}\Psi_n^{'}$. Then the equations of motion for ϕ_n will yield

$$\Phi_n = \psi_n - \Box^{-n+1}\Psi_n^{'} = 0. \tag{5.116}$$

Again, it is sufficient to replace $\psi_n - \Box^{-n+1}\Psi_n^{'} = 0$ with $\psi_n - \Box^{-n+1}\Psi_n^{'} \approx 0$ satisfied on the constraint surface. As a result, there are n primary constraints in Φ_n. Moreover, considering the equations of motion for χ_n's and ϕ_n's simultaneously yields the *original* action given by (5.107). The time evolutions of the Ξ_n's & Φ_n's fix the corresponding Lagrange multipliers λ^{Ξ_n} & λ^{Φ_n} in the total Hamiltonian (when we add the terms $\lambda^{\Xi_n}\Xi_n$ & $\lambda^{\Phi_n}\Phi_n$ to the integrand in (5.93)); hence, the

Ξ_n's & Φ_n's do not induce secondary constraints.

In order to classify these constraints, one can show that the following Poisson brackets involving Φ_n on the constraint surface ($\pi_N \approx 0, \pi_i \approx 0, \mathcal{H}_N \approx 0, \mathcal{H}_i \approx 0, \Xi_n \approx 0, \Phi_n \approx 0$) are satisfied [1]:

$$\{\Phi_n, \pi_N\} = \{\Phi_n, \pi_i\} = \{\Phi_n, \mathcal{H}_N\} = \{\Phi_n, \mathcal{H}_i\} = \{\Phi_m, \Xi_n\} = \{\Phi_m, \Phi_n\} \approx 0, \tag{5.117}$$

which means that the Φ_n's can be treated as first-class constraints. We should point out that we have checked that the Poisson brackets of all possible pairs among the constraints vanish on the constraint surface Γ_1; as a result, there are no second-class constraints. From (5.16) and (5.104), we obtain infinitely many degrees of freedom. Hence, we see that an injudicious choice for $\mathcal{F}(\bar{\Box})$ can lead to infinitely many degrees of freedom (there are many such examples). However, our aim is to come up with a concrete example whereby IDG shall be determined solely by the massless spin-2 graviton and at most one massive scalar.

5.5.2 Exponential case

In the definition of $\mathcal{F}(\bar{\Box})$ given by (5.105), if

$$c(\bar{\Box}) = e^{\gamma(\bar{\Box})}, \tag{5.118}$$

where $\gamma(\bar{\Box})$ is an entire function, we can decompose the propagator into partial fractions and have just one extra pole apart from the spin-2 graviton. Consequently, in order to have just one extra degree of freedom, we have to impose conditions on the coefficients in the $\mathcal{F}(\bar{\Box})$ series expansion. Moreover, to avoid $\Box^{-1}$ terms appearing in the $\mathcal{F}(\bar{\Box})$, we must have that

$$c(\bar{\Box}) = \sum_{n=0}^{\infty} c_n \bar{\Box}^n, \tag{5.119}$$

[1] Let us note again that Γ_1 is a smooth submanifold of the phase space determined by the *primary* and *secondary constraints*; hereafter in this section, we shall exclusively use the "$\approx$" notation to denote equality on Γ_1.

with the first coefficient $c_0 = 1$. Hence,

$$\mathcal{F}(\bar{\Box}) = \left(\frac{M_P}{M}\right)^2 \sum_{n=0}^{\infty} c_{n+1} \bar{\Box}^n. \tag{5.120}$$

Suppose we have $c(\bar{\Box}) = e^{-\bar{\Box}}$. Using (5.105), we get

$$\mathcal{F}(\bar{\Box}) = \sum_{n=0}^{\infty} f_n \bar{\Box}^n, \tag{5.121}$$

where the coefficients f_n are of the form

$$f_n = \left(\frac{M_P}{M}\right)^2 \frac{(-1)^{n+1}}{(n+1)!}. \tag{5.122}$$

This particular choice of $c(\bar{\Box})$ is very well motivated from string field theory [41]. In fact, the above choice of $\gamma(\bar{\Box}) = -\bar{\Box}$ contains at most one extra zero in the propagator corresponding to one extra scalar mode in the spin-0 component of the graviton propagator [56, 87]. We can rewrite the action (around Minkowski space) as follows,

$$S_{eqv} = \frac{1}{2} \int d^4x \sqrt{-g} \left\{ M_P^2 \left[A + A \left(\frac{e^{-\bar{\Box}} - 1}{\Box} \right) A \right] + B(R - A) \right\}. \tag{5.123}$$

The equation of motion for A is

$$M_P^2 \left[1 + 2 \left(\frac{e^{-\bar{\Box}} - 1}{\Box} \right) A \right] - B = 0. \tag{5.124}$$

In momentum space, we can solve the equation above:

$$e^{\bar{k}^2} = 1 - \frac{k^2(BM_P^{-2} - 1)}{2A}, \tag{5.125}$$

where, going to momentum space, $\Box \to -k^2$ (on a flat background) while $\bar{k} \equiv k/M$. From (L.11) in Appendix L, we have $e^{\bar{k}^2} = \frac{1}{3}$. Therefore, solving (5.125) yields

$$B = M_P^2 \left(1 + \frac{4A}{3k^2}\right). \tag{5.126}$$

Note that we obtain only one extra solution (apart from the one for the massless spin-2 graviton). We observe that there is a finite number of real solutions; hence, there are also finitely many degrees of freedom. The form of the solution can be written schematically as follows (where Ω represents the solution and b_1 is a parameter),

$$\Omega = \Box A + b_1 A = 0, \tag{5.127}$$

or, in momentum space,

$$-Ak^2 + Ab_1 = 0 \Rightarrow k^2 = b_1. \tag{5.128}$$

Following again the prescription laid down in Section 5.3.2, we can parameterise the terms of the form $\Box A$, $\Box^2 A$, etc. with the help of the auxiliary fields χ_l and η_l, for $l \geq 1$. Therefore, equivalently,

$$\Omega^{'} = \eta_1 + b_1 A = 0, \tag{5.129}$$

where $\Omega^{'}$ represents the parameterised solution ($\Box A$ has been parameterised in terms of η_1). Upon taking the equations of motion for the field ρ, one can rewrite $A + M_P^{-2} A\mathcal{F}(\bar{\Box})A$ as follows,

$$A + M_P^{-2} A\mathcal{F}(\bar{\Box})A = b_0 \omega \mathcal{G}(A, \eta_1, \eta_2, \dots). \tag{5.130}$$

Hence, we can recast the action given by (5.123) as follows,

$$S_{eqv} = \frac{1}{2}\int d^4x\sqrt{-g}\Big[M_P^2 b_0\omega\ \mathcal{G}(A,\eta_1,\eta_2,\dots) + B(R-A) + \chi_1 A(\eta_1 - \Box A) + \sum_{l=2}^{\infty}\chi_l A(\eta_l - \Box\eta_{l-1}) + \rho\big(\omega - \Omega^{'}\big)\Big], \tag{5.131}$$

where b_0 is a constant and ρ is a Lagrange multiplier while taking the equation of motion for ρ yields $\omega = \Omega^{'}$. The equation of motion for ρ yields

$$\Theta = \omega - \Omega^{'} = 0. \tag{5.132}$$

Note that $\Theta = \omega - \Omega^{'} \approx 0$ will suffice on the constraint surface determined by the primary and secondary constraints ($\pi_N \approx 0, \pi_i \approx 0, \mathcal{H}_N \approx 0, \mathcal{H}_i \approx 0, \Xi_n \approx 0, \Theta \approx 0$). As a result, Θ is a primary constraint. The time evolutions of the Ξ_n's & Θ fix the corresponding Lagrange multipliers λ^{Ξ_n} & λ^{Θ} in the total Hamiltonian (when we add the terms $\lambda^{\Xi_n}\Xi_n$ & $\lambda^{\Theta}\Theta$ to the integrand in (5.93)); hence, the Ξ_n's & Θ do not induce secondary constraints.

Taking the equations of motion for the χ_n's and ρ simultaneously yields the same equation of motion as that for the action given by (5.123). The Poisson bracket of Θ with other constraints gives

$$\{\Theta,\pi_N\} = \{\Theta,\pi_i\} = \{\Theta,\mathcal{H}_N\} = \{\Theta,\mathcal{H}_i\} = \{\Theta,\Xi_n\} = \{\Theta,\Theta\} \approx 0, \tag{5.133}$$

where $\approx$ would have been sufficient. Thus, Θ is a first-class constraint. Hence,

we can calculate the number of the physical degrees of freedom as follows,

$$
\begin{aligned}
2\mathcal{A} &\equiv 2 \times \Big\{(h_{ij}, \pi^{ij}), (N, \pi_N), (N^i, \pi_i), (B, p_B), (A, p_A), \underbrace{(\eta_1, p_{\eta_1}), (\eta_2, p_{\eta_2}), \cdots}_{n=1,\ 2,\ 3, \cdots \infty}\Big\} \\
&= 2 \times (6 + 1 + 3 + 1 + 1 + \infty) = \infty, \\
\mathcal{B} &= 0, \\
2\mathcal{C} &\equiv 2 \times (\pi_N, \pi_i, \mathcal{H}_N, \mathcal{H}_i, \Xi_n, \Theta) = 2(1 + 3 + 1 + 3 + \infty + 1) = \infty, \\
\mathcal{N} &= \frac{1}{2}(2\mathcal{A} - \mathcal{B} - 2\mathcal{C}) = \frac{1}{2}(24 - 0 - 18) = 3,
\end{aligned}
\tag{5.134}
$$

since there is a one-to-one correspondence between each pair (η_n, p_{η_n}) and Ξ_n. This gives 2 degrees of freedom from the massless spin-2 graviton in addition to an extra degree of freedom as expected from the propagator analysis. One may consult Appendix L for more details.

5.6 Summary

In this chapter, we have carried out a Hamiltonian analysis of an infinite derivative gravitational theory (IDG) and evaluated the number of degrees of freedom for the theory. IDG contains infinitely many derivatives acting on the Ricci scalar [41].

From a Lagrangian point of view, the number of dynamical degrees of freedom can be determined from the propagator. Specifically, it hinges on the number of poles arising in the propagator. In the case of IDG, one can see from the spin-0 and spin-2 components of the propagator that, for a Gaussian kinetic term in the Lagrangian, there exist just two dynamical degrees of freedom. In order to guarantee that there are no additional poles in the propagator apart from those being already present in the original theory, one can impose that the propagator be suppressed by the exponential of an entire function. It should be pointed out that an entire function does not give rise to poles in the finite complex plane. Therefore, the kinetic term in the Lagrangian for infinite derivative theories should be modified accordingly. For a scalar toy model, the kinetic term is of the form $\mathcal{F}(\bar{\Box}) = \Box e^{-\bar{\Box}}$. In the context of gravity, we have $\mathcal{F}(\bar{\Box}) = M_p^2 \Box^{-1}(e^{-\bar{\Box}} - 1)$.

From a Hamiltonian point of view, in order to compute the number of dynamical degrees of freedom, one has to write down first the configuration space variables and first- & second-class constraints. For instance, infinite derivative theories contain infinitely many configuration space variables and, accordingly, first- and second-class constraints. However, for a Gaussian kinetic term, $\mathcal{F}(\bar{\Box})$, the number of degrees of freedom is finite, which holds for both scalar and gravitational Hamiltonian densities.

Chapter 6

Conclusion

In this thesis, we have looked into classical and quantum aspects of infinite derivative field theories and infinite derivative gravity. In particular, we have mainly focused on a ghost-free and singularity-free infinite derivative theory of gravity. Here we outline the results which have been presented so far.

Outline of Results

In Chapter 2, we have written down the infinite derivative gravitational action. Moreover, we have presented the corresponding tree-level propagator when metric perturbations around a Minkowski background, $g_{\mu\nu} = \eta_{\mu\nu} + h_{\mu\nu}$, are considered. Inspired by the shift-scaling symmetries of the field equations in GR, we have motivated an infinite derivative scalar toy model which encapsulates the basic features and behaviour of infinite derivative gravity.

The free part of the infinite derivative scalar toy model gives rise to a propagator that is exponentially suppressed in the UV. Furthermore, after considering metric perturbations around a Minkowski background, we have computed the $\mathcal{O}(h^3)$ part of the infinite derivative gravitational action. As a result, we derived the interaction terms in the infinite derivative scalar toy model. The interaction terms give rise to exponentially enhanced vertex factors. We observe that the propagator and the vertex factors exhibit opposing momentum dependence. This compensatory behaviour is a generic feature of gauge field theories.

Consequently, we have derived the modified superficial degree of divergence for the infinite derivative scalar toy model. In contrast to the superficial degree of divergence for GR, where the superficial degree of divergence increases as the number of loops increases, rendering GR non-renormalisable, the modified superficial degree of divergence for the infinite derivative scalar toy model decreases as the number of loops L increases. Consequently, loop amplitudes are superficially convergent when $L > 1$. This fact is a promising hint as far as the renormalisability of the infinite derivative scalar toy model is concerned.

In Chapter 3, we have looked into radiative corrections for an infinite derivative scalar field theory toy model resembling the UV properties of infinite derivative gravity. We wrote down the Feynman rules for our toy model, that is, the propagator and the vertex factors. Next, we evaluated the 1-loop, 2-point diagram with arbitrary external momenta, which gives rise to a Λ^4 divergence, where Λ is a momentum cutoff. The highest divergence for 2-loop diagrams with vanishing external momenta is Λ^4 as well, meaning that we do not get higher divergences as the loop-order increases. In the 1-loop, 2-point function, we got a $e^{\frac{3\bar{p}^2}{2}}$ external momentum dependence at high energies, which appears as a subdivergence in higher-loop diagrams. This property renders all higher-loop and higher-point diagrams finite once bare propagators are replaced with dressed propagators. Specifically, the exponential suppression coming from the dressed propagator is stronger than the exponential enhancement engendered by the vertices. When we replace the bare propagators with dressed propagators in the 1-loop, 2-point function, the corresponding Feynman integrals are convergent. The 1-loop, N-point functions with vanishing external momenta are now finite in the UV; the same holds for 2-loop integrals with zero external momenta. To that end, we have also established the UV finiteness of n-loop, 2- & 3-point diagrams constructed out of lower-loop, 2- & 3-point diagrams.

In general, we have shown that, by employing dressed vertices and dressed propagators, n-loop, N-point diagrams constructed out of lower-loop, 2- & 3-point and, in general, N_i-point diagrams are UV finite. This implies that the most general one-particle irreducible (1PI) Feynman diagrams within the framework of infinite derivative field theories are finite in the UV. Hence, no UV divergences arise and no new counterterm is necessary.

In addition, we have demonstrated that the external momentum dependences of n-loop, N-point diagrams constructed out of lower-loop, 2- & 3-point and, in general, N_i-point diagrams decrease as the loop-order increases and the external momentum divergences are eliminated at sufficiently high loop-order.

In Chapter 4, we have investigated the external momentum dependence of scattering diagrams within the framework of infinite derivative field theories and gravity. For a finite-order, higher-derivative scalar field theory, the cross section of tree-level scattering diagrams blows up at large external momenta. If we dress the propagators and the vertices by making propagator and vertex loop corrections to the bare vertices of the scattering diagrams, the external momentum growth can still not be tamed. We observe that dressing the propagators somewhat softens the external momentum growth.

Subsequently, we have investigated a scalar field theory with infinite derivative kinetic and interaction terms. The propagators are exponentially suppressed while the vertices are exponentially enhanced. We have obtained that the corresponding tree-level cross section blows up when the external momenta are large. Only if we dress the propagators and the vertices by making renormalised propagator and vertex loop corrections to the bare vertices at sufficiently high loop-order (the loop-order n being greater than or equal to four) can the cross section be made finite in the UV. As the loop-order increases, the dressed vertices give rise to negative exponents so that scattering amplitudes are ameliorated at high energies. Hence, the cross section does not blow up in the UV. One can surmise that, in that context, scattering scalar wave packets with infinite derivative interactions would not engender black hole singularities, which can potentially assist us with understanding the high-energies properties of gravity within the framework of an infinite derivative gravitational paradigm.

Next, we have looked into high-energy scattering diagrams in an infinite derivative scalar toy model motivated by the infinite derivative gravitational action. In particular, we have established that dressing the vertices and the propagators indeed gives rise to a finite cross section and convergent scattering diagrams at large external momenta. It would be illuminating to demonstrate that non-locality can ameliorate the trans-Planckian scattering problem and prevent the formation of a black hole singularity. Armed with these findings, one

could attempt to resolve the black hole singularity and cosmological singularity problems in a time-dependent setup.

Finally, in Chapter 5, we have carried out a Hamiltonian analysis of an infinite derivative gravitational theory (IDG) and evaluated the number of degrees of freedom for the theory. The IDG action contains infinitely many derivatives acting on the Ricci scalar [41] and is simpler compared with the infinite derivative gravitational action given by (1.10). From a Lagrangian point of view, the number of dynamical degrees of freedom can be determined from the propagator. Specifically, it hinges on the number of poles arising in the propagator. In the case of IDG, one can see from the spin-0 and spin-2 components of the propagator that, for a Gaussian kinetic term in the Lagrangian, there exist just two dynamical degrees of freedom. In order to guarantee that there are no additional poles in the propagator apart from those being already present in the original theory, one can impose that the propagator be suppressed by the exponential of an entire function. It should be pointed out that an entire function does not give rise to poles in the finite complex plane. Therefore, the kinetic term in the Lagrangian for infinite derivative theories should be modified accordingly. For a scalar toy model, the kinetic term is of the form $\mathcal{F}(\bar{\Box}) = \Box e^{-\bar{\Box}}$. In the context of gravity, we have $\mathcal{F}(\bar{\Box}) = M_p^2 \Box^{-1}(e^{-\bar{\Box}} - 1)$. Evidently, Hamiltonian and Lagrangian analyses should give rise to coincident physical interpretations.

From a Hamiltonian point of view, in order to compute the number of dynamical degrees of freedom, one has to write down first the configuration space variables and first- & second-class constraints. For instance, infinite derivative theories contain infinitely many configuration space variables and, accordingly, first-class and second-class constraints. However, for a Gaussian kinetic term, $\mathcal{F}(\bar{\Box})$, the number of degrees of freedom is finite, which holds for both scalar and gravitational Hamiltonian densities.

Future Work

- Infinite derivative gravitational theories can resolve the black hole singularity problem in the weak field regime. It would be interesting to see whether

one can avoid singularities in the case of astrophysical black holes.

- Addressing the cosmological singularity issue in the presence of matter sources is an open question. Moreover, the exact cosmological solutions were only obtained in the presence of a cosmological constant. A realistic cosmological scenario must include a graceful exit from the inflationary phase. Currently, a scheme to analyse such a transition is lacking and any progress in this direction would be greatly beneficial.

- So far, infinite derivative gravitational models have been studied around a Minkowski background. It would be interesting to explore the classical and quantum properties of infinite derivative gravitational theories around de Sitter (dS) and Friedmann-Lemaître-Robertson-Walker (FLRW) backgrounds (see [157, 158] for related recent work).

- In this thesis, we have shown that, by employing dressed vertices and dressed propagators, n-loop, N-point diagrams constructed out of lower-loop, 2- & 3-point and, in general, N_i-point diagrams are UV finite. Moreover, we have shown that the external momentum dependences of n-loop, N-point diagrams constructed out of lower-loop, 2- & 3-point and, in general, N_i-point diagrams decrease as the loop-order increases and the external momentum divergences are eliminated at sufficiently high loop-order. We would like to further generalise these results and apply them to the infinite derivative gravitational theory given by (1.10). Showing that an infinite derivative theory of gravity is renormalisable or even finite at higher loop-order would be a big achievement by itself and a major step towards establishing a UV-complete quantum gravitational theory.

- In order to establish unitarity within the framework of infinite derivative theories, novel prescriptions may have to be employed. Establishing unitarity and causality of infinite derivative theories of gravity would be a major step towards the construction of a fully satisfactory theory of quantum gravity.

- Regarding scattering diagrams, it would be instructive to consider scattering diagrams within the context of the infinite derivative gravitational action given by (1.10). We expect that, by using dressed propagators and dressed vertices, we would obtain finite cross sections, thereby rendering the scattering diagrams under consideration convergent at large external momenta.

- As far as Hamitonian analysis is concerned, it would be interesting as a future exercise to write down the Hamiltonian density and compute the number of degrees of freedom for the full infinite derivative gravitational action given by (1.10). That way, one could compare the results from Hamiltonian analysis to the ones we have already obtained from Lagrangian analysis.

Appendix A

Conventions and notations

The metric signature employed in this thesis is

$$g_{\mu\nu} = (-, +, +, +). \tag{A.1}$$

In natural units ($\hbar = c = 1$),

$$M_P = \kappa^{-\frac{1}{2}} = \sqrt{\frac{\hbar c}{8\pi G_N^{(4)}}}, \tag{A.2}$$

where M_P is the (reduced) Planck mass and $G_N^{(4)}$ is Newton's gravitational constant in four-dimensional spacetime.
Here are the mass dimensions of some quantities:

$$[dx] = [x] = [t] = M^{-1}, \tag{A.3}$$

$$[\partial_\mu] = [p_\mu] = [k_\mu] = M^1, \tag{A.4}$$

$$[\text{velocity}] = \frac{[x]}{[t]} = M^0. \tag{A.5}$$

Hence,

$$[d^4x] = M^{-4}. \tag{A.6}$$

The action is a dimensionless quantity:

$$[S] = [\int d^4x \ \mathcal{L}] = M^0. \tag{A.7}$$

Therefore,

$$[\mathcal{L}] = M^4. \tag{A.8}$$

The Christoffel symbol is given by

$$\Gamma^{\lambda}_{\mu\nu} = \frac{1}{2} g^{\lambda\tau}(\partial_\mu g_{\nu\tau} + \partial_\nu g_{\mu\tau} - \partial_\tau g_{\mu\nu}). \tag{A.9}$$

The Riemann tensor is given by

$$R^{\lambda}{}_{\mu\sigma\nu} = \partial_\sigma \Gamma^{\lambda}_{\mu\nu} - \partial_\nu \Gamma^{\lambda}_{\mu\sigma} + \Gamma^{\lambda}_{\sigma\rho}\Gamma^{\rho}_{\nu\mu} - \Gamma^{\lambda}_{\nu\rho}\Gamma^{\rho}_{\sigma\mu}, \tag{A.10}$$

and satisfies

$$R_{\mu\nu\lambda\sigma} = -R_{\nu\mu\lambda\sigma} = -R_{\mu\nu\sigma\lambda} = R_{\lambda\sigma\mu\nu}, \tag{A.11}$$

$$R_{\mu\nu\lambda\sigma} + R_{\mu\lambda\sigma\nu} + R_{\mu\sigma\nu\lambda} = 0. \tag{A.12}$$

The Ricci tensor is given by

$$R_{\mu\nu} = R^{\lambda}{}_{\mu\lambda\nu} = \partial_\lambda \Gamma^{\lambda}_{\mu\nu} - \partial_\nu \Gamma^{\lambda}_{\mu\lambda} + \Gamma^{\lambda}_{\lambda\rho}\Gamma^{\rho}_{\nu\mu} - \Gamma^{\lambda}_{\nu\rho}\Gamma^{\rho}_{\lambda\mu}, \tag{A.13}$$

and satisfies

$$R_{\mu\nu} = R_{\nu\mu}. \tag{A.14}$$

The Ricci scalar is given by

$$R = g^{\mu\nu}R_{\mu\nu} = g^{\mu\nu}\partial_\lambda \Gamma^{\lambda}_{\mu\nu} - \partial^\mu \Gamma^{\lambda}_{\mu\lambda} + g^{\mu\nu}\Gamma^{\lambda}_{\lambda\rho}\Gamma^{\rho}_{\nu\mu} - g^{\mu\nu}\Gamma^{\lambda}_{\nu\rho}\Gamma^{\rho}_{\lambda\mu}. \tag{A.15}$$

The Weyl tensor is given by

$$C^{\mu}{}_{\alpha\nu\beta} \equiv R^{\mu}{}_{\alpha\nu\beta} - \frac{1}{2}(\delta^\mu_\nu R_{\alpha\beta} - \delta^\mu_\beta R_{\alpha\nu} + R^\mu_\nu g_{\alpha\beta} - R^\mu_\beta g_{\alpha\nu}) + \frac{R}{6}(\delta^\mu_\nu g_{\alpha\beta} - \delta^\mu_\beta g_{\alpha\nu}), \tag{A.16}$$

$$C^{\lambda}{}_{\mu\lambda\nu} = 0. \tag{A.17}$$

The Einstein tensor is given by

$$G_{\mu\nu} = R_{\mu\nu} - \frac{1}{2} g_{\mu\nu} R. \tag{A.18}$$

Varying the Einstein-Hilbert action,

$$S_{EH} = \frac{1}{2} \int d^4x \sqrt{-g} \left(M_P^2 R - 2\Lambda \right), \tag{A.19}$$

where Λ is the cosmological constant of mass dimension 4, yields the Einstein equation,

$$M_P^2 G_{\mu\nu} + g_{\mu\nu}\Lambda = T_{\mu\nu}, \tag{A.20}$$

where $T_{\mu\nu}$ is the energy-momentum tensor. When considering perturbations around a Minkowski background, the cosmological constant Λ is set equal to zero.

The formula for the commutation of covariant derivatives is given by

$$\begin{aligned} [\nabla_\rho, \nabla_\sigma] X^{\mu_1 \ldots \mu_k}{}_{\nu_1 \ldots \nu_l} = {} & R^{\mu_1}{}_{\lambda\rho\sigma} X^{\lambda\mu_2 \ldots \mu_k}{}_{\nu_1 \ldots \nu_l} + R^{\mu_2}{}_{\lambda\rho\sigma} X^{\mu_1 \lambda \mu_3 \ldots \mu_k}{}_{\nu_1 \ldots \nu_l} + \ldots \\ & - R^{\lambda}{}_{\nu_1\rho\sigma} X^{\mu_1 \ldots \mu_k}{}_{\lambda \ldots \nu_l} - R^{\lambda}{}_{\nu_2\rho\sigma} X^{\mu_1 \ldots \mu_k}{}_{\nu_1 \lambda \nu_3 \ldots \nu_l} - \ldots . \end{aligned} \tag{A.21}$$

The Bianchi identity is given by

$$\nabla_\kappa R_{\mu\nu\lambda\sigma} + \nabla_\sigma R_{\mu\nu\kappa\lambda} + \nabla_\lambda R_{\mu\nu\sigma\kappa} = 0. \tag{A.22}$$

Contracting (A.22) with $g^{\mu\lambda}$ gives the contracted Bianchi identity,

$$\nabla_\kappa R_{\nu\sigma} - \nabla_\sigma R_{\nu\kappa} + \nabla^\lambda R_{\lambda\nu\sigma\kappa} = 0. \tag{A.23}$$

Contracting (A.23) with $g^{\nu\kappa}$, we obtain

$$\nabla_\kappa R^\kappa_\sigma = \frac{1}{2} \nabla_\sigma R, \tag{A.24}$$

yielding

$$\nabla^\sigma \nabla_\kappa R^\kappa_\sigma = \frac{1}{2}\Box R \tag{A.25}$$

and

$$\nabla_\mu G^\mu_\nu = 0. \tag{A.26}$$

Appendix B

Ghosts

Higher-derivative gravitational theories usually suffer from *ghosts*. Ghosts are fields which have negative kinetic energy. The existence of ghosts at the classical level usually indicates vacuum instabilities while ghosts arising at the quantum level may imply violation of unitarity. In gravity, ghosts are associated with negative residues in the graviton propagator [86, 106].
On the other hand, *tachyons* are particles which have imaginary mass, that is, $m^2_{\text{tachyon}} < 0$.

B.1 General Relativity

In General Relativity, there exists a ghost but it is not harmful. The four-dimensional graviton propagator,

$$\Pi_{GR} = \frac{\mathcal{P}^2}{k^2} - \frac{\mathcal{P}^0_s}{2k^2}, \tag{B.1}$$

has a negative residue at the $k^2 = 0$ pole. However, the aforementioned pole merely corresponds to the physical graviton.

B.2 $f(R)$ gravity

The action of $f(R)$ gravitational theories is given by (1.7). When $f(R) = M_P^2 R + \alpha_0 R^2$, the corresponding propagator can be written as

$$\Pi_{R^2} = \Pi_{GR} + \frac{1}{2}\frac{\mathcal{P}_s^0}{k^2 + m^2}. \tag{B.2}$$

We observe that there is an additional degree of freedom in the scalar sector of the propagator. This spin-0 particle is not a ghost and is non-tachyonic if $m^2 \geq 0$.

B.3 Weyl squared gravity

The action of Weyl squared gravity is of the form

$$\mathcal{L}_W \sim M_P^2 R + C^{\mu\nu\lambda\sigma} C_{\mu\nu\lambda\sigma}. \tag{B.3}$$

It can easily be verified that

$$C^2 \equiv C^{\mu\nu\lambda\sigma} C_{\mu\nu\lambda\sigma} = R_{\mu\nu\lambda\sigma} R^{\mu\nu\lambda\sigma} - 2R_{\mu\nu} R^{\mu\nu} + \frac{1}{3} R^2. \tag{B.4}$$

The propagator for Weyl squared gravity is given by

$$\Pi_{C^2} = \frac{\mathcal{P}^2}{(1 - (2k/M_P)^2 k^2} - \frac{\mathcal{P}_s^0}{2k^2} = \Pi_{GR} - \frac{\mathcal{P}^2}{k^2 + m^2}. \tag{B.5}$$

We observe that there is an extra spin-2 degree of freedom which has a negative residue. This is termed the *Weyl ghost* and it violates unitarity.

Appendix C

Unitarity

Unitarity plays a crucial role in determining the viability of a theory. Unitarity in non-local theories has been studied in [27, 29, 30, 31, 32, 39, 40, 65, 92, 93, 94, 95, 96]. In order to check unitarity at higher-loop order, the optical theorem plays a very important role. Let us now expand on the optical theorem [12, 119].

The $\mathcal{S}$-matrix describes the initial and final states of a system during a scattering process. As a state $|\Psi;t\rangle$ evolves in time, its norm should stay the same:

$$\langle\Psi;t|\Psi;t\rangle = \langle\Psi;0|\Psi;0\rangle \tag{C.1}$$

Since

$$|\Psi;t\rangle = e^{-iHt}|\Psi;0\rangle, \tag{C.2}$$

where H is the Hamiltonian, one should have $H^\dagger = H$ so that H is Hermitian. In order to ensure conservation of probability, the $\mathcal{S}$-matrix, which is given by $\mathcal{S} = e^{-iHt}$, has to be unitary. That is,

$$\mathcal{S}^\dagger\mathcal{S} = 1, \tag{C.3}$$

where $\mathcal{S}^\dagger$ is the Hermitian conjugate of $\mathcal{S}$. One can write the $\mathcal{S}$-matrix as follows,

$$\mathcal{S} = 1 + i\mathcal{T}, \tag{C.4}$$

where the elements of the $\mathcal{T}$-matrix (transfer matrix) are defined by the following relation,

$$\langle f\,|\mathcal{T}|\,i\rangle = (2\pi)^4\delta^4(p_f - p_i)\widetilde{\mathcal{T}}(i \to f), \tag{C.5}$$

where $\widetilde{\mathcal{T}}(i \to f)$ is a scattering amplitude ($|i\rangle$ and $|f\rangle$ now denote initial and final states, respectively). From (C.4), we have

$$\mathcal{S}^\dagger\mathcal{S} = 1 = \left(1 - i\mathcal{T}^\dagger\right)(1 + i\mathcal{T}) \tag{C.6}$$

$$\Rightarrow i\left(\mathcal{T}^\dagger - \mathcal{T}\right) = \mathcal{T}^\dagger\mathcal{T}, \tag{C.7}$$

where $\mathcal{T}^\dagger$ is the Hermitian conjugate of $\mathcal{T}$. It should be pointed out that (C.6) is the condition for unitarity and implies conservation of probability. Employing an orthonormal and complete [1] set of states $|n\rangle$,

$$\langle n|m\rangle = \delta_{nm}, \tag{C.10}$$

$$\sum_n |n\,\rangle\langle\, n| = 1, \tag{C.11}$$

we can express each state $|n\rangle$ in terms of the momenta k_i. Therefore, (C.11) becomes

$$1 = \sum_n \int d\Pi_n\, |n\,\rangle\langle\, n| \tag{C.12}$$

$$= \sum_n \prod_{j\in n} \int \frac{dk_j}{(2\pi)^3}\frac{1}{2E_j}\, |k_1, k_2, \ldots, k_n\,\rangle\langle\, k_1, k_2, \ldots, k_n|\,. \tag{C.13}$$

[1] Completeness in Hilbert space means that [12]

$$\mathbb{1} = \sum_X \int d\Pi_X |X\rangle\langle X|, \tag{C.8}$$

where the sum is over states $|X\rangle$ and

$$d\Pi_X \equiv \prod_{j\in X} \frac{d^3p_j}{(2\pi)^3}\frac{1}{2E_j}. \tag{C.9}$$

$d\Pi_X$ is proportional to the Lorentz-invariant phase space of the particles in state $|X\rangle$, that is, $d\Pi_{\text{LIPS}} = (2\pi)^4\delta^4(\Sigma p)d\Pi_X$.

The left-hand side of (C.7) is

$$\langle f|i\big(\mathcal{T}^\dagger - \mathcal{T}\big)|i\rangle = i(2\pi)^4\delta^4(p_f - p_i)\left(\widetilde{\mathcal{T}}^*(f \to i) - \widetilde{\mathcal{T}}(i \to f)\right), \tag{C.14}$$

where the superscript * denotes complex conjugation. Using (C.13), we get

$$\langle f|\mathcal{T}^\dagger\mathcal{T}|i\rangle = \sum_n \int d\Pi_n \langle f|\mathcal{T}^\dagger|n\rangle \langle n|\mathcal{T}|i\rangle \tag{C.15}$$

$$= (2\pi)^4 \sum_n \int d\Pi_n \; \delta^4(p_f - p_n)(2\pi)^4\delta^4(p_n - p_i)\widetilde{\mathcal{T}}^*(f \to n)\widetilde{\mathcal{T}}(i \to n). \tag{C.16}$$

Then (C.7) gives the *Generalised Optical Theorem*:

$$\widetilde{\mathcal{T}}(i \to f) - \widetilde{\mathcal{T}}^\dagger(f \to i) = i\sum_n \int d\Pi_n (2\pi)^4\delta^4(p_n - p_i)\widetilde{\mathcal{T}}^*(f \to n)\widetilde{\mathcal{T}}(i \to n). \tag{C.17}$$

The aforementioned theorem should be valid perturbatively order-by-order. On the left-hand side, we have matrix elements while, on the right-hand side, we have matrix elements squared. Hence, at order λ^2 where λ is some coupling, the left-hand side should be a loop while the right-hand side should correspond to a tree-level computation. If there are no loops in an interacting theory, unitarity is violated.

When $|f\rangle = |i\rangle = |X\rangle$ and $|X\rangle$ is a 1-particle state, (C.17) yields

$$\text{Im } \widetilde{\mathcal{T}}(X \to X) = m_X \sum_n \Gamma(X \to n). \tag{C.18}$$

where $\Gamma(X \to n)$ is a decay rate. What (C.18) means is that the imaginary part of the propagator is given by the sum of all possible decay rates.

If $|X\rangle$ is a 2-particle state, we can obtain the *Optical Theorem* (in the centre-of-mass frame):

$$\text{Im } \widetilde{\mathcal{T}}(X \to X) = 2E_{CM}|\vec{p}_{CM}| \sum_n \sigma(X \to n), \tag{C.19}$$

where E_{CM} is the total centre-of-mass energy and $\vec{p}_{CM}$ is the momentum of the particles in the centre-of-mass frame. Hence, the imaginary part of the forward scattering amplitude is proportional to the total cross section.

Within the framework of infinite derivative theories, novel prescriptions may have to be employed in order for unitarity to be established. Establishing unitarity and causality [1] of infinite derivative theories of gravity would be a major step towards the construction of a fully satisfactory theory of quantum gravity.

[1] Causality in ordinary QFT means that a measurement carried out at one point cannot influence a measurement at another point, where the two points are spacelike-separated [119].

Appendix D

Quantised infinite derivative gravitational action

If we consider metric fluctuations around a Minkowski background,

$$g_{\mu\nu} = \eta_{\mu\nu} + h_{\mu\nu}, \tag{D.1}$$

we can define the quantum theory in harmonic gauge,

$$\partial_\nu \bar{h}^{\mu\nu} = 0, \tag{D.2}$$

where

$$\bar{h}_{\mu\nu} = h_{\mu\nu} - \frac{1}{2}\eta_{\mu\nu}h \Rightarrow \bar{h}^{\mu\nu} = h^{\mu\nu} - \frac{1}{2}\eta^{\mu\nu}h. \tag{D.3}$$

$\bar{h}_{\mu\nu}$ is called the trace-reverse of $h_{\mu\nu}$ since $\bar{h} = \eta^{\mu\nu}\bar{h}_{\mu\nu} = -h$, where $h = \eta^{\mu\nu}h_{\mu\nu}$. Note that $h^{\mu\nu} = \eta^{\mu\rho}\eta^{\nu\sigma}h_{\rho\sigma} \Rightarrow \bar{h}^{\mu\nu} = \eta^{\mu\rho}\eta^{\nu\sigma}\bar{h}_{\rho\sigma}$. Furthermore, $h_{\mu\nu} = \bar{h}_{\mu\nu} - \frac{1}{2}\eta_{\mu\nu}\bar{h}$.

Therefore, we can write down the quantised infinite derivative gravitational

action action as follows [100, 159],

$$S_{\texttt{quantised}} = S + S_{\texttt{GF}} + S_{\texttt{ghost}} \tag{D.4}$$

$$= \frac{1}{2}\int d^4x\sqrt{-g}\left[M_P^2 R + R\mathcal{F}_1(\bar{\Box})R + R_{\mu\nu}\mathcal{F}_2(\bar{\Box})R^{\mu\nu} + R_{\mu\nu\lambda\sigma}\mathcal{F}_3(\bar{\Box})R^{\mu\nu\lambda\sigma}\right]$$

$$- \frac{1}{2\xi}\int d^4x\left(F_\tau \mathcal{G}(\Box)F^\tau\right) + \int d^4x\left(\bar{C}_\tau \vec{F}^\tau_{\mu\nu} D^{\mu\nu}_\alpha C^\alpha\right), \tag{D.5}$$

where S is given by (1.10) and $\bar{\Box} = \Box/M^2$. $S_{\texttt{GF}}$ is the gauge-fixing term given by (D.12) and $S_{\texttt{ghost}}$ is the ghost-antighost action given by (D.14) while ξ is a finite parameter. We have that $F^\tau = \vec{F}^\tau_{\mu\nu}h^{\mu\nu}$ and $\vec{F}^\tau_{\mu\nu} = \delta^\tau_\mu\vec{\partial}_\nu - \frac{1}{2}\delta^\tau_\sigma\eta^{\sigma\rho}\eta_{\mu\nu}\vec{\partial}_\rho$ (the arrow indicates the direction in which the derivative acts). C^σ is the ghost field and $\bar{C}_\tau$ is the antighost field; both are anticommuting. $D^{\mu\nu}_\alpha$ is the operator generating gauge transformations in the graviton field $h^{\mu\nu}$, given an arbitrary infinitesimal vector field $\xi^\alpha(x)$ (corresponding to $x^{'\mu} = x^\mu - \xi^\mu$).
That is,

$$\delta h_{\mu\nu} = \delta g_{\mu\nu} = \pounds_\xi g_{\mu\nu} = \xi^\rho\partial_\rho g_{\mu\nu} + g_{\mu\rho}\partial_\nu\xi^\rho + g_{\rho\nu}\partial_\mu\xi^\rho = D_{\mu\nu\alpha}\xi^\alpha, \tag{D.6}$$

where $\pounds$ is the Lie derivative and

$$D_{\mu\nu\alpha}\xi^\alpha = \partial_\mu\xi_\nu + \partial_\nu\xi_\mu + h_{\alpha\nu}\partial_\mu\xi^\alpha + h_{\mu\alpha}\partial_\nu\xi^\alpha + \xi^\alpha\partial_\alpha h_{\mu\nu}. \tag{D.7}$$

Accordingly,

$$D_{\mu\nu\alpha} = \eta_{\alpha\nu}\partial_\mu + \eta_{\mu\alpha}\partial_\nu + h_{\alpha\nu}\partial_\mu + h_{\mu\alpha}\partial_\nu + \partial_\alpha h_{\mu\nu}. \tag{D.8}$$

We can raise the indices in (D.8) using the Minkowski tensors.
Moreover, the $\mathcal{F}_i$'s, $i = 1, 2, 3$, are analytic functions of $\bar{\Box}$,

$$\mathcal{F}_i(\bar{\Box}) = \sum_{n=0}^{\infty} f_{i_n}\bar{\Box}^n, \tag{D.9}$$

where the f_{i_n}'s are real coefficients.

$\mathcal{G}(\Box)$ is given by

$$\mathcal{G}(\Box) = -\Box e^{-\bar{\Box}} = \sum_{n=0}^{\infty} \frac{(-1)^{n+1}\Box^{n+1}}{n!M^{2n}}. \tag{D.10}$$

If we change the gauge-fixing term to read $F^\tau = e^\tau(x)$ [84], with $e^\tau(x)$ an arbitrary four-vector function, we can smear out the gauge condition with a weighting functional. Choosing the weighting functional

$$\omega(e^\tau) = \exp\left[i\left(-\frac{1}{2\xi}\int d^4x\, e_\tau \mathcal{G}(\Box)e^\tau\right)\right], \tag{D.11}$$

where ξ is a finite parameter, we obtain the gauge-fixing term (see [84] for a derivation of the gauge-fixing term in non-local theories)

$$S_{\texttt{GF}} = -\frac{1}{2\xi}\int d^4x\,(F_\tau \mathcal{G}(\Box)F^\tau)\,. \tag{D.12}$$

Finally, the Faddeev-Popov ghost-antighost action is given by

$$S_{\texttt{ghost}} = \int d^4x\left(\bar{C}_\tau\, \mathcal{G}(\Box)\vec{F}^\tau_{\mu\nu}D^{\mu\nu}_\alpha C^\alpha\right). \tag{D.13}$$

If we perform integration by parts $2l$ times for each $\Box^l$ term in (D.13) arising from the power series expansion of $\mathcal{G}(\Box)$ and redefine appropriately the antighost field, the ghost-antighost action will become

$$S_{\texttt{ghost}} = \int d^4x\left(\bar{C}_\tau \vec{F}^\tau_{\mu\nu}D^{\mu\nu}_\alpha C^\alpha\right). \tag{D.14}$$

It should be pointed out that the Faddeev-Popov ghost fields are benign (in contrast to the Weyl ghost).

Appendix E

Newtonian potential

Let us consider the Newtonian potential in the weak-field limit. The Newtonian approximation of a perturbed metric for a static point source is given by [12, 160]

$$ds^2 = (\eta_{\mu\nu} + h_{\mu\nu})dx^\mu dx^\nu = -(1+2\Phi(r))dt^2 + (1-2\Psi(r))(dx^2+dy^2+dz^2), \quad \text{(E.1)}$$

where

$$h_{\mu\nu} \equiv \begin{pmatrix} -2\Phi(r) & 0 & 0 & 0 \\ 0 & -2\Psi(r) & 0 & 0 \\ 0 & 0 & -2\Psi(r) & 0 \\ 0 & 0 & 0 & -2\Psi(r) \end{pmatrix}. \quad \text{(E.2)}$$

The trace and 00-component of the field equations around a flat background for an infinite derivative gravitational action (see (2.34)) are given by

$$\begin{aligned} -\kappa T_{00} &= \frac{1}{2}(a(\bar{\Box}) - 3c(\bar{\Box}))R, \\ \kappa T_{00} &= a(\bar{\Box})R_{00} + \frac{1}{2}c(\bar{\Box})R, \end{aligned} \quad \text{(E.3)}$$

where $T_{\mu\nu}$ is the stress-energy tensor and T_{00} gives the energy density. In the static, linearised limit, $\Box = \nabla^2 = \partial_i\partial^i$ (that is, the flat-space d'Alembertian

becomes the Laplace operator), yielding

$$-\kappa T_{00} = (a(\bar{\Box}) - 3c(\bar{\Box}))(2\nabla^2\Psi - \nabla^2\Phi)$$
$$\kappa T_{00} = (a(\bar{\Box}) - c(\bar{\Box}))\nabla^2\Phi + 2c(\bar{\Box})\nabla^2\Psi. \tag{E.4}$$

Thus,

$$\kappa T_{00} = \frac{a(\bar{\Box})\left(a(\bar{\Box}) - 3c(\bar{\Box})\right)}{a(\bar{\Box}) - 2c(\bar{\Box})}\nabla^2\Phi = \kappa m_g \delta^3(\vec{r}). \tag{E.5}$$

T_{00} is the point source, that is, $T_{00} = m_g\delta^3(\vec{r})$, m_g is the mass of the object generating the gravitational potential while δ^3 is the three-dimensional Dirac delta-function and is given by

$$\delta^3(\vec{r}) = \int \frac{d^3k}{(2\pi)^3}\, e^{ik\vec{r}}. \tag{E.6}$$

Hence, taking the Fourier components of (E.5) yields

$$\Phi(r) = -\frac{\kappa m_g}{(2\pi)^3}\int_{-\infty}^{\infty} d^3k\, \frac{a(-k^2) - 2c(-k^2)}{a(-k^2)(a(-k^2) - 3c(-k^2))}\frac{e^{ik\vec{r}}}{k^2} \tag{E.7}$$
$$= -\frac{\kappa m_g}{2\pi^2 r}\int_0^{\infty} dk\, \frac{(a(-k^2) - 2c(-k^2))}{a(-k^2)(a(-k^2) - 3c(-k^2))}\frac{\sin(kr)}{k} \tag{E.8}$$

and

$$\Psi(r) = \frac{\kappa m_g}{2\pi^2 r}\int_0^{\infty} dk\, \frac{c(-k^2)}{a(-k^2)(a(-k^2) - 3c(-k^2))}\frac{\sin(kr)}{k}. \tag{E.9}$$

If $a(-k^2) = c(-k^2)$, no additional degrees of freedom are introduced in the scalar sector of the propagator and the only degrees of freedom we have are those of the massless graviton. In that case, we obtain

$$\Phi(r) = \Psi(r) = -\frac{\kappa m_g}{(2\pi)^2 r}\int_0^{\infty} dk\, \frac{\sin(kr)}{a(-k^2)k}. \tag{E.10}$$

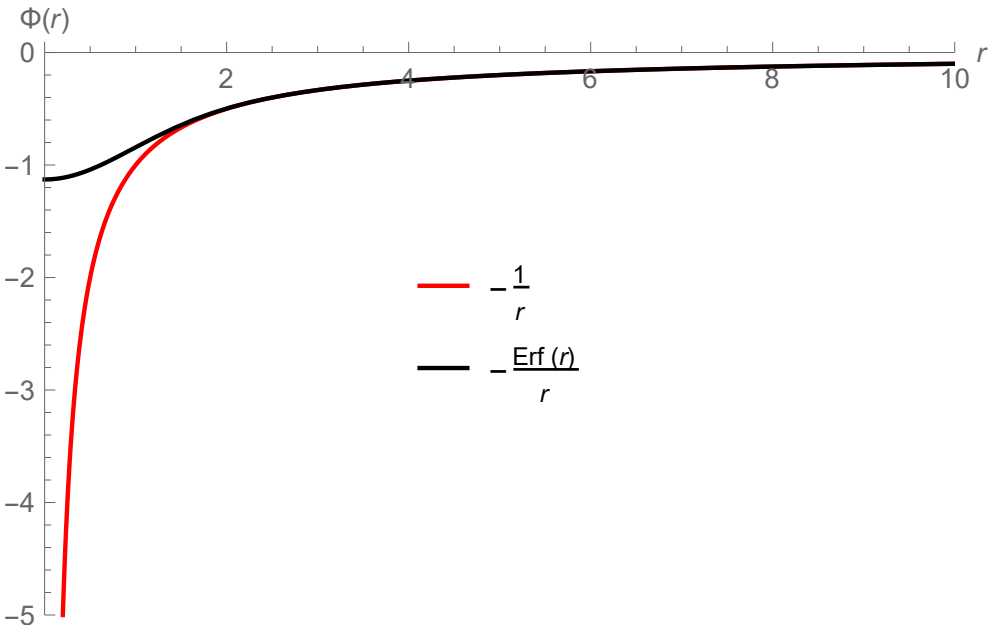

Figure E.1: Newtonian potentials. The red line denotes the (singular) Newtonian potential in GR while the black line indicates the (non-singular) Newtonian potential in IDG.

Making the choice $a(\bar{\Box}) = e^{-\bar{\Box}}$, we get [56]

$$\Phi(r) = \Psi(r) = -\frac{\kappa m_g}{(2\pi)^2 r}\int_0^\infty dk\ \frac{\sin(kr)}{k e^{\frac{k^2}{M^2}}} \tag{E.11}$$

$$= -\frac{\kappa m_g \mathrm{Erf}\left(\frac{Mr}{2}\right)}{8\pi r}. \tag{E.12}$$

As $r \to \infty$ (or if $M \to \infty$), $\mathrm{Erf}\left(\frac{Mr}{2}\right) \to 1$ and we recover the $-\frac{1}{r}$ divergence of GR. When $r \to 0$, we have that

$$\lim_{r\to 0}\Phi(r) = \lim_{r\to 0}\Psi(r) = -\frac{\kappa m_g M}{8\pi^{3/2}}, \tag{E.13}$$

which is a constant. We observe that the Newtonian potential is non-singular (see also Fig. E.1).

Appendix F

Scale of non-locality

It is known that higher-derivative gravitational theories come with a mass scale so that the correct dimensionality of the covariant derivatives is ensured. This mass scale is known as the scale of non-locality. In [99], it was demonstrated that the scattering amplitude becomes more exponentially suppressed as the number of particles in a scattering event increases. Subsequently, in [111], it was shown that, by considering a higher-derivative scalar field theory toy model, the effective mass scale for a system of n particles is inversely proportional to the square root of the number of particles and that, as the number of particles increases, the corresponding effective mass scale associated with the scattering amplitude decreases. Hence, the effective mass scale M_{eff} satisfies, for large n, $M_{\text{eff}} \sim M/\sqrt{n}$, where M is the mass scale, *i.e.*, scale of non-locality, and n is the number of particles. Below we expand on this result.

We want to find the scale of non-locality for a system of n particles. Let us consider the scalar toy model that is given by (4.46). The Feynman rules are given in Section 4.3. From (4.56), we see that the dressed propagator goes roughly as $e^{-\frac{3\bar{p}^2}{2}}$ when p^2 is large.

Suppose we have a tree-level six-point scattering amplitude (see Fig. F.1). We

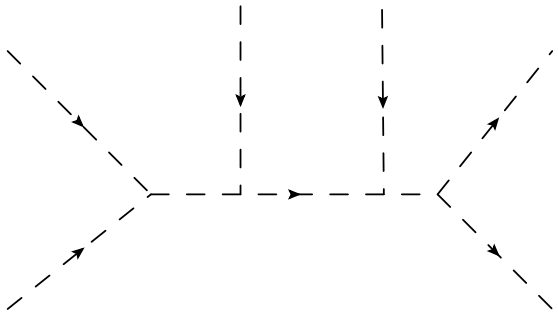

Figure F.1: The tree-level 6-point scattering diagram. The external momenta in the middle are p_5 and p_6.

have that

$$\begin{aligned} i\mathcal{T} &= \lambda^4 V(p_1, p_2, -p_1 - p_2) V(p_3, p_4, p_1 + p_2 + p_5 + p_6) V(p_1 + p_2, p_5, -p_1 - p_2 - p_5) \\ &\quad \times V(p_1 + p_2 + p_5, p_6, -p_1 - p_2 - p_5 - p_6) \frac{i}{(p_1 + p_2)^2 e^{(\bar{p}_1 + \bar{p}_2)^2}} \frac{1}{(p_1 + p_2 + p_5)^2 e^{(\bar{p}_1 + \bar{p}_2 + \bar{p}_5)^2}} \\ &\quad \times \frac{1}{(p_1 + p_2 + p_5 + p_6)^2 e^{(\bar{p}_1 + \bar{p}_2 + \bar{p}_5 + \bar{p}_6)^2}}. \end{aligned} \tag{F.1}$$

From conservation of momentum, we have that $p_1 + p_2 + p_3 + p_4 + p_5 + p_6 = 0$.

Now, suppose we have n vertices in the tree-level diagram and we want to find M_{eff}. From (F.1), we have

$$\begin{aligned} \mathcal{T} &= \lambda^4 \Big\{ \Big[p_1^2 (e^{\bar{p}_2^2} + e^{(\bar{p}_1 + \bar{p}_2)^2}) + p_2^2 (e^{\bar{p}_1^2} + e^{(\bar{p}_1 + \bar{p}_2)^2}) + (p_1 + p_2)^2 (e^{\bar{p}_1^2} + e^{\bar{p}_2^2}) \Big] \\ &\quad \times \Big[p_3^2 (e^{\bar{p}_4^2} + e^{(\bar{p}_1 + \bar{p}_2 + \bar{p}_5 + \bar{p}_6)^2}) + p_4^2 (e^{\bar{p}_3^2} + e^{(\bar{p}_1 + \bar{p}_2 + \bar{p}_5 + \bar{p}_6)^2}) + (p_1 + p_2 + p_5 + p_6)^2 (e^{\bar{p}_3^2} + e^{\bar{p}_4^2}) \Big] \\ &\quad \times \Big[p_5^2 (e^{(\bar{p}_1 + \bar{p}_2)^2} + e^{(\bar{p}_1 + \bar{p}_2 + \bar{p}_5)^2}) + (p_1 + p_2)^2 (e^{\bar{p}_5^2} + e^{(\bar{p}_1 + \bar{p}_2 + \bar{p}_5)^2}) + (p_1 + p_2 + p_5)^2 (e^{\bar{p}_5^2} + e^{(\bar{p}_1 + \bar{p}_2)^2}) \Big] \\ &\quad \times \Big[p_6^2 (e^{(\bar{p}_1 + \bar{p}_2 + \bar{p}_5)^2} + e^{(\bar{p}_1 + \bar{p}_2 + \bar{p}_5 + \bar{p}_6)^2}) + (p_1 + p_2 + p_5)^2 (e^{\bar{p}_6^2} + e^{(\bar{p}_1 + \bar{p}_2 + \bar{p}_5 + \bar{p}_6)^2}) \\ &\quad + (p_1 + p_2 + p_5 + p_6)^2 (e^{\bar{p}_6^2} + e^{(\bar{p}_1 + \bar{p}_2 + \bar{p}_5)^2}) \Big] \Big\} \\ &\quad \times \frac{1}{(p_1 + p_2)^2 e^{(\bar{p}_1 + \bar{p}_2)^2}} \frac{1}{(p_1 + p_2 + p_5)^2 e^{(\bar{p}_1 + \bar{p}_2 + \bar{p}_5)^2}} \frac{1}{(p_1 + p_2 + p_5 + p_6)^2 e^{(\bar{p}_1 + \bar{p}_2 + \bar{p}_5 + \bar{p}_6)^2}}. \end{aligned} \tag{F.2}$$

If we expand (F.2), we shall get terms of the form,

$$\sum(\text{polynomial in p})e^{\sum(\text{polynomial in p})/M^2}, \tag{F.3}$$

coming from the vertices.

Suppose now that we dress the four vertices. At sufficiently high loop order n (when $n \geqslant 4$), the exponents in the dressed vertices become negative. The vertex factors are:

$$e^{\alpha^n \bar{p}_1^2 + \beta^n \bar{p}_2^2 + \gamma^n \bar{p}_3^2}, \tag{F.4}$$

where p_1, p_2, p_3 are the incoming vertex momenta. When the loop order n of the dressed vertices is equal to 4, that is, $n = 4$, the exponents for the dressed vertices in (F.4) become negative [99, 100]:

$$\alpha^4 = \beta^4 = \gamma^4 = -\frac{11}{27}. \tag{F.5}$$

Then we have, for the largest external momentum contribution ($n = 4$),

$$\begin{aligned}
\mathcal{T} &\sim e^{-\frac{11\bar{p}_1^2}{27}} e^{-\frac{11\bar{p}_2^2}{27}} e^{-\frac{11\bar{p}_3^2}{27}} e^{-\frac{11\bar{p}_4^2}{27}} e^{-\frac{11\bar{p}_5^2}{27}} e^{-\frac{11\bar{p}_6^2}{27}} e^{-\frac{22(p_1+p_2)^2}{27M^2}} e^{-\frac{22(p_1+p_2+p_5)^2}{27M^2}} e^{-\frac{22(p_1+p_2+p_5+p_6)^2}{27M^2}} \\
&\quad \times e^{-\frac{(p_1+p_2)^2}{M^2}} e^{-\frac{(p_1+p_2+p_5)^2}{M^2}} e^{-\frac{(p_1+p_2+p_5+p_6)^2}{M^2}} \\
&= e^{-\frac{11\bar{p}_1^2}{27}} e^{-\frac{11\bar{p}_2^2}{27}} e^{-\frac{11\bar{p}_3^2}{27}} e^{-\frac{11\bar{p}_4^2}{27}} e^{-\frac{11\bar{p}_5^2}{27}} e^{-\frac{11\bar{p}_6^2}{27}} e^{-\frac{49(p_1+p_2)^2}{27M^2}} e^{-\frac{49(p_1+p_2+p_5)^2}{27M^2}} e^{-\frac{49(p_1+p_2+p_5+p_6)^2}{27M^2}}.
\end{aligned} \tag{F.6}$$

If $|p_1| = |p_2| = |p_3| = |p_4| = |p_5| = |p_6| = |p|$ and $p_1 = p_3 = p_5 = p$, $p_2 = p_4 = p_6 = -p$, then

$$\mathcal{T} \sim e^{-\frac{115\bar{p}^2}{27}}. \tag{F.7}$$

Now suppose we have an eight-point tree-level scattering diagram. Then we

have, for the largest external momentum contribution ($n = 4$),

$$\begin{aligned}
\mathcal{T} \sim\ & e^{-\frac{11\bar{p}_1^2}{27}} e^{-\frac{11\bar{p}_2^2}{27}} e^{-\frac{11\bar{p}_3^2}{27}} e^{-\frac{11\bar{p}_4^2}{27}} e^{-\frac{11\bar{p}_5^2}{27}} e^{-\frac{11\bar{p}_6^2}{27}} e^{-\frac{11\bar{p}_7^2}{27}} e^{-\frac{11\bar{p}_8^2}{27}} \\
& \times e^{-\frac{22(p_1+p_2)^2}{27M^2}} e^{-\frac{22(p_1+p_2+p_5)^2}{27M^2}} e^{-\frac{22(p_1+p_2+p_5+p_6)^2}{27M^2}} e^{-\frac{22(p_1+p_2+p_5+p_6+p_7)^2}{27M^2}} e^{-\frac{22(p_1+p_2+p_5+p_6+p_7+p_8)^2}{27M^2}} \\
& \times e^{-\frac{(p_1+p_2)^2}{M^2}} e^{-\frac{(p_1+p_2+p_5)^2}{M^2}} e^{-\frac{(p_1+p_2+p_5+p_6)^2}{M^2}} e^{-\frac{(p_1+p_2+p_5+p_6+p_7)^2}{M^2}} e^{-\frac{(p_1+p_2+p_5+p_6+p_7+p_8)^2}{M^2}} \\
& = e^{-\frac{11\bar{p}_1^2}{27}} e^{-\frac{11\bar{p}_2^2}{27}} e^{-\frac{11\bar{p}_3^2}{27}} e^{-\frac{11\bar{p}_4^2}{27}} e^{-\frac{11\bar{p}_5^2}{27}} e^{-\frac{11\bar{p}_6^2}{27}} e^{-\frac{11\bar{p}_7^2}{27}} e^{-\frac{11\bar{p}_8^2}{27}} e^{-\frac{49(p_1+p_2)^2}{27M^2}} e^{-\frac{49(p_1+p_2+p_5)^2}{27M^2}} e^{-\frac{49(p_1+p_2+p_5+p_6)^2}{27M^2}} \\
& \times e^{-\frac{49(p_1+p_2+p_5+p_6+p_7)^2}{27M^2}} e^{-\frac{49(p_1+p_2+p_5+p_6+p_7+p_8)^2}{27M^2}}. \qquad \text{(F.8)}
\end{aligned}$$

Again, from conservation of momentum,

$$p_1 + p_2 + p_3 + p_4 + p_5 + p_6 + p_7 + p_8 = 0. \qquad \text{(F.9)}$$

If $|p_1| = |p_2| = |p_3| = |p_4| = |p_5| = |p_6| = |p_7| = |p_8| = |p|$ and $p_1 = p_3 = p_5 = p_7 = p$, $p_2 = p_4 = p_6 = p_8 = -p$, then

$$\mathcal{T} \sim e^{-\frac{186\bar{p}^2}{27}} = e^{-\frac{62\bar{p}^2}{9}}. \qquad \text{(F.10)}$$

We observe that the eight-point diagram is even more strongly exponentially suppressed in the UV as compared to the 6-point diagram.

For a $2n$-point tree-level diagram with dressed vertices, where $|p_i| = p$, $i = 1, \ldots, 2n$, $p_{2j-1} = p$, $p_{2j} = -p$, $j = 1, \ldots, n$, we have ($n \geq 2$)

$$\mathcal{T} \sim e^{-\frac{(22n+49(n-2))\bar{p}^2}{27}} = e^{-\frac{(71n-98)\bar{p}^2}{27}}. \qquad \text{(F.11)}$$

We can write the equation above as follows,

$$\mathcal{T} \sim e^{-\left(\frac{p}{M_{\text{eff}}}\right)^2}, \qquad \text{(F.12)}$$

where

$$M_{\text{eff}} = \left(\frac{27}{71n - 98}\right)^{1/2} M\,. \qquad \text{(F.13)}$$

Now suppose we have external momenta on the external legs in a 6-point, tree-level diagram (one on one of the legs on the left-hand side of the diagram and the other on one of the legs on the right-hand side of the diagram). Employing dressed vertices, we obtain

$$\mathcal{T} \sim e^{-\frac{115\bar{p}^2}{27}}. \tag{F.14}$$

F.1 Dressing the vertices with 1-loop diagram in the middle

A 1-loop diagram with external momenta p, $-p$ goes as $e^{3\bar{p}^2/2}$ for large external momenta. Adding a 1-loop diagram in the middle in Fig. 4.1, where the propagators and the vertices are both dressed, gives us a scattering amplitude that goes to zero for large external momenta. Thus

$$\begin{aligned}\mathcal{T} &\sim e^{-\frac{11\bar{p}_1^2}{27}} e^{-\frac{11\bar{p}_2^2}{27}} e^{-\frac{11\bar{p}_3^2}{27}} e^{-\frac{11\bar{p}_4^2}{27}} e^{-\frac{11\bar{p}_5^2}{27}} e^{-\frac{11\bar{p}_6^2}{27}} e^{-\frac{22(p_1+p_2)^2}{27M^2}} e^{-\frac{22(p_1+p_2+p_5)^2}{27M^2}} e^{-\frac{22(p_1+p_2+p_5+p_6)^2}{27M^2}} \\ &\quad \times e^{-\frac{(p_1+p_2)^2}{M^2}} e^{-\frac{2(p_1+p_2+p_5)^2}{M^2}} e^{\frac{3(p_1+p_2+p_5)^2}{2M^2}} e^{-\frac{(p_1+p_2+p_5+p_6)^2}{M^2}} \\ &= e^{-\frac{11\bar{p}_1^2}{27}} e^{-\frac{11\bar{p}_2^2}{27}} e^{-\frac{11\bar{p}_3^2}{27}} e^{-\frac{11\bar{p}_4^2}{27}} e^{-\frac{11\bar{p}_5^2}{27}} e^{-\frac{11\bar{p}_6^2}{27}} e^{-\frac{49(p_1+p_2)^2}{27M^2}} e^{-\frac{71(p_1+p_2+p_5)^2}{54M^2}} e^{-\frac{49(p_1+p_2+p_5+p_6)^2}{27M^2}}.\end{aligned} \tag{F.15}$$

If $|p_1| = |p_2| = |p_3| = |p_4| = |p_5| = |p_6| = |p|$ and $p_1 = p_3 = p_5 = p$, $p_2 = p_4 = p_6 = -p$, then,

$$\mathcal{T} \sim e^{-\frac{203\bar{p}^2}{54}}. \tag{F.16}$$

For a $2n$-point tree-level diagram with dressed vertices, where $|p_i| = p$, $i = 1, \ldots, 2n$, $p_{2j-1} = p$, $p_{2j} = -p$, $j = 1, \ldots, n$, we have ($n \geq 2$)

$$\mathcal{T} \sim e^{-\frac{(44n+98(n-2)-27)\bar{p}^2}{54}} = e^{-\frac{(142n-223)\bar{p}^2}{54}}. \tag{F.17}$$

We can write the equation above as

$$\mathcal{T} \sim e^{-\left(\frac{p}{M_{\text{eff}}}\right)^2}, \tag{F.18}$$

where

$$M_{\text{eff}} = \left(\frac{54}{142n-223}\right)^{1/2} M. \tag{F.19}$$

F.2 Dressing both the propagators and the vertices

Suppose we dress both the propagators and the vertices in Fig 4.1. We wish to find the behaviour of the scattering amplitude $\mathcal{T}$ for large external momenta. We have

$$\begin{aligned}\mathcal{T} &\sim e^{-\frac{11\bar{p}_1^2}{27}} e^{-\frac{11\bar{p}_2^2}{27}} e^{-\frac{11\bar{p}_3^2}{27}} e^{-\frac{11\bar{p}_4^2}{27}} e^{-\frac{11\bar{p}_5^2}{27}} e^{-\frac{11\bar{p}_6^2}{27}} e^{-\frac{22(p_1+p_2)^2}{27M^2}} \\ &\times e^{-\frac{22(p_1+p_2+p_5)^2}{27M^2}} e^{-\frac{22(p_1+p_2+p_5+p_6)^2}{27M^2}} e^{-\frac{3(p_1+p_2)^2}{2M^2}} e^{-\frac{3(p_1+p_2+p_5)^2}{2M^2}} e^{-\frac{3(p_1+p_2+p_5+p_6)^2}{2M^2}} \\ &= e^{-\frac{11\bar{p}_1^2}{27}} e^{-\frac{11\bar{p}_2^2}{27}} e^{-\frac{11\bar{p}_3^2}{27}} e^{-\frac{11\bar{p}_4^2}{27}} e^{-\frac{11\bar{p}_5^2}{27}} e^{-\frac{11\bar{p}_6^2}{27}} e^{-\frac{125(p_1+p_2)^2}{54M^2}} e^{-\frac{125(p_1+p_2+p_5)^2}{54M^2}} e^{-\frac{125(p_1+p_2+p_5+p_6)^2}{54M^2}}.\end{aligned} \tag{F.20}$$

If $|p_1| = |p_2| = |p_3| = |p_4| = |p_5| = |p_6| = |p|$ and $p_1 = p_3 = p_5 = p$, $p_2 = p_4 = p_6 = -p$, then

$$\mathcal{T} \sim e^{-\frac{257\bar{p}^2}{54}}. \tag{F.21}$$

For a $2n$-point tree-level diagram with dressed vertices, where $|p_i| = p$, $i = 1, \ldots, 2n$, $p_{2j-1} = p$, $p_{2j} = -p$, $j = 1, \ldots, n$, we have ($n \geq 2$)

$$\mathcal{T} \sim e^{-\frac{(44n+125(n-2))\bar{p}^2}{54}} = e^{-\frac{(169n-250)\bar{p}^2}{54}}. \tag{F.22}$$

We can write the equation above as:

$$\mathcal{T} \sim e^{-\left(\frac{p}{M_{\text{eff}}}\right)^2}, \tag{F.23}$$

where

$$M_{\text{eff}} = \left(\frac{54}{169n-250}\right)^{1/2} M. \tag{F.24}$$

We observe that M_{eff} decreases as the number of particles n increases. By dimensional analysis, one can write down the effective length scale L_{eff} as $L_{\text{eff}} \sim M_{\text{eff}}^{-1}$. Thus, one can see that the effective length scale L_{eff} increases as the number of particles n increases.

Appendix G

Generalised boundary term

In [112], the derivation of the generalised Gibbons-Hawking-York (GHY) boundary term for the infinite derivative gravitational action given by (1.10) was presented; ADM decomposition (see Section 5.3) and coframe slicing were employed in the derivation of the result.

The coframe metric reads as follows,

$$ds^2_{\text{coframe}} = g_{\alpha\beta}\theta^\alpha\theta^\beta = -N^2(\theta^0)^2 + g_{ij}\theta^i\theta^j, \tag{G.1}$$

where

$$\begin{aligned} \theta^0 &= dt, \\ \theta^i &= dx^i + \beta^i dt. \end{aligned} \tag{G.2}$$

The extrinsic curvature in coframe slicing is given by

$$K_{ij} = -\frac{1}{2N}\Big(h_{il}\partial_j(\beta^l) + h_{jl}\partial_i(\beta^l) - \bar{\partial}_0 h_{ij}\Big), \tag{G.3}$$

where h_{ij} is the induced metric on the $t = \texttt{constant}$ hypersurface and

$$\begin{aligned}\partial_0 &\equiv \frac{\partial}{\partial t} - \beta^i \partial_i, \\ \partial_i &\equiv \frac{\partial}{\partial x^i}.\end{aligned} \tag{G.4}$$

As shown in [161], for a generic gravitational action

$$S_{\texttt{gravity}} = \frac{1}{16\pi G_N^{(4)}} \int_{\mathcal{M}} d^4x \sqrt{-g} f(\mathcal{R}_{\mu\nu\rho\sigma}), \tag{G.5}$$

one can write down the following equivalent action,

$$S_{\texttt{eqv}} = \frac{1}{16\pi G_N^{(4)}} \int_{\mathcal{M}} d^4x \sqrt{-g} \left[f(\varrho_{\mu\nu\rho\sigma}) + \varphi^{\mu\nu\rho\sigma} \left(\mathcal{R}_{\mu\nu\rho\sigma} - \varrho_{\mu\nu\rho\sigma} \right) \right], \tag{G.6}$$

where $\varrho_{\mu\nu\rho\sigma}$ and $\varphi^{\mu\nu\rho\sigma}$ are auxiliary fields; taking the equation of motion for $\varphi^{\mu\nu\rho\sigma}$ yields $\varrho_{\mu\nu\rho\sigma} = \mathcal{R}_{\mu\nu\rho\sigma}$. $\mathcal{M}$ is the manifold over which the integration takes place and $\partial\mathcal{M}$ is its boundary. Using the method in [161], one can deduce that the infinite derivative gravitational action, now including the corresponding boundary term, is given by [112]

$$\begin{aligned}
S_{\texttt{total}} &= S_{\texttt{eqv}} + S_{\texttt{boundary}} \\
&= \frac{1}{16\pi G_N^{(4)}} \int_{\mathcal{M}} d^4x \sqrt{-g} \Big[\varrho + M_P^{-2} \big(\varrho \mathcal{F}_1(\bar{\Box}) \varrho + \varrho_{\mu\nu} \mathcal{F}_2(\bar{\Box}) \varrho^{\mu\nu} \\
&+ \varrho_{\mu\nu\rho\sigma} \mathcal{F}_3(\bar{\Box}) \varrho^{\mu\nu\rho\sigma} \big) + \varphi^{\mu\nu\rho\sigma} \left(\mathcal{R}_{\mu\nu\rho\sigma} - \varrho_{\mu\nu\rho\sigma} \right) \Big] \\
&+ \frac{1}{8\pi G_N^{(4)}} \oint_{\partial\mathcal{M}} d\Sigma_\mu n^\mu \Big[K + M_P^{-2} \big(2K\mathcal{F}_1(\bar{\Box}) \rho - 4K\mathcal{F}_1(\bar{\Box}) \Omega \\
&- K\mathcal{F}_2(\bar{\Box}) \Omega - K_{ij} \mathcal{F}_2(\bar{\Box}) \Omega^{ij} + K_{ij} \mathcal{F}_2(\bar{\Box}) \rho^{ij} - 4K_{ij} \mathcal{F}_3(\bar{\Box}) \Omega^{ij} - 2X_1^{ij} - \frac{1}{2} X_2^{ij} \big) \Big],
\end{aligned} \tag{G.7}$$

where $\Omega_{ij} = n^\gamma n^\delta \varrho_{\gamma i \delta j}$, $\Omega = h^{ij}\Omega_{ij}$, $\rho_{ij} = h^{km}\rho_{ijkm}$, $\rho = h^{ij}\rho_{ij}$, $K = h^{ij}K_{ij}$ and K_{ij} is the extrinsic curvature given by (G.3). The form of the X terms is complicated and shall not be presented here; one can find the full expressions and

the method employed in deriving them in [112].

Appendix H

Wald entropy

In [114], Wald's gravitational entropy [162, 163] was evaluated in (Anti-)de Sitter space for the following infinite derivative gravitational action,

$$S = \frac{1}{16\pi G_N^{(D)}} \int d^D x \sqrt{-g} \left[R - 2M_P^{-2}\Lambda + \alpha \left(R\mathcal{F}_1(\bar{\Box})R + R_{\mu\nu}\mathcal{F}_2(\bar{\Box})R^{\mu\nu} + R_{\mu\nu\lambda\sigma}\mathcal{F}_3(\bar{\Box})R^{\mu\nu\lambda\sigma} \right) \right], \tag{H.1}$$

and the entropy was found to be

$$S_{Wald}^{(A)dS} = \frac{A_H^{(A)dS}}{4G_N^{(D)}} \{1 \pm \frac{2\alpha}{l^2} \left[f_{1_0} D(D-1) + f_{2_0}(D-1) + 2f_{3_0} \right]\}, \tag{H.2}$$

where $A_H^{(A)dS}$ is the area of the horizon, f_{1_0}, f_{2_0}, f_{3_0} are the first coefficients in the expansions $\mathcal{F}_i(\bar{\Box}) = \sum_{n=0}^{\infty} f_{i_n} \bar{\Box}^n$ $(i = 1, 2, 3)$, Λ is the cosmological constant and its mass dimension is 4. α is a constant of mass dimension -2 while l is a length scale. The cosmological constant is given in (A)dS space by

$$\Lambda = \pm \frac{M_P^2 (D-1)(D-2)}{2l^2}, \tag{H.3}$$

where the positive sign corresponds to dS space and the negative one to AdS space.

Regarding the following action (where $\mathcal{F}_2(\bar{\Box})$ and $\mathcal{F}_3(\bar{\Box})$ have been set to zero

in (H.1)),

$$S = \frac{1}{16\pi G_N^{(4)}} \int d^4x \sqrt{-g} \left[R - 2M_P^{-2}\Lambda + \alpha R \mathcal{F}_1(\bar{\Box}) R \right], \tag{H.4}$$

the entropy in four-dimensional de Sitter space was found to be as follows,

$$S_{Wald} = \frac{A_H^{dS}}{4G_N^{(4)}} \left(1 + 8 f_{1_0} \alpha M_P^{-2} \Lambda \right). \tag{H.5}$$

If the following inequality holds,

$$M_P^2 + 8\alpha\Lambda f_{1_0} < 0, \tag{H.6}$$

we obtain an unphysical, negative entropy.

Appendix I

Loop integrals

I.1 1-loop integrals with arbitrary external momenta

To compute a 1-loop, 2-point integral with arbitrary external momenta, p and $-p$, we have to evaluate integrals of the form

$$\int \frac{d^4k}{(2\pi)^4}\, f(p,k),$$

where f is a function of the external momentum p, and the loop momentum k. We analytically continue the integrand, so that we can work in Euclidean space,

$$d^4k \to id^4k, \quad k^2 \to k_E^2, \quad p\cdot k \to (p\cdot k)_E, \quad p^2 \to p_E^2,$$

since $k_0 \to ik_0$ and $p_0 \to ip_0$ [1]. Then, by spherical symmetry, we express d^4k_E as follows,

$$d^4k_E = 4\pi k_E^3 \sqrt{1-x^2}\, dx dk_E, \tag{I.1}$$

[1] In Minkowski space (mostly plus metric signature), $k^2 = -k_0^2 + \vec{k}^2$, where $\vec{k}^2 = k_1^2 + k_2^2 + k_3^2$. After analytic continuation, $k_E^2 = k_4^2 + \vec{k}^2$, where $k_4 = -ik_0$. For brevity, we shall suppress the subscript E in the notation.

where x is the cosine of the angle between p_E and k_E. We assume p_E to be the z-axis, so $p_E \cdot k_E = p_E k_E x$ and p_E & k_E are the norms of p_E and k_E.

We then integrate with respect to x from -1 to 1. If the integral converges, we subsequently integrate with respect to k_E from 0 to ∞. If the integral diverges, we integrate with respect to k_E from 0 to Λ, where Λ is the momentum cutoff.

I.2 2-loop integrals with vanishing external momenta

Let us compute the integral resulting in (3.22). The integral is given by

$$W = \int \frac{d^4k_1}{(2\pi)^4}\frac{d^4k_2}{(2\pi)^4}\frac{(k_1^2+k_2^2+k_3^2)^2}{16M_P^4 k_1^2 k_2^2 k_3^2} e^{k_1^2/2M^2} e^{-(k_2-k_3)^2/2M^2}. \tag{I.2}$$

This can be written as

$$W = \frac{1}{16M_P^4}\int_0^\Lambda da \int_0^\infty db \int_{-1}^1 dx \frac{\sqrt{1-x^2}\,(4\pi a^3 2\pi^2 b^3)\left(\frac{3a^2}{2}+\frac{b^2}{2}\right)^2 \exp\left(\frac{a^2}{2M^2}\right)\exp\left(-\frac{b^2}{2M^2}\right)}{16(2\pi)^8 a^2 \frac{1}{4}\left(a^2+b^2+2abx\right)\frac{1}{4}\left(a^2+b^2-2abx\right)}, \tag{I.3}$$

where x is the cosine of the angle between k_1 and $k_2 - k_3$, a is the norm of k_1 in the Euclidean space, and b is the norm of $k_2 - k_3$ in the Euclidean space. The factor $1/16$ in front of the integral is the Jacobian $\left(\frac{1}{2}\right)^4$.

Integrating with respect to x from -1 to 1, we get

$$W = \frac{1}{2048\pi^5 M_P^4}\int_0^\Lambda da \int_0^\infty db \frac{\pi\left(a^2+b^2-(a+b)\,|a-b|\right)}{4a^2b^2\left(a^2+b^2\right)} ab^3\left(3a^2+b^2\right)^2 \exp\left(\frac{a^2}{2M^2}\right) \times \exp\left(-\frac{b^2}{2M^2}\right). \tag{I.4}$$

The integration with respect to b is split into two parts: i) from 0 to a and ii)

from a to ∞. The first part becomes $(a^2+b^2-(a+b)(a-b)=2b^2)$

$$W_1=\frac{1}{4096\pi^4M_P^4}\int_0^{\Lambda}da\int_0^{a}db\frac{b^3}{a(a^2+b^2)}\left(3a^2+b^2\right)^2\exp\left(\frac{a^2}{2M^2}\right)\exp\left(-\frac{b^2}{2M^2}\right) \tag{I.5}$$

and gives (see (3.24) for the definition of the exponential-integral function $\mathrm{Ei}(z)$)

$$\begin{aligned}W_1=\frac{1}{4096\pi^4M_P^4}\int_0^{\Lambda}da\,\frac{-2}{a}\Bigg(&M^2\left(a^2M^2\left(7-5e^{\frac{a^2}{2M^2}}\right)-4M^4\left(e^{\frac{a^2}{2M^2}}-1\right)+a^4\left(5-2e^{\frac{a^2}{2M^2}}\right)\right)\\&+a^6e^{\frac{a^2}{M^2}}\mathrm{Ei}\left(-\frac{a^2}{M^2}\right)-a^6e^{\frac{a^2}{M^2}}\mathrm{Ei}\left(-\frac{a^2}{2M^2}\right)\Bigg).\end{aligned} \tag{I.6}$$

The second part becomes $(a^2+b^2-(a+b)(b-a)=2a^2)$

$$W_2=\frac{1}{4096\pi^4M_P^4}\int_0^{\Lambda}da\int_a^{\infty}db\frac{ab}{a^2+b^2}\left(3a^2+b^2\right)^2\exp\left(\frac{a^2}{2M^2}\right)\exp\left(-\frac{b^2}{2M^2}\right) \tag{I.7}$$

and gives

$$W_2=\frac{1}{4096\pi^4M_P^4}\int_0^{\Lambda}da\,\frac{1}{4}a\left(24a^2M^2+8M^4-8a^4e^{\frac{a^2}{M^2}}\mathrm{Ei}\left(-\frac{a^2}{M^2}\right)\right). \tag{I.8}$$

In (I.6), there are four terms which diverge exponentially; those terms are the terms in the integrand involving $-5e^{a^2/2M^2}$, $e^{a^2/2M^2}-1$, $-2e^{a^2/2M^2}$ and $-a^6e^{a^2/M^2}\mathrm{Ei}(-a^2/2M^2)$. For those terms, we first write $M^2=-\tilde{M}^2$ and then analytically continue back the integrals to obtain them as a function of M^2 [1]. We should mention that we get Λ^4, Λ^2 and $\log\left(\frac{\Lambda}{M}\right)$ divergences after we apply that prescription in (I.6). The full result is (see (3.25) for the definition of the

[1]While going to Euclidean space, we always have a choice, either $t\to it$ or $x\to ix$, and that depends on the overall sign of the exponents. When we write $M^2=-\tilde{M}^2$ in Appendix I.2, we simply mean that rather than $t\to it$, we choose $x\to ix$. And, as we have now checked, once the integrals are evaluated correctly, we do not find any inconsistencies since all the loop amplitudes are purely imaginary, leading to terms that are real in the effective action. Perhaps it is also worth pointing out that the analytic continuations followed here are not new and have been used in previous non-local quantum field theory literature with consistent results. In particular, in [65, 70], it was shown that, in the $M^2\to\infty$ limit, one recovers the local field theory results, as one should.

Euler-Mascheroni constant γ)

$$W_1 = \frac{M^2}{8192\pi^4 M_P^4}\left(-4\Lambda^4 - 4(5+\gamma)M^4 - 18\Lambda^2 M^2 - 2e^{\frac{\Lambda^2}{M^2}}\left(\Lambda^4 - 2\Lambda^2 M^2 + 2M^4\right)\mathrm{Ei}\left(-\frac{\Lambda^2}{M^2}\right)\right.$$
$$+ 8M^4\left(\frac{1}{2}\mathrm{Ei}\left(-\frac{\Lambda^2}{2M^2}\right) + \log\left(\frac{2M}{\Lambda}\right)\right) + 20M^4 e^{-\frac{\Lambda^2}{2M^2}} - 4\Lambda^2 M^2 e^{-\frac{\Lambda^2}{2M^2}}$$
$$\left.+4\Lambda^2 M^2 e^{-\frac{\Lambda^2}{M^2}}\mathrm{Ei}\left(\frac{\Lambda^2}{2M^2}\right) + 2\Lambda^4 e^{-\frac{\Lambda^2}{M^2}}\mathrm{Ei}\left(\frac{\Lambda^2}{2M^2}\right) + 4M^4 e^{-\frac{\Lambda^2}{M^2}}\mathrm{Ei}\left(\frac{\Lambda^2}{2M^2}\right)\right). \tag{I.9}$$

Integrating (I.8) with respect to a from 0 to Λ yields

$$W_2 = \frac{M^2}{8192\pi^4 M_P^4}\left(-2e^{\frac{\Lambda^2}{M^2}}\left(\Lambda^4 - 2\Lambda^2 M^2 + 2M^4\right)\mathrm{Ei}\left(-\frac{\Lambda^2}{M^2}\right) + 4\Lambda^4 + 8M^4\log\left(\frac{\Lambda}{M}\right)\right.$$
$$\left.+4\gamma M^4 - 2\Lambda^2 M^2\right). \tag{I.10}$$

Summing (I.9) and (I.10), we obtain

$$W = W_1 + W_2 \tag{I.11}$$
$$= \frac{M^2}{2048\pi^4 M_P^4}\left(-e^{\frac{\Lambda^2}{M^2}}\left(\Lambda^4 - 2\Lambda^2 M^2 + 2M^4\right)\mathrm{Ei}\left(-\frac{\Lambda^2}{M^2}\right) - 5M^2\left(\Lambda^2 + M^2\right)\right.$$
$$+ 2M^4\left(\frac{1}{2}\mathrm{Ei}\left(-\frac{\Lambda^2}{2M^2}\right) + \log(2)\right) + 5M^4 e^{-\frac{\Lambda^2}{2M^2}} - \Lambda^2 M^2 e^{-\frac{\Lambda^2}{2M^2}}$$
$$\left.+\Lambda^2 M^2 e^{-\frac{\Lambda^2}{M^2}}\mathrm{Ei}\left(\frac{\Lambda^2}{2M^2}\right) + \frac{1}{2}\Lambda^4 e^{-\frac{\Lambda^2}{M^2}}\mathrm{Ei}\left(\frac{\Lambda^2}{2M^2}\right) + M^4 e^{-\frac{\Lambda^2}{M^2}}\mathrm{Ei}\left(\frac{\Lambda^2}{2M^2}\right)\right). \tag{I.12}$$

If we expand (I.12) for large Λ, we get a quadratic divergence, as expected:

$$W = \frac{M^4}{2048\pi^4 M_P^4}\left(M^2\left(\log(4) - 8\right) - 4\Lambda^2\right). \tag{I.13}$$

Finally,

$$\Gamma_{2,2,\mathtt{ii}} = \frac{3iW}{2} = \frac{3iM^4}{4096\pi^4 M_P^4}\left(M^2\left(\log(4) - 8\right) - 4\Lambda^2\right). \tag{I.14}$$

Appendix J

Dimensional regularisation

If we want to dimensionally regularise an integral, we should follow a certain procedure, see [12, 164, 165]. First, we make the following replacement:

$$\int \frac{d^4k}{(2\pi)^4} \frac{g(p,k)}{h(p,k)} \to \int \frac{d^Dk}{(2\pi)^D} \frac{g(p,k)}{h(p,k)}, \tag{J.1}$$

as we now wish to perform the integral in D dimensions, where D is an arbitrary complex number. Then we express the terms appearing in the denominator $h(p,k)$ as integrals, using the following relation for positive x:

$$\frac{1}{x} = \int_0^\infty d\alpha \; e^{-\alpha x}; \tag{J.2}$$

α is called a Schwinger parameter. We complete the square in the exponent of the integrand and then shift the loop momentum variable, so we just have to perform a Gaussian integral. Regarding the numerator $g(p,k)$, we accordingly shift the loop momentum variable (the integration measure is invariant) in order to be consistent, and drop terms linear in the (shifted) k as they integrate symmetrically to 0. In the context of dimensional regularisation, we can also make the replacement $k^\mu k^\nu \to \frac{\delta^{\mu\nu}k^2}{D}$, when evaluating the loop integrals (in Euclidean space, after analytic continuation).

For the sake of convenience, let us list the following generalised Gaussian

integrals ($a > 0$) in D-dimensional Euclidean space, where D is a complex parameter [164]:

$$\int \frac{d^D k}{(2\pi)^D} \exp\left[-ak^2\right] = \frac{1}{(4\pi a)^{D/2}}, \tag{J.3}$$

$$\int \frac{d^D k}{(2\pi)^D} k_\mu \exp\left[-ak^2\right] = 0, \tag{J.4}$$

$$\int \frac{d^D k}{(2\pi)^D} k_\mu k_\nu \exp\left[-ak^2\right] = \frac{\delta_{\mu\nu}}{2a(4\pi a)^{D/2}}, \tag{J.5}$$

$$\int \frac{d^D k}{(2\pi)^D} k^2 \exp\left[-ak^2\right] = \frac{D}{2a(4\pi a)^{D/2}}, \tag{J.6}$$

$$\int \frac{d^D k}{(2\pi)^D} k_\mu k_\nu k_\rho \exp\left[-ak^2\right] = 0, \tag{J.7}$$

$$\int \frac{d^D k}{(2\pi)^D} k_\mu k_\nu k_\rho k_\sigma \exp\left[-ak^2\right] = \frac{\delta_{\mu\nu}\delta_{\rho\sigma} + \delta_{\mu\rho}\delta_{\nu\sigma} + \delta_{\mu\sigma}\delta_{\nu\rho}}{4a^2(4\pi a)^{D/2}}, \tag{J.8}$$

$$\int \frac{d^D k}{(2\pi)^D} k^4 \exp\left[-ak^2\right] = \frac{D(D+2)}{4a^2(4\pi a)^{D/2}}, \tag{J.9}$$

where k_μ is a vector in D-dimensional Euclidean space. Partial differentiation of (J.3) with respect to a yields the other formulae. All integrals involving odd powers of k vanish.

After the Gaussian integration, there are only some parameter integrals remaining. For instance, if there are two parameter integrals remaining $\int_0^\infty d\alpha_1 \int_0^\infty d\alpha_2$, we can make the following substitutions:

$$\alpha_1 + \alpha_2 = s, \quad \alpha_1 = s\alpha, \quad \alpha_2 = s(1-\alpha), \tag{J.10}$$

where $0 < s < \infty$ and $0 < \alpha < 1$ while $d\alpha_1 d\alpha_2 = s ds d\alpha$.

If the integral we are trying to dimensionally regularise is very complicated, we may follow an alternative procedure. We can employ the following relation for the volume element of a $D-1$-dimensional surface:

$$d\Omega_D = d\Omega_{D-1} \left(1 - z^2\right)^{\frac{D-3}{2}} dz, \tag{J.11}$$

where $z \equiv \cos(\theta)$ (θ may be defined to be the angle between p and k in 1-loop Feynman integrals with arbitrary external momenta or the angle between k_1 and k_2 in 2-loop Feynman integrals with the external momenta set equal to zero) and $d\Omega_D$ denotes the differential solid angle of the D-dimensional unit sphere:

$$d\Omega_D = \sin^{D-2}(\phi_{D-1}) \sin^{D-3}(\phi_{D-2}) \cdots \sin(\phi_2) d\phi_1 \cdots d\phi_{D-1}, \tag{J.12}$$

where ϕ_i is the angle to the i-th axis, with $0 \leq \phi_1 < 2\pi$ and $0 \leq \phi_i < \pi$ for $i > 1$ [12].

Then we can use

$$\int d^D k = \int d\Omega_D \int k^{D-1} dk. \tag{J.13}$$

and, subsequently, insert (J.11), for which

$$\Omega_{D-1} = \int d\Omega_{D-1} = \frac{2\pi^{\frac{(D-1)}{2}}}{\Gamma\left(\frac{D-1}{2}\right)}; \tag{J.14}$$

$\Gamma(x)$ is the Gamma function.

After all the Gaussian integrals and as many as possible of the parameter integrals have been carried out, we write D as $D = 4 - \epsilon$ and, then, perform a series expansion in ϵ about 0. To make the result dimensionally correct, we may have to multiply it by factors of M^ϵ, where M is a mass scale at which the non-local modifications become important. If we get a pole in ϵ, say $\frac{1}{\epsilon}$, this means we have a divergence. Otherwise, the integral is finite within the framework of dimensional regularisation; this does not necessarily mean that the integral is convergent in the conventional sense.

J.1 $e^{2\bar{p}\cdot\bar{k}}$ integrals

The eighth and the ninth terms in (3.37), *i.e.*,

$$\left(e^{2\left(\frac{\bar{p}}{2}+\bar{k}\right)^2} - e^{\left(\frac{\bar{p}}{2}+\bar{k}\right)^2} e^{\left(\frac{\bar{p}}{2}-\bar{k}\right)^2}\right)$$

and

$$\left(e^{2\left(\frac{\bar{p}}{2}-\bar{k}\right)^2} - e^{\left(\frac{\bar{p}}{2}+\bar{k}\right)^2} e^{\left(\frac{\bar{p}}{2}-\bar{k}\right)^2}\right),$$

give rise to integrals containing the terms $e^{2\bar{p}\cdot\bar{k}} - 1$ and $e^{-2\bar{p}\cdot\bar{k}} - 1$, respectively. Dimensionally regularising, the sum of the integrals associated with the terms $e^{2\bar{p}\cdot\bar{k}} - 1$ and $e^{-2\bar{p}\cdot\bar{k}} - 1$ is equal to 0. That is, we refer to the integrals

$$Q_1 = \frac{i}{2M_P^2}\int \frac{d^4k}{(2\pi)^4}\,\frac{C^2(e^{2\bar{p}\cdot\bar{k}}-1)}{(\frac{p}{2}+k)^2(\frac{p}{2}-k)^2} \tag{J.15}$$

and

$$Q_2 = \frac{i}{2M_P^2}\int \frac{d^4k}{(2\pi)^4}\,\frac{C^2(e^{-2\bar{p}\cdot\bar{k}}-1)}{(\frac{p}{2}+k)^2(\frac{p}{2}-k)^2}, \tag{J.16}$$

where

$$C = \frac{1}{4}\left[p^2 + \left(\frac{p}{2}+k\right)^2 + \left(\frac{p}{2}-k\right)^2\right]. \tag{J.17}$$

Using a Taylor series expansion, one obtains

$$e^{2\bar{p}\cdot\bar{k}} - 1 = \sum_{m=1}^{\infty}\frac{(2\bar{p}\cdot\bar{k})^m}{m!} \tag{J.18}$$

and

$$e^{-2\bar{p}\cdot\bar{k}} - 1 = \sum_{m=1}^{\infty}\frac{(-2\bar{p}\cdot\bar{k})^m}{m!}. \tag{J.19}$$

Therefore, we have that

$$(e^{2\bar{p}\cdot\bar{k}} - 1) + (e^{-2\bar{p}\cdot\bar{k}} - 1) = 2\sum_{m=1}^{\infty}\frac{(2\bar{p}\cdot\bar{k})^{2m}}{(2m)!}. \tag{J.20}$$

Each of the terms in the following sum,

$$Q_1 + Q_2 = \sum_{m=1}^{\infty}\frac{i}{M_P^2}\int \frac{d^4k}{(2\pi)^4}\,\frac{C^2(2\bar{p}\cdot\bar{k})^{2m}}{(\frac{p}{2}+k)^2(\frac{p}{2}-k)^2(2m)!}, \tag{J.21}$$

is equal to zero within the framework of dimensional regularisation. To elaborate, we want to compute the integrals of the form

$$\frac{i}{M_P^2}\int \frac{d^Dk}{(2\pi)^D}\frac{C^2(2\bar{p}\cdot\bar{k})^{2m}}{(\frac{p}{2}+k)^2(\frac{p}{2}-k)^2(2m)!},$$

where $m = 1, \ldots, \infty$ and D is an arbitrary complex number. First, we Schwinger-parameterise the terms in the denominator

$$\frac{1}{(\frac{\bar{p}}{2}+\bar{k})^2} = \int_0^\infty d\alpha_1\ e^{-\alpha_1(\frac{\bar{p}}{2}+\bar{k})^2}, \tag{J.22}$$

$$\frac{1}{(\frac{\bar{p}}{2}-\bar{k})^2} = \int_0^\infty d\alpha_2\ e^{-\alpha_2(\frac{\bar{p}}{2}-\bar{k})^2}. \tag{J.23}$$

Then we complete the square in the exponent of the integrand so as to write the integrand in the form $e^{-(\alpha_1+\alpha_2)\bar{k}'^2}$ (multiplied by polynomials of p and k'), where k' is the shifted loop momentum variable and $\bar{k}' \equiv k'/M$. Consequently, we evaluate the Gaussian integrals with respect to the loop momentum variable k' in Euclidean space (the integrals are convergent since the integrands are exponentially suppressed). There remain parameter integrals with respect to a_1 and a_2 to be performed; therefore, we make the following change of variables for the parameter integrals with respect to a_1 and a_2:

$$\alpha_1 + \alpha_2 = s, \quad \alpha_1 = s\alpha, \quad \alpha_2 = s(1-\alpha), \tag{J.24}$$

where $0 < s < \infty$, $0 < \alpha < 1$ and $d\alpha_1 d\alpha_2 = sdsd\alpha$. Finally, we write D as $D = 4 - \epsilon$ and perform a series expansion in ϵ about 0. We get no pole in ϵ and the finite part of the integral is equal to zero. That is, dimensionally regularising, we obtain

$$\frac{i}{M_P^2}\int \frac{d^Dk}{(2\pi)^D}\frac{C^2(2\bar{p}\cdot\bar{k})^{2m}}{(\frac{p}{2}+k)^2(\frac{p}{2}-k)^2(2m)!} = 0. \tag{J.25}$$

Therefore,

$$\Gamma_{2,1,iii}(p^2) = Q_1 + Q_2 = 0. \tag{J.26}$$

Appendix K

c_N coefficients

The c_N coefficients (see (3.74)), which depend on N, the number of external lines, are always positive. For instance, when $N = 4$, *i.e.*, for an n-loop, four-point diagram constructed out of lower-loop, three-point diagrams, we have, from the internal propagators and dressed vertices comprising the n-loop, four-point diagram, that (assuming symmetrical routing of momenta in the 1-loop square)

$$\begin{aligned}
&\left(\bar{k}+\frac{\bar{p}_1}{4}+\frac{2\bar{p}_2}{4}-\frac{\bar{p}_3}{4}\right)^2+\left(\bar{k}+\frac{\bar{p}_2}{4}+\frac{2\bar{p}_3}{4}-\frac{\bar{p}_4}{4}\right)^2+\left(\bar{k}+\frac{\bar{p}_3}{4}+\frac{2\bar{p}_4}{4}-\frac{\bar{p}_1}{4}\right)^2 \\
&+\left(\bar{k}+\frac{\bar{p}_4}{4}+\frac{2\bar{p}_1}{4}-\frac{\bar{p}_2}{4}\right)^2 \\
&=4\bar{k}^2+\frac{3}{8}\left(\bar{p}_1^2+\bar{p}_2^2+\bar{p}_3^2+\bar{p}_4^2\right)-\frac{1}{4}\left(p_1\cdot p_3+p_2\cdot p_4\right)\ . \qquad \text{(K.1)}
\end{aligned}$$

Now, even if $p_1 = p_3 = p$ and $p_2 = p_4 = -p$, (K.1) is equal to

$$4\bar{k}^2+\frac{1}{4}\left(\bar{p}_1^2+\bar{p}_2^2+\bar{p}_3^2+\bar{p}_4^2\right)\ .$$

We see that the coefficient $\frac{1}{4}$ is greater than zero. When $N = 5$, *i.e.*, for an n-loop, five-point diagram constructed out of lower-loop three-point diagrams, we

have (again assuming symmetrical routing of momenta in the 1-loop pentagon)

$$\begin{aligned}
&\left(\bar{k}+\frac{\bar{p}_1}{5}+\frac{2\bar{p}_2}{5}+\frac{3\bar{p}_3}{5}-\frac{\bar{p}_4}{5}\right)^2+\left(\bar{k}+\frac{\bar{p}_2}{5}+\frac{2\bar{p}_3}{5}+\frac{3\bar{p}_4}{5}-\frac{\bar{p}_5}{5}\right)^2 \\
&+\left(\bar{k}+\frac{\bar{p}_3}{5}+\frac{2\bar{p}_4}{5}+\frac{3\bar{p}_5}{5}-\frac{\bar{p}_1}{5}\right)^2+\left(\bar{k}+\frac{\bar{p}_4}{5}+\frac{2\bar{p}_5}{5}+\frac{3\bar{p}_1}{5}-\frac{\bar{p}_2}{5}\right)^2 \\
&+\left(\bar{k}+\frac{\bar{p}_5}{5}+\frac{2\bar{p}_1}{5}+\frac{3\bar{p}_2}{5}-\frac{\bar{p}_3}{5}\right)^2 \\
=&5\bar{k}^2+\frac{3}{5}\left(\bar{p}_1^2+\bar{p}_2^2+\bar{p}_3^2+\bar{p}_4^2\right)+\frac{2}{5}\left(p_1\cdot p_2+p_2\cdot p_3+p_3\cdot p_4+p_4\cdot p_5+p_5\cdot p_1\right) .
\end{aligned} \tag{K.2}$$

Even when $p_1 = 2p$, $p_2 = -p$, $p_3 = p$, $p_4 = -p$, $p_5 = -p$, (K.2) is equal to

$$5\bar{k}^2+\frac{7}{20}\left(\bar{p}_1^2+\bar{p}_2^2+\bar{p}_3^2+\bar{p}_4^2+\bar{p}_5^2\right) .$$

Again, the coefficient $\frac{7}{20}$ is greater than zero. One can proceed in a similar fashion for the other higher-point diagrams.

Appendix L

Finding the physical degrees of freedom from propagator analysis

Let us consider the action given by (5.52) or, equivalently, (5.53). The propagator around Minkowski spacetime is given by (2.49), where $a(\bar{\Box}) = 1$ and $c(\bar{\Box}) = 1 + M_P^{-2}\mathcal{F}\left(\bar{\Box}\right)\Box$. Hence,

$$\Pi(-k^2) = \frac{\mathcal{P}^2}{k^2} + \frac{\mathcal{P}_s^0}{k^2(-2 + 3M_P^{-2}k^2\mathcal{F}(-k^2/M^2))}. \tag{L.1}$$

We know that $\mathcal{F}(\bar{\Box})$ is given by (5.105). Only if $c(\bar{\Box})$ is the exponent of an entire function can we decompose into partial fractions and have just one extra pole.

The upshot is that, in order to have just one extra degree of freedom, we have to impose conditions on the coefficients in $\mathcal{F}\left(\bar{\Box}\right)$. In order to avoid $\Box^{-1}$ terms appearing in $\mathcal{F}(\bar{\Box})$, we must have that

$$c(\bar{\Box}) = \sum_{n=0}^{\infty} c_n \bar{\Box}^n \tag{L.2}$$

and $c_0 = 1$. Hence,

$$\mathcal{F}(\bar{\Box}) = \left(\frac{M_P}{M}\right)^2 \sum_{n=0}^{\infty} c_{n+1}\bar{\Box}^n. \tag{L.3}$$

To get infinitely many poles and, hence, degrees of freedom, one could have, for instance, that

$$c(\bar{\Box}) = \cos(\bar{\Box}), \tag{L.4}$$

so that $c_0 = 1$. Then (5.53) becomes

$$S = \frac{1}{2}\int d^4x\sqrt{-g}\left[M_P^2 A + M_P^2 A\left(\frac{\cos(\bar{\Box})-1}{\Box}\right)A + B(R-A)\right]. \tag{L.5}$$

Using (L.1), apart from the $k^2 = 0$ pole, we have poles when

$$\cos\left(\frac{k^2}{M^2}\right) = \frac{1}{3}. \tag{L.6}$$

We see that (L.6) has infinitely many solutions due to the periodicity of the cosine function and, therefore, the propagator has infinitely many poles and, hence, degrees of freedom. We can write the solutions as $\bar{k}^2 = 2m\pi$, where $m = 0, 1, 2, \ldots$. The following relations are also useful,

$$\cos(-\bar{k}^2) = \prod_{l=1}^{\infty}\left(1 - \frac{4\bar{k}^4}{(2l-1)^2\pi^2}\right) \tag{L.7}$$

or, equivalently,

$$\cos(\bar{\Box}) = \prod_{l=1}^{\infty}\left(1 - \frac{4\bar{\Box}^2}{(2l-1)^2\pi^2}\right). \tag{L.8}$$

Now, to get just one extra degree of freedom, one can make, for instance, the choice $c(\bar{\Box}) = e^{-\bar{\Box}}$. Then

$$\mathcal{F}(\bar{\Box}) = \sum_{n=0}^{\infty} f_n \bar{\Box}^n, \tag{L.9}$$

where

$$f_n = \left(\frac{M_P}{M}\right)^2 \frac{(-1)^{n+1}}{(n+1)!}. \tag{L.10}$$

Using (L.1), apart from the $k^2 = 0$ pole, we have poles when

$$e^{k^2/M^2} = \frac{1}{3}. \tag{L.11}$$

There is just one extra pole and, hence, degree of freedom. In total, there are three degrees of freedom.

References

[1] A. Einstein, "The Foundation of the General Theory of Relativity", *Annalen Phys.* **49** (1916) 769–822, [Annalen Phys.14,517(2005)]. 1

[2] M. J. G. Veltman, "Quantum Theory of Gravitation", *Conf. Proc.* **C7507281** (1975) 265–327. 1

[3] B. S. DeWitt, "Quantum Theory of Gravity. 2. The Manifestly Covariant Theory", *Phys. Rev.* **162** (1967) 1195–1239. 1

[4] B. S. DeWitt, "Quantum Theory of Gravity. 3. Applications of the Covariant Theory", *Phys. Rev.* **162** (1967) 1239–1256. 1

[5] B. S. DeWitt, "Quantum Theory of Gravity. 1. The Canonical Theory", *Phys. Rev.* **160** (1967) 1113–1148. 1

[6] B. S. DeWitt and G. Esposito, "An Introduction to quantum gravity", *Int. J. Geom. Meth. Mod. Phys.* **5** (2008) 101–156, `arXiv:0711.2445`. 1

[7] K. G. Wilson, "The Renormalization Group: Critical Phenomena and the Kondo Problem", *Rev. Mod. Phys.* **47** (1975) 773. 1

[8] G. 't Hooft and M. J. G. Veltman, "One loop divergencies in the theory of gravitation", *Ann. Inst. H. Poincare Phys. Theor.* **A20** (1974) 69–94. 1

[9] M. H. Goroff and A. Sagnotti, "The Ultraviolet Behavior of Einstein Gravity", *Nucl. Phys.* **B266** (1986) 709–736. 1

[10] M. H. Goroff and A. Sagnotti, "Quantum gravity at two loops", *Phys. Lett.* **160B** (1985) 81–86. 1

[11] A. E. M. van de Ven, "Two loop quantum gravity", *Nucl. Phys.* **B378** (1992) 309–366. 1

[12] M. D. Schwartz, "Quantum Field Theory and the Standard Model", Cambridge University Press, 2014. 2, 5, 153, 154, 160, 179, 181

[13] A. Conroy, "Infinite Derivative Gravity: A Ghost and Singularity-free Theory", PhD thesis, Lancaster U., 2017. arXiv:1704.07211. 2, 10, 13

[14] J. Polchinski, "String theory. Vol. 1: An introduction to the bosonic string", Cambridge University Press, 2007. 2, 72

[15] J. Polchinski, "String theory. Vol. 2: Superstring theory and beyond", Cambridge University Press, 2007. 2, 72

[16] A. Ashtekar, "Introduction to loop quantum gravity and cosmology", *Lect. Notes Phys.* **863** (2013) 31–56, arXiv:1201.4598. 2, 73

[17] H. Nicolai, K. Peeters, and M. Zamaklar, "Loop quantum gravity: An Outside view", *Class. Quant. Grav.* **22** (2005) R193, arXiv:hep-th/0501114. 2, 73

[18] J. Henson, "The Causal set approach to quantum gravity", arXiv:gr-qc/0601121. 2, 73

[19] D. A. Eliezer and R. P. Woodard, "The Problem of Nonlocality in String Theory", *Nucl. Phys.* **B325** (1989) 389. 2, 9

[20] E. Witten, "Noncommutative Geometry and String Field Theory", *Nucl. Phys.* **B268** (1986) 253–294. 2, 3, 72

[21] W. Siegel, "Introduction to string field theory", *Adv. Ser. Math. Phys.* **8** (1988) 1–244, arXiv:hep-th/0107094. 2

[22] P. G. O. Freund and M. Olson, "Nonarchimedean strings", *Phys. Lett.* **B199** (1987) 186–190. 2, 3, 72, 88

[23] B. Dragovich, "Zeta strings", arXiv:hep-th/0703008. 2

[24] M. R. Douglas and S. H. Shenker, "Strings in Less Than One-Dimension", *Nucl. Phys.* **B335** (1990) 635. 2, 3

[25] D. Z. Freedman and A. Van Proeyen, "Supergravity", Cambridge Univ. Press, Cambridge, UK, 2012. 2

[26] E. Tomboulis, "Renormalizability and Asymptotic Freedom in Quantum Gravity", *Phys. Lett.* **97B** (1980) 77–80. 2, 5, 6

[27] E. T. Tomboulis, "Unitarity in Higher Derivative Quantum Gravity", *Phys. Rev. Lett.* **52** (1984) 1173. 2, 3, 5, 6, 153

[28] E. T. Tomboulis, "Renormalization and asymptotic freedom in quantum gravity". In *Christensen, S.m. (Ed.): Quantum Theory Of Gravity*, 251-266, 1983. 2, 5, 6

[29] E. T. Tomboulis, "Superrenormalizable gauge and gravitational theories", `arXiv:hep-th/9702146`. 2, 5, 6, 153

[30] E. T. Tomboulis, "Nonlocal and quasilocal field theories", *Phys. Rev.* **D92** (2015) 125037, `arXiv:1507.00981`. 2, 6, 153

[31] L. Modesto, "Super-renormalizable Quantum Gravity", *Phys. Rev.* **D86** (2012) 044005, `arXiv:1107.2403`. 2, 5, 6, 153

[32] L. Modesto and L. Rachwal, "Super-renormalizable and finite gravitational theories", *Nucl. Phys.* **B889** (2014) 228–248, `arXiv:1407.8036`. 2, 5, 6, 153

[33] A. O. Barvinsky and Yu. V. Gusev, "New representation of the nonlocal ghost-free gravity theory", *Phys. Part. Nucl.* **44** (2013) 213–219, `arXiv:1209.3062`. 2, 5

[34] A. O. Barvinsky, "Aspects of Nonlocality in Quantum Field Theory, Quantum Gravity and Cosmology", *Mod. Phys. Lett.* **A30** (2015), no. 03n04, 1540003, `arXiv:1408.6112`. 2, 5

[35] D. Anselmi, "Weighted scale invariant quantum field theories", *JHEP* **02** (2008) 051, arXiv:0801.1216. 2

[36] D. Anselmi, "Properties Of The Classical Action Of Quantum Gravity", *JHEP* **05** (2013) 028, arXiv:1302.7100. 2

[37] J. W. Moffat, "Ultraviolet Complete Quantum Gravity", *Eur. Phys. J. Plus* **126** (2011) 43, arXiv:1008.2482. 2, 5

[38] L. Modesto, J. W. Moffat, and P. Nicolini, "Black holes in an ultraviolet complete quantum gravity", *Phys. Lett.* **B695** (2011) 397–400, arXiv:1010.0680. 2, 5

[39] A. Addazi and G. Esposito, "Nonlocal quantum field theory without acausality and nonunitarity at quantum level: is SUSY the key?", *Int. J. Mod. Phys.* **A30** (2015) 1550103, arXiv:1502.01471. 2, 5, 153

[40] A. Addazi, "Unitarization and causalization of nonlocal quantum field theories by classicalization", *Int. J. Mod. Phys.* **A31** (2016) 1650009, arXiv:1505.07357. 2, 5, 153

[41] T. Biswas, A. Mazumdar, and W. Siegel, "Bouncing universes in string-inspired gravity", *JCAP* **0603** (2006) 009, arXiv:hep-th/0508194. 2, 3, 5, 6, 24, 102, 114, 116, 117, 132, 136, 139, 144

[42] T. Biswas, T. Koivisto, and A. Mazumdar, "Towards a resolution of the cosmological singularity in non-local higher derivative theories of gravity", *JCAP* **1011** (2010) 008, arXiv:1005.0590. 2, 3, 113

[43] T. Biswas, A. S. Koshelev, A. Mazumdar, and S. Yu. Vernov, "Stable bounce and inflation in non-local higher derivative cosmology", *JCAP* **1208** (2012) 024, arXiv:1206.6374. 2, 3, 113

[44] B. Craps, T. De Jonckheere, and A. S. Koshelev, "Cosmological perturbations in non-local higher-derivative gravity", *JCAP* **1411** (2014) 022, arXiv:1407.4982. 2

[45] G. Calcagni, L. Modesto, and P. Nicolini, "Super-accelerating bouncing cosmology in asymptotically-free non-local gravity", *Eur. Phys. J.* **C74** (2014) 2999, arXiv:1306.5332. 2

[46] A. S. Koshelev and S. Yu. Vernov, "On bouncing solutions in non-local gravity", *Phys. Part. Nucl.* **43** (2012) 666–668, arXiv:1202.1289. 2

[47] J. Khoury, "Fading gravity and self-inflation", *Phys. Rev.* **D76** (2007) 123513, arXiv:hep-th/0612052. 2

[48] T. Biswas, R. Brandenberger, A. Mazumdar, and W. Siegel, "Non-perturbative Gravity, Hagedorn Bounce & CMB", *JCAP* **0712** (2007) 011, arXiv:hep-th/0610274. 2

[49] I. Dimitrijevic, B. Dragovich, J. Grujic, and Z. Rakic, "New Cosmological Solutions in Nonlocal Modified Gravity", *Rom. J. Phys.* **58** (2013) 550–559, arXiv:1302.2794. 2

[50] F. Briscese, A. Marcian, L. Modesto, and E. N. Saridakis, "Inflation in (Super-)renormalizable Gravity", *Phys. Rev.* **D87** (2013) 083507, arXiv:1212.3611. 2

[51] F. Briscese, L. Modesto, and S. Tsujikawa, "Super-renormalizable or finite completion of the Starobinsky theory", *Phys. Rev.* **D89** (2014) 024029, arXiv:1308.1413. 2

[52] S. Deser and R. P. Woodard, "Nonlocal Cosmology", *Phys. Rev. Lett.* **99** (2007) 111301, arXiv:0706.2151. 2

[53] S. Nojiri and S. D. Odintsov, "Modified non-local-F(R) gravity as the key for the inflation and dark energy", *Phys. Lett.* **B659** (2008) 821–826, arXiv:0708.0924. 2

[54] K. Krasnov and Y. Shtanov, "Non-Metric Gravity. II. Spherically Symmetric Solution, Missing Mass and Redshifts of Quasars", *Class. Quant. Grav.* **25** (2008) 025002, arXiv:0705.2047. 2

[55] A. Conroy, A. S. Koshelev, and A. Mazumdar, "Geodesic completeness and homogeneity condition for cosmic inflation", *Phys. Rev.* **D90** (2014) 123525, arXiv:1408.6205. 3, 13

[56] T. Biswas, E. Gerwick, T. Koivisto, and A. Mazumdar, "Towards singularity and ghost free theories of gravity", *Phys. Rev. Lett.* **108** (2012) 031101, arXiv:1110.5249. 3, 5, 6, 7, 10, 18, 20, 24, 25, 26, 28, 88, 113, 132, 136, 162

[57] P. G. O. Freund and E. Witten, "Adelic string amplitudes", *Phys. Lett.* **B199** (1987) 191. 3

[58] L. Brekke, P. G. O. Freund, M. Olson, and E. Witten, "Nonarchimedean String Dynamics", *Nucl. Phys.* **B302** (1988) 365–402. 3

[59] P. H. Frampton and Y. Okada, "Effective Scalar Field Theory of P^-adic String", *Phys. Rev.* **D37** (1988) 3077–3079. 3

[60] E. Brezin and V. A. Kazakov, "Exactly Solvable Field Theories of Closed Strings", *Phys. Lett.* **B236** (1990) 144–150. 3

[61] D. Ghoshal, "p-adic string theories provide lattice discretization to the ordinary string worldsheet", *Phys. Rev. Lett.* **97** (2006) 151601, arXiv:hep-th/0606082. 3

[62] D. J. Gross and A. A. Migdal, "Nonperturbative Solution of the Ising Model on a Random Surface", *Phys. Rev. Lett.* **64** (1990) 717. 3

[63] T. Biswas, M. Grisaru, and W. Siegel, "Linear Regge trajectories from worldsheet lattice parton field theory", *Nucl. Phys.* **B708** (2005) 317–344, arXiv:hep-th/0409089. 3, 6, 73

[64] M. J. Ablowitz and A. S. Fokas, "Complex Variables: Introduction and Applications", Cambridge Univ. Press, Cambridge, UK, 2003. 3

[65] T. Biswas and N. Okada, "Towards LHC physics with nonlocal Standard Model", *Nucl. Phys.* **B898** (2015) 113–131, arXiv:1407.3331. 4, 73, 153, 177

[66] T. Biswas, J. A. R. Cembranos, and J. I. Kapusta, "Thermal Duality and Hagedorn Transition from p-adic Strings", *Phys. Rev. Lett.* **104** (2010) 021601, arXiv:0910.2274. 4, 6, 73

[67] T. Biswas, J. A. R. Cembranos, and J. I. Kapusta, "Thermodynamics and Cosmological Constant of Non-Local Field Theories from p-Adic Strings", *JHEP* **10** (2010) 048, arXiv:1005.0430. 4, 6, 73

[68] T. Biswas, J. A. R. Cembranos, and J. I. Kapusta, "Finite Temperature Solitons in Non-Local Field Theories from p-Adic Strings", *Phys. Rev.* **D82** (2010) 085028, arXiv:1006.4098. 4, 6, 73

[69] J. W. Moffat, "Finite nonlocal gauge field theory", *Phys. Rev.* **D41** (1990) 1177–1184. 4

[70] T. Biswas, J. Kapusta, and A. Reddy, "Thermodynamics of String Field Theory Motivated Nonlocal Models", *JHEP* **12** (2012) 008, arXiv:1201.1580. 4, 40, 73, 177

[71] R. Bluhm, "Particle fields at finite temperature from string field theory", *Phys. Rev.* **D43** (1991) 4042–4050. 4, 40

[72] J. E. Lidsey, "Stretching the inflaton potential with kinetic energy", *Phys. Rev.* **D76** (2007) 043511, arXiv:hep-th/0703007. 4

[73] N. Barnaby, T. Biswas, and J. M. Cline, "p-adic Inflation", *JHEP* **04** (2007) 056, arXiv:hep-th/0612230. 4

[74] N. Barnaby and J. M. Cline, "Large Nongaussianity from Nonlocal Inflation", *JCAP* **0707** (2007) 017, arXiv:0704.3426. 4

[75] L. Joukovskaya, "Dynamics in nonlocal cosmological models derived from string field theory", *Phys. Rev.* **D76** (2007) 105007, arXiv:0707.1545. 4

[76] I. Ya. Aref'eva, L. V. Joukovskaya, and S. Yu. Vernov, "Bouncing and accelerating solutions in nonlocal stringy models", *JHEP* **07** (2007) 087, arXiv:hep-th/0701184. 4

[77] I. Ya. Aref'eva, L. V. Joukovskaya, and S. Yu. Vernov, "Dynamics in nonlocal linear models in the Friedmann-Robertson-Walker metric", *J. Phys.* **A41** (2008) 304003, arXiv:0711.1364. 4

[78] I. Ya. Aref'eva and A. S. Koshelev, "Cosmological Signature of Tachyon Condensation", *JHEP* **09** (2008) 068, arXiv:0804.3570. 4

[79] G. Calcagni, M. Montobbio, and G. Nardelli, "A Route to nonlocal cosmology", *Phys. Rev.* **D76** (2007) 126001, arXiv:0705.3043. 4

[80] D. J. Mulryne and N. J. Nunes, "Diffusing non-local inflation: Solving the field equations as an initial value problem", *Phys. Rev.* **D78** (2008) 063519, arXiv:0805.0449. 4

[81] G. Calcagni and G. Nardelli, "Nonlocal instantons and solitons in string models", *Phys. Lett.* **B669** (2008) 102–106, arXiv:0802.4395. 4

[82] S. Yu. Vernov, "Localization of the SFT inspired Nonlocal Linear Models and Exact Solutions", *Phys. Part. Nucl. Lett.* **8** (2011) 310–320, arXiv:1005.0372. 4

[83] F. Galli and A. S. Koshelev, "Perturbative stability of SFT-based cosmological models", *JCAP* **1105** (2011) 012, arXiv:1011.5672. 4

[84] K. S. Stelle, "Renormalization of Higher Derivative Quantum Gravity", *Phys. Rev.* **D16** (1977) 953–969. 4, 17, 159

[85] K. S. Stelle, "Classical Gravity with Higher Derivatives", *Gen. Rel. Grav.* **9** (1978) 353–371. 4

[86] P. Van Nieuwenhuizen, "On ghost-free tensor lagrangians and linearized gravitation", *Nucl. Phys.* **B60** (1973) 478–492. 4, 5, 22, 151

[87] T. Biswas, T. Koivisto, and A. Mazumdar, "Nonlocal theories of gravity: the flat space propagator", in "Proceedings, Barcelona Postgrad Encounters on Fundamental Physics", pp. 13–24. 2013. arXiv:1302.0532. 4, 5, 6, 18, 20, 22, 24, 25, 26, 28, 88, 113, 126, 132, 136

[88] T. P. Sotiriou and V. Faraoni, "f(R) Theories Of Gravity", *Rev. Mod. Phys.* **82** (2010) 451–497, arXiv:0805.1726. 4

[89] A. A. Starobinsky, "A New Type of Isotropic Cosmological Models Without Singularity", *Phys. Lett.* **91B** (1980) 99–102. 5

[90] W. Siegel, "Stringy gravity at short distances", arXiv:hep-th/0309093. 5, 73

[91] A. A. Tseytlin, "On singularities of spherically symmetric backgrounds in string theory", *Phys. Lett.* **B363** (1995) 223–229, arXiv:hep-th/9509050. 5, 73

[92] V. A. Alebastrov and G. V. Efimov, "Causality in quantum field theory with nonlocal interaction", *Commun. Math. Phys.* **38** (1974) 11–28. 5, 153

[93] V. A. Alebastrov and G. V. Efimov, "A proof of the unitarity of S-matrix in a nonlocal quantum field theory", *Commun. Math. Phys.* **31** (1973) 1–24. 5, 153

[94] G. V. Efimov, "Non-local quantum theory of the scalar field", *Commun. Math. Phys.* **5** (1967) 42–56. 5, 153

[95] G. V. Efimov and S. Z. Seltser, "Gauge invariant nonlocal theory of the weak interactions", *Annals Phys.* **67** (1971) 124–144. 5, 153

[96] G. V. Efimov, "On the construction of nonlocal quantum electrodynamics", *Annals Phys.* **71** (1972) 466–485. 5, 153

[97] Yu. V. Kuzmin, "The convergent nonlocal gravitation. (in Russian)", *Sov. J. Nucl. Phys.* **50** (1989) 1011–1014, [Yad. Fiz.50,1630(1989)]. 5

[98] T. Biswas and S. Talaganis, "String-Inspired Infinite-Derivative Theories of Gravity: A Brief Overview", *Mod. Phys. Lett.* **A30** (2015) 1540009, arXiv:1412.4256. 7

[99] S. Talaganis and A. Mazumdar, "High-Energy Scatterings in Infinite-Derivative Field Theory and Ghost-Free Gravity", *Class. Quant. Grav.* **33** (2016) 145005, arXiv:1603.03440. 7, 8, 35, 163, 165

[100] S. Talaganis, T. Biswas, and A. Mazumdar, "Towards understanding the ultraviolet behavior of quantum loops in infinite-derivative theories of gravity", *Class. Quant. Grav.* **32** (2015) 215017, arXiv:1412.3467. 7, 35, 79, 113, 158, 165

[101] S. Talaganis, "Quantum Loops in Non-Local Gravity", *PoS* **CORFU2014** (2015) 162, arXiv:1508.07410. 7

[102] S. Talaganis, "Towards UV Finiteness of Infinite Derivative Theories of Gravity and Field Theories", arXiv:1704.08674. 7

[103] H. Elvang and Y.-t. Huang, "Scattering Amplitudes", arXiv:1308.1697. 7, 72

[104] M. Ostrogradsky, "Mémoires sur les équations différentielles, relatives au problème des isopérimètres", *Mem. Acad. St. Petersbourg* **6** (1850) 385–517. 8, 102

[105] R. P. Woodard, "Ostrogradsky's theorem on Hamiltonian instability", *Scholarpedia* **10** (2015) 32243, arXiv:1506.02210. 8, 9, 102

[106] T. Clifton, P. G. Ferreira, A. Padilla, and C. Skordis, "Modified Gravity and Cosmology", *Phys. Rept.* **513** (2012) 1–189, arXiv:1106.2476. 9, 151

[107] S. Talaganis and A. Teimouri, "Hamiltonian Analysis for Infinite Derivative Field Theories and Gravity", arXiv:1701.01009. 9

[108] T. Biswas, A. Conroy, A. S. Koshelev, and A. Mazumdar, "Generalized ghost-free quadratic curvature gravity", *Class. Quant. Grav.* **31** (2014) 015022, arXiv:1308.2319, [Erratum: Class. Quant. Grav.31,159501(2014)]. 10

[109] J. Edholm, A. S. Koshelev, and A. Mazumdar, "Behavior of the Newtonian potential for ghost-free gravity and singularity-free gravity", *Phys. Rev.* **D94** (2016) 104033, arXiv:1604.01989. 10

[110] J. Edholm and A. Conroy, "Newtonian Potential and Geodesic Completeness in Infinite Derivative Gravity", *Phys. Rev.* **D96** (2017) 044012, arXiv:1705.02382. 10

[111] S. Talaganis and A. Teimouri, "Scale of non-locality for a system of n particles", arXiv:1705.07759. 11, 163

[112] A. Teimouri, S. Talaganis, J. Edholm, and A. Mazumdar, "Generalised Boundary Terms for Higher Derivative Theories of Gravity", *JHEP* **08** (2016) 144, arXiv:1606.01911. 11, 12, 170, 171, 172

[113] A. Conroy, A. Mazumdar, and A. Teimouri, "Wald Entropy for Ghost-Free, Infinite Derivative Theories of Gravity", *Phys. Rev. Lett.* **114** (2015) 201101, arXiv:1503.05568. 12

[114] A. Conroy, A. Mazumdar, S. Talaganis, and A. Teimouri, "Nonlocal gravity in D dimensions: Propagators, entropy, and a bouncing cosmology", *Phys. Rev.* **D92** (2015) 124051, arXiv:1509.01247. 12, 22, 173

[115] S. Talaganis and A. Teimouri, "Rotating black hole and entropy for modified theories of gravity", arXiv:1705.02965. 12

[116] A. Conroy, A. S. Koshelev, and A. Mazumdar, "Defocusing of Null Rays in Infinite Derivative Gravity", *JCAP* **1701** (2017) 017, arXiv:1605.02080. 13

[117] A. Conroy, T. Koivisto, A. Mazumdar, and A. Teimouri, "Generalized quadratic curvature, non-local infrared modifications of gravity and Newtonian potentials", *Class. Quant. Grav.* **32** (2015) 015024, arXiv:1406.4998. 13

[118] A. Teimouri, "Entropy of non-local gravity", arXiv:1705.11164. 13

[119] M. E. Peskin and D. V. Schroeder, "An Introduction to quantum field theory", Addison-Wesley, Reading, USA, 1995. 35, 36, 153, 156

[120] M. Srednicki, "Quantum field theory", Cambridge University Press, 2007. 36

[121] S. R. Coleman and E. J. Weinberg, "Radiative Corrections as the Origin of Spontaneous Symmetry Breaking", *Phys. Rev.* **D7** (1973) 1888–1910. 40

[122] S. Hassani, "Mathematical Physics: A Modern Introduction to its Foundations", Springer, 2013. 44

[123] "*NIST Digital Library of Mathematical Functions*". http://dlmf.nist.gov/, Release 1.0.17 of 2017-12-22, December 2017. F. W. J. Olver, A. B. Olde Daalhuis, D. W. Lozier, B. I. Schneider, R. F. Boisvert, C. W. Clark, B. R. Miller and B. V. Saunders, eds. 51

[124] J. F. Donoghue and T. Torma, "Infrared behavior of graviton-graviton scattering", *Phys. Rev.* **D60** (1999) 024003, `arXiv:hep-th/9901156`. 53

[125] S. Weinberg, "The Quantum theory of fields. Vol. 1: Foundations", Cambridge University Press, 2005. 72

[126] D. Amati, M. Ciafaloni, and G. Veneziano, "Planckian scattering beyond the semiclassical approximation", *Phys. Lett.* **B289** (1992) 87–91. 72, 73

[127] M. Fabbrichesi, R. Pettorino, G. Veneziano, and G. A. Vilkovisky, "Planckian energy scattering and surface terms in the gravitational action", *Nucl. Phys.* **B419** (1994) 147–188, `arXiv:hep-th/9309037`. 72

[128] G. Veneziano and J. Wosiek, "Exploring an S-matrix for gravitational collapse", *JHEP* **09** (2008) 023, `arXiv:0804.3321`. 72

[129] G. Veneziano, "String-theoretic unitary S-matrix at the threshold of black-hole production", *JHEP* **11** (2004) 001, `arXiv:hep-th/0410166`. 72

[130] D. Amati, M. Ciafaloni, and G. Veneziano, "Towards an S-matrix description of gravitational collapse", *JHEP* **02** (2008) 049, arXiv:0712.1209. 72

[131] S. B. Giddings and M. Srednicki, "High-energy gravitational scattering and black hole resonances", *Phys. Rev.* **D77** (2008) 085025, arXiv:0711.5012. 72, 73

[132] S. B. Giddings, M. Schmidt-Sommerfeld, and J. R. Andersen, "High energy scattering in gravity and supergravity", *Phys. Rev.* **D82** (2010) 104022, arXiv:1005.5408. 72, 73

[133] S. B. Giddings and S. D. Thomas, "High-energy colliders as black hole factories: The End of short distance physics", *Phys. Rev.* **D65** (2002) 056010, arXiv:hep-ph/0106219. 72

[134] D. M. Eardley and S. B. Giddings, "Classical black hole production in high-energy collisions", *Phys. Rev.* **D66** (2002) 044011, arXiv:gr-qc/0201034. 72

[135] D. J. Gross and A. Jevicki, "Operator Formulation of Interacting String Field Theory", *Nucl. Phys.* **B283** (1987) 1–49. 72

[136] G. Veneziano, "Construction of a crossing - symmetric, Regge behaved amplitude for linearly rising trajectories", *Nuovo Cim.* **A57** (1968) 190–197. 72

[137] D. J. Gross and P. F. Mende, "String Theory Beyond the Planck Scale", *Nucl. Phys.* **B303** (1988) 407–454. 72

[138] S. B. Giddings, D. J. Gross, and A. Maharana, "Gravitational effects in ultrahigh-energy string scattering", *Phys. Rev.* **D77** (2008) 046001, arXiv:0705.1816. 72, 73

[139] D. J. Gross and P. F. Mende, "The High-Energy Behavior of String Scattering Amplitudes", *Phys. Lett.* **B197** (1987) 129–134. 72, 73

[140] W. Staessens and B. Vercnocke, "Lectures on Scattering Amplitudes in String Theory", in "5th Modave Summer School in Mathematical Physics Modave, Belgium, August 17-21, 2009". 2010. arXiv:1011.0456. 72

[141] P. Don, S. Giaccari, L. Modesto, L. Rachwal, and Y. Zhu, "Scattering amplitudes in super-renormalizable gravity", *JHEP* **08** (2015) 038, arXiv:1506.04589. 73

[142] D. Amati, M. Ciafaloni, and G. Veneziano, "Effective action and all order gravitational eikonal at Planckian energies", *Nucl. Phys.* **B403** (1993) 707–724. 73

[143] D. Amati, M. Ciafaloni, and G. Veneziano, "Higher Order Gravitational Deflection and Soft Bremsstrahlung in Planckian Energy Superstring Collisions", *Nucl. Phys.* **B347** (1990) 550–580. 73

[144] D. Amati, M. Ciafaloni, and G. Veneziano, "Can Space-Time Be Probed Below the String Size?", *Phys. Lett.* **B216** (1989) 41–47. 73

[145] D. Amati, M. Ciafaloni, and G. Veneziano, "Superstring Collisions at Planckian Energies", *Phys. Lett.* **B197** (1987) 81. 73

[146] J. L. Anderson and P. G. Bergmann, "Constraints in covariant field theories", *Phys. Rev.* **83** (1951) 1018–1025. 102, 104, 106

[147] P. A. M. Dirac, "Generalized Hamiltonian dynamics", *Proc. Roy. Soc. Lond.* **A246** (1958) 326–332. 102, 104

[148] P. A. M. Dirac, "The Theory of gravitation in Hamiltonian form", *Proc. Roy. Soc. Lond.* **A246** (1958) 333–343. 102, 104

[149] P. A. Dirac, "Lectures on Quantum Mechanics", Dover Publications Inc., 2003. 102, 104

[150] R. L. Arnowitt, S. Deser, and C. W. Misner, "The Dynamics of general relativity", *Gen. Rel. Grav.* **40** (2008) 1997–2027, arXiv:gr-qc/0405109. 102, 115

[151] E. Gourgoulhon, "3+1 formalism and bases of numerical relativity", arXiv:gr-qc/0703035. 102, 115, 116

[152] A. W. Wipf, "Hamilton's formalism for systems with constraints", *Lect. Notes Phys.* **434** (1994) 22, arXiv:hep-th/9312078. 104

[153] M. Henneaux and C. Teitelboim, "Quantization of gauge systems", Princeton University Press, 1992. 104, 105, 106, 107

[154] H.-J. Matschull, "Dirac's canonical quantization program", arXiv:quant-ph/9606031. 106

[155] E. Sudarshan and N. Mukunda, "Classical Dynamics: A Modern Perspective", Wiley, New York, 1974. 107

[156] J. Kluson, "Non-Local Gravity from Hamiltonian Point of View", *JHEP* **09** (2011) 001, arXiv:1105.6056. 108, 122

[157] T. Biswas, A. S. Koshelev, and A. Mazumdar, "Gravitational theories with stable (anti-)de Sitter backgrounds", *Fundam. Theor. Phys.* **183** (2016) 97–114, arXiv:1602.08475. 145

[158] T. Biswas, A. S. Koshelev, and A. Mazumdar, "Consistent higher derivative gravitational theories with stable de Sitter and anti-de Sitter backgrounds", *Phys. Rev.* **D95** (2017), no. 4, 043533, arXiv:1606.01250. 145

[159] S. Talaganis, "Slavnov Identities for Infinite Derivative Theory of Gravity", arXiv:1705.08569. 158

[160] I. Quandt and H.-J. Schmidt, "The Newtonian limit of fourth and higher order gravity", *Astron. Nachr.* **312** (1991) 97, arXiv:gr-qc/0109005. 160

[161] N. Deruelle, M. Sasaki, Y. Sendouda, and D. Yamauchi, "Hamiltonian formulation of f(Riemann) theories of gravity", *Prog. Theor. Phys.* **123** (2010) 169–185, arXiv:0908.0679. 171

[162] R. M. Wald, "Black hole entropy is the Noether charge", *Phys. Rev.* **D48** (1993) R3427–R3431, arXiv:gr-qc/9307038. 173

[163] T. Jacobson, G. Kang, and R. C. Myers, "On black hole entropy", *Phys. Rev.* **D49** (1994) 6587–6598, arXiv:gr-qc/9312023. 173

[164] G. Leibbrandt, "Introduction to the Technique of Dimensional Regularization", *Rev. Mod. Phys.* **47** (1975) 849. 179, 180

[165] H. Osborn, "Lecture Notes on Advanced Quantum Field Theory". http://www.damtp.cam.ac.uk/user/ho/AQFTNotes.pdf, May 2016. 179